POLISH NATIONAL COMMITTEE
FOR
INTERNATIONAL UNION OF GEODESY AND GEOPHYSICS

POLISH NATIONAL REPORT ON GEODESY

2019–2022

Presented to 28th General Assembly
of the International Union of Geodesy and Geophysics
in Berlin, Germany, 2023

Committee on Geodesy, Polish Academy of Sciences
Warsaw, 2023

Preface

National Committee for the International Union of Geodesy and Geophysics of the Polish Academy of Sciences (PAS) – the adhering organization representing Poland to IUGG and its Associations, coordinates the flow of information in both directions between IUGG and the respective Polish scientific community. For a number of decades, the reports on activities on geodesy in Poland in the quadrenium were presented to the International Association of Geodesy (IAG) by the Committee on Geodesy of the Polish Academy of Sciences on the request of the Polish National Committee for IUGG.

This report has been prepared by the Committee on Geodesy of PAS for submission to the IAG at its General Assembly in Berlin, Germany, during the 28th IUGG General Assembly, 10–21 July 2023. It consists a summary of research activity in geodesy performed in a period of 2019–2022 in Poland.

The Polish National Report on Geodesy 2019–2022 is in the form of the six peer-reviewed review papers (chapters):

1. Research on reference frames and reference networks in Poland in 2019–2022 (Jan Krynski and Tomasz Liwosz);
2. Research on gravity field modelling and gravimetry in Poland in 2019–2022 (Jan Krynski, Przemyslaw Dykowski, Walyeldeen Godah and Malgorzata Szelachowska);
3. Research on Earth rotation and geodynamics in Poland in 2019–2022 (Janusz Bogusz, Aleksander Brzezinski, Walyeldeen Godah and Jolanta Nastula);
4. Research on GNSS positioning and applications in Poland in 2019–2022 (Jacek Paziewski, Tomasz Hadas, Witold Rohm and Pawel Wielgosz);
5. Global Geodetic Observing System in Poland 2019–2022 (Krzysztof Sosnica, Radosław Zajdel and Jaroslaw Bosy);
6. Research on general theory and methodology in geodesy in Poland in 2019–2022 (Anna Klos, Marcin Ligas and Marek Trojanowicz);

which were developed in cooperation with the researchers from the following universities and research institutes:

- AGH University of Science and Technology in Krakow;
- Institute of Geodesy and Cartography in Warsaw;
- Military University of Technology in Warsaw;
- Space Research Centre of the Polish Academy of Sciences in Warsaw;
- University of Warmia and Mazury in Olsztyn;
- Warsaw University of Technology;
- Wroclaw University of Environmental and Life Sciences.

The report is published in the Advances in Geodesy and Geoinformation, the official journal of the Committee on Geodesy of the Polish Academy of Sciences. Many thanks the authors of all articles (chapters), reviewers and all those who contributed to develop the final form of the report.

Jan Krynski

President

Polish National Committee for IUGG

Research on reference frames and reference networks in Poland in 2019-2022

Jan Krynski[1], Tomasz Liwosz[2]*

[1]Institute of Geodesy and Cartography, Warsaw, Poland,
[2]Warsaw University of Technology, Warsaw, Poland,
*Corresponding author: Tomasz Liwosz, e-mail: tomasz.liwosz@pw.edu.pl

Abstract: The article presents the reviewed and summarised research activities of Polish research groups on reference frames and reference networks in a period of 2019–2022. It contains the results on the implementation of latest resolutions on reference systems of the International Union of Geodesy and Geophysics and the International Astronomical Union focusing on changes in the consecutive issues of the Astronomical Almanac of the Institute of Geodesy and Cartography, Warsaw. It further presents the status of the implementation of the European Terrestrial Reference System 1989 (ETRS89) in Poland, monitoring the terrestrial reference frame, including research on global terrestrial reference frames, GNSS data analysis within the EUREF Permanent Network, research on GNSS receiver antenna phase centres, research on impact of non-tidal loading effects on position solutions, and on station velocities. Then the activities concerning the realization of ITRS and ETRS89 in Poland are discussed, including operational work of GNSS IGS/EPN stations as well as operational work of the laser ranging station of the International Laser Ranging Service, with special emphasis on the Polish active GNSS network for the realization of ETRS89 and maintenance of the vertical control network. Extensive research activities are observed in the field of implementation of the International Terrestrial Gravity Reference Frame in Poland, maintenance and modernization of gravity control network in Poland but also in Sweden, establishment of gravity control network in Ireland based on absolute gravity survey as well as maintenance of the national magnetic control network in Poland which is traditionally performed on a regular basis.

Keywords: reference system, reference frame, vertical control, gravity control, magnetic control

Accepted Article

1. Introduction

The article presents the achievements of Polish research and government institutions in the years 2019–2022, concerning the issues related to the implementation of global and regional reference systems, integration of geodetic, gravimetric and magnetic measurements for the realization and maintenance of a unified reference frame and reference networks, mainly in Poland but also in some other countries. Results of research conducted by the teams affiliated in the following Polish institutions: AGH University of Science and Technology in Cracow (AGH), Polish Head Office of Geodesy and Cartography (GUGiK), Institute of Geodesy and Cartography in Warsaw (IGiK), Military University of Technology in Warsaw (MUT), Rzeszow University of Technology (RUT), Space Research Centre of the Polish Academy of Sciences (SRC PAS), Warsaw University of Technology (WUT), University of Warmia and

This article has been accepted for publication in the journal Advances in Geodesy and Geoinformation, issue 72/2, 2023. It has not yet undergone the process of copyediting, typesetting, pagination and proofreading. This may lead to differences between this version and the final published version. The article may be cited as DOI: 10.24425/agg.2023.146156.

Mazury in Olsztyn (UWM), Wroclaw University of Environmental and Life Sciences (UPWr), are presented.

Research on the implementation of resolutions of General Assemblies of the International Astronomical Union (IAU) and the International Union of Geodesy and Geophysics (IUGG) regarding celestial reference systems, time systems as well as transformations between celestial and terrestrial systems has been continued at the Centre of Geodesy and Geodynamics of IGiK. The latest resolutions of IAU and IUGG are consequently implemented in consecutive editions of the Astronomical Almanac (pol. *Rocznik Astronomiczny*). The Astronomical Almanac is developed and published by IGiK every year since 1946. Recent releases of the Astronomical Almanac of IGiK are shortly presented in Section 2.

Control networks in Poland: horizontal, vertical, gravimetric, and magnetic are integrated in a common reference system – the European Terrestrial Reference System 1989 (ETRS89) which is a standard reference system in Europe adopted in 1990 by EUREF – the Regional Reference Frame Sub-commission for Europe acting under the Commission 1 on Reference Frames of the International Association of Geodesy (IAG). Since 1992 the ETRS89 has been realized in Poland by means of the Global Navigation Satellite System (GNSS). The latest realization of ETRS89 in Poland (PL-ETRF2000), was developed in 2011 through the network of 103 GNSS permanent stations, i.e. the Active Geodetic Network – European Position Determination System (ASG-EUPOS), and was officially adopted in 2013 ([41]Krynski et al., 2019a). More information on the realizations of ETRS89 in Poland is provided in Section 3, while the status of the ASG-EUPOS system is given in Section 6.

Polish GNSS and Satellite Laser Ranging (SLR) stations operate also within IAG services and support the international geodetic community in the realization of global and regional terrestrial reference frames. Several GNSS stations are part of the International GNSS Service (IGS) and EUREF Permanent Network (EPN). The satellite laser ranging station in Poland operates within the International Laser Ranging Service (ILRS). More details on the operational work of Polish stations are given in Section 5.

Polish institutions contribute also to the maintenance of the ETRS89 at the pan-European level. Two EPN analysis centres (ACs) at MUT and WUT regularly process GNSS data and estimate coordinates of stations belonging to their EPN sub-networks. Since 2014, WUT and MUT are also running the EPN Analysis Combination Centre (ACC). The ACC analyses and combines the GNSS solutions of 16 EPN analysis centres. The activities of the ACC and the Polish ACs in 2019–2022 are presented in Section 4.2.

For several years, Polish groups have been conducting research on various topics related to global and regional reference frames. Research on global terrestrial reference frames and the improvement of the determination of global geodetic parameters and future ITRFs was conducted at UPWr (Section 4.1). Research on issues related to receiver antenna phase center correction was conducted at UWM, MUT, and AGH. It concerned the development of a field calibration procedure, and the analysis of the influence of the use of different receiver antenna calibrations on station positions (Section 4.3). The impact of non-tidal loading effects (atmospheric, oceanic and hydrospheric) on the results of satellite navigation techniques was investigated in UPWr, and MUT (Section 4.4) and on the results of space gravity missions in IGiK (Section 7). The research on the determination of station velocities and their uncertainties was conducted at MUT (Section 4.5).

In 2014, the PL-EVRF2007-NH reference frame was adopted for the Polish fundamental vertical network. Since then, local authorities started implementing the PL-EVREF2007-NH for the detailed vertical network. In 2020, GUGiK initiated works for the new country-wide levelling campaign. The status of the PL-EVRF2007-NH implementation and the preparations for the new levelling campaign are presented in Section 7.

Accepted Article

The reference surface for heights in the vertical system in Poland is a static quasigeoid derived from a gravity field considered to be invariant in time. For last 20 years temporal variations of gravity are monitored using data from Gravity Recovery and Climate Experiment (GRACE) and GRACE Follow-On satellite missions. Global Geopotential Models (GGMs) obtained from those missions were used by the team of IGiK in the research on modelling and predicting temporal variations of gravity functionals, in particular geoid heights over Central Europe, in the context of the definition and realization of a modern vertical reference system. The results of those investigations are also summarized in Section 7.

The gravity control in Poland, based on the network of absolute gravity stations, was established in 2012–2013. The review and maintenance of that network in 2022 will be followed by surveying campaigns in next few years. An extensive activity of IGiK towards implementation of the International Terrestrial Gravity Reference System/Frame (ITGRS/ITGRF) in Poland was observed. In particular it concerns on preparing the Borowa Gora (BG) Observatory infrastructure to become a reference station of ITGRF.

The activities of IGiK related to gravity control were extended beyond Polish borders. They concerned the modernization of the gravity control network in Sweden as well as extended works on designing surveying the gravity control network in Ireland. More detail information on the subject is given in Section 8.

The magnetic control network in Poland was established in 1955 (Section 9). The network is regularly surveyed and maintained by IGiK. Presently the magnetic control network consists of 21 repeat stations. Two magnetic observatories of the global international network for monitoring geomagnetic field (INETRMAGNET) together with two permanent magnetic stations in Poland provide data that are used to control magnetic surveys.

The activities of Polish research groups related to terrestrial reference frames, geodynamics and gravity in Poland are integrated within the Research Network for Global Geodetic Observing System (GGOS-PL). In years 2017–2022, IGiK, MUT, and UPWr together with the Institute of Geophysics of the Polish Academy of Sciences and with several other institutions carried out a regional project EPOS-PL on the development of the Polish Earth science infrastructure. The project was integrated with the European Plate Observing System Programme (EPOS) ([43]Krynski et al., 2019c). Within the project, centres of research infrastructure for geomagnetic and magnetotelluric data, GNSS data, gravimetric data, and integrated data for GGOS-PL have been developed, and all new data is regularly supplied to the relevant databases.

2. Implementation of IUGG and IAU resolutions on reference systems

The team of the Centre of Geodesy and Geodynamics of IGiK traditionally has implemented consecutive IAU and IUGG resolutions in computing programs or in developed new algorithms for calculating ephemeris for the Astronomical Almanac of IGiK (AA IGiK).

The full version of the AA IGiK, containing a complete set of tables, is available on web pages of IGiK[1] in pdf format. Starting from 2014, presentation of high precision astrometric and geodetic data in the AA IGiK was consequently modified considering the latest achievements in the field of reference systems. In 2015, an "on-line" calculator of apparent places of stars was developed and made available on web pages of IGiK[2]. It has been extended in 2017 by calculations of mean positions of stars and reduction terms for the computation of apparent places at arbitrary time ([41]Krynski et al., 2019a). The Internet "on-line" AA IGiK based on

[1]http://www.igik.edu.pl/pl/rocznik-astronomiczny/

[2]http://www.igik.edu.pl/pl/Rocznik-Astronomiczny-On-Line/

Accepted Article

direct calculations ensures significantly better accuracy than the traditional Astronomical Almanac of a reasonable volume. Simultaneously, the content of tables of the printed version of the AA IGiK has been reduced. The consecutive issues of the AA IGiK for the years 2020 ([40]Krynski and Sekowski, 2019), 2021 ([44]Krynski and Sekowski, 2020), 2022 ([46]Krynski and Sekowski, 2021), 2023 ([47]Krynski and Sekowski, 2022) (Fig. 1) are in agreement with recent resolutions of IAU and IUGG and contain all updates to their previous editions.

Fig. 1. The Astronomical Almanacs of IGiK issued in the years 2019–2022

3. Implementation of the ETRS89 in Poland

The ETRS89 is a geodetic reference system for Europe which was adopted by EUREF in 1990. The ETRS89 coincides with the International Terrestrial Reference System (ITRS) at epoch 1989.0, and is fixed to the stable part of the Eurasian Plate.

Presently, two ETRS89 realizations, namely PL-ETRF2000 and PL-ETRF89, are officially used in Poland ([41]Krynski et al., 2019a). The PL-ETRF89 (in Poland named also EUREF-89) was developed on the basis of GPS observations collected during two surveying campaigns (in 1992, and in 1994–1995) and includes coordinates of 348 passive ground stations, while the PL-ETRF2000 was realized on the basis of GPS observations collected at Polish permanent GNSS stations (during 66 days in 2008 and 2010/2011) belonging to the ASG-EUPOS network (Section 9), which was established in 2008 and is maintained by GUGiK. The PL-ETRF2000 reference frame was adopted by GUGiK in 2013.

The PL-ETRF2000 reference frame is based on GPS data collected at the ASG-EUPOS stations up to March 2011. Since then, most stations included in this reference frame experienced a change of GNSS equipment (antenna, receiver), which caused coordinate changes on some stations (e.g., [53]Liwosz and Ryczywolski, 2016). Also, several new stations were established after the PL-ETRF2000 was developed and 14 new stations are planned to be installed in 2023. Therefore, to take into account the changes on the ASG-EUPOS stations, and to include all new stations, an update of the ETRS89 realization in Poland is required; the preparation of the new realization of the ETRS89 is foreseen after the installation of new stations in 2023.

Accepted

4. Monitoring the terrestrial reference frame

In this section research conducted by Polish institutions on various topics related to global and regional reference frames has been summarized.

4.1 Research on global terrestrial reference frames

The research on global terrestrial reference frames (TRF) and possible improvement of the determination of global geodetic parameters such as geocenter and pole coordinates, as well as future ITRFs was conducted by the group at the Wroclaw University of Environmental and Life Sciences. [72]Zajdel et al. (2019a) analysed the impact of various factors on GNSS products, e.g., station coordinates, geocenter coordinates, Earth orientation parameters, and GNSS orbits obtained from a double-differenced multi-GNSS (GPS, GLONASS, Galileo) global processing. The authors found that when no-net-translation minimum constraints are not applied in the GNSS solution, the station position repeatability is degraded by 70% for the north, 55% for the east, and 25% for the up component, as compared to the solution in which those constraints were applied and the network origin coincided with the ITRF. The authors concluded that it is mandatory to apply the no-net-translation minimum constraints in global GNSS solutions.

[73]Zajdel et al. (2019b) analysed the impact of various approaches of the TRF realization using minimum-constraints as well as the selection of reference stations on the estimated coordinates of SLR stations, TRF scale, Earths orientation parameters and geocenter coordinates. The authors found that when using a robust station selection for TRF realization, the repeatability of station positions may be improved by 8% for the north, 4% for the east, and 6% for the vertical component. On the other hand, the impact of the selection of stations used for the TRF realization on the scale of resulting SLR solutions was found negligible.

The possibility to use new SLR and GNSS observations for the determination of the global parameters was studied ([66]Sosnica et al., 2019; [67]Strugarek et al., 2019; [6]Bury et al., 2021a; [74]Zajdel et al., 2022). [66]Sosnica et al. (2019) analysed the contribution of SLR observations performed to GNSS satellites for the realization of an SLR terrestrial reference frame and the determination of global parameters. It was concluded that those observations increase the number of coordinate solutions with respect to SLR-only solutions and improve the repeatability of station positions, and thus they should be considered for the future ITRF realizations. [67]Strugarek et al. (2019) investigated the quality of global geodetic parameters and reference frame parameters obtained from SLR observations performed to active Sentinel-3A/3B satellites for which orbits were determined using GPS observations. The authors found that those observations may be used for determination of precise station coordinates and global parameters e.g., geocenter and pole co-ordinates. Also, after increasing the number of active SLR satellites and extending the observation period, those observations could be considered in further realizations of TRFs. In 2019, the BeiDou Satellite Navigation System (BDS) released the antenna phase center corrections for BeiDou satellites. Since then, the BDS constellation became a potential second GNSS contributor (in addition to Galileo) to the realization of the scale in future ITRF realizations. [74]Zajdel et al. (2022) analysed the possibility to use BeiDou-3 observations to realize the scale of the terrestrial reference frame. It was found that the estimated scale depends on the frequencies of signals used for GNSS data processing. The common usage of GNSS and SLR-to-GNSS observations in the realization of TRF was analyzed ([7]Bury et al., 2021b). In the approach applied the co-location between SLR and GNSS techniques takes place in space, on board of GNSS satellites. Such co-location in space

Accepted Article

could replace in future local ties between SLR and GNSS stations. The authors found that the best results in terms of TRF realization can be obtained when imposing NNT and NNR conditions on both GNSS and SLR core stations.
Development of multi-year GNSS solutions involves the correction of discontinuities in station position time series in order to reliably estimate station velocities. [60]Najder (2020) used the FODITS program of the Bernese GNSS Software ([8]Dach et al., 2015) to automatically detect the discontinuities in station positions of selected global IGS stations and compared the results with ITRF2014 and JTRF2014 (the Jet Propulsion Laboratory realization of the ITRS). [60]Najder (2020) provided confidence intervals for automatic detection of the discontinuities, but also indicated some drawbacks of this approach in the identification of the discontinuities epochs and velocity changes..

4.2 GNSS analysis in the frame of the EUREF Permanent Network

The purpose of the EUREF Permanent Network (EPN) is to provide access to the ETRS89. Presently EPN consists of about 400 permanent GNSS stations located in Europe. Two Polish analysis centres (ACs) operating at the WUT and the MUT, regularly analyze GNSS observations and provide their solutions (station coordinates and tropospheric zenith delays) to EPN.
Since 2014, WUT and MUT are also responsible for operating the EPN Analysis Combination Centre (ACC). The tasks of the EPN ACC include the analysis and combination of GNSS coordinate solutions generated by 16 EPN analysis centres. Since 2016, EPN daily and weekly combined solutions have been developed at WUT ([56]Liwosz, 2022a). The EPN daily combined solutions are the input for the EUREF reference frame solution ([50]Legrand, 2022). The ACC website[3] containing plots of EPN station position time series and AC position residuals is maintained at MUT. In 2019–2022, the ACC tasks were continued.
The EPN combined solutions, as the EUREF reference frame product, are also provided by WUT to the EPOS (European Plate Observing System) GNSS products portal within the EPOS-GNSS thematic core service ([18]Fernandes et al., 2022).
In 2019 the ACC investigated the impact of adding Galileo observations to AC solutions (in addition to GPS and GLONASS) on combined EPN station positions. For majority of stations the mean position differences between the two-system (GPS, GLONASS) and three-system (GPS, GLONASS, Galileo) solutions were up to 1 mm for the east and north components, and up to 3 mm for the vertical component. It was also found that for stations with antennas for which type-mean calibrations were used, larger position differences were obtained, especially for the vertical component, than for stations with individually calibrated antennas ([54]Liwosz and Araszkiewicz, 2019a). Since the beginning of GPS week 2044 (10 March 2019), 11 EPN ACs have started including Galileo observations (in addition to GPS and GLONASS) in their operational products.
In 2019 the ACC analyzed also the impact of adding globally distributed stations to the EPN regional network on the positions of EPN stations. The official EPN combined solution (regional) was compared to the combined solution in which additional global stations were included. The differences in station positions between both solutions resulted mostly from a different alignment of each solution (global, regional) to the reference frame. Time series of position differences were also compared to series of modelled non-tidal loadings (due to atmosphere and continental water) and good agreement was obtained ([55]Liwosz and Araszkiewicz, 2019b).

[3]http://www.epnacc.wat.edu.pl/epnacc/

Accepted Article

On 27 November 2022 (start of GPS week 2238) the IGS switched from the IGb14 to the IGS20 reference frame and IGS repro3 standards for the generation of its operational products. The EPN ACC and ACs also started preparations for the switch to the IGS20 in EPN analysis. The details regarding the switch were discussed at the EPN Analysis Centres Workshop on 3 November 2022 (virtual meeting). Minutes and presentations from this meeting are available at the EPN CB webpage[4]. Changes in the EPN analysis after the switch to IGS20 will include, e.g. the use of the consistent three-system (GPS, GLONASS, Galileo) IGS AC final products, the adoption of the new EPN receiver antenna model (based on the IGS type-mean model with additional calibrations for antenna-radome pairs not included in the IGS model), the consideration of receiver antenna misalignments from true north, the use of the FES2014b ocean tide loading model, the use of the VMF3 for troposphere modelling, and the adoption of the new long filename IGS convention for the EPN products. The activities of the EPN ACC in 2019–2022 were regularly presented at the EUREF Symposia and EPN Analysis Centres Workshops (e.g., [54]Liwosz and Araszkiewicz, 2019a; [55]2019b; [58]2022; [57]Liwosz, 2022b).

4.3 Research on GNSS receiver antenna calibrations

The GNSS receiver antenna phase center issues are closely related to GNSS reference frames. The research on antenna calibrations in Poland concerned the development of a field calibration procedure, and the analysis of the influence of receiver antenna calibrations on station positions.

In 2019, the UWM and Astri Polska, started a European Space Agency (ESA) project dedicated to the development of the receiver antenna field absolute calibration procedure for a multi-frequency and multi-GNSS signals. The methodology and algorithms proposed are based on the principles developed at the University of Hannover, with implementing own innovations. The initial results were published ([49]Krzan et al., 2020; [9]Dawidowicz et al., 2021). The calibrations obtained from the independent UWM analysis for selected GNSS antennas showed good consistency (within 2 mm); slightly larger differences were observed for low zenith angles as well as at certain azimuth ranges in high zenith angles. The comparison of antenna models developed at the UWM with type-mean calibrations included in the IGS model showed that differences up to 3–4 mm could also be found for low elevation angles. The obtained results demonstrated a consistent performance for the Astri/UWM calibration procedure. However, some aspects, e.g. the modelling of phase center corrections at low elevations need to be further investigated.

Research team from the UWM investigated also offsets in the station position components caused by the receiver antenna changes at selected EPN stations ([10]Dawidowicz et al., 2023), in particular, the correlation between the occurrence of the offset and phase center correction model calibration type (type-mean, individual robot, individual chamber) as well as multipath values changes after the antenna replacement. GNSS data from 12 EPN stations from 2017–2019 were analysed. The results proved that the antenna replacement is critical in the context of station coordinates stability and, in most cases, it causes visible shifts in the position time series. Depending on the solution type, multipath changes after the antenna replacement are responsible for 21% – 42% of variations in the coordinates. In other cases, the imperfections in phase center correction models were the most probable reason for the observed position shifts.

The impact of various receiver antenna phase centre calibrations on the estimated positions of GNSS stations was investigated at the MUT. [1]Araszkiewicz et al. (2019) analysed the differences between individual and type-mean antenna models, and evaluated the impact of

[4]http://www.epncb.eu/_newseventslinks/workshops/EPNLACWS_2022/

Accepted Article

applying those models on estimated station heights. The authors found that both models give very similar results in terms of stability of the determined height and its variability caused by changing the elevation mask. The impact of applying GPS receiver antenna corrections to Galileo observations on GNSS positions was also investigated ([2]Araszkiewicz and Kiliszek, 2020). It was found that the use of GPS L2 corrections for the Galileo E5a signals may change the estimated height up to 8 mm; similar results were obtained for absolute and relative positioning methods.
[4]Borowski et al. (2022) analyzed the reliability of selected receiver antenna phase center calibrations included in models published by the IGS. Height differences for close stations obtained from different GPS solutions (EPN, PPP, short baseline) were compared with the measurements of spirit levelling. The best consistency with the levelling results was obtained for a short-baseline L1-only GPS solution. For one of the tested antennas, a change of the antenna calibration from IGS08 to IGS14 model resulted in 8 mm difference in height.

4.4 Research on impact of non-tidal loading effects on position solutions

Non-tidal loading effects due to atmosphere, ocean and continental water cause deformation of the Earth's surface. Although these effects are visible in position determined using space geodetic techniques, they are not modelled in official operational analysis and are subject to research.
[33]Klos et al. (2021) examined the sensitivity of GPS to the non-tidal loading effects for a set of Eurasian permanent GNSS stations. The authors found that correcting vertical GPS displacements by the atmospheric non-tidal loading effect leads to the reduction of the time series variances, and to the improvement in the uncertainty of the GPS vertical velocities by a factor of 2. They recommended application of the atmospheric non-loading at the observation level, while application of the hydrological loading to the resulting position time series.
[5]Bury et al. (2019) analysed the impact of the atmospheric non-tidal loading on the determination of global geodetic parameters using SLR observations to GNSS satellites. The authors found that neglecting the atmospheric non-tidal loading effect causes the systematic shift of station positions (so-called Blue-Sky effect) up to 2.3 mm for inland stations; it also causes systematic effects in the estimates of geocenter coordinates and satellite orbits. They concluded that the atmospheric non-tidal loading should be applied by all space geodetic techniques to remove systematic effects from estimated global parameters and to improve consistency between techniques.
[29]Kaczmarek (2019) analysed time series predicted from the non-tidal atmospheric, non-tidal ocean, and hydrological loading models and compared them to the global GNSS position time series of eight stations in Europe. The author computed correlation coefficients between the corresponding time series and found that the atmospheric non-tidal loading had the greatest influence on GNSS position time series at the considered area.

4.5 Research on vertical displacements

Detecting and monitoring vertical displacements are crucial for the realization and the maintenance of the vertical reference frame. Research in that field on both regional and global scale is conducted by numerous research groups all over the world.
The applicability of the co-kriging method for modelling vertical movements of the Earth's crust in Poland with the use of precise levelling data from the vertical control network and GNSS data from permanently operating stations was investigated by the team of UWM ([36]Kowalczyk et al., 2020). The authors indicated the difference in terms of isotropy between levelling and GNSS data. Strong dependence of the evaluation of vertical movements on the

Accepted Article

data set applied was observed in the results obtained. Thus co-kriging was found to not be a suitable method for modelling vertical movements of the Earth's crust based on combination of levelling and GNSS data.
Possibility of the determination of the most relevant common points in hybrid networks, i.e. network of repeated levelling measurements combined with a network of permanent GNSS stations, using scale-free network theory with the distance criterion for modelling vertical movements of the Earth's crust was examined ([37]Kowalczyk et al., 2021a). The computing tests per-formed using the UELN + EPN hybrid network provided successful results for identification the most significant pseudo-nodal points in large hybrid networks.
[38]Kowalczyk et al. (2021b) analysed the accuracy of determining the vertical movements of the Earth's crust based on time series of four techniques: satellite altimetry, tide gauges, GNSS and radar interferometry. The authors found that the accuracies of vertical movements obtained from the radar interferometry were similar to those obtained from GNSS position time series. On the other hand, the vertical movements of the Earth's crust determined from GNSS data differed from the results obtained on the basis of data from other techniques.

4.6 Research on GNSS stations velocities

Station velocities derived from GNSS solutions can be used for the analysis and interpretation of geodynamic phenomena. Estimation of station velocities from the position time series requires careful modelling of seasonal signals, discontinuities in positions, non-linearity of velocity, noise processes to reliably estimate the values of velocities and their uncertainties. [3]Bogusz et al. (2019) proposed a methodology for the position time series analysis, recommended to be used to obtain reliable GPS vertical station velocities, in particular for studying the post-glacial re-bound. The authors validated their methodology for 469 stations in Europe. They found that velocity uncertainties may be underestimated up to 8 times when assuming only white noise instead of power-law and white noise together during the position time series analysis. [31]Klos et al. (2019a) proposed the Wiener filter to model the time-varying seasonal amplitudes in position time series. The model was applied to synthetic and real GPS position time series. The authors showed that the proposed method provides optimal modelling of seasonal signals, while the underlying noise properties of the time series are not altered.
[32]Klos et al. (2019b) studied sea level changes at gauge stations focusing on vertical land motions (VLM). The authors proposed a new methodology for modelling of GPS-derived non-linear VLM. In addition to standard linear VLM model, the authors proposed to account also for co-seismic offsets, changes in the vertical velocities, and postseismic transient. The new methodology was applied for GPS station position time series (spanning years 1993-2015) in the earthquake affected Western North Pacific region. The authors found that introducing the new non-linear VLM model improves absolute tide gauge sea level estimates by 20% on average. It was also found that the new non-linear VLM model reduced the difference between altimetry and tide gauge derived absolute sea level trend estimates

4.7 Research on estimation of tectonic plates motion parameters

Tectonic plate motion models are needed for various geodetic and geodynamical applications. Such models can be computed on the basis of station velocities derived from space geodetic techniques, i.e.: GNSS, SLR, Very Long Baseline Interferometry (VLBI), Doppler Orbitography and Radiopositioning Integrated by Satellite (DORIS). [27]Jagoda et al. (2020a) estimated plate motion parameters for six plates: Eurasian, North American, Pacific, Australian, African and Antarctic using ITRF2008 station velocities. The plate parameters were

Accepted Article

computed separately for SLR, VLBI and DORIS techniques using different number of stations until stability in determined plate parameters was observed. The results were compared with the APKIM2005 (Actual Plate Kinematic and Crustal Deformation Model) plate motion model and good agreement was obtained. The estimation of plate motion parameters of the six plates mentioned using only VLBI station velocities was studied in more detail in [25]Jagoda and Rutkowska (2020a). [26]Jagoda and Rutkowska (2020b) analysed the motion of Eurasian plate using GNSS station velocities from the ITRF2014 solution. The authors estimated Eurasian plate motion parameters using four different station sets. The final parameters were computed using all (120) GNSS stations analysed in this study. The results were compared with the APKIM2005 model and with another model based on GPS observations from years 1991.0-1996.3.

5. Stations in Poland involved in realization of ITRS and ETRS89

An overview of Polish GNSS and SLR stations that are part of the IAG services and that support the international geodetic community in the realization of terrestrial reference frames is provided in this Section. Several Polish GNSS stations operate within the International GNSS Service (IGS) and the EUREF Permanent Network (EPN). The only SLR station in Poland operates within the International Laser Ranging Service (ILRS).

5.1 Operational work of GNSS permanent IGS/EPN stations

Permanent IGS and EPN GNSS stations have been operating in Poland for the last 29 years. Presently 19 permanent GNSS stations (Fig. 2) operate in Poland within the EPN network and 6 of them operate also within the IGS network[5].
In 2022, the WUT installed two GNSS permanent stations (WUTH00NOR, PPSH00NOR) in the Stanislaw Siedlecki Polish Polar Station in Hornsund, located at the bay of Isbjørnhamna in the southern part of Svalbard. The stations operate in cooperation with the Institute of Geophysics of the Polish Academy of Sciences. The two new GNSS stations have been included in the EPN and the European Plate Observing System (EPOS). The station WUTH00NOR was also proposed to join the IGS and was accepted in March 2023.
Seven stations (BOGI, BOGO, BOR1, JOZ2, JOZE, LAMA, WROC) were included in the ITRF2020 – the latest realization of the ITRS (published in April 2022). Two Polish stations: BOR1 and JOZE, were used for the estimation of official transformation parameters between ITRF2020 and ITRF2014; they were also included in the latest IGS terrestrial reference frame – IGS20, which is based on the ITRF2020.
Data from the above mentioned stations are regularly uploaded to two Regional Data Centres located at the BKG (Federal Agency for Cartography and Geodesy, Germany) and at the BEV (Federal Office of Metrology and Surveying, Austria). Stations BOGI, BOR1, JOZ2 and WROC provided also data for the IGS Real-time GNSS Data project[6]. All stations belonging to the IGS are additionally included into the IGS Multi-GNSS Experiment (MGEX) pilot project[7].

[5]http://www.epncb.eu/_networkdata/stationlist.php/
[6]http://igs-ip.net/home/
[7]http://igs.org/mgex/

Accepted Article

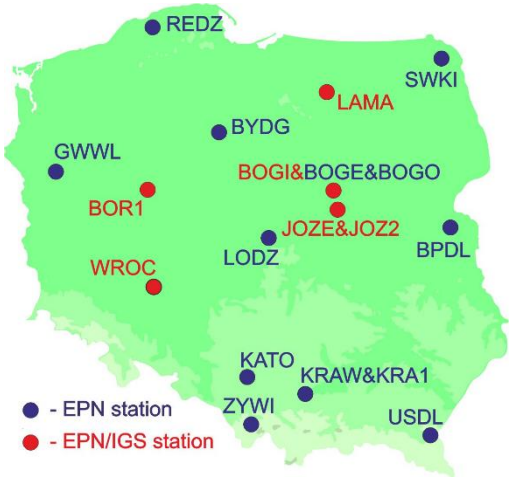

Fig. 2. EPN/IGS permanent GNSS stations in Poland (as of January 2023) ([45]Krynski and Rogowski, 2021)

Stations at Borowa Gora (BOGI), Borowiec (BOR1), Jozefoslaw (JOZ2), Cracow (KRAW, KRA1), Lamkowko (LAMA), and Wroclaw (WROC) provide also data for the EUREF-IP project[8]. Since 2005 the AGH University of Science and Technology has been operating the Ntrip Broadcaster[9].

5.2 Operational work of ILRS laser ranging station BORL

The Satellite Laser Ranging Station Borowiec (BORL) of the SRC PAS tracks satellites and space debris (cooperative and uncooperative targets) on regular basis: in 2019 – 82 objects, in 2020 – as many as 97 targets ([45]Krynski and Rogowski, 2021), in 2021 – 99 objects ([59]Liwosz and Dykowski, 2022), while in 2022 – 64 objects.
The station operates within the framework of the International Laser Ranging Service (ILRS) and EUROLAS Consortium as well as, since 2015, in the framework of the Space Debris Study Group run by the ILRS and internal contracts signed with the European Space Agency (ESA) and the European Consortium EUSST[10]. Tracking space debris and determining their position as well as their rotation/tumbling and orientation in space is of great importance from the perspective of future debris removal missions (e.g. ENVISAT). The number of space debris grows rapidly; more than 25 000 orbiting objects of diameter above 10 cm was counted in 2022 ([59]Liwosz and Dykowski, 2022).
The current information about the position of the objects like rocket bodies is very crucial and critical, from the point of view of the Space Surveillance and Tracking services, i.e. re-entry, collision avoidance or anti-satellite-weapon. Data provided by the BORL station contribute to global research on the determination of space debris spin dynamics (ENVISAT, ERS-1, ERS-2, OICETS, Seasat-1, TOPEX/Poseidon, and others). The results obtained were sent to the Crustal Dynamics Data Information System (CDDIS), EUROLAS Data Center (EDC), EUSST databank, and Space Debris databank in Graz ([45]Krynski and Rogowski, 2021). Table 1 presents a brief summary of SLR observations at BORL station in 2019–2022.

Table 1. SLR observation at BORL station in 2019–2022

[8]https://igs.bkg.bund.de/ntrip/
[9]http://home.agh.edu.pl/~kraw/ntrip.php/
[10]https://www.eusst.eu/

Accepted Article

Year	Satellites observed	Passes	Successful passes		RMS of a single shot [cm]
			normal points	single shots	
2019	44 SLR (30 LEO + 14	1079	15 197	743734	1.20 – 3.81
	38 space debris objects	388	4 074	188499	2.04 – 221.72
2020	40 SLR (27 LEO + 13	1352	18 644	918999	1.49 – 4.11
	57 space debris objects	698	7 396	300046	1.42 – 187.58
2021	53 SLR (37 LEO + 16	1396	17 923	885119	2.05
	46 space debris objects	382	4 686	214575	22.19
2022	51 SLR (27 LEO + 24	1356	16955	842882	1.13 – 3.87
	13 space debris objects	226	3643	136292	1.31 – 141.05

Twelve geodetic-geodynamic satellites: Ajisai, Etalon-1, Etalon-2, Geo-IK-2, GRACE-FO-1, GRACE-FO-2, LAGEOS-1, LAGEOS-2, LARES, LARETS, STARLETTE, and Stella, were tracked at BORL in the years 2019–2022. Summary of observational statistics of these satellites in the years 2019, 2020 ([45]Krynski and Rogowski, 2021), 2021 ([59]Liwosz and Dykowski, 2022) with indicating the largest number of passes, returns and normal points are given in Tables 2, 3, 4, and 5, respectively.

Table 2. SLR observations of geodetic satellites in 2019

Satellite name	Passes	Returns	Normal points	Avgerage RMS [cm]
Ajisai	62	84860	785	3.81
Etalon-1	3	453	14	3.76
Etalon-2	4	295	20	2.60
Geo-IK-2	3	4229	31	2.19
GRACE-FO-1	23	9880	564	3.08
GRACE-FO-2	11	5291	285	2.88
LAGEOS-1	**100**	**125946**	**923**	1.76
LAGEOS-2	43	43780	440	1.82
LARES	75	37186	821	1.55
LARETS	56	21245	405	2.16
STARLETTE	53	46889	573	2.31
Stella	13	7851	103	2.07
Total	443		4933	

Table 3. SLR observations of geodetic satellites in 2020

Satellite name	Passes	Returns	Normal points	Average RMS [cm]
Ajisai	**111**	**189595**	**1387**	3.41
Etalon-1	0	0	0	0
Etalon-2	3	364	14	3.61

Accepted Article

Geo-IK-2	6	4705	38	2.22
GRACE-FO-1	21	10077	432	3.45
GRACE-FO-2	15	7731	350	3.19
LAGEOS-1	46	45220	423	1.73
LAGEOS-2	50	30870	388	1.78
LARES	104	36486	1004	1.51
LARETS	92	37412	713	1.98
STARLETTE	97	70903	931	2.02
Stella	7	5109	65	2.02
Total	552		5745	

Table 4. SLR observations of geodetic satellites in 2021

Satellite name	Passes	Returns	Normal points	Avgerage RMS [cm]
Ajisai	90	**131444**	**1240**	3.12
Etalon-1	2	100	7	2.90
Etalon-2	2	130	9	3.57
Geo-IK-2	23	10136	547	3.35
GRACE-FO-1	13	5720	312	3.76
GRACE-FO-2	5	6151	57	2.56
LAGEOS-1	**100**	95514	1047	1.77
LAGEOS-2	65	23544	590	1.76
LARES	70	23744	516	1.90
LARETS	87	36161	942	1.53
STARLETTE	74	62326	760	1.81
Stella	11	6746	85	1.87
Total	542		6112	

Table 5. SLR observations of geodetic satellites in 2022

Satellite name	Passes	Returns	Normal points	Avgerage RMS [cm]
Ajisai	84	**134618**	1314	3.32
Etalon-1	7	903	31	3.32
Etalon-2	0	0	0	0
Geo-IK-2	8	7516	70	2.09
GRACE-FO-1	12	5917	286	2.87
GRACE-FO-2	15	6858	396	3.55
LAGEOS-1	**122**	113752	**1344**	1.85
LAGEOS-2	51	23711	491	1.83
LARES	60	21909	458	1.93
LARETS	81	29145	868	1.54
STARLETTE	74	33032	592	1.82
Stella	11	7330	96	2.13
Total	519		5976	

Accepted Article

A novelty in 2022 is LARES-2 passive geodynamic satellite[11] launched on 13 July 2022. First successful observation of this satellite made by BORL station was performed on 3 August 2022. In total, 4 passes of this satellite with 938 returns, 30 normal points and mean RMS 1.59 cm were recorded by BORL station.

Tracking results of LAGEOS-1 and LAGEOS-2 satellites are used for evaluation of the BORL laser sensor quality. Report on the station performance is regularly delivered by ILRS. Both quality and effectiveness of the laser measurements at BORL are significantly improved as compared to the previous years of its operational activity. For example, in 2020 the average LAGEOS RMS was at the level 17–18 mm, and approximately 150 average LAGEOS measurements in a normal point as well as approximately 1800 average LAGEOS full rate measurements per pass were observed.

Since many years the BORL station keeps its products quality on an equal and very good level. Based on the quality report for 2022 performed by four independent analysis centres (Hitotsubashi University, Joint Center for Earth System Technology/Goddard Space Flight Center, Russian Mission Control Centre and Shanghai Astronomical Observatory), the average LAGEOS normal point RMS, a short-term stability, and a long-term stability of BORL station are 3.9 mm, 9.7 mm, and 4.9 mm, respectively.

A new software dedicated to reduction of laser measurements, adopted to the newest operating systems (Windows/Linux) and equipped with a very flexible graphic interface, was developed by the team of the Borowiec Observatory in the years 2020–2021. Its code is compatible with the specifications and requirements given by ILRS. The software allows for the determination of a number of parameters, i.e. residuals O–C, normal points, RMS of normal points, RMS of observation, time bias, range bias can be determined with that software. The final works are underway and are planned to be completed with a quarantine procedure launched by ILRS in 2023.

In 2019, orbits of 13 space debris objects (Russian and Chinese boosters from LEO regime) were calculated. The improvement of orbits of the tracked rockets by using laser ranging data from a single station was investigated. Calculations were performed with the advanced orbital programme GEODYN-II, using laser measurements from BORL. The ephemerides based on initial orbital elements (TLE) were compared with positions obtained from laser measurements (Fig. 3).

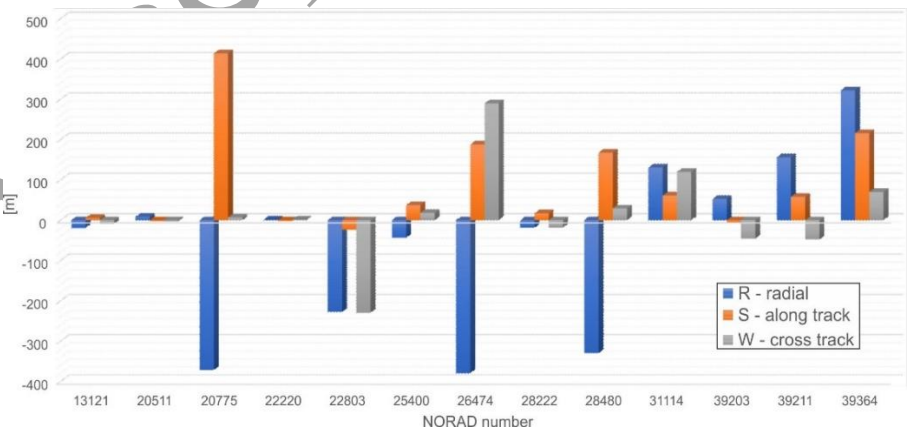

Fig. 3. Input TLE ephemerides vs. laser measurements in RSW frame

For all analysed targets the differences between the ephemerides based on TLE and observations performed at BORL (corrected elements/positions) are given in the radial, along-

[11]https://ilrs.gsfc.nasa.gov/missions/satellite_missions/current_missions/lrs2_general.html.

Accepted Article

track, cross-track (RSW) frame. The results obtained showed that a single short observation (from a dozen to several dozen seconds) of analysed objects improves the variance-covariance matrix by as much as 20–40% ([51]Lejba et al., 2020). In 2022 the positions and velocities of objects such as rocket bodies from the LEO regime and their covariance matrix based on full-rate laser measurements collected by the laser sensor BORL were determined. The purpose of those calculations was to show that a single short laser observation is sufficient to maintain a high-quality orbit of the LEO junk objects like rocket bodies. The results of those calculations are under preparation for publication.

The SST/Space Safety programme dominating amongst the activities of the team of BORL station in the years 2019–2022 constitutes one of the pillars of the Space Situational Awareness programme implemented by both ESA (Space Safety in the next years), and the EUSST Consortium ([34]Konacki et al., 2019). It is dedicated to monitoring both active and inactive satellites, discarded debris orbiting the Earth. Responsibility for the research and development in SLR in the project, in which Poland is an official member of the EUSST Consortium, and the SRC PAS is one of the members of the Polish SST consortium, is entrusted to the team of the BORL station. A second independent optical-laser system, dedicated to the SST programme also operates at the BORL station ([39]Krynski and Rogowski, 2019; [68]Suchodolski, 2019). The results of computation of coordinates of the BORL station based on LAGEOS measurements performed by the ILRS network in the years 2016–2019 which was one of the most important scientific achievements of the station team in 2020, confirm the high quality of data provided by the BORL station.

One of the most important scientific achievements in 2021 was the determination of the BORL station coordinates from laser observations of LARES as well as LAGEOS-1 and LAGEOS-2 satellites, to intercompare them and to assess their quality. The coordinates of 17 selected stations were computed the for weekly arcs from 29 February 2012 to 31 December 2015 with the use of the NASA GSFC GEODYN-II software. In the first stage, the coordinates were calculated only from the observations of the LARES satellite, in the second stage – only from LAGEOS-1 and LAGEOS-2 satellites, and in the third stage – of all three satellites LARES + LAGEOS-1 + LAGEOS-2. The results from the 1st stage (LARES only) indicate significant errors in stations' coordinates, mainly due to the low satellite orbit (1450 km) and large distances between stations (continental effect). The average 3DRMS of the positions of all stations was 23.5 mm with the uncertainty of ±6.5 mm. In the 2nd stage (LAGEOS only) the results were significantly better and amounted to 9.9 mm ±3.6 mm, respectively. The 3rd stage (LARES + LAGEOS) provided the best results; the mean RMS of 9.9 mm with the uncertainty of ±3.2 mm (Fig. 4). It has been concluded that the solution from three satellites (LARES + LAGEOS-1 + LAGEOS-2) gives slightly better results for determining the coordinates of SLR stations and should be taken into account in subsequent realizations of ITRF ([62]Schillak et al., 2021).

Accepted Article

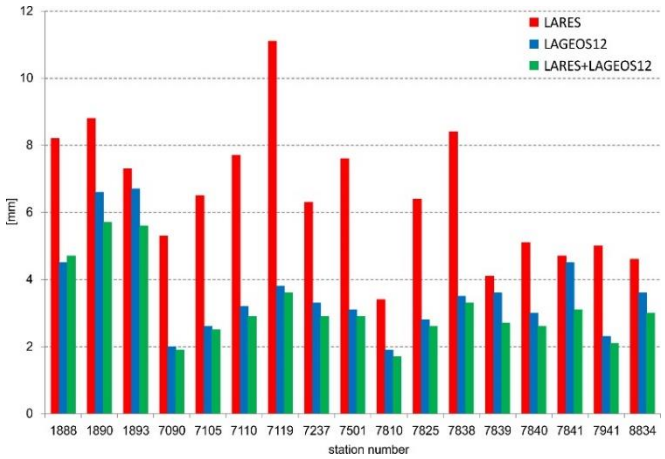

Fig. 4. The average 3D precision for each station for three solutions: LARES only (red), LAGEOS-1+LAGEOS-2 (blue), LARES+LAGEOS-1+LAGEOS-2 (green) ([62]Schillak et al., 2021)

Coordinates of the BORL station determined as both geocentric and topocentric ones for the period July 1993 – December 2019 were analysed and the activity of SLR third generation system was summarized. The BORL station has been providing high-quality observations since the installation of the 3rd generation laser in July 1993. Since then, SLR observations of LAGEOS-1 and LAGEOS-2 satellites – the basic satellites for determining the coordinates of stations – were regularly performed. The station coordinates were determined from 168 monthly orbital arcs with 28 168 normal points using the GSFC NASA GEODYN-II orbital program. 3DRMS stability of the determined positions throughout the period investigated was estimated as 12.7 mm with the uncertainty of ±4.3 mm. A very high level of agreement of the results for both satellites LAGEOS-1 and LAGEOS-2 was observed; for the orbital RMS of fit, i.e. 21.3 mm and 21.0 mm, and for the range bias and its long-term stability -7.3 mm ±11.0 mm and -6.3 mm ±2.4 mm, respectively. Coordinates of BORL determined over the entire 26.5 year period exhibit high consistency with a slight improvement in quality with time (Fig. 5).

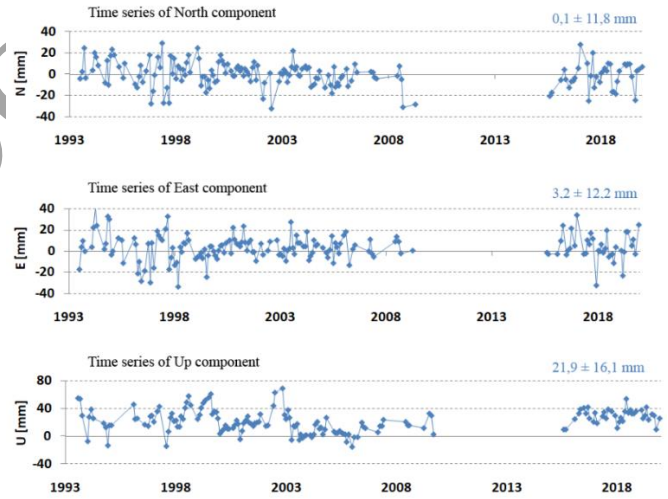

Fig. 5. De-trended for epoch 2010.0 topocentric coordinates N, E, U of BORL station in 1993-2019 ([63]Schillak et al., 2022)

Accepted Article

Only a 2 cm jump in the vertical component was detected at the turn of 2002/2003, caused by a change in the parameters of the constant-fraction discriminator in the "stop" channel. The velocity and direction of the station motion were also assessed. Due to the very long period of 26.5 years, the obtained results for the velocity of the BORL station determined are fully consistent with ITRF2014, 24.9 mm/year and 25.0 mm/year, respectively. The work can be a template for the other SLR stations for assessing the quality of the observations, making it easier to find and correct random and systematic errors ([63]Schillak et al., 2022).
The laser measurements of space debris objects performed by BORL station in the years 2016–2020 have been the subject of a detail analysis. The BORL station is tracking now regularly 80–90 different space debris objects. The sum of all successful passes registered in the years 2016–2020 is 1936 with 23 436 normal points. The average RMS of objects equipped with SLR-dedicated retroreflectors ranges from 1.5 cm to 14 cm, and of objects without such retroreflectors – from 8 cm to 222 cm ([65]Smaglo et al., 2022).
The analysis of the local Love and Shida numbers (h2 and l2 parameters) using SLR measurements to Stella, STARLETTE, LAGEOS-1 and LAGEOS-2 satellites, conducted at the Australian Yarragadee and Mount Stromlo SLR stations from 1 January 2014 to 1 January 2019 was performed ([28]Jagoda et al., 2020b).

6. Active GNSS station networks for the realization of ETRS89 in Poland

ASG-EUPOS – a multifunctional precise satellite positioning system in Poland

The ASG-EUPOS is a GNSS permanent network in Poland which was established in 2008. Stations belonging to the ASG-EUPOS constitute the fundamental geodetic control network which is used for the official realization of the ETRS89 in Poland (Section 3). The ASG-EUPOS is also a multifunctional augmentation system for precise GNSS positioning. The ASG-EUPOS is maintained by GUGiK. Presently, the ASG-EUPOS network consists of 129 GNSS permanent GNSS reference stations of which 107 are located in Poland, and 22 – in neighbouring countries near the Polish border (Fig. 6). In December 2022 GUGiK has signed the agreement with the State Service of Ukraine for Geodesy, Cartography and Cadastre to include Ukrainian stations located near the Polish-Ukrainian border to the ASG-EUPOS system (GUGiK, 2023).

Accepted Article

Fig. 6. Reference stations of the ASG-EUPOS system (as of February 2023, www.asgeupos.pl)

In 2021 the densification of the reference network has been undertaken to increase availability and accuracy of real time services. In 2022, 4 new reference stations were installed, and in 2023 the additional 14 new reference stations will be established.
In the years 2017–2019, the ASG-EUPOS system was upgraded and since then the provided services are based on 4 GNSS constellations: GPS, GLONASS, Galileo, and BeiDou. Presently, all reference stations operating within the ASG-EUPOS network are tracking all 4 GNSS constellations. However, since GNSS receivers installed on 43 stations do not track the BeiDou-3 satellites, it is planned to replace them in the years 2024–2025, so that all receivers in the ASG-EUPOS network could track all available signals from 4 GNSS constellations ([24]GUGiK, 2023). Since 2021, the GNSS data from ASG-EUPOS stations are stored in RINEX 3 format.
In cooperation with MUT, GUGiK participates in the EPN Densification project[12] ([30]Kenyeres et al., 2019). The purpose of that project is to realize a dense, homogeneous, and high quality position and velocity product for Europe. Within the project, GUGiK regularly provides the GNSS solutions of the ASG-EUPOS network which are included in the successive releases of the densification product.

7. Maintenance of the vertical control network in Poland

In 2014 the PL-EVRF2007-NH was adopted as the official reference frame for the Polish fundamental vertical network. The implementation of the PL-EVRF2007-NH by local authorities for the detailed vertical network is still in progress. In accordance with Polish regulations, the EVRF2007 reference frame is to be implemented locally by the end of 2023. Currently (March 2023) over 80% of the local units have completed the implementation ([24]GUGiK, 2023). Also the new quasigeoid model (PL-GEOID2021-NH) for the PL-EVRF2007-NH was developed by UPWr and published in 2022 on the GUGiK website.
Activities related to the new levelling campaign in Poland have been initiated by GUGiK in 2020. GNSS/levelling surveys were performed in 2021 for more than 100 UELN benchmarks. In 2022 GUGiK has completed the designing works of the levelling campaign for about 25% area of Poland. The designing works for the remaining part of Poland are planned to be done in 2023.
Data provided by geodetic space techniques, i.e. GNSS and gravity field dedicated satellite missions to, allow to monitor temporal variations of the reference surface for heights caused by temporal variations of the gravity field due to mass displacements in the Earth system. An extensive research on monitoring, assessing, and modelling mass variations in the Earth system was conducted at IGiK.
Temporal variations of orthometric/normal heights induced by hydrological mass variations over 24 large river basins over the world were assessed by the team of IGiK using GRACE-based GGMs (Godah et al., 2020a). They exhibit a distinctive seasonal pattern. Correlation between them and temporal variations of equivalent water thickness ΔEWT obtained from the WGHM hydrological model were observed in 88% of subareas of river basins investigated, exhibiting strong correlation in 48% of them. It was also shown that the amplitudes of orthometric/normal heights variations in large river basins investigated significantly differ from each other, e.g. 8 cm over the Amazon river basin, and 2 cm for the Orange river basin. In many

[12] http://www.epncb.oma.be/_densification/

Accepted Article

cases hydrological mass changes patterns substantially differ among subareas of the same large river basin, what results in significant differences between the variations of orthometric/normal heights at those subareas. For example, at the Congo river basin they even exceed a triple amplitude of the average of variations of orthometric/normal heights over the entire river basin.
Inter-annual hydrology-induced crustal deformations in Europe were investigated by the team of MUT using RL06 GRACE-based GGMs and WGHM and GLDAS hydrological models ([52]Lenczuk et al., 2020). The strength of the deformation signal from three data sources was found not uniform. The largest long-term non-linear variations in surface deformation time series from all three datasets were observed at the eastern part of Europe; the further from the Atlantic Ocean the larger. Correlation between precipitation and an uplift was discussed and the contribution of GRACE mission to hydrology-induced crustal deformations was highlighted.
Vertical deformations of the Earth's surface determined using GRACE-based GGMs and GNSS data were investigated in terms of EWT variations in Southeastern Poland ([19]Godah et al., 2019; [21]2020b). The authors confirmed that GNSS data can provide information valuable for the determination of ΔEWT. They also showed that the combination of ΔEWT obtained from GNSS and GRACE data fits better to ΔEWT obtained from WGHM hydrological model than ΔEWT obtained from GRACE data only. Vertical deformations of the Earth's surface determined using GRACE-based GGMs compared with those from GNSS data show the local temporal mass variation signal which can be sensed by GNSS observations but not by GRACE data ([21]Godah et al., 2020b).
The use of national GNSS CORS networks for the determination of temporal mass variations within the Earth system as well as for improving GRACE/GRACE-FO solutions was investigated. The case for Poland with the ASG-EUPOS CORS network was considered ([22]Godah et al., 2020c). Temporal variations of EWT as well as vertical deformations of the Earth's surface were determined at the stations of the ASG-EUPOS network. ΔEWT solutions from GNSS data were combined with the corresponding ones from GRACE data. Strong correlations (correlation coefficients from 0.6 to 0.9) between detrended vertical deformations of the Earth's surface determined from GRACE/GRACE-FO data and the corresponding ones from GNSS data were observed at 93% of GNSS stations investigated. It was shown that the temporal mass variations determined from GNSS data from CORS network stations provide valuable information to complement those obtained from GRACE data.
The dynamics of physical heights and their use for the determination of accurate orthometric/normal heights were further extensively investigated. Temporal variations of orthometric/normal heights over Poland obtained using GRACE data reach up to 23 mm. It was shown that they can be modelled with 1 mm accuracy, and predicted with the accuracy of ca. 1–2 mm ([23]Godah et al., 2021). Those variations in Central Europe were assessed at the level of 23 mm, and in Turkey – 25 mm ([69]Szelachowska et al., 2022a). The authors showed that having geoid/quasigeoid obtained from local gravimetric geoid/quasigeoid model or dedicated gravity satellite missions with 1 cm accuracy, one could determine the height with GNSS levelling with the accuracy of a few centimetres using PPP solution, and the accuracy of a few millimetres using double-differencing.
As a continuation of a previous study a contribution of GRACE data to the determination of precise levelling corrected for their dynamics was investigated at the territory of Poland as a test area ([70]Szelachowska et al., 2022b). The new approach of determining such heights was proposed. First, height variations were obtained using Release 6 GRACE-based GGMs and Love numbers from the preliminary reference Earth model. Then they were modelled and predicted using the Seasonal Decomposition Method. It was shown that the major part of the

Accepted Article

signal, i.e., ca. 66% of variations of orthometric/normal heights results from the variation of the ellipsoidal height, while its remaining part is due to the variation of geoid/quasigeoid height. The research conducted indicate the importance of the knowledge of the dynamics of physical heights for the determination of reliable orthometric/normal heights, which are still considered static over the majority of the Earth land areas ([20]Godah et al., 2020a; [70]Szelachowska et al., 2022b). It is fundamental for precise levelling to fulfil the contemporary geodetic scientific and applications purposes ([23]Godah et al., 2021; [69]Szelachowska et al., 2022a). It was shown that monitoring variations of orthometric/normal heights can significantly mitigate artifacts and aliasing of repeated levelling measurements ([70]Szelachowska et al., 2022b).
The determination of vertical land movements is important to investigate the factors affecting the sea level change on a sea coast. The sensitivity of satellite altimetry, tide gauge and GNSS observations to changes in vertical displacements was investigated in the area of the Adriatic Sea coast by the team of UWM in cooperation with Riga Technical University (Pajak et al., 2021). The results obtained show highly coherent regional patterns of sea level change on both Italian and Croatian costs simultaneously indicating land subsidence on both coasts of Croatia and Italy, and the rise of sea level. The authors suggested more pronounced geophysical processes in the area investigated in the last decades. Changes in mean sea level on the Polish coast of the Baltic sea derived from tide gauge data from the years 1811–2015 were investigated using several statistical methods ([35]Kowalczyk, 2019). It was shown that the use of Fourier function with the moving average window of 19 years which corresponds to the 18.6 years nutation cycle provides best fitting linear trend. A gradual, slight increase in the mean sea level ranging from +0.8 mm/y to +2.4 mm/y was observed for tide gauge stations considered.

8. Maintenance and modernization of the International Terrestrial Gravity Reference Frame

Maintenance and modernization of national gravity control as well as implementation of developments in gravimetry within the IAG, are a continuous and ongoing subject of activities in Poland. The team of IGiK continued, the initiated in 2018, modernization of national gravity control of the Republic of Ireland and Northern Ireland, performing the absolute gravity survey with the use of the A10-020 gravimeter. The gravity system in Sweden (the RG2000) established in cooperation with Polish researchers was finalized and published. Gravity control in Poland went through a maintenance and review process in 2022 in order to evaluate its current condition. The development of the International Terrestrial Gravity Reference System/Frame (ITGRS/F) was implemented at the Borowa Gora Observatory of IGiK to make it fully suitable as a reference station of ITGRS. In addition to two absolute gravimeters: A10-020 (IGiK), and FG5-230 (WUT), operating in Poland, IGiK acquired in 2021 the Absolute Quantum Gravimeter (AQG sn B07) manufactured by iXblue, providing new capabilities for modernization and maintenance of gravity reference frames.

8.1. Maintenance and modernization of the gravity control network in Poland

Within the period of 2019–2022 no dedicated gravity survey was conducted on both fundamental stations (located indoors) and base stations (located outdoors) of the national gravity control in Poland. In 2022 the gravity control in Poland underwent a thorough review and maintenance ordered by GUGiK and performed by the team of WUT. As a result 6 fundamental stations and 8 base stations were found destroyed (and/or no longer available for survey) and their replacement locations have been selected. The establishment of replaced

Accepted Article

stations is planned by GUGiK for early 2023 while the re-measurement of the fundamental gravity stations for 2023, and base gravity stations for the years 2024–2025.
Independently, the team of IGiK performed repeated absolute gravity measurements at selected fundamental and base stations of the Polish gravity control as part of other activities, such as EPOS-PL project (4 base stations in the Upper Silesia region), EPOS-PL+ project (fundamental station at Borowiec Observatory of SRC PAS), and regular activities of IGiK (fundamental stations at the Central Gravimetric Calibration Baseline). These additional surveys will be helpful in long term evaluation of the stability of the gravity control in Poland. They are described in more detail in [48]Krynski et al. (2023).

8.2. Implementation of the International Terrestrial Gravity Reference System/Frame in Poland

Resolution 4 on "Establishment of the Infrastructure for the International Gravity Reference Frame" of the IAG, adopted at the XXVII IUGG 2019 General Assembly[13], 2019), encourages national institutions to establish absolute gravity stations with regular gravity observations on them. In accordance to IGRS 2020 Conventions ([71]Wziontek et al., 2021), the so called "reference stations" would serve as basic realization of ITGRF. At such stations, "gravity reference function" is strongly suggested to be established to maintain continuous gravity record with a superconducting gravimeter supplemented with periodic gravity measurements with absolute gravimeters (at least every 2 months, 6 times per year). Those absolute gravimeters are supposed to participate in international comparisons of absolute gravimeters in order to assure traceability to the internationally established gravity reference value.
Within the period of 2019–2022 IGiK focused on building up and preparing the Borowa Gora (BG) Observatory infrastructure to become a reference station of ITGRF. Since 2016 the iGrav-027 superconducting gravimeter was running continuously at BG Observatory. Simultaneously, regular monthly gravity measurements with the A10-020 gravimeter (operated since 2008) were performed along with several gravity comparison campaigns with the FG5-230 gravimeter (owned by WUT). Starting from late 2021, regular gravity measurements at BG Observatory have also be conducted with the AQG-B07 quantum gravimeter.
Within the last seven years, the A10-020 gravimeter participated in 3 significant absolute gravimeter comparisons: Belval in 2015, Wettzell in 2018 ([17]Falk et al., 2020), and Onsala in 2022. Results from 2015 and 2018 absolute gravimeter comparison campaigns were used for combining of iGrav-027 and A10-020 results to establish the gravity reference function and evaluate the drift rate of the iGrav instrument ([13]Dykowski et al., 2019c) (Fig. 7).

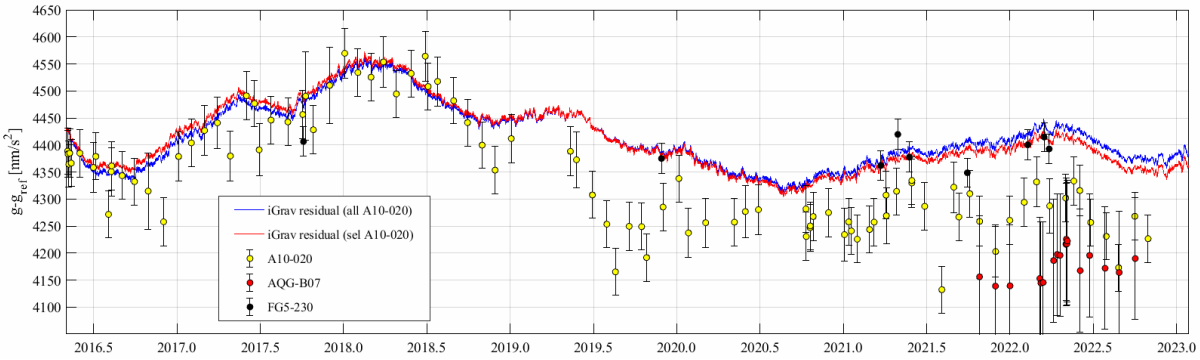

[13]https://iag-aig.org/doc/GH2020/209_IAG%20Resolutions.pdf

Accepted Article

Fig. 7. Gravity reference function at BG Observatory with gravity surveyed with the A10-020, AQG-B07, and FG5-230 gravimeters; g_{ref} = 9 812 500 000 nm/s^2 ([13]Dykowski et al., 2019c)

Up to early 2019 results obtained with the A10-020 gravimeter agree with those from the iGrav-027, i.e. both are referenced to the international gravity reference level. Linear drift of the iGrav-027 in the period 2016–2019 was estimated for 2 variants: 1) with the use of all available surveys with the A10-020 gravimeter (var. A – +4.9 nm/s2/year), and 2) selected (within single Total Uncertainty (T.U.) to iGrav-027 results) A10-020 gravity surveys (var B – -1.1 nm/s2/year). The gravity reference function realized by the iGrav-027 gravimeter (Fig. 7) is also presented in two versions of drift estimates: 1) reduced for var. A (Fig. 7 – blue curve), and 2) var. B (Fig. 7 – red curve). To constrain the gravity reference function at the BG Observatory from 2019 until 2022, another comparison campaign of absolute gravimeters is required. In June 2022 all three instruments, i.e. FG5-230 (owned by WUT), and A10-020 and AQG-B07 (owned by IGiK), participated in the NKG-CAG2022 comparison campaign organized by the Nordic Geodetic Commission in the Onsala Space Observatory in Sweden. Results from that comparison are not yet available at the time of this publication what makes impossible a complete evaluation of the gravity reference function.
Starting from mid-2019 (Fig. 7) offsets for none of the absolute gravimeters are included and only approximate estimates can be made as to the systematic effects of the instruments. At this level of analysis the approximate offsets within the period of 2019–2022 are within single tens of nm/s2 for the FG5-230, -100 nm/s2 for the A10-020 and -200 nm/s2 for the AQG-B07. For the A10-020 gravimeter this is an expected level based on the instrument performance before 2019. For the AQG-B07 during 2022 both systematic effects as well as uncertainty budget were still under evaluation.
Maintaining a gravity reference function proved to be especially important in this period because of the Covid-19 pandemic, which effectively reduced the possibility to perform international absolute gravimeter comparisons. Evaluated offsets from the gravity reference function at BG Observatory were and will be used in all gravity activities carried out by IGiK, therefore disseminating the international gravity reference level.

8.3. Modernization of gravity control in Sweden

No new measurements were conducted by Polish teams in the years 2019–2022. Final results of the RG 2000 establishment and adjustment were completed and published in 2019 ([16]Engfeldt et al., 2019).

8.4. Establishment of gravity control in the Republic of Ireland and Northern Ireland

The team of IGiK, in cooperation with the Ordnance Survey Ireland (Republic of Ireland) and Ordnance Survey of Northern Ireland (Northern Ireland) established the national gravity control on the Ireland island (both Republic of Ireland and Northern Ireland). The work was initiated in mid-2018 following a design approved by both OSI and OSNI. The main concept of the new gravity control in Ireland (Absolute Gravity Network – AGN) assumes that the gravity at all its stations, homogenously distributed over the island of Ireland (selected after extensive studies and field reconnaissance) are determined with the use of the A10-type absolute gravimeter ([11]Dykowski et al., 2019a; [12]2019b). For all stations vertical gravity gradients were also determined with a set of two LaCoste&Romberg (LCR) gravimeters.
AGN Ireland consists of 57 stations of which more than 20 stations are co-located with permanent GNSS stations of the active GNSS network for the island of Ireland (Fig. 8). A number of 51 AGN Ireland stations, so-called Network Stations are located outdoors, typically

Accepted Article

on bedrock or church steps. Six AGN Ireland stations located indoors (confirmed solid concrete), forming the traverse running meridionally, were designed specifically to serve as a gravimetric calibration baseline. Additionally seven gravity stations were identified as stations of the previous most recent reference network established in late 1960s, recognised as World Relative Gravity Reference Network (WRGRN) stations ([39]Krynski and Rogowski, 2019).

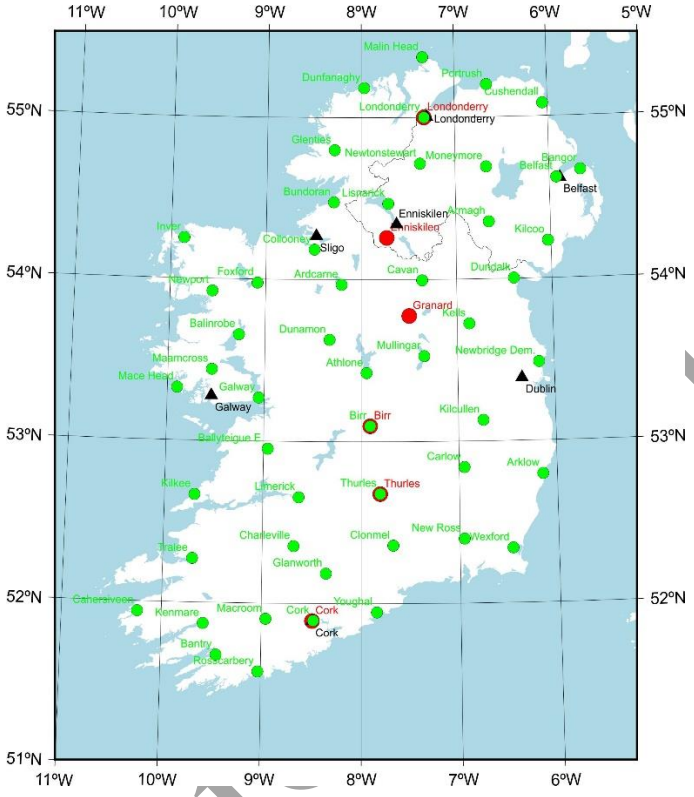

Fig. 8. The Absolute Gravity Network in Ireland: Network Stations (green circles), gravimetric calibration baseline stations (red circles), WRGRN stations (black triangles) ([39]Krynski and Rogowski, 2019)

Gravity survey at the stations of a new gravity control in Ireland, disrupted by Covid-19 pandemic, was carried out in three campaigns: September 2018, August/September 2019, and June/August 2021. At the AGN stations gravity was surveyed with the A10-020 absolute gravimeter ([41]Krynski et al., 2019a; [42]2019b), and the vertical gravity gradient was determined using two LCR gravimeters (G-1012 and G-1036) of IGiK, except 4 WRGRN stations which have been connected to Network Stations with relative gravity survey using also two LaCoste&Romberg gravimeters (G-1012 and G-1036) of IGiK.

For the evaluation of absolute gravity values within the project the following corrections were used with compliance of the recently established IGRS 2020 conventions ([71]Wziontek et al., 2021): gravimetric Earth tides, polar motion, effect of atmospheric mass variations, ocean tidal loading, vertical gravity gradient reduction, self-attraction correction, diffraction correction ([15]Dykowski et al., 2022).

As an important element of the project, the spring gravimeter LCR G-1084 of IGiK with dedicated self-programmed recording system based on a Raspberry Pi device was installed at the OSi headquarters in the Phoenix Park, Dublin, to evaluate the ocean tide model best fitting for the Irish region (following the recommendations of IGRS 2020 Conventions). Raw tidal data was recorded in the period September 2018 – February 2021. For tidal analysis with the ETERNA software (version: et34 x v80 gnusim, [64]Schueller, 2015) ~500 days of best quality

Accepted Article

record was used. In total 29 different ocean tidal models (OTL models obtained from Chalmers Loading Provider M.S. Bos and H-G. Scherneck[14]) were tested in combination with the Tamura body tide model against the adjusted local tidal model. As a result of the study, standard deviations and max-min differences of the residual signal remaining from subtracting the combination of the Tamura tide model with each of the ocean tide models from the local model (result of tidal analysis) were defined as the parameter for selecting the best fit ocean tidal loading model (Fig. 9). Both estimated parameters indicate the CSR4.0 model as the best one for Ireland ([14]Dykowski et al., 2021). This model was used in processing all gravimetric measurements made in Ireland.

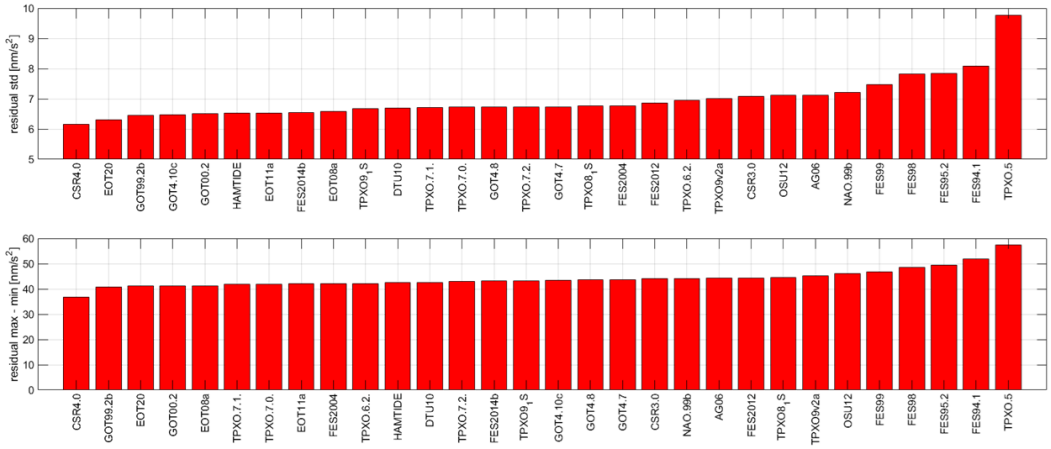

Fig. 9. The results of the analysis determining the most suitable tidal model for Ireland ([14]Dykowski et al., 2021)

Positions and heights of the AGN stations were determined during the course of the project by the teams of the Ordnance Survey Ireland and the Ordnance Survey of Northern Ireland. Results from the establishment of AGN Ireland will be tied to the ITGRF gravity reference level.

9. Maintenance of the magnetic control network in Poland

The magnetic control in Poland has been established in 1955 and regularly maintained since then providing data on variability of geomagnetic field over the territory of Poland which allow to determine its actual parameters. It consists of 21 repeat stations (Fig. 10) and is traditionally surveyed with full metrological consistency, and maintained by IGiK, following the rules of the Magnetic Network of Europe (MagNetE) of the International Association of Geomagnetism and Aeronomy of IUGG. The magnetic control is densified by magnetic points, in particular in the areas of strong magnetic anomalies.

Due to quick and irregular variability of the magnetic field of the Earth, three independent components of the intensity vector of the geomagnetic field, i.e. magnetic declination D, magnetic inclination I, and the module of the magnetic intensity vector F are measured roughly every 2–3 years at each repeat magnetic station, starting from 1970. During each survey the benchmarks of repeat stations and their eccentric stations are carefully checked; the actual horizontal gradient of the geomagnetic field at the stations are examined. When necessary, a new location of the benchmark is found and new monumentation of the repeat station is

[14]http://holt.oso.chalmers.se/loading/

Accepted

established, which is followed by the magnetic survey performed using a special procedure to ensure the continuity of observations.

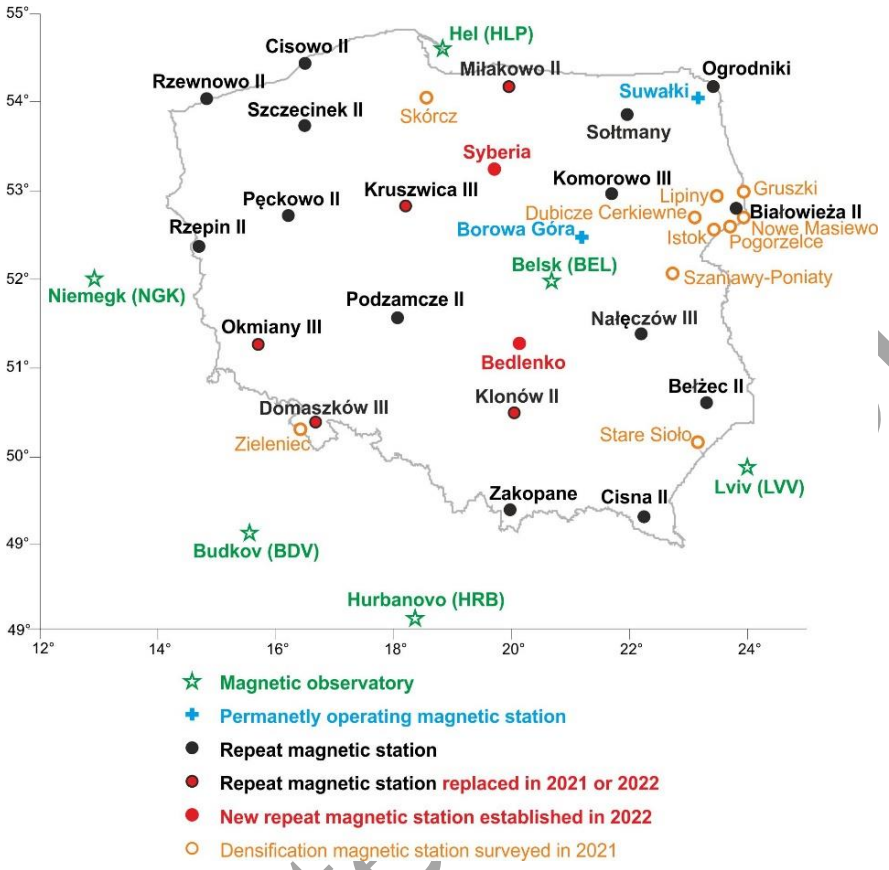

Fig. 10. Polish magnetic repeat station network 2022

Secular variations of the Earth's magnetic field in Poland are determined from repeated survey of the magnetic control as well as using data from the magnetic observatories which operate in the framework of the global international network INETRMAGNET: two Polish magnetic observatories run by the Institute of Geophysics of the Polish Academy of Sciences (IGF PAS): Central Geophysical Observatory in Belsk and Magnetic Observatory in Hel as well as four magnetic observatories of neighbouring countries: Niemegk (Germany), Budkov (Czech Republic), Hurbanovo (Slovakia), and Lviv (Ukraine) (Fig. 10) ([39]Krynski and Rogowski, 2019; [45]2021; [59]Liwosz and Dykowski, 2022). Additional data used to control magnetic surveys in Poland are provided by two permanently operating magnetic stations (Fig. 10): Borowa Gora of IGiK, and Suwalki of IGF PAS.

The *X*, *Y*, *Z* components of the magnetic intensity vector at the magnetic stations are calculated using magnetic declination *D*, magnetic inclination *I* and the module of the magnetic intensity vector *F*, determined at those stations, reduced to the mid-year period using data from magnetic observatories of the INTERMAGNET network. The results of magnetic data processing are regularly submitted to the magnetic database of IGiK and partially to the World Data Centre for Geomagnetism in Edinburgh, UK.

The Polish magnetic repeat station network is regularly maintained and improved following the European standards defined by MagNetE ([39]Krynski and Rogowski, 2019; [45]2021). The list of the Polish magnetic repeat stations surveyed in the years 2019–2022 is given in Table 6. Some magnetic repeat stations were replaced with the new ones and monumented in new locations. In 2021, station Milakowo was replaced by Milakowo II, Klonow – by Klonow

Accepted

II, and Okmiany II – by Okmiany III. In 2022, a complementary design of the fundamental magnetic control addressed the need for new locations of two existing repeat stations: Kruszwica II, and Domaszkow II as well as for the establishment of two new magnetic repeat stations: Bedlenko and Syberia (Fig. 10). In the same year two replaced repeat stations: Kruszwica III, and Domaszkow III as well as two new repeat stations: Bedlenko and Syberia (Fig. 10) were monumented and magnetic declination *D*, magnetic inclination *I* as well as the module of the magnetic intensity vector *F* were measured at those stations.

Table 6. Polish magnetic repeat stations surveyed in the years 2019–2022

No	Station name	2019	2020	2021	2022
1	Cisowo II	-	×	×	-
2	Ogrodniki	×	-	×	-
3	Milakowo II	-	-	×	-
4	Rzewnowo II	-	×	×	-
5	Soltmany	-	-	×	-
6	Szczecinek II	-	×	×	-
7	Komorowo III	×	-	×	-
8	Bialowieza II	×	-	×	-
9	Kruszwica II/ Kruszwica III	-	-	×/-	-/×
10	Peckowo II	×	-	×	-
11	Rzepin II	×	-	×	-
12	Podzamcze II	-	-	×	-
13	Naleczow III	-	×	×	-
14	Okmiany II/Okmiany III	-	-	×/×	-
15	Belzec II	-	-	×	-
16	Klonow/ Klonow II	×/-	-	×/×	-
17	Domaszkow II/ Domaszkow III	-	-	×/-	-/×
18	Zakopane	×	-	×	-
19	Cisna II	-	-	×	-
20	Bedlenko	-	-	-	×
21	Syberia	-	-	-	×

In 2022 an inspection of 14 eccentric stations of the magnetic repeat stations (Fig. 11) was carried out accompanied with the examination of the horizontal gradient of the geomagnetic field in the close vicinity of the stations.

Accepted Article

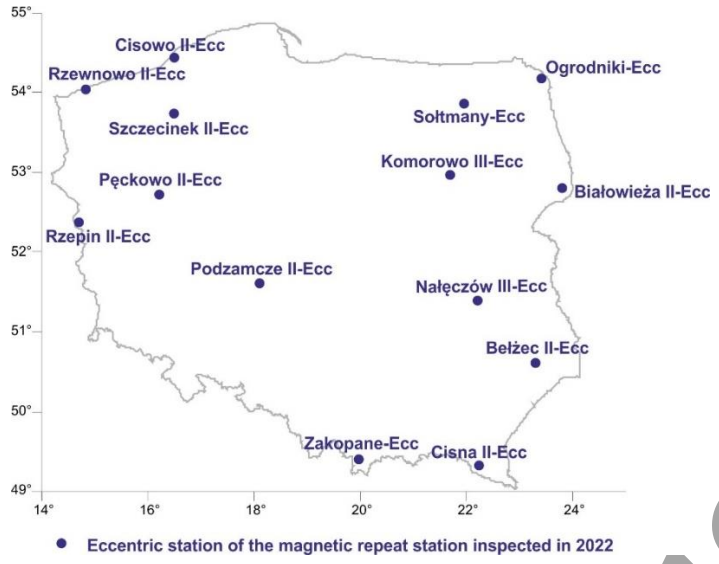

Fig. 11. Eccentric stations of the magnetic repeat stations inspected in 2022

10. Summary and conclusions

The article contains the summary of activities of Polish research and government institutions in the years 2019–2022 in the areas related to the implementation of regional and global reference frames, integration of geodetic, gravimetric and magnetic observations for the realization and maintenance of a unified reference frame and reference networks.

Traditionally the team of IGiK continued in the years 2019–2022 developing the Astronomical Almanac series. The almanacs were in agreement with resolutions of recent General Assemblies of IAU and IUGG. They contain all updates to their previous editions. The development of the on-line version of the Almanac made possible to reduce the printed version of the Almanac as compared with its full version – both available on IGiK web page.

The presently used ETRS89 realization in Poland – PL-ETRF2000, was adopted by GUGiK in 2013. It is based on GPS data collected up to March 2011 at the permanent stations of the ASG-EUPOS network. Since then, GNSS equipment (antenna, receiver) was changed on most ASG-EUPOS network stations which caused coordinate changes on some stations. There were also new stations established, and 14 additional stations are planned to be installed in 2023. To take into account all changes that occurred after the PL-ETRF2000 was developed a new realization of the ETRS89 in Poland is required.

The ASG-EUPOS system established in 2008 operates and is maintained by the GUGiK. Since 2019 the system provides services based on 4 GNSS constellations: GPS, GLONASS, Galileo, and BeiDou. In 2021 the reference network started to be densified to increase availability and accuracy of real time services. In 2022 four new stations were established and 14 additional are planned for 2023. Presently there are 107 permanent GNSS stations of the ASG-EUPOS network. ASG-EUPOS stations together with 22 stations operating in neighbouring countries are the official reference stations for precise positioning in Poland.

Nineteen Polish permanent GNSS stations continued their operational work within the international IAG services: EUREF and IGS (6 of 19 stations). In 2022 two new GNSS stations were installed by WUT at the Polish Polar Station in Hornsund, Norway; both of them were included in the EPN and one in the IGS. The only SLR station in Poland (BORL at Borowiec) continued laser ranging measurements to Earth's satellites and space debris; the number of measured space objects at the BORL station grows each year. These measurements are

Accepted Article

performed within the International SLR Service (ILRS), EUROLAS Consortium, as well as internal contracts signed with the ESA and the European Consortium EUSST.
The research on global terrestrial reference frames and the improvement of the determination of global geodetic parameters (e.g., geocenter and pole coordinates) as well as future ITRFs was conducted by the team of UPWr. For example, the possibility to use new GNSS observations to BeiDou-3 satellites and SLR observations to GNSS and Sentinel-3A/3B satellites and their impact on the estimation of global parameters was analyzed. Also, the common usage of GNSS and SLR-to-GNSS observations in the realization of terrestrial reference frame was investigated. In the proposed approach the co-location between SLR and GNSS techniques took place in space, on board of GNSS satellites. Such co-locations could replace the presently used local ties between stations.
Teams of WUT and MUT continued the activities of the EPN analysis centres and the EPN Analysis Combination Centre (ACC). The impact of adding Galileo observations on EPN combined solutions was analyzed. Also, the preliminary works on adding a number of globally distributed stations to the EPN network were done and its impact on solutions for station positions was analyzed. Recent activities of the ACC included the preparations for the switch to the IGS20 reference frame and new IGS standards in the EPN analysis.
In recent years, the research on receiver antenna calibrations was also conducted in Poland. In 2019, the UWM in cooperation with Astri Polska started a European Space Agency project on developing and implementing a field calibration procedure for a multi-frequency and multi-GNSS. The initial calibrations obtained from independent UWM analysis showed good consistency (at the 2 mm level). Similar consistency was obtained in comparison with the type-mean IGS model. However, it was indicated that some aspects, e.g. the modelling of phase center corrections for low elevations, needs to be further investigated.
The PL-EVRF2007-NH reference frame has been implemented by local authorities for the detailed vertical network in Poland for over 80% of the country. The preparations for the new levelling campaign in Poland started in 2020. In 2022 the designing works were completed for 25% of the Polish territory and the works are going to be continued in 2023.
Geoid height variations as well as vertical displacements of the Earth surface were extensively investigated using GRACE mission data in the context of the realization of a modern vertical reference system in different areas of the world, in particular in Central Europe, including Poland. It was shown that temporal variations of orthometric/normal heights over Poland obtained using GRACE data reach up to 23 mm, that they can be modelled with 1 mm accuracy, and predicted with the accuracy of ca. 1–2 mm. It was also shown that the major part of those variations results from the variation of the ellipsoidal height, while its remaining part is due to the variation of geoid/quasigeoid height.
Advanced research and activities towards the implementation of the International Terrestrial Gravity Reference System/Frame in Poland was conducted. The gravimetric infrastructure of the Borowa Gora (BG) Observatory has been supplemented with the AQG-B07 quantum gravimeter. Metrological activities concerning the gravimetric infrastructure of IGiK are regularly performed and the gravity reference function is regularly maintained. The Observatory has been prepared to become a reference station of ITGRF. The survey of the Absolute Gravity Network in Ireland has been completed. The measurements have been processed applying all state-of-the-art corrections. The long-term record of the spring gravimeter LCR G-1084 of IGiK equipped with the self-programmed recording system, installed at the OSi headquarters in the Phoenix Park, Dublin, was used to evaluate the ocean tide model best fitting for the Irish region.
Magnetic control network in Poland, due to strong variability of the geomagnetic field, needs to be regularly maintained. It is surveyed on regular basis (approximately every two years)

Accepted Article

which ensures that the parameters describing secular variations of magnetic field in Poland are up to date. In the years 2019–2022, 21 magnetic repeat stations and 10 densification stations were surveyed at least once, and 14 eccentric stations of magnetic repeat stations were maintained.

Author contributions

Conceptualization: J.K., T.L.; original draft preparation: J.K., T.L.

Data availability statement

No datasets were used in this research.

Acknowledgements

The paper was elaborated in the framework of the statutory project "Problems of geodesy and geodynamics" of IGiK (financially supported by the Polish Ministry of Education and Science), and within the activities of the Section of Geodesy and Geodynamics of the Committee on Geodesy of the Polish Academy of Sciences. Valuable help was provided by Przemyslaw Dykowski, Anna Ejsmont, Pawel Lejba, Jaroslaw Somla. The authors would like to thank the anonymous reviewers for valuable comments and suggestions to improve the manuscript

References

[1]Araszkiewicz, A., Podkowa, A. and Kiliszek, D. (2019). Height variation depending on the source of antenna phase centre corrections: LEIAR25.R3 case study. *Sensors*, 2019, 19(18), 4010. DOI: 10.3390/s19184010.
[2]Araszkiewicz, A. and Kiliszek, D. (2020). Impact of Using GPS L2 Receiver Antenna Corrections for the Galileo E5a Frequency on Position Estimates. *Sensors*, 20, 5536. DOI: 10.3390/s20195536.
[3]Bogusz, J., Klos, A., and Pokonieczny, K. (2019). Optimal Strategy of a GPS Position Time Series Analysis for Post-Glacial Rebound Investigation in Europe. *Remote* Sens., 11, 1209. DOI: 10.3390/rs11101209.
[4]Borowski, L., Kudrys, J., Kubicki, B. et al. (2022). Phase Centre Corrections of GNSS Antennas and Their Consistency with ATX Catalogues. *Remote Sens.*, 14, 3226. DOI: 10.3390/rs14133226.
[5]Bury, G., Sosnica, K., and Zajdel, R. (2019). Impact of the Atmospheric Non-tidal Pressure Loading on Global Geodetic Parameters Based on Satellite Laser Ranging to GNSS. *IEEE Trans. Geosci. Remote Sens.*, 57(6), 3574-3590. DOI: 10.1109/TGRS.2018.2885845.
[6]Bury, G., Sosnica, K., Zajdel, R. et al. (2021a). Determination of precise Galileo orbits using combined GNSS and SLR observations. *GPS Solut.*, 25, 11. DOI: 10.1007/s10291-020-01045-3.
[7]Bury, G., Sosnica, K., Zajdel, R. et al. (2021b). Geodetic datum realization using SLR-GNSS co-location onboard Galileo and GLONASS. *J. Geophys. Res. Solid Earth*, 126, e2021JB022211. DOI: 10.1029/2021JB022211.

Accepted Article

[8]Dach, R., Lutz, S., Walser, P. et al. (2015). *Bernese GNSS Software Version 5.2*. DOI: 10.7892/boris.72297.
[9]Dawidowicz, K., Rapinski, J., Smieja, M. et al. (2021). Preliminary Results of an Astri/UWM EGNSS Receiver Antenna Calibration Facility. *Sensors*, 21. DOI: 10.3390/s21144639.
[10]Dawidowicz, K., Krzan, G., and Wielgosz, P. (2023). Offsets in the EPN station position time series resulting from antenna/radome changes: PCC type-dependent model analyses. *GPS Solut.*, 27, 9. DOI: 10.1007/s10291-022-01339-8.
[11]Dykowski, P., Kane, P., Krynski, J. et al. (2019a). Towards the establishment of the Absolute Gravity Network Ireland. In: Symposium of the IAG Subcommission for Europe (EUREF), 22–24 May 2019, Tallinn, Estonia.
[12]Dykowski, P., Krynski, J., Sekowski, M. et al. (2019b). Establishment of the Absolute Gravity Network Ireland – first results. In: 5th IAG Symposium on Terrestrial Gravimetry: Static and Mobile Measurements TG-SMM, 1–4 October 2019, St. Petersburg, Russia.
[13]Dykowski, P., Krynski, J. and Sekowski, M. (2019c). A 3 year-long AG/SG gravity time series at Borowa Gora Geodetic Geodetic-Geophysical Observatory. In: 27th IUGG General Assembly 2019, 8–18 July 2019, Montreal, Canada.
[14]Dykowski, P., Karkowska, K., Sekowski, M. et al. (2021). Ocean tidal loading models assessment using 28 months of gravimetric tidal records in Dublin, Ireland. In: EGU General Assembly 2021, 19–30 April 2021, Vienna, Austria.
[15]Dykowski, P., Krynski, J., Sekowski, M. et al. (2022). Establishment of a modern gravity control in Ireland. In: IGRF2022 Workshop, 11–13 April 2022, Leipzig, Germany.
[16]Engfeldt, A., Lidberg, M., Sekowski, M. et al. (2019). RG 2000 – the new gravity reference frame of Sweden. *Geophys.*, 54(1), 69–92.
[17]Falk, R., Pálinkáš, V., Wziontek, H. et al. (2020). Final report of EURAMET.M.G-K3 regional comparison of absolute gravimeters. *Metrologia*, 57, 1A. DOI: 10.1088/0026-1394/57/1A/07019.
[18]Fernandes, R., Bruyninx, C., Crocker, P. et al. (2022). A new European service to share GNSS Data and Products. *Ann. Geophys.*, 65, 3, DM317,2022. DOI:10.4401/ag-8776.
[19]Godah, W., Szelachowska, M., Ray, J.D. et al. (2019). A model of temporal mass variations within the Earth system developed using GRACE and GNSS data. In: 27 IUGG General Assembly 2019, 8–18 July 2019, Montreal, Canada.
[20]Godah, W., Szelachowska, M., Krynski, J. et al. (2020a). Assessment of temporal variations of ortho-metric/normal heights induced by hydrological mass variations over large river basins using GRACE mission data. *Remote Sens.*, 12(18), 3070. DOI:10.3390/rs12183070.
[21]Godah, W., Szelachowska, M., Ray, J.D. et al. (2020b). Comparison of vertical deformations of the Earth's surface obtained using GRACE-based GGMs and GNSS data – A case study of South-Eastern Po-land. *Acta Geodyn. et Geomater.*, 17, 2(198), 169–176. DOI: 10.13168/AGG.2020.0012.
[22]Godah, W., Ray, J.D., Szelachowska, M. et al. (2020c). The use of national GNSS CORS networks for the determination of temporal mass variations within the Earth's system as well as for improving GRACE/GRACE-FO solutions – a case study of Poland. *Remote Sens.*, 12(20), 3359. DOI: 10.3390/rs12203359.
[23]Godah, W., Szelachowska, M., and Krynski, J. (2021). On the dynamics of physical heights and their use for the determination of accurate orthometric/normal heights. In: EGU General Assembly 2021, 19–30 April, Vienna, Austria.
[24]GUGiK (2023). GUGiK Bulletin No 4 – March 2023 (in Polish). https://www.gov.pl/web/gugik/wydanie-4---marzec-2023.

Accepted Article

[25]Jagoda, M., and Rutkowska, M. (2020a). Use of VLBI measurement technique to determination of the tectonic plates motion parameters. *Metrology and Measurements Systems*, 27(1), 151-165. DOI: 10.24425/mms.2020.131722.
[26]Jagoda, M., and Rutkowska, M. (2020b). An Analysis of the Eurasian Tectonic Plate Motion Parameters Based on GNSS Stations Positions in ITRF2014. *Sensors*, 20(21), 6065. DOI: 10.3390/s20216065.
[27]Jagoda, M., Rutkowska, M., Suchocki, C. et al. (2020a). Determination of the tectonic plates motion parameters based on SLR, DORIS and VLBI stations positions. *J. Appl. Geod.*, 14(2), 121-131. DOI: 10.1515/jag-2019-0053.
[28]Jagoda, M., Rutkowska, M., Lejba, P. et al. (2020b). Satellite Laser Ranging for Retrieval of the Local Values of the Love h2 and Shida l2 Numbers for the Australian ILRS Stations. *Sensors*, 20(23), 6851. DOI: 10.3390/s20236851.
[29]Kaczmarek, A. (2019). Influence of Geophysical Signals on Coordinate Variations GNSS Permanent Stations in Central Europe. *Artificial Satellites, Journal of Planetary Geodesy*, 54(3), 57-71. DOI: 10.2478/arsa-2019-0006.
[30]Kenyeres, A., Bellet, J.G., Bruyninx, C. et al. (2019). Regional integration of long-term national dense GNSS network solutions. *GPS Solut.*, 23, 122. DOI: 10.1007/s10291-019-0902-7.
[31]Klos, A., Bos, M.S., Fernandes, R.M.S. et al. (2019a). Noise-Dependent Adaption of the Wiener Filter for the GPS Position Time Series. *Math. Geosci.*, 51, 53-73. DOI: 10.1007/s11004-018-9760-z.
[32]Klos, A., Kusche, J., Fenoglio-Marc, L., Bos, M.S., Bogusz, J. (2019b). Introducing a vertical land motion model for improving estimates of sea level rates derived from tide gauge records affected by earthquakes. GPS Solut 23, 102 (2019). https://doi.org/10.1007/s10291-019-0896-1.
[33]Klos, A., Dobslaw, H., Dill, R. and Bogusz, J. (2021). Identifying the sensitivity of GPS to non-tidal loadings at various time resolutions: examining vertical displacements from continental Eurasia. *GPS Solut.*, 25, 89. DOI: 10.1007/s10291-021-01135-w.
[34]Konacki, M., Malacz, A., Chimicz, A. et al. (2019). Optical, Laser and Processing Capabilities of the New Polish Space Situational Awareness Centre. In: Advanced Maui Optical and Space Surveillance Technologies Conference (AMOS), 17–20 September.
[35]Kowalczyk, K. (2019). Changes in mean sea level on the Polish coast of the Baltic sea based on tide gauge data from the years 1811–2015. *Acta Geodyn. et Geomater.*, 16(2), 194. DOI: 10.13168/AGG.2019.0016.
[36]Kowalczyk, K., Kowalczyk, A.M., and Chojka, A. (2020). Modeling of the vertical movements of the Earth's crust in Poland with the co-kriging method based on various sources of data. *Appl. Sci.*, 10, 9. DOI: 10.3390/app10093004.
[37]Kowalczyk, K., Kowalczyk, A.M., and Rapinski, J. (2021a). Identification of common points in hybrid geodetic networks to determine vertical movements of the Earth's crust. *J. Appl. Geod.*, 15(2). DOI: 10.1515/jag-2021-0002.
[38]Kowalczyk, K., Pajak, K., Wieczorek, B. et al. (2021b). An Analysis of Vertical Crustal Movements along the European Coast from Satellite Altimetry, Tide Gauge, GNSS and Radar Interferometry. *Remote Sens.*, 13, 2173. DOI: 10.3390/rs13112173.
[39]Krynski, J., and Rogowski, J.B. (2019). National Report of Poland to EUREF 2019. In: Symposium of the IAG Subcommission for Europe (EUREF), 22–24 May 2019, Tallinn, Estonia.
[40]Krynski, J., and Sekowski, M. (2019). *Rocznik Astronomiczny na rok 2020*. Instytut Geodezji i Kartografii, Warszawa, http://www.igik.edu.pl/pl/a/Rocznik-Astronomiczny-2020.

Accepted Article

[41]Krynski, J., Rogowski, J.B., and Liwosz, T. (2019a). Research on reference frames and reference networks in Poland in 2015-2018. *Geod. Cartogr.*, 68(1). DOI: 10.24425/gac.2019.126093.
[42]Krynski, J., Dykowski, P., and Olszak, T. (2019b). Research on gravity field modelling and gravimetry in Poland in 2015-2018. *Geod. Cartogr.*, 68(1). DOI: 10.24425/gac.2019.126094.
[43]Krynski, J., Olszewska, D., Gorka-Kostrubiec, B. et al. (2019c). EPOS PL Polish national infrastructure fulfilling European Plate Observing System goals. In: 27th IUGG General Assembly 2019, 08–18 July 2019, Montreal, Canada.
[44]Krynski, J., and Sekowski, M. (2020). *Rocznik Astronomiczny na rok 2021*. Instytut Geodezji i Kartografii, Warszawa, http://www.igik.edu.pl/pl/a/Rocznik-Astronomiczny-2021.
[45]Krynski, J., and Rogowski, J.B. (2021). National Report of Poland to EUREF 2019-2020. In: Symposium of the IAG Subcommission for Europe (EUREF), 26–28 May 2021, Ljubliana, Slovenia.
[46]Krynski, J., and Sekowski, M. (2021). *Rocznik Astronomiczny na rok 2022*. Instytut Geodezji i Kartografii, Warszawa, http://www.igik.edu.pl/pl/a/Rocznik-Astronomiczny-2022.
[47]Krynski, J., and Sekowski, M. (2022). *Rocznik Astronomiczny na rok 2023*. Instytut Geodezji i Kartografii, Warszawa, http://www.igik.edu.pl/pl/a/Rocznik-Astronomiczny-2023.
[48]Krynski, J., Dykowski, P., Godah, W. et al. (2023). Research on gravity field modelling and gravimetry in Poland in 2019-2022. *Adv. Geod. Geoinf.*, 72(2), e46. DOI: 10.24425/agg.2023.146158.
[49]Krzan, G., Dawidowicz, K., and Wielgosz, P. (2020). Antenna phase center correction differences from robot and chamber calibrations: the case study LEIAR25. *GPS Solut.*, 24, 44. DOI: 10.1007/s10291-020-0957-5.
[50]Legrand, J. (2022). EPN multi-year position and velocity solution CWWWW. Retrieved 01 March, 2023 from Royal Observatory of Belgium. DOI: 10.24414/ROB-EUREF-CWWWW.
[51]Lejba, P., Suchodolski, T., and Michalek, P. (2020). Laser Ranging to Space Debris in Poland: Tracking and Orbit Determination. In: Proceedings of the Advanced Maui Optical and Space Surveillance Technologies Conference (AMOS), 15–18 September 2020.
[52]Lenczuk, A., Leszczuk, G., Klos, A. et al. (2020). Study on the inter-annual hydrology-induced deformations in Europe using GRACE and hydrological models. *J. Appl. Geod.*, 14(4). DOI: 10.1515/jag-2020-0017.
[53]Liwosz, T., and Ryczywolski, M. (2016). Verification of the Polish geodetic reference frame by means of a new solution based on permanent GNSS data from the years 2011–2014. *Rep. Geod. Geoinf.*, 102. DOI: 10.1515/rgg-2016-0027.
[54]Liwosz, T., and Araszkiewicz, A. (2019a). Report of the EPN Analysis Centres Coordinator. Inclusion of Galileo observations in EPN coordinate products. In: Symposium of the IAG Subcommission for Europe (EUREF), 22–24 May 2019, Tallinn, Estonia.
[55]Liwosz, T., and Araszkiewicz, A. (2019b). EPN Analysis Centres Coordinator Report. In: EPN Analysis Center Workshop, 16–17 October 2019, Warsaw, Poland.
[56]Liwosz, T. (2022a). EPN daily and weekly combined position solutions. Warsaw University of Technology, Poland. DOI: 10.17388/WUT-EUREF-CMBPOS.
[57]Liwosz, T. (2022b). Report of EPN Analysis Centres Coordinator: status of EPN coordinate products and preparations for the switch to IGS20. EPN Analysis Centres Workshop, November 3, 2022. http://www.epncb.eu/_newseventslinks/workshops/EPNLACWS_2022/pdf/Liwosz_ACC_report_AC_workshop.pdf.

Accepted Article

[58]Liwosz, T., and Araszkiewicz, A. (2022). Report of the EPN Analysis Centres Coordinator. In: Symposium of the IAG Subcommission for Europe (EUREF), 31 May – 03 June 2022, Zagreb, Croatia.
[59]Liwosz, T., and Dykowski, P. (2022). National Report of Poland to EUREF 2022. In: Symposium of the IAG Sub-commission for Europe (EUREF), 31 May – 03 June 2022, Zagreb, Croatia.
[60]Najder, J. (2020). Automamatic detection of discontinuities in the station position time series of the reprocessed global GNSS network using Bernese GNSS Software. *Acta Geodyn. et Geomater*., 17(4), 439–451. DOI: 10.13168/AGG.2020.0032.
[61]Pajak, K., Kowalczyk, K., Kaminski, J. et al. (2021). Studying the sensitivity of satellite altimetry, tide gauge and GNSS observations to changes in vertical displacements. *Geomatics Environ. Eng.*, 15(4). DOI: 10.7494/geom.2021.15.4.45.
[62]Schillak, S., Lejba, P., and Michalek, P. (2021). Analysis of the Quality of SLR Station Coordinates Determined from Laser Ranging to the LARES Satellite. *Sensors*, 21(3), 737. DOI: 10.3390/s21030737.
[63]Schillak, S., Lejba, P., Michalek, P. et al. (2022). Analysis of the Results of the Borowiec SLR Station (7811) for the period 1993-2019 as an Example of the Quality Assessment of Satellite Laser Ranging Stations. *Sensors*, 22(2), 616. DOI: 10.3390/s22020616.
[64]Schueller, K. (2015). Theoretical basis for Earth Tide analysis with the new ETERNA34-ANA-V4.0 program. *Bull.Inf. Marées Terrestres*, 149, 12024-12061.
[65]Smaglo, A., Lejba, P., Schillak, S. et al. (2021). Measurements to Space Debris in 2016–2020 by Laser Station at Borowiec Poland. *Artificial Satellites, Journal of Planetary Geodesy*, 56(4), 119-134. DOI: 10.2478/arsa-2001-0009.
[66]Sosnica, K., Bury, G., Zajdel, R. et al. (2019). Estimating global geodetic parameters using SLR observations to Galileo, GLONASS, BeiDou, GPS, and QZSS. *Earth Planets Space*, 71(20), 1–11. DOI: 10.1186/s40623-019-1000-3.
[67]Strugarek, D., Sosnica, K., Arnold, D. et al. (2019). Determination of Global Geodetic Parameters Using Satellite Laser Ranging Measurements to Sentinel-3 Satellites. *Remote Sens.*, 11(19), 2282. DOI: 10.3390/rs11192282.
[68]Suchodolski, T. (2019). CBK PAS Borowiec Second Satellite Tracking System. ILRS Technical Workshop in Stuttgart, Germany, 21–25 October. Retrieved from https://cddis.nasa.gov/2019_ Technical_Workshop/Program/index.html.
[69]Szelachowska, M., Godah, W., and Krynski, J. (2022a). On the need of considering temporal variations of or-thometric/normal heights induced by mass transport in the Earth's system for precise levelling. In: NKG Working Groups GEO & FHSG, 14–18 March, Gävle, Sweden.
[70]Szelachowska, M., Godah, W., and Krynski, J. (2022b). Contribution of GRACE satellite mission to the determi-nation of orthometric/normal heights corrected for their dynamics – A case study of Poland. *Remote Sens.*, 14(17), 19. DOI 10.3390/rs14174271.
[71]Wziontek, H., Bonvalot, S., Falk, R. et al. (2021). Status of the International Gravity Reference System and Frame. *J. Geod.* 95, 7. DOI: 10.1007/s00190-020-01438-9.
[72]Zajdel, R., Sosnica, K., Dach, R. et al. (2019a). Network effects and handling of the geocenter motion in multi-GNSS processing. *J. Geophys. Res. Solid Earth*, 124(6), 5970-5989. DOI: 10.1029/2019JB017443.
[73]Zajdel, R., Sosnica, K., Drozdzewski, M. et al. (2019b). Impact of network constraining on the terrestrial reference frame realization based on SLR observations to LAGEOS. *J. Geod.*, 93(11), 2293–2313. DOI: 10.1007/s00190-019-01307-0.
[74]Zajdel, R., Steigenberger, P., and Montenbruck, O. (2022). On the potential contribution of BeiDou-3 to the realization of the terrestrial reference frame scale. *GPS Solut.*, 26(109), 1–18. DOI: 10.1007/s10291-022-01298-0.

Accepted Article

Research on gravity field modelling and gravimetry in Poland in 2019-2022

Jan Krynski*, Przemyslaw Dykowski, Walyeldeen Godah, Malgorzata Szelachowska

Institute of Geodesy and Cartography, Centre of Geodesy and Geodynamics, Warsaw, Poland, *Corresponding author: Jan Krynski, e-mail: krynski@igik.edu.pl

Abstract: The article presents the reviewed and summarised research activities of the Polish research groups on gravimetry and gravity field modelling in the period of 2019–2022. It contains the results of absolute gravity surveys for the maintenance of the international gravity reference level in Poland and Europe, and for geodynamic research with an emphasis on metrological aspects. It also contains relative gravimetry issues as well as the results of marine gravity surveys in the southern Baltic Sea. Non-tidal gravity changes were extensively investigated. Long-term gravity variations were monitored at the Borowa Gora Geodetic-Geophysical Observatory and in a few other locations in Poland. The contribution of gravimetric records to seismic studies was investigated. Temporal variations of the gravity field from GRACE (Gravity Recovery and Climate Experiment) and GRACE-FO (GRACE Follow-On) data, in particular, deformations of the Earth's surface as well as temporal variations of heights, total water storage and groundwater storage were investigated. Moreover, GRACE-based products and the performance of monthly Global Geopotential Models (GGMs) were a subject of research. GGMs developed in last years were evaluated. The research on developing new approaches in geoid modelling and their validation was conducted. New regional and local geoid models were determined for Poland and Ethiopia. The use of different techniques for estimating the absolute sea level at sites of the selected network in the Baltic Sea was investigated.

Keywords: geoid, gravity field, absolute gravity measurements, gravimetry, GRACE/GRACE-FO satellite missions

Accepted Article

1. Introduction

Research activities of the Polish research groups in the years 2019–2022 in gravimetry and gravity field modelling are a consequent continuation/extension of those from the period of 2015–2018 ([27]Krynski et al., 2019).

The new definition of the International Terrestrial Gravity Reference System/Frame (ITGRS/F) challenges activities related to the maintenance of gravity control ([50]Wziontek et al., 2021), especially at the Borowa Gora Geodetic-Geophysical Observatory (BG) of the Institute of Geodesy and Cartography (IGiK) utilizing the continuous operation of the iGrav-027 superconducting gravimeter. In particular, it concerns gravimetric metrology. Multiple initiatives have been started for periodic absolute gravity surveys with two absolute gravimeters (AGs): the FG5-230 and the A10-020 at several locations in Poland selected for geodynamic monitoring. The capabilities of absolute gravimetry at IGiK have been expanded in late 2021 by the absolute quantum gravimeter AQG-B07 installed at the BG Observatory. All three AGs

This article has been accepted for publication in the journal Advances in Geodesy and Geoinformation, issue 72/2, 2023. It has not yet undergone the process of copyediting, typesetting, pagination and proofreading. This may lead to differences between this version and the final published version. The article may be cited as DOI: 10.24425/agg.2023.146158.

operating in Poland: FG5-230, A10-020, and AQG-B07 participated in 2022 in an absolute gravimeter comparison campaign.
The calibration of gravimeters is necessary to ensure consistency and reliability of gravimetric survey, in particular, to efficiently monitor non-tidal gravity changes. Relative LaCoste&Romberg (LCR) gravimeters of IGiK, calibrated on the gravimetric calibration baseline, were successfully used to calibrate spring gPhoneX tidal gravimeters in Poland within the EPOS-PL (European Plate Observing System - Poland) and EPOS-PL+ (continuation/extension of EPOS-PL) projects. Joint measurements of AGs and the iGrav-027 gravimeter at the BG Observatory allowed for an updated drift evaluation and long term stability assessment providing an insight into long term gravity variations at the Observatory.
The combination of tidal gravimetric and seismic records provides promising material for advance seismic studies. Detail analysis showed that the stability of tidal gravimeters allows deeper insight into Earth structure than the one from standard seismic records.
The products of GRACE (Gravity Recovery and Climate Experiment) and GRACE-FO (GRACE Follow-On) satellite missions provide extremely valuable information for monitoring temporal variations of the Earth's gravity field. These variations can further be interpreted in terms of hydrological mass change (e.g. temporal variations of total water storage and groundwater storage), deformations of the Earth's surface (i.e. ellipsoidal height change) induced by temporal mass loadings, and temporal variations of geoid/quasigeoid heights resulted from gravity change. They are a subject of growing interest among worldwide scientific community in terms of both analysis and software development.
The newly developed Global Geopotential Models (GGMs) require evaluation, before being used for geoid modelling. It is particularly important for quality estimate of modelled geoid. Also new approaches to geoid modelling on regional and local scale are the subject of research of numerous research groups.

2. Gravity measurements

The research in Poland applying gravity survey for geodesy and geodynamics was related in the last years to terrestrial gravity surveys (absolute gravity surveys and tidal gravity records) as well as marine gravity surveys. Within the period of 2019–2022, major developments in recording Earth tides in Poland were observed, up to a large extend due to the involvement in the EPOS-PL and EPOS-PL+ projects ([8]Dykowski et al., 2021a). Majority of repeated gravity surveys with AGs were performed at the BG Observatory. New marine gravity surveys were conducted with a Micro-g Marine Gravity System by the team of the Gdansk University of Technology in the Baltic Sea region in Poland. Research utilizing gravity tidal records for seismic studies was continued by IGiK.

2.1 Absolute gravity surveys

For over a decade, two institutions in Poland: the Warsaw University of Technology (WUT), and IGiK were conducting gravity surveys with AGs: FG5-230, and A10-020, respectively. Both gravimeters were used in various projects in Poland as well as in a number of European countries for the maintenance of gravity control, geodynamic research and metrology. Starting from October 2021, a new AG – the Absolute Quantum Gravimeter (AQG-B07) of IGiK – is used in Poland ([10]Dykowski et al., 2022b; [11]2022c). It is the first commercial type of gravimeter based on a quantum sensor with a variety of applications in the field of geodesy and geophysics ([35]Ménoret et al., 2018). Thus, three AGs are currently operational in Poland allowing to utilize all of them for research in the field of geodesy and geophysics.

Accepted Article

Absolute gravity surveys for the maintenance of the international gravity reference level in Poland and Europe

Current status of the new definition of the ITGRS/F essentially states that AGs now define the system ([50]Wziontek et al., 2021). Within the period of 2019–2022, absolute gravity measurements related to the maintenance of the international gravity reference level were performed with all three AGs in Poland (A10-020, AQG-B07, FG5-230) at the BG Observatory.

In mid-2021, the team of IGiK concluded absolute gravity surveys in the Republic of Ireland and Northern Ireland within the AGN Ireland project related to the establishment of a modern gravity control on the island of Ireland. Aspects of absolute gravity measurements related to the maintenance of the international gravity reference frames for Poland and other European countries with a contribution of Polish teams are discussed in [29]Krynski and Liwosz (2023).

Absolute gravity surveys for geodynamic research

Multiple activities oriented towards quasi-permanent monitoring of gravity changes in Poland were carried out in the years 2019–2022. Three main research and infrastructure projects contributed to activities concerned geodynamical monitoring the EPOS-PL (2017-2021), EPOS-PL+ (2020-2023), and the Monitoring of Geodynamics in Poland (MGP) (started in 2012, AG measurements since 2018).

Within the framework of the EPOS-PL project, the team of IGiK performed a periodic (every 6 months) absolute gravity survey with the A10-020 gravimeter on 10 field stations (Fig. 1 – red dots) of the Multidisciplinary Upper Silesian Episodes (MUSE) polygons, one in a non-active and the other in still active mining areas in the Upper Silesian Region (UPR). Those absolute gravity determinations provided a reliable gravity reference for periodic relative gravity surveys conducted also every 6 months on nearly 200 stations of MUSE (Fig. 1 – black dots) by the Central Mining Institute (GIG). On those nearly 200 stations, precise GNSS (Global Navigation Satellite System) surveys were performed to assess the deformations induced by mining ([7]Dykowski et al., 2019). Measurements were completed by the end of 2021. Results of gravity survey at two stations (also being points of national gravity control PBOG) of the 10 absolute gravity stations for the period of the EPOS-PL project as well as a gravity value from 2012 to 2015 measurements for the realization of the Polish gravity control are presented in Figure 2 ([10]Dykowski et al., 2022a). Variability of gravity changes at Oswiecim station (Fig. 2. – bottom) indicates the need for repeatable periodic gravity measurements for continuous monitoring of the state of the gravity control.

Accepted Article

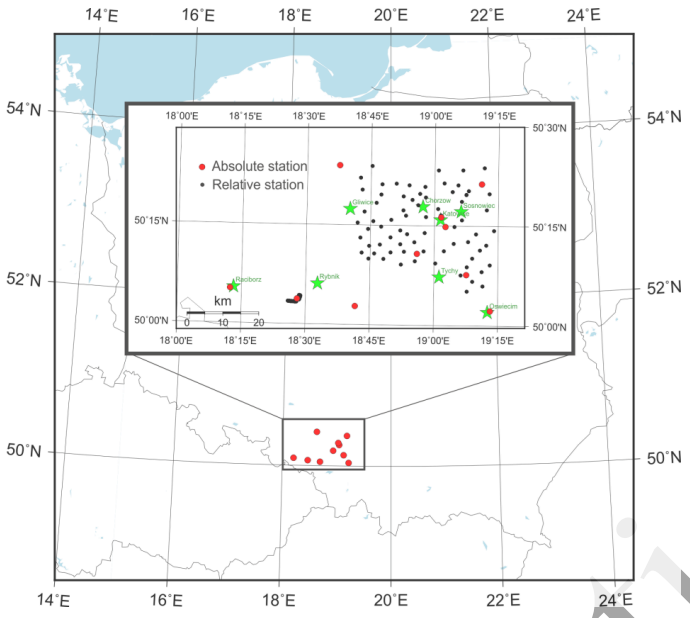

Fig. 1. Gravity stations surveyed within the EPOS-PL project at MUSE polygons

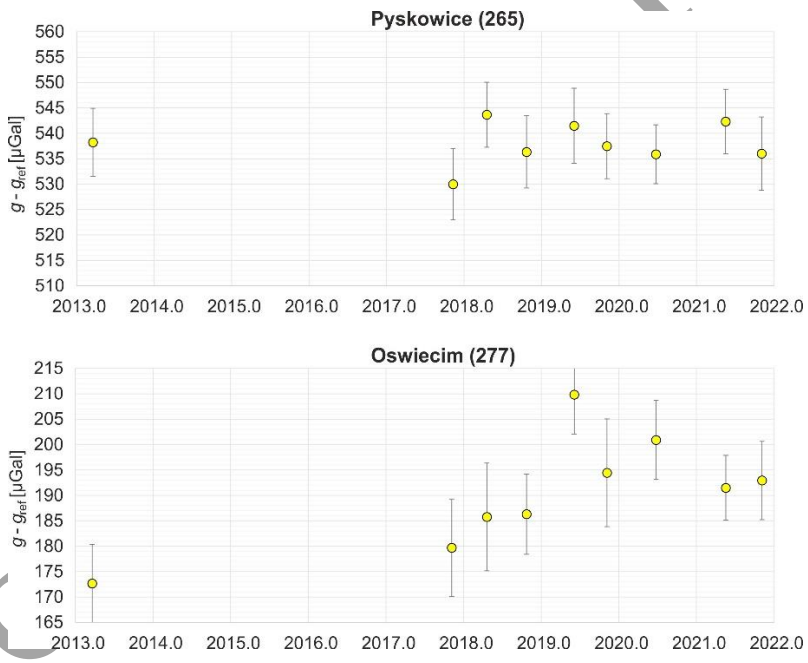

Fig. 2. Absolute gravity measurements conducted within the EPOS-PL project at PBOG stations in Pyskowice (g_{ref} = 981 069 000; top) and Oswiecim (g_{ref} = 981 034 000; bottom); error bars indicate the total uncertainty of gravity value determined with A10-020 gravimeter, reduced to benchmark level, single coverage k = 1, 67%

Repeated absolute gravity measurements are being conducted within the EPOS-PL+ project by the team of IGiK every 6 months for GIG and for the Space Research Centre of the Polish Academy of Sciences (SRC PAS). Gravity surveys for GIG which are carried out on an active exploration site in Marklowice in UPR provide absolute gravity reference for relative gravity measurements at nearly 100 field stations in that area. Gravity surveys for SRC PAS are conducted at the Astrogeodynamic Observatory in Borowiec, mainly with the A10-020, but also with the AQG-B07 gravimeter, to monitor gravity long term supporting tidal records by the gPhoneX-161 gravimeter ([37]Nastula et al., 2022).

Article

Since 2017 the absolute gravity measurements with the FG5-230 gravimeter were performed by WUT at two permanent stations: Dziwie (Wielkopolska Voivodeship), and Holowno (Lubelskie Voivodeship) of MGP, a project maintained by the Geohazards Centre at the Polish Geological Institute – National Research Institute. Those locations supplement 7 seismic stations operating within the Polish Seismological Network. The MGP stations are equipped with modern broad-band seismic, magnetic, tidal gravimetric (only Holowno station), GNSS, meteorological and hydrogeological infrastructure, installed in very stable conditions to provide long-term observations. Results of repeated absolute gravity measurements with the FG5-230 gravimeter on both stations are shown in Figure 3.

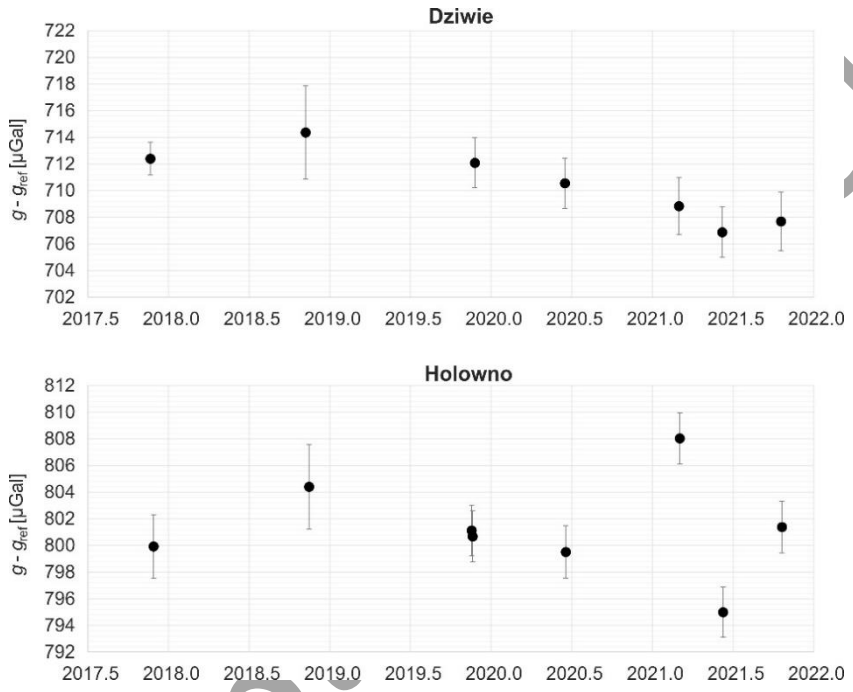

Fig. 3. Absolute gravity measurements within MGP project at stations in Dziwie (g_{ref} = 981 216 000; top) and Holowno (g_{ref} = 981 115 000; bottom); error bars indicate the total uncertainty of gravity determined by the FG5-230 gravimeter at 125.0 cm height above benchmark level, single coverage k = 1.67%

Metrological aspects in absolute gravimetry

Absolute gravimeters in Poland undergo regular metrological control, internally at the level of calibration of gravimeter's subcomponents, and externally either against reference gravity values and/or against the gravity reference function at the BG Observatory as well as international comparisons of AGs. Metrological control is crucial for maintaining and keeping a high quality gravity standard in Poland with the use of all three AGs: A10-020, AQG-B07 of IGiK and FG5-230 of WUT. This control is on one hand carried out by calibration of subcomponents (laser, rubidium clock and barometer) of AGs at the Polish Central Office of Measures (GUM) with respect to national metrological standards of length, time, and pressure, respectively. This type of control cannot be performed with the AQG-B07 quantum gravimeter. Master laser and quartz oscillator calibration used to control the measurement in the quantum gravimeter is performed internally, using spectroscopy against rubidium Rb^{87} atoms ([35]Ménoret et al., 2018).

The long term stability of the A10-020 absolute gravimeter is continuously monitored and analysed ([9]Dykowski et al., 2021b). In order to assure a full reliability of the A10-020

Accepted Article

gravimeter several periodic control activities were implemented. The most basic one concerned calibration of the A10-020 internal components: a helium–neon (He-Ne) laser, rubidium oscillator, and the barometer. In the period from 2008 to 2022, all three components of the A10-020 gravimeter were calibrated at least once a year. Calibrations were performed in multiple National Metrological Institutes as well as in associated institutions equipped with a relevant infrastructure.

Results of the calibrations of the laser of the A10-020 gravimeter are shown in Figure 4. In 2019 the A10-020 gravimeter underwent a laser exchange, hence the gap in Figure 4. For both lasers, the red/blue lock drifts are symmetrical with respect to the central frequency change, which has a linear trend, and after 10 years became smaller by ~9 MHz than the initial calibration value (corresponds to ~18 μGal difference in the calculated gravity value) which is very significant. Laser drift after laser exchange shows a similar character, yet stronger in terms of linear drift of central frequency of ~7 Mhz in only 3 years of operation. This indicates the necessity for monitoring laser frequency on a regular basis.

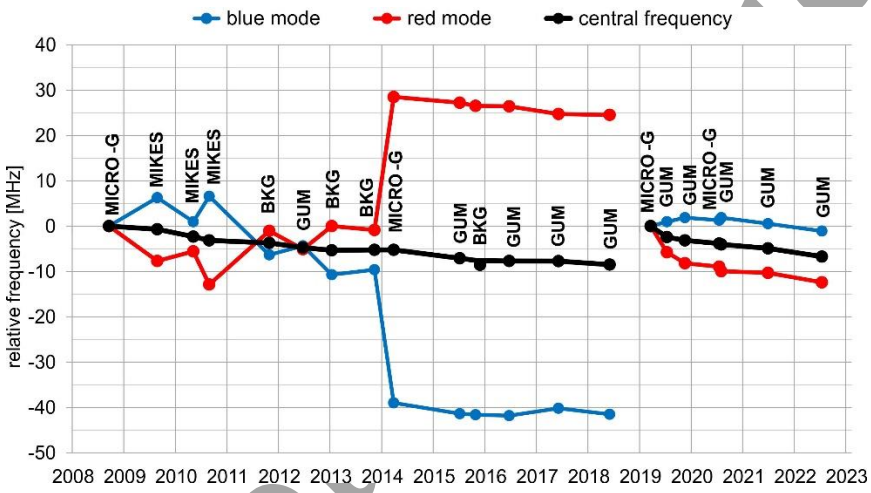

Fig. 4. Results of calibrations of the laser of the A10-020 gravimeter in 2009-2022; MICRO-G – Micro-g LaCoste Inc., MIKES – National Metrological Institute of Finland, GUM – National Metrological Institute of Poland, BKG – Federal Agency of Geodesy and Cartography, Germany

On the other hand, AGs can be metrologically controlled on regular basis against a gravity reference function, e.g. at the BG Observatory ([29]Krynski and Liwosz, 2023). The gravity reference function needs to be constrained by results of participation in international comparisons of AGs.

In mid-2018, the EURAMET.M.G-K3 Key Comparison ([13]Falk, et al., 2020) took place at the Wettzell Observatory. From Poland, only the A10-020 gravimeter participated in that comparison campaign; its resulting offset was estimated as -8.9 μGal (Key Comparison solution). Due to the Covid-19 Pandemic, multiple initiatives of organizing international AGs comparisons in Europe were either cancelled or postponed. It did not allow for effective maintenance of the international gravity reference level. In May–July 2022, a regional AG comparison campaign (NKG-CAG-2022 Additional Comparison) was conducted by the Nordic Commission of Geodesy (NKG) at the Onsala Space Observatory. All three AGs from Poland: A10-020, AQG-B07 (Fig. 5), and the FG5-230 participated in the comparison. Results from the comparison will be publicly available in 2023. They will allow for a comprehensive elaboration of the gravity reference function at the BG Observatory.

Accepted article

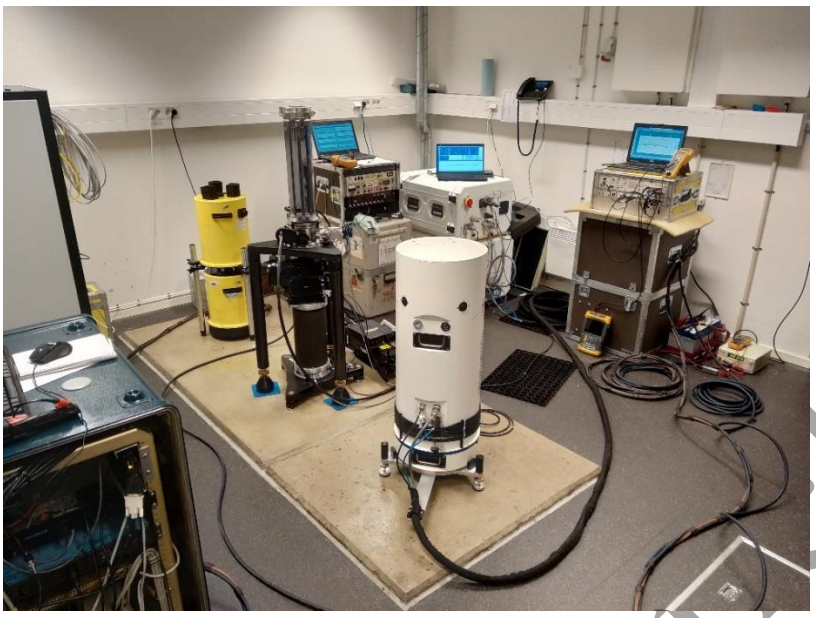

Fig. 5. NKG-CAG 2022 AG comparison at the Onsala Space Observatory. From the left: A10-020 (IGiK, Poland), FG5X-206 (EOST, France), AQG-B07 (IGiK, Poland)

To summarize, Polish teams of IGiK and WUT are active in fulfilling the requirements for supporting and maintaining gravity reference levels of their designated gravity infrastructure toward fulfilling the new definition of the new International Terrestrial Gravity Reference System (ITGRS) as a future replacement to IGSN71 ([50]Wziontek et al., 2021). In the currently being established structure of the ITGRF, presently two stations in Poland: Borowa Gora and Jozefoslaw have the required gravimetric infrastructure to serve as reference stations.

2.2 Metrological aspects in relative gravimetry

Metrological control of relative gravimeters is essential for the most precise terrestrial gravimetric measurements, especially for tidal records. Within the period of 2019–2022, the tidal gravimetric infrastructure in Poland expanded by multiple gPhoneX gravimeters ([8]Dykowski et al., 2021a). All tidal gravimetric records of at least 3 months in length conducted in the recent years are shown in Figure 6. The iGrav, and four gPhoneX gravimeters marked green provide near real time data to the Gravimetric Observations Research Infrastructure Centre (CIBOG) maintained by IGiK. One LCR gravimeter, marked green in Figure 6, is no longer used for continuous tidal records; its tidal gravity series from 2012 until 2018 are, however, collected within CIBOG.

Accepted Article

Fig. 6. Tidal gravimeters in Poland, marked green, are active instruments providing data to CIBOG (status by the end of 2022)

All tidal gravimeters providing data to CIBOG went through a consistent scale factor determination procedure by joint records with a pair of relative spring gravimeters, as important parts of the EPOS-PL and EPOS-PL+ projects ([8]Dykowski et al., 2021a; [37]Nastula et al., 2022). The procedure utilized two LaCoste&Romberg model G gravimeters with automatic feedback systems, for joint gravimetric records with the calibrated tidal gravimeter. Joint records lasted at least 60 days (up to 120 days). The scale factor for the tidal gravimeter was calculated using the least squares adjustment. Results of these calibrations for the iGrav-027 and four gPhoneX gravimeters are summarized in Table 1. Because of the methodology applied, an essential part of the procedures included calibration of the LaCoste&Romberg gravimeters on gravimetric calibration baselines in Poland, supplemented with absolute gravity measurements with the A10-020 gravimeter ([37]Nastula et al., 2022). The achieved accuracy of the scale factor determinations of tidal gravimeters with the use of LCR gravimeters was below 0.1% which is the threshold to be achieved for precise tidal records analysis.

Table 1. Summary of scale factor determinations for tidal gravimeters in the framework of the EPOS-PL and EPOS-PL+ projects

Gravimeter	Date	$k \pm m_K$
iGrav-027 (Borowa Gora)	2022.06 – 2022.09	-1060.25 ± 0.24
gPhoneX-155 (Rybnik)	2019.04 – 2019.06	1.00337 ± 0.00033
gPhoneX-157 (Katowice)	2019.06 – 2019.07	0.99642 ± 0.00037
gPhoneX-164 (Wroclaw)	2020.10 – 2021.01	0.99949 ± 0.00010

Accepted Article

gPhoneX-171 (Borowiec)	2021.10 – 2022.01	0.99743 ± 0.00018

2.3 Marine gravity surveys

In recent years, the team from the Gdansk University of Technology has conducted a number of marine gravimetric measurements in the Baltic Sea within the MORGRAV project. The internal accuracy of these shipborne gravity data in the Gulf of Gdansk was assessed by using a cross-section analysis ([39]Pyrchla et al., 2020). Internal consistency of the measurements was estimated as 1.13 mGal. The free-air anomalies determined on the basis of the acquired marine gravimetric data compared with the corresponding ones determined from the SGG-UTM-1 combined GGM exhibited some significant differences. The analysis showed that those discrepancies were caused by data deterioration due to external conditions.

3. Investigations of non-tidal gravity changes

Non-tidal gravity changes investigated are related to tidal gravity records and focused either on long term gravity variation or on the use of high frequency raw tidal gravity records for seismic studies. A consistent program of monitoring long term gravity changes is currently being carried out at the BG Observatory of IGiK with the use of AGs and a superconducting gravimeter. With the extension of the tidal infrastructure by a number of gPhoneX gravimeters (mentioned in Section 2.1) more stations in Poland are now suitable for monitoring gravity variations in the non-tidal frequency band, seasonal and longer periods as well as for seismic studies. Separate studies were carried out specifically to use tidal gravity records for in-depth seismic studies.

3.1 Monitoring of long term gravity variations at tidal gravity stations

Monitoring gravity variations at the Borowa Gora Geodetic-Geophysical Observatory
In the period of 2019–2022, the iGrav-027 superconducting gravimeter continued, with no major interruption, high precision gravimetric records started in 2016. Throughout the period from 2016 to 2022 the records of the iGrav-027 gravimeter have been supplemented with absolute gravity determinations with the use of all three AGs currently operating in Poland. The FG5-230 gravimeter of WUT performed survey several times in that period, the A10-020 gravimeter – on a regular monthly basis ([9]Dykowski et al., 2021b) and the AQG-B07 quantum gravimeter – also on a regular monthly basis ([12]Dykowski et al., 2022c). Data from the iGrav-027 gravimeter is partially submitted to the International Geodynamics and Earth Tide Service (IGETS) database ([5]Dykowski et al., 2018a; [6]2018b).
Several years of continuous operation with the iGrav-027 gravimeter, supplemented with absolute gravity surveys with the use of gravimeters that participated in international AG comparisons allowed not only to evaluate the drift of the superconducting gravimeter, but also to tie the gravity record to the ITGRF gravity level.
In 2021, a joint analysis of gravity records from the A10-020 and iGrav-027 gravimeters at the BG Observatory was performed ([9]Dykowski et al., 2021b). The drift of the iGrav gravimeter was evaluated with the distinction of its two periods of operation. First eight months (~200 days 2016.05 - 2017.01, the end marked with a green dashed line) were considered as an exponential decay due to internal temperature stabilization of the iGrav-027. Second period of the iGrav drift from 2017.01 – 2019.01 (the end marked with a green dashed line) when the A10-020 gravimeter did not undergo service was considered as a linear trend. For both periods drift rates were evaluated using two solutions with respect to the A10-020 result, i.e. utilizing

Accepted Article

all A10-020 gravimeter results and selected results (within single total uncertainty of the A10-020 gravimeter with respect to the iGrav-027 gravimeter). Both solutions are presented in Figure 7 with indication of the described periods. Using all A10-020 results, the exponential decay resulted in a time constant (tc) of 35.5 days with a linear fit of -0.11 μGal/year while using selected A10-020 gravimeter results, the exponential decay resulted in a time constant of 34.1 days and a linear fit of +0.49 μGal/year. Both solutions indicate exceptional stability of the iGrav-027 superconducting gravimeter, yet in a long term period of several years they considerably drift apart from each other indicating a need for further evaluation.
Beyond 2019, the iGrav-027 drift is assumed linear and has not yet been evaluated due to the lack of participation of AGs operating at the BG Observatory in absolute gravimeter comparisons, mostly postponed and/or cancelled due to the Covid-19 pandemic. In May–July 2022 a regional AG comparison campaign – NKG-CAG-2022 Additional Comparison – was conducted with the participation of the A10-020 and AQG-B07, yet results were not available at the time of preparation of this paper.

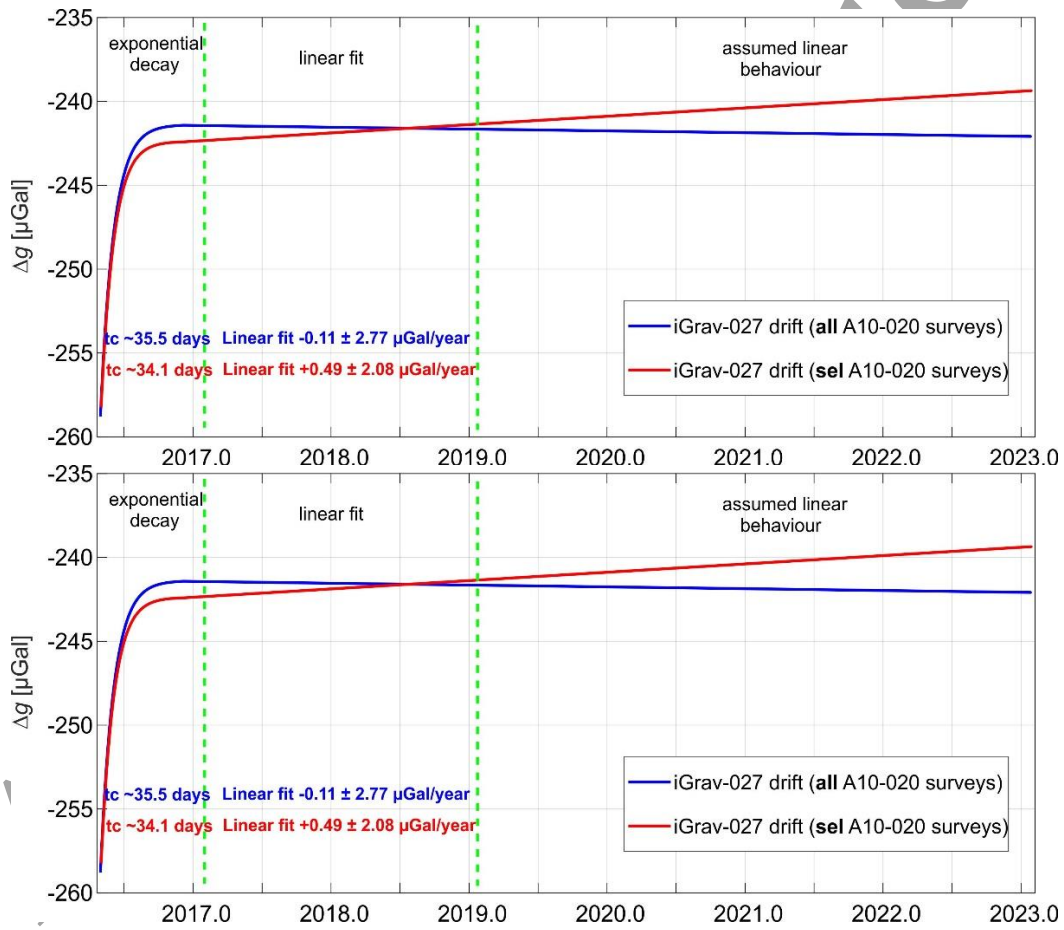

Fig. 7. Drift evaluation of the iGrav-027 gravimeter over first couple of years of operation (all A10-020 results – blue, selected – red)

The residual signal (after removing Earth tides – Tamura, ocean tides – FES04, barometric effect, polar motion) obtained from the iGrav-027 gravimeter tidal record for both above-mentioned solutions to remove the gravimeters drift are presented in Figure 8. They provide very interesting insights at long term non-tidal gravity change: small scale annual signals, and strong several yearlong trends, both of which are suspected to be of hydrological origin related specifically to the location of the BG Observatory. Within the period of 2016–2022, the peak

to peak gravity variation exceeds 25 μGal. The long term gravity variation available from the iGrav-027 gravimeter is a very important tool for the evaluation of AGs, especially the A10-020 and AQG-B07, in terms of their performance and stability, thus may play an important role in defining the ITGRF.

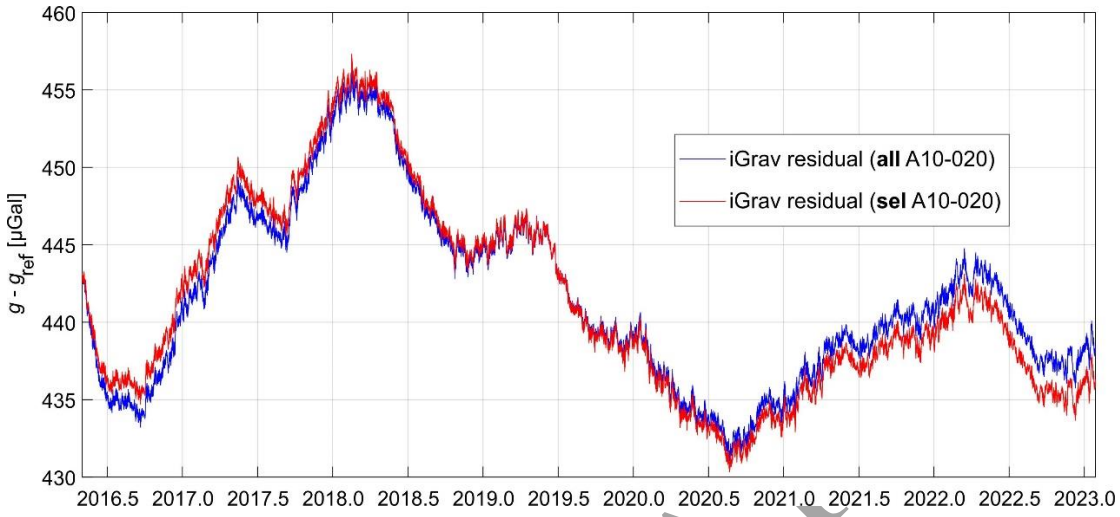

Fig. 8. Residual signal of the iGrav-027 (after drift removal and tie to ITGRF); all A10-020 results – blue, selected – red

Monitoring gravity variations in other locations in Poland

As already mentioned in Section 2.1, within the period of 2019–2022, the tidal gravimetric infrastructure in Poland expanded to five gPhoneX type gravimeters with the support of the EPOS-PL, EPOS-PL+, and MOG projects, hence giving new capabilities for monitoring gravity in Poland.

On selected gPhoneX locations, i.e. Holowno, and Borowiec, periodic absolute gravity surveys are being conducted ([37]Nastula et al., 2022), however, no studies using the long term gravity change from the tidal gravimeter have yet been performed.

Currently, the use of the gPhoneX#165 in Holowno of the Polish Geological Institute – National Research Institute focuses on its capability of recording seismic signals within the MGP project. Events recorded by the instrument are used to prepare periodic reports on seismicity in Poland and around the world.

Tidal gravimeters gPhoneX #155 (Rybnik) and #157 (Katowice) owned by GIG are mainly used to evaluate seismic tremors in mining areas caused by mining exploration ([26]Kotyrba et al., 2020). Using gravimeters to such studies supplements research on understanding the effects of mining exploration, especially in terms of evaluation of tremor strength as a function of distance and magnitude.

The use of the gPhoneX gravimeter at the Borowiec Astrogeodynamic Observatory of SRC PAS primarily focuses on utilizing the results to support the activities related to the Cesium Fountain operating currently at the Observatory. This includes as well short term and long term gravity variation analysis which is undergoing with the support of the IGiK ([37]Nastula et al., 2022).

3.2 Contribution of gravimetric records to seismic studies

Gravimetric recordings of earthquakes show excellent capabilities in long-period seismology. Tidal gravimeters can detect surface waves of periods even up to 500–600 s, while a typical

Accepted Ar

broad-band seismic sensor, due to its mechanical limitation, can detect them only up to periods of 200–300 s. Consequently, gravimetric data can complement seismic recordings for longer periods, depending on what seismometer the station is equipped with and what the seismometer's cut-off period is. A superconducting gravimeter can act as a single-dimension of a very broad-band seismometer (only the vertical component).

Research conducted at the IGiK allowed for the detailed analysis of the transfer function of gravimeters and, as a result, to define a period range when a sensitivity coefficient (calibration factor) and a time lag value only, can be used to adequately describe the properties of instruments ([24]Karkowska et al., 2022a). A joint analysis of the gravimetric and seismometric recordings allows for studying a wider response for incoming seismic wave. Methods developed during the seismic-gravimetric experiment at the BG Geodetic-Geophysical Observatory ([23]Karkowska et al., 2021) have been adopted to selected worldwide stations with co-located typical broad-band seismic sensors and superconducting gravimeters ([25]Karkowska et al., 2022b). Simultaneous seismic and gravity recordings at the same location allow for exploring a broader response for incoming seismic waves. In this way, one joint group-velocity dispersion curve of Rayleigh surface waves for a broader range of periods has been estimated for all stations. All curves were then inverted by linear inversion (together with the determination of resolution matrices, Fig. 9a) and Monte Carlo methods to calculate a distribution of shear-wave seismic velocity with depth in the Earth's mantle (Fig. 9b). Analyses of the fundamental mode of Rayleigh surface waves recorded by typical broadband seismometers (120 s) can give information about the Earth's structure up to 600 km (periods up to 300 s), while in the case of tidal gravimeters up to 1200 km (periods up to 500 s).

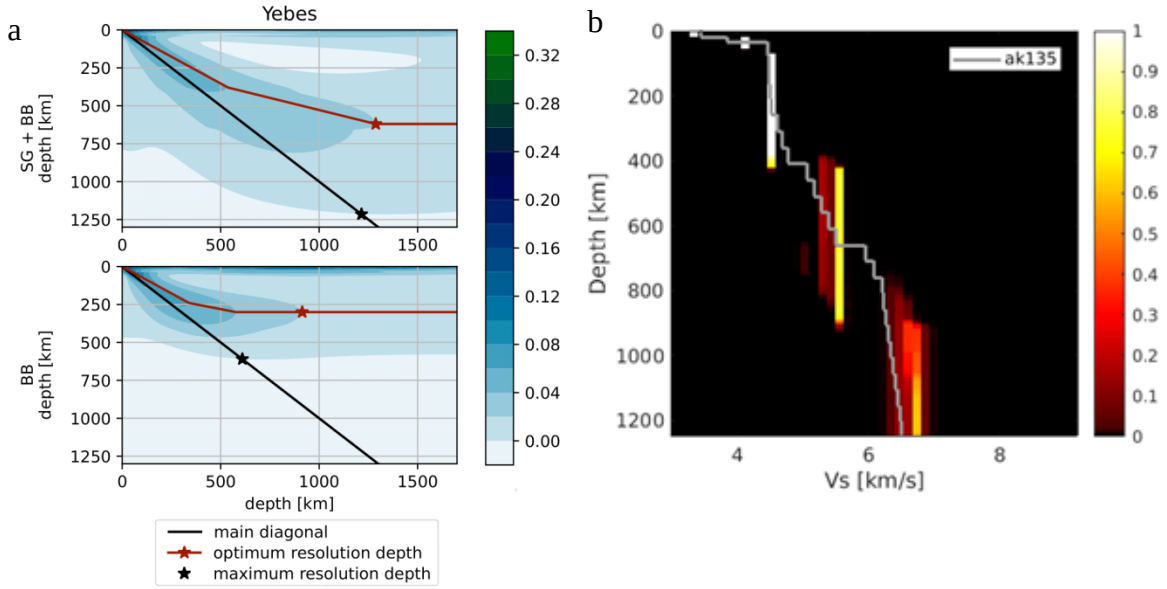

Fig. 9. a) Resolution matrices of the inversion scheme for the joint dispersion curve (SG+BB) and only seismic data dispersion curve (BB). The maximum resolution depth is marked with a black star and the optimum resolution depth with a red star. A resolution matrix relates the estimated model to the true one. A resolution matrix is an identity matrix when the true model and estimated one are identical. b) Results of Monte Carlo inversion performed for Yebes station on joint dispersion curve. The plot represents the a posteriori probability of S-wave velocity (Vs) at each depth; white color shows high probabilities, and red one - low probabilities

3.3 Temporal variations of the gravity field from GRACE/GRACE-FO data

Article

Software for the determination of temporal variations of the Earth gravity field

A novel scientific software, named IGiK–TVGMF (Instytut Geodezji i Kartografii – Temporal Variations of Gravity/Mass Functionals) for the determination of TVGMFs within the Earth's system using GRACE data as well as for analysing and modelling TVGMFs using the seasonal adjustment (SA) and the Principal Component Analysis/Empirical Orthogonal Function (PCA/EOF) methods was developed as a computing tool in the Gravimetric Observations Research Infrastructure Centre of the EPOS-PL project ([14]Godah, 2019). The MATLAB R2017a App Designer was used to develop this software. Three Graphical User Interfaces (GUIs): TVGMF–Computation, TVGMF–Analysis (PCA/EOF), and TVGMF–Analysis (SA) were included in the IGiK–TVGMF software. The TVGMF–Computation allows to calculate thirteen TVGMFs from monthly release 05 GRACE-based GGMs. The user can select monthly GGMs from those provided by seven different computation centres and setup different parameters, e.g. degree-2 spherical harmonic coefficient, reference model, reference system, maximum degree and order (d/o), decorrelation (DDK) filters, and Gaussian filter. The TVGMF–Analysis (PCA/EOF) and the TVGMF–Analysis (SA) allow to analyse and model the TVGMF using PCA and seasonal adjustment methods, respectively. A good agreement, e.g. sub-mm level in terms of temporal variations of geoid height (ΔN), between TVGMFs determined using the IGiK–TVGMF software and the corresponding ones determined using the GRAVSOFT and the International Centre for Global Earth Models (ICGEM[1]) interactive online tool were obtained.

Research on deformations of the Earth's surface and temporal variations of heights

An extended research on vertical displacements and deformations of the Earth's surface, temporal variations of geoid heights and orthometric/normal height changes was conducted by the IGiK's team. Vertical displacements of the Earth's surface (Δh) in the period of 2008–2013 at 25 sites (of presently 129 stations) of the Active Geodetic Network of the European Position Determination System (ASG-EUPOS) in south-eastern Poland determined using GRACE products were compared with those determined using GNSS data ([17]Godah et al., 2020a). The results obtained revealed that monthly Δh obtained from GRACE data are generally in good agreement with the corresponding ones obtained from GNSS data. The Pearson coefficients of correlation between those Δh were in the range from 0.6 to 0.9. Standard deviations of differences between Δh obtained from GRACE and GNSS data were in the range of 2.6–5.7 mm. Overall, the results obtained indicated the need for further investigations concerning Δh determined using GNSS data from the remaining ASG-EUPOS stations as well as for a longer period, i.e. more than 5 years, that are needed to better understand geodynamic processes, and to monitor mass transport within the Earth's system (MTES) over the area of Poland.

The use of GNSS data from national Continuously Operating Reference Stations (CORS) networks, in particular, all GNSS stations of the ASG-EUPOS network, for the determination of MTES and for improving GRACE solutions was investigated ([18]Godah et al., 2020b). The results obtained revealed good agreement between the annual seasonal pattern of Δh from GNSS (Δh_{GNSS}) and the respective one from GRACE/GRACE-FO data ($\Delta h_{G/GF}$). The median values of peak-to-peak variations of Δh_{GNSS} and $\Delta h_{G/GF}$ were at the level of ca. 20 cm. Strong correlations (i.e. Pearson correlation coefficients ranging from 0.6 to 0.9) between Δh_{GNSS} and $\Delta h_{G/GF}$ at 93% of ASG-EUPOS sites investigated were observed. In terms of secular variations of Δh, the results obtained exhibited disagreement between linear trends of Δh_{GNSS} and the respective ones of $\Delta h_{G/GF}$ as GNSS data can include additional local deformations signal.

[1] http://icgem.gfz-potsdam.de/

Accepted Article

Furthermore, the combination of Δ*EWT* determined by inverting Δh_{GNSS} with the corresponding ones from GRACE/GRACE-FO data improve the determination of Δ*EWT* over the area of Poland; the differences between Δ*EWT* obtained from this combination and Δ*EWT* from the WGHM (WaterGAP Global Hydrology Model) exhibited strong correlations at 83% of the ASG-EUPOS sites investigated and their standard deviations were of 4 cm. Overall, the results obtained clearly showed that national GNSS CORS networks may provide valuable information for modelling MTES. However, the use of other national GNSS CORS networks operated worldwide for determining MTES as well as for improving GRACE/GRACE-FO satellite missions' solutions can be recommended as subjects for future research.

Significant efforts of the IGiK's team have been put into the estimation of orthometric/normal height changes (Δ*H*/Δ*H**) over 24 large river basins ([19]Godah et al., 2020c) as well as for the areas of Turkey ([38]Öztürk et al., 2020) and Poland ([44]Szelachowska et al., 2022) using GRACE satellite mission data. For the river basin of a weak hydrological signal, such as the Orange river basin, Δ*H*/Δ*H** do not exceed ±1 cm, while Δ*H*/Δ*H** can reach 8 cm in the case of the river basin of strong hydrological signal, e.g. the Amazon river basin ([19]Godah et al., 2020c). The analyses of Δ*H*/Δ*H** obtained indicated that due to spatio-temporal patterns such as unusual floods, extreme drought, and rainfall seasonality within the entire river basin as well as the location of the upstream and downstream areas of the river basin, clear differences (e.g. ±2 cm in the Amazon river basin) for Δ*H*/Δ*H** can be found within subareas of the same river basin ([19]Godah et al., 2020c). For the area of Turkey, the differences between Δ*H*/Δ*H** in the same area at different epochs reach up to 25 mm, while those differences at the same epoch and different areas reach up to 9 mm ([38]Öztürk et al., 2020). The seasonal decomposition (SD) method was selected as the appropriate one for analysing Δ*H*/Δ*H** over Turkey; the correlations and standard deviations of the differences between Δ*H*/Δ*H** data and Δ*H*/Δ*H** models developed using the SD method were at the level of ca. 96 ± 1%, and the range from 0.9 to 1.2 mm, respectively. Moreover, the use of Green's function for the determination of Δ*H*/Δ*H** from Δ*EWT* obtained from the WGHM was recommended ([38]Öztürk et al., 2020). For the area of Poland, the need for monitoring Δ*H*/Δ*H** to correct orthometric/normal heights was investigated ([44]Szelachowska et al., 2022). Firstly, the relation between temporal mass variations within the Earth system with respect to geoid/quasigeoid height changes, Δ*h*, and Δ*H*/Δ*H** was described. Then, the procedure for the determination of orthometric/normal height corrected from their dynamics was formulated. The Δ*H*/Δ*H** were determined at the sites of the ASG-EUPOS network using GRACE data and the NKG2016LU (Nordic Commission of Geodesy Land Uplift 2016) model. It was shown that Δ*H*/Δ*H** over the area of Poland reached up to 23 mm. Those Δ*H*/Δ*H** can be modelled and predicted for the next 6 months with an accuracy of 1 mm and ca.1–2 mm, respectively. Overall, the results obtained indicate the need of Δ*H*/Δ*H** for the determination of accurate orthometric/normal heights that fulfil the contemporary geodetic scientific requirements and high-precision applications associated with physical heights ([44]Szelachowska et al., 2022).

With the use of GPS (Global Positioning System) and GRACE data, the seasonal horizontal deformations of the Earth's surface for the period 2003–2014 were investigated at 36 GPS stations located mostly in northeast India and Nepal Himalaya (Ray et al., 2021). Positive coefficient of correlations between time series of horizontal seasonal deformations of the Earth's surface in the north component obtained from GPS and GRACE data was determined at nearly 89% of GPS stations investigated. The median values of correlation coefficients in the east and north components are 0.20 and 0.61, respectively. They also revealed a positive reduction of Weighted Root Mean Square (WRMS) at ~83% of GPS stations investigated in the case of the north component. In the case of the east component, this positive reduction of

Accepted Article

WRMS was observed in 58% of GPS stations investigated. Median values of Nash-Sutcliffe model Efficiency (NSE) in the east and north components are –0.01 and 0.28, respectively.
The suitability of GGMs developed using data from Non-Dedicated Gravimetric Satellite Missions (NDGSM) for determining Δ*N* was investigated ([16]Godah et al., 2019b). Two areas, i.e. Poland and the Amazon river basin, which are characterized by different signal strengths of temporal mass variations within the Earth's system were considered. The results obtained indicated that GGMs developed on the basis of data from TanDEM-X, Swarm-comb, Swarm-2 and Sentinel-3A seem, to some extent, suitable for the reliable determination of Δ*N* for the Amazon river basin but unsuitable for the determination of Δ*N* for areas with a weak mass transport signal as in the case of Poland.

Temporal variations of total water storage and groundwater storage
Temporal variations of total water storage (Δ*TWS*) and groundwater storage were investigated by the team of the University of Warmia and Mazury in Olsztyn (UWM). Δ*TWS* from GRACE-FO data, monthly precipitation and evapotranspiration as well as sea level change from tide gauge data over Venezia Islands were analysed ([4]Birylo and Rzepecka, 2020). The lack of dependence between Δ*TWS* obtained from GRACE-FO data and the temporal variations of evapotranspiration and evapotranspiration was observed, however, those Δ*TWS* and mean sea level change exhibited a similar phase change. The authors concluded that atmospheric budget analysis of the MERRA (Modern-Era Retrospective analysis for Research and Applications) model can provide a good prediction for the availability of fresh water.
Variations of groundwater level obtained from direct measurements in wells located in Poland were compared with temporal variations of groundwater storage (Δ*GWS*) determined using GRACE products and global land data assimilation (GLDAS) models ([41]Rzepecka and Birylo, 2020). It was found that Δ*TWS* from GRACE and wells data were highly correlated; the cross-correlation function values reached up to 0.9. The Δ*GWS* obtained from GRACE data and GLDAS model were shifted (delayed) with respect to measurements in wells by three months. The values of cross-correlation function between those Δ*GWS* ranged from ca. 0.2 to 0.6. Amplitudes of variations in water levels in the wells are much higher than the amplitudes of Δ*TWS* from GRACE data and Δ*GWS* from GRACE and GLDAS data. This might be ascribed to disagreement between mean soil porosity values, as the amplitudes of the thickness of the unsaturated zone at the well locations are about four times larger than the corresponding amplitudes of Δ*GWS* from the GRACE products and GLDAS models.
The Δ*TWS* and Δ*GWS* over main river basins in Poland, i.e. the Vistula river and Odra river basins, determined from GRACE data, GLDAS hydrological sub-models (the Community Land Model (CLM), the Mosaic (MOS) model, the Variable Infiltration Capacity (VIC) model and the Noah model-, CMIP5 (World Climate Research Programme's Coupled Model Intercomparison Project Phase 5) climate models (the Flexible Global Ocean-Atmosphere-Land System Model Grid-point Version 2 (FGOALS-g2), the Geophysical Fluid Dynamics Laboratory Earth System Model Version 2G (GFDL-ESM2G), the NASA Goddard Institute for Space Studies E2-H Model (GISS-E2-H), the Russian Institute for Numerical Mathematics' model (inmcm4), the Model for Interdisciplinary Research on Climate version 5 (MIROC5), and the Max Planck Institute Earth System Model (MPI-ESM-LR) and direct measurements in wells were determined and analysed ([45]Sliwinska et al., 2019). The results obtained showed that the CLM, GFD-ESM2G and MIROC5 models agree well with GRACE data. The highest agreement between in-situ well measurements and Δ*GWS* from the combination of GRACE and hydrological and climate models was found for the CLM, FGOALS-g2 and MPI-ESM-LR models.

Accepted Article

RL06 GRACE-based products and the performance of monthly GGMs

Researchers from Polish research institutions participated in examining RL06 GRACE-based products and investigating the performance of monthly GGMs. The variance of signal contained in two types of RL06 GRACE-based products: spherical harmonics (SH) solution and mass concentration blocks (mascons) was examined ([30]Lenczuk et al., 2020). For SH solution, spherical harmonics coefficients (SHCs) up to d/o 96, provided by JPL (Jet Propulsion Laboratory), GFZ (GeoForschungsZentrum) and CSR (Center for Space Research at University of Texas, Austin) were used. For the mascons values of Δ*TWS* provided by the CSR, JPL, and the Goddard Space Flight Center (GSFC) computing centres converted to SHCs (GRACE-M-based GGMs) up to d/o 96 were utilized. It was found that applying the anisotropic DDK3 filter to SH solutions maintain more signal compared to the use of the isotropic Gaussian filter. For mascons, GSFC solution contains much more gravity signal than those of CSR and JPL ones. Differences in signal variance arise from different background models as well as various shape and size of mascons used during processing GRACE observations. It was proved that GGMs obtained from mascon solutions are more appropriate to retrieve the change of gravity signal on a local scale. Furthermore, degree variances and signal contained in GRACE solutions were compared for individual d/o of SHCs. The lowest signal variance was obtained for low SHCs up to d/o 34 of GRACE-based GGMs filtered with DDK3. It was concluded that the method of GRACE-based GGMs filtering has a stronger impact on the final signal than various processing approaches and background models used. The differences in variances were identified for GRACE-based GGMs and GRACE-M-based GGMs.

The research on selecting a proper filter, i.e. an isotropic Gaussian filter and anisotropic decorrelation filters, for RL06 and RL05 releases of monthly GRACE-based GGMs was conducted ([43]Szabó and Marjanska, 2020). The square root of degree variances of spherical harmonics for RL05, RL06 and the difference between RL06 and RL05 for CSR centre using different filters were calculated. The DDK filter shows better stability for higher degrees/orders of spherical harmonic coefficients than the Gaussian filter. For Gaussian filters with radii 500 and 600 km, a better agreement between RL06 and RL05 is noted. Moreover, gravity disturbances determined from filtered GRACE-based GGMs were compared with the corresponding ones obtained from the FG5-230 absolute gravimetric measurements conducted in Jozefoslaw Astro-Geodetic Observatory of WUT. RL05a and RL06 solutions from CSR, GFZ and JPL centres filtered with the use of DDK1–DDK8 filters as well as Gaussian filters with radii 200, 300, 400, 500 and 600 km were analysed. For both releases (except RL6 GGMs from GFZ) very good consistency with the FG5-230 measurements was obtained. The best fit, i.e. a cross-correlation coefficient of 0.7–0.8 and the RMSE (Root Mean Square Error) at the level of 4–5 μGal, was found for GRACE-based solutions filtered using DDK3 – DDK6 filters ([43]Szabó and Marjanska, 2020).

Mass changes and vertical displacements from Swarm satellite mission data were assessed ([40]Richter et al., 2021). A new approach of such an assessment with two variants was considered. In the first one, the entire observed mass change signal was decomposed using the PCA method. In the second variant, the GRACE and Swarm residuals were used as an input for the PCA method, giving solutions that can be considered as the combination of GRACE interpolation/extrapolation with the Swarm reconstruction method. Following this assessment, global temporal variations of equivalent water height (Δ*EWH*) were reconstructed. It was found that the reconstructed Δ*EWH* were much closer to GRACE-based solutions than Swarm-only-based ones. For d/o 40, monthly Swarm-only Δ*EWH* have a global RMSE of 1.39 m at the beginning of the Swarm mission, then decreasing to 0.29 m. The reconstructed Δ*EWH* have a lower RMSE of 0.02–0.08 m. The reconstruction approach enables to obtain reliable monthly Δ*EWH* for d/o 40 which is not possible in the case of the Swarm-only monthly solutions.

Accepted Article

The performance of monthly GGMs developed up to d/o 90 using satellite laser ranging (SLR) and high-low satellite-to-satellite tracking (HLSST) data from 20 Low Earth Orbit (LEO) satellites and 9 SLR satellites including data from CHAMP (CHAllenging Minisatellite Payload), GRACE, and GOCE (Gravity Field and Steady-state Ocean Circulation Explorer) satellite missions was analysed ([51]Zhong et al., 2021). The accuracies of combined HLSST+SLR solutions were found comparable to the respective ones obtained from GRACE for SHCs below d/o 10, and significantly better than the solutions from SLR-only and HLSST-only. The effective spatial resolution of the combined solutions can reach d/o 20, and is higher than that of the HLSST-only solutions ([51]Zhong et al., 2021). Moreover, the global mass redistribution and its magnitudes can be well identified from combined HLSST+SLR solutions at 1000 km spatial resolution. The seasonal mass variations over the Amazon river basin and the long-term trend of mass variations over Greenland, in terms of ΔEWT, determined from combined HLSST+SLR solutions match to the respective ones from the GRACE solutions. The RMS of mass variations was estimated to 282 Gt for the Amazon river basin, and 192 Gt for Greenland.

The influence of solar, geomagnetic, and ionospheric activities on the quality of kinematic and reduced-dynamic GOCE orbits using SLR residuals of GPS-based GOCE orbits was investigated ([42]Strugarek et al., 2019). A substantial sensitivity of kinematic orbit solutions to the F10.7 Solar Radio Flux Index and the ionospheric activity measured by the variations of the Total Electron Content (TEC) values as well as the minor sensitivity of kinematic orbits to the magnetic field activity index Kp was observed. The reduced-dynamic orbits were almost insensitive to indices describing ionospheric, solar, and geomagnetic activities. Moreover, the quality of data provided by individual SLR stations detecting time biases by the use of ascending and descending sun-synchronous GOCE orbit passes was investigated as well as the analysis of SLR station residuals as a function of the nadir angle and horizontal angle of the SLR observations was conducted. It was shown that some of them are affected by time bias errors. The analysis of SLR station residuals as a function of the nadir angle and horizontal angle of the SLR observations indicated a variability of 2–4 cm for stations Monument Peak, Greenbelt and Mount Stromlo. Moreover, differences of SLR residuals between kinematic and reduced-dynamic orbits indicated that kinematic orbits were frequently affected by radial, along-track and cross-track errors. For some stations, incorrect station coordinates and insufficient troposphere delay modelling can be noted.

Time series of monthly gravity field solutions derived by satellite laser ranging (SLR) observations to geodetic satellites, by GPS observations and a dual frequency K-band range-rate measurements of the GRACE mission, and by GPS observations of the three Swarm satellites were determined, evaluated and mutually compared ([36]Meyer et al., 2019). The combined monthly gravity field solutions obtained from Swarm and SLR data generated on the normal equation level that can be helpful to bridge the gap between GRACE and GRACE Follow-On satellite missions were proposed ([36]Meyer et al., 2019). The combined Swarm and SLR solutions were validated using GRACE solutions. The best fit between the SLR/Swarm combination of mass estimation and GRACE-based mass estimation for the mentioned period was achieved when SLR and Swarm normal equations are combined with almost equal weights. The combined gravity field solutions match GRACE ones significantly better than solutions based on SLR-only.

4. Research on static gravity field

4.1. Evaluation of Global Geopotential Models

Accepted Article

GGMs developed in years 2019–2022, i.e. satellite-only GGMs: GO_CONS_GCF_2_TIM_R6, GO_CONS_GCF_2_DIR_R6, GO_CONS_GCF_2_TIM_R6e, and Tongji-GMMG2021S, as well as combined GGMs: SGG-UGM-2 and XGM2019e, were validated at IGiK. Those models are available on the website of the ICGEM. They were assessed over the area of Poland in terms of height anomalies with the use of GNSS/levelling data at ASG-EUPOS network stations, and in terms of free-air gravity anomalies with the use of absolute gravity data at the stations of the Polish gravity control.
For satellite-only GGMs: GO_CONS_GCF_2_TIM_R6, GO_CONS_GCF_2_DIR_R6, GO_CONS_GCF_2_TIM_R6e, standard deviations of differences of height anomalies at d/o 200 are at the level of 25 cm and they decrease to ca. 3 cm when the omitted gravity signal, i.e. the signal in the spectral range from applied d/o 200 to d/o 2190, is compensated using the Earth Gravitational Model 2008 (EGM2008). In the case of Tongji-GMMG2021S model the standard deviation of differences of height anomalies at d/o 200 is 2.9 cm when the omitted gravity signal is taken from the EIGEN-6C4 combined GGM.
The accuracy of the combined GGM SGG-UGM-2, in terms of the standard deviation of the gravity anomaly differences, is ca. 1.8 mGal which is almost at the same level as the ones of the EGM2008, EIGEN and GECO combined GGMs. Standard deviations of differences of height anomalies obtained from XGM2019e and from GNSS/levelling data are 3 cm at d/o 2159 and 2190. However, the accuracy of XGM2019e, in terms of the standard deviation of the gravity anomaly differences at maximum d/o, i.e. 5540, is almost 4 mGal which is twice larger than the corresponding standard deviations obtained for the EGM2008 and EIGEN-6C4 models ([28]Krynski and Rogowski, 2021). The lower quality of the XGM2019e model compared to the quality of the EGM2008 and EIGEN-6C4 models for Poland may result from the use of terrestrial gravimetric data with a resolution of 15'×15' from the resources of the National Geospatial-Intelligence Agency (NGA) of the United States.
The contribution of dedicated gravity satellite missions to the modelling of the Earth's gravity field over East Africa, in particular, the area of Sudan, Ethiopia and Uganda, was assessed. Gravity functionals, e.g. geoid/quasigeoid height, gravity anomaly, and gravity disturbance, obtained from recent combined and satellite-only GGMs were evaluated using terrestrial gravity data available in Sudan and Ethiopia as well as GNSS/levelling data in Uganda. The results obtained revealed substantial improvements in GGMs developed with the use of GOCE satellite mission data compared to GGMs that do not include GOCE data, e.g. the EGM2008. In the area of Ethiopia and Uganda, these improvements reach ca. 40% and ca. 50%, respectively. This may reflect and confirm the contribution of dedicated gravity satellite missions to improve the modelling of the Earth's gravity field over East Africa ([15]Godah et al., 2019a).
The European Gravimetric Geoid models EGG2008 and EGG2015 were validated on the territory of Poland. Height anomalies determined from these models were compared with those obtained from GNSS/levelling data. In the case of EGG2015 model the fit is at the level of 2 cm and it decreases to 1.3 cm when the trigonometric polynomials fit is additionally applied ([33]Marjanska et al., 2019).

4.2. Geoid modelling

The research team from Wroclaw University of Environmental and Life Sciences (UPWr) continued their investigations concerning geoid modelling and issues related to this process. In particular, they investigated the use of the Geophysical Gravity data Inversion (GGI) method for modelling the disturbing potential and quasigeoid surface over the area of Poland. Different reference crust's densities as well as two types of GGI models: (1) type A – with the disturbing potential from the EGM2008, and (2) type B – without the disturbing potential from EGM2008,

Accepted Article

were considered. It was concluded that height anomalies and gravity disturbances can be determined with high accuracy from both model types applied in the GGI method as well as the accuracy of height anomalies determined depends on the reference crust's density applied ([46]Trojanowicz, 2019).

The GGI method was applied within the Colorado geoid experiment to model the quasigeoid using terrestrial and airborne gravity data as well as SRTM (Shuttle Radar Topography Mission) digital elevation model (DEM) of a spatial resolution of 3 arc-second, and the XGM2016 (the experimental global gravity field model 2016). In order to model the geoid surface, geoid-to-quasigeoid separation (GQS) was estimated. Over 700 height anomalies from GPS/levelling data: ~500 points from historical data and over 200 points for the Geoid Slope Validation Surveys 2017 profile (GSVS17) were used to validate quasigeoid/geoid models developed. Standard deviations of the differences between geoid/quasigeoid heights determined using the GGI method and their corresponding ones from historical and GSVS17 profile GPS/levelling data are at the level of 1−2 cm. The results obtained exhibited the robustness of the GGI method for modelling the local geoid/quasigeoid surface ([49]Trojanowicz et al., 2021).

The UPWr team also focused on the interpolation methods implemented for local geoid/quasigeoid modelling. In particular, they investigated (1) the effect of neglecting terrestrial gravity data in the geoid/quasigeoid modelling process (2) the effect of the accuracy of the GGM on the quality of a local geoid/quasigeoid model, and (3) the density of GNSS/levelling points to keep the accuracy at the level of the gravimetric geoid/quasigeoid model. An analysis based on comparisons of four approaches for modelling the local geoid/quasigeoid surface was performed. The 1st and 2nd approaches were based only on GGM and GNSS/levelling data interpolated using the least squares collocation method (LSC) and the thin plate spline, respectively. The 3rd and 4th approaches incorporate in addition terrestrial gravity data and elevations from DEM. The 3rd approach was based on Molodensky's theory and the LSC method, while the 4th approach was based on the GGI method. The differences between the results obtained from all four methods investigated do not exceed 1 mm when using a high-quality GGM and a dense network of GNSS/levelling data (ca.1 point per 30 km^2). In such a case, there is no need to use gravity data and develop advanced geoid/quasigeoid modelling methods. The differences between the results from the four methods implemented became notable when using coarse GNSS/levelling data and lower-quality GGM ([47]Trojanowicz et al., 2020a).

The use of the global topographic mass density model developed by the University of New Brunswick (UNB_TopoDens) for determining the differences between geoid/quasigeoid heights ($\delta = N - \zeta$) and Bouguer anomalies over the area of the Western Carpathians was also investigated by the UPWr team. The results obtained indicated that Bouguer anomalies without using data from UNB_TopoDens model range from approx. –74 to +23 mGal, and δ range from ca. -10 to +5 cm. When data from UNB_TopoDens model are considered, these ranges can be reduced by ~40 mGal for Bouguer anomalies, and ~8 cm for δ. For the highest areas of the Western Carpathians, the difference between δ determined using complete Bouguer anomalies and simple Bouguer anomalies can reach 9 cm ([48]Trojanowicz et al., 2020b).

The research team from IGiK continued their activities towards precise geoid/quasigeoid modelling for the area of Poland. New mean gravity anomalies were generated in two spatial resolutions 5′×5′ and 1′×1′. The coarser grid represented mean free-air gravity anomalies was developed to be included in the EGM2020. The finer grid represented mean Faye anomalies was generated for geoid modelling for the territory of Poland ([28]Krynski and Rogowski, 2021). More accurate formula for the free-air gravity gradient was applied instead of the commonly used constant coefficient equal to 0.3086. The new gravimetric quasigeoid model

Accepted Article

GDQM-PL-19 for Poland was calculated using the updated mean Faye anomalies. The accuracy of that model, in terms of standard deviations of differences between height anomalies with respect of GNSS/levelling data, is at the level of 1.5 cm.
Gravimetric quasigeoid models GDQM-PL13 and GDQM-PL19 developed in the last decade by the IGiK team were compared with two official Polish quasigeoid models. One is gugik-geoid2011-PL-KRON86-NH – based on the PL-KRON86-NH vertical reference frame, and the other is gugik-geoid2011-PL-EVRF2007-NH – compatible with the PL-EVRF2007-NH vertical reference frame. Both were obtained by fitting height anomalies from the EGM2008 into the corresponding ones determined using GNSS/levelling data. Both GDQM-PL13 and GDQM-PL19 quasigeoid models were developed using the EGM2008, mean 1′×1′ Faye gravity anomalies for the area of Poland (different ones for GDQM-PL13 and GDQM-PL19), free-air gravity anomalies for territories surrounding the country, deflections of the vertical for Poland and applying the remove-compute-restore technique with the LSC method. Standard deviations of differences between height anomalies obtained from GDQM-PL13 and GDQM-PL19 models and the corresponding ones determined from fitted gugik-geoid2011-PL-KRON86-NH and gugik-geoid2011-PL-EVRF2007-NH models are at the level of 1.5 cm ([28]Krynski and Rogowski, 2021).
The IGiK's team participated in the research on geoid modelling for the area of Ethiopia. A new gravimetric geoid model over Ethiopia (named the ETH–GM21) was developed. The model is based on terrestrial and airborne free-air gravity anomalies as well as the SRTM3 DEM and EIGEN-6C4 combined GGM. The LSC method and the remove-compute-restore technique were implemented to develop the ETH–GM21. Geoid heights obtained from this model range from 3 m in northern Ethiopia to –35 m in southeast Ethiopia. The estimated accuracy of geoid heights from the ETH–GM21 gravimetric geoid model, in terms of the standard deviation of differences *dN* between geoid heights from this model and the corresponding ones obtained from 46 GNSS/levelling, is ca. 15 cm. After applying the 7-parameter transformation model, this accuracy improved to 13 cm ([2]Belay et al., 2021).
Then, a GQS model for the area of Ethiopia (ETH-GQS) with the use of airborne free-air gravity anomalies and the topographic information retrieved from the SRTM3 DEM, was developed. Sjöberg's strict formula was used to compute the ETH-GQS. The use of GQS values obtained from the ETH-GQS substantially improved the agreement between geoid heights obtained from GNSS/levelling data and the corresponding ones determined from GGMs. In terms of the standard deviation of differences between geoid heights from GNSS/levelling data and the ones from the EIGEN-6C4 GGM, this improvement is ~75%, i.e. from ~24 to ~6 cm ([3]Belay et al., 2022).
The local quasigeoid model QuasigeoidKR2019 was developed for the area of Krakow. The model is based on repeatable static GNSS observations at 66 points and normal heights referenced to the detailed vertical control network. Height anomalies derived were used to develop an approximation function that models the residual quasigeoid heights with respect to the EGM2008; planar coordinates in the PL-2000 coordinate frame are the input data to that approximation function. The quality of GNSS and levelling measurements was evaluated based on the repeatability of height anomalies from two independent determinations at 22 points. The estimated accuracy of the local QuasigeoidKR2019 model in the Krakow area is higher than that of the PLgeoid2011 national model. The maximum difference between models and empirical GNSS/levelling data reaches up to 14 mm for the local model and 44 mm for the national model. The mean absolute difference of 5 mm for the local model and 16 mm for the national model was obtained ([1]Banasik et al., 2020).
The problem of interpolation in modelling a local geoid using GNSS/levelling data was investigated. Two methods of interpolation were intercompared: the ordinary kriging/LSC with

Accepted Article

constant trend and inverse distance weighting (IDW) using leave-one-out and random (Monte Carlo) cross-validation. Ordinary kriging and IDW performance was tested using various planar covariance function models for kriging and various exponents for IDW. Practically no difference between interpolation results of kriging/LSC and IDW with suitably chosen parameters was observed for analysed dataset. However, differences between results within a method and between methods in the whole range of steering parameters may become significant. Generally, for the area investigated, the accuracy in terms of absolute, root mean square and median absolute errors, is below 1 cm ([31]Ligas et al., 2022).

The new quasigeoid model for the Baltic Sea area was determined with the Helmert method ([32]Lyszkowicz et al., 2021) using airborne gravity anomalies from the Baltic Sea and terrestrial gravity anomalies from Denmark, Finland, Latvia, Lithuania, Poland, and Sweden. The terrain corrections were calculated using SRTM30 digital terrain model. Three different GGMs, i.e. GOCE-DIR6, GOCO06s, and EIGEN-6C4 were used; thus three solutions were obtained. The quasigeoid models determined were validated using GNSS/levelling data at the stations of the ASG-EUPOS network. Their accuracy was assessed as 4 cm.

A quasigeoid model for the area of Poland developed by the team of the Wroclaw University of Environmental and Life Sciences was selected in the competition announced by the Head Office of Geodesy and Cartography in 2021, and on 4 April 2022 was established as the official quasigeoid model PL-geoid2021 for Poland. The theoretical part, i.e. the description of the adopted methodology and the cohesion of the models with the vertical geodetic control network, was assessed. The model was first verified using satellite/levelling data at 24 control points located throughout the country and then at 62 points of the geodetic control network which were surveyed in two 12-hour GNSS sessions. It was also compared with the PL-geoid2011 – previous official quasigeoid model for Poland (Table 2).

Table 2. Statistics illustrating the verification of the PL-geoid2021 quasigeoid model for Poland

quasigeoid model	24 control points		62 control points	
	mean (m)	std (m)	mean (m)	std (m)
PL-geoid2011	0.005	0.023	-0.015	0.038
PL-geoid2021	-0.002	0.019	-0.012	0.026

At both sets of control points the new PL-geoid2021 quasigeoid model performs better than the PL-geoid2011 model ([21]GUGiK, 2022).

The influence of noise variance in the prediction of geophysical phenomena was investigated using methods based on the least squares theory, such as Kriging and LSC ([22]Jarmolowski, 2019). In particular, the relation between signal spectral range and uncorrelated noise (e.g. noise induced by measurement error and noise resulted from high frequency signal in the spectral bands beyond the spatial resolution of the data) variance was verified. Two data sets of Bouguer anomalies were utilized: the first one presenting terrestrial data obtained from the United States of America gravity database, and the second one determined from the EGM2008. Three different estimators were used to assess the noise variance size. They were based on the average of a priori noise standard error, the minimum of the differences between the data used and their prediction, and a posteriori noise standard error, respectively. The results obtained revealed that the noise in Bouguer anomalies was related to the spatial resolution of the data used rather than the measurement errors.

The contradictions between the guidelines concerning aeronautical data quality requirements (DQR) and the geodetic legal regulations in Poland were pointed out ([34]Marjanska, 2022). The differences between the coordinates data obtained from the ASG-EUPOS network stations and the corresponding ones documented in the aforementioned guidelines were determined.

Accepted Article

The results obtained indicated that these differences reach up to of 30 cm for the horizontal position and 1 cm for the ellipsoidal height. Moreover, the differences between quasigeoid heights obtained from the EGM96 (Earth Gravitational Model 1996) GGM that is used in the aviation and the respective ones from the official quasigeoid models for Poland were found at the level of up to 1 m ([34]Marjanska, 2022).

4.3. Estimation of sea level

The research associated with the use of the Synthetic Aperture Radar (SAR), GNSS, tide gauge (TG), and geoid heights data for estimating the absolute sea level at sites of the selected network in the Baltic Sea (SNBS) were conducted within the ESA's project entitled "Geodetic SAR for Baltic Height System Unification (SAR-HSU)" ([20]Gruber et al., 2022). Within the project, ten active electronic corner reflectors (ECRs) tied to the existing TGs and/or permanent GNSS stations, were installed at the SNBS. In order to determine the absolute sea level and height system unification for the SNBS, positions obtained from SAR and GNSS as well as geoid/quasigeoid heights obtained from gravimetric geoid/quasigeoid model, and mean sea level obtained from TG data were combined considering the technique-specific processing standards for each geodetic technique. Moreover, the ECR stations were connected with the TG or GNSS stations using conventional spirit levelling. The absolute sea level obtained from SAR, GNSS, and TG data as well as gravimetric quasigeoid models for the SNBS are not fully consistent; the difference reaches up to 0.5 m. Thus, further research concerning the performance of the ECRs and the instrument calibration as well as the methods and procedures applied by SAR positioning technique to meet the contemporary accuracy of the geodetic measurements were recommended ([20]Gruber et al., 2022). All data and products associated with the SAR-HSU project as well as their supplementary information are available for public use via the website[2].

5. Summary and conclusions

The article contains the summary of activities of Polish research and government institutions in the years 2019–2022 in gravimetry with special emphasis on its metrological aspects, and in modelling gravity field with considering its temporal variations.

Extensive research activities were conducted toward the implementation of ITGRF in Poland. In mid-2022 all three absolute gravimeters operating in Poland i.e., FG5-230, A10-020, and AQG-B07, participated in AG comparison campaign in Onsala, organized by the Nordic Commission of Geodesy. As all gravimeters also performed joint surveys together with the iGrav-027 superconducting gravimeter at the Borowa Gora Geodetic-Geophysical Observatory, results from the comparison will allow a reliable traceability to the ITGRF reference level. It was shown that the maintenance of the international gravity reference system requires, besides careful metrological control, consideration of the impact of non-tidal gravity variations and that the true gravity variations are larger than the accuracies currently achievable with AGs.

Installation of the absolute quantum gravimeter AQG-B07 in the BG Observatory further expanded the gravimetric infrastructure required for reliable realization of the gravity standard in Poland as well as for supporting the operation of the iGrav-027 gravimeter.

The A10-020 absolute gravimeter was used in the EPOS-PL and EPOS-PL+ projects related to monitoring deformations in mining areas in the Upper Silesian region in Poland. Gravimetric

[2] https://www.asg.ed.tum.de/iapg/baltic/

Accepted Article

measurements with the FG5-230 gravimeter were performed for geodynamic research at stations Dziwie and Holowno in multiple survey campaigns within MOG project.
Research on non-tidal gravity changes was successfully continued with the use of data recorded at the BG Observatory as well as at multiple stations newly equipped with gPhoneX gravimeters. Time series of tidal gravimeter records together with quasi-regular absolute gravity measurements at the BG Observatory allowed for analysis of long term gravity variations reaching peak to peak values of 25 μGal. Linear drift estimates at the level of below ±1 μGal/year confirm great stability of the iGrav-027 gravimeter over the period of 2017–2022.
Joint research in the fields of geodesy and seismicity concerning contribution of gravimetric records to seismic studies was continued. Transfer functions of gravimeters used in the seismic analysis were determined. Monte Carlo methods were used to calculate a distribution of shear-wave seismic velocity with depth in the Earth's mantle. It was shown that signals recorded by typical broadband seismometers (120 s) can give information about the Earth's structure up to 600 km (periods up to 300 s), while in the case of tidal gravimeters up to 1200 km (periods up to 500 s).
Temporal variations of the gravity field were subject of extensive research. A novel scientific software IGiK–TVGMF for the determination, analysis and modelling temporal variations of gravity/mass functionals (TVGMF) from GRACE/GRACE-FO data was developed as a computing tool in the Gravimetric Observations Research Infrastructure Centre of the EPOS-PL project. Vertical displacements and deformations of the Earth's surface, in particular temporal variations of geoid heights and orthometric/normal height changes, were widely investigated with the use of GRACE/GRACE-FO and GNSS data. Also the suitability of non-dedicated gravity satellite missions were examined. In general, results from GNSS data match to those from GRACE data. Variations of orthometric/normal heights were investigated in large river basins of both weak and strong hydrological signal on five continents and specifically in Poland, Turkey, northeast India and Nepal Himalaya. Seasonal signals obtained vary from 1 cm to 8 cm. It was shown that national GNSS CORS networks provide valuable information for modelling TVGMF and can efficiently complement those functionals modelled with the use of GRACE data. Some research was focused on temporal variations of total water storage and groundwater storage with the use of GRACE/GRACE-FO data. An important conclusion was that atmospheric budget analysis of the MERRA model can provide a good prediction for the availability of fresh water.
RL06 GRACE-based products and the performance of monthly GGMs were investigated. GGMs obtained from mascon solutions were found more appropriate to retrieve the change of gravity signal in a local scale. The products of different computing centres were mutually compared in terms of signal strengths in the provided solutions. The superiority of DDK3 filter over the isotropic Gaussian filter was proved.
Monthly GGMs developed up to d/o 90 as a combination of SLR and high-low satellite-to-satellite tracking data from LEO satellites and SLR satellites including data from CHAMP, GRACE, and GOCE satellite missions were analysed. Monthly GGMs obtained from SLR observations to geodetic satellites were mutually compared with those obtained from GPS and K-band range-rate data of the GRACE mission, and from GPS observations of the three Swarm satellites showing the SLR and Swarm combined gravity field solutions match GRACE ones significantly better than those based on SLR-only.
GGMs developed in years 2019–2022 were carefully evaluated with the use of GNSS/levelling data at ASG-EUPOS network stations in Poland as well as with the use of absolute gravity data at the stations of the Polish gravity control. The contribution of gravity dedicated satellite missions products to the Earth's gravity field modelling over the area of Sudan, Ethiopia and Uganda, was assessed. GGMs from satellite missions considerably improve the modelling of

Accepted Article

the Earth's gravity field over East Africa, e.g. by as much as 40% and 50% in the area of Ethiopia and Uganda, respectively.
Research on geoid modelling and issues related to this process were continued. The use of the Geophysical Gravity data Inversion (GGI) method for modelling the disturbing potential and quasigeoid surface over the area of Poland as well as Colorado was investigated. The role of the reference crust's density applied as well as the interpolation methods implemented for local geoid/quasigeoid modelling was discussed. Determination of differences between geoid/quasigeoid heights and Bouguer anomalies with the use of the global topographic mass density model developed by the University of New Brunswick (UNB_TopoDens) over the area of the Western Carpathians was investigated.
The 5′×5′ grid of mean free-air gravity anomalies was developed to be included in the EGM2020. The 1′×1′ grid of mean Faye gravity anomalies was generated for developing new gravimetric quasigeoid model for Poland of 1.5 cm accuracy. A number of existing geoid/quasigeoid models for Poland were intercompared. In 2022 a new official quasigeoid model for Poland PL-geoid2011 has been adopted. Also a new quasigeoid model for the Baltic Sea area as well as a local geoid model for the area of Krakow were developed. The Polish team participated in the research on geoid modelling for the area of Ethiopia.
The research on the estimation of sea level with the use of SAR, GNSS, tide gauge, and geoid heights data was conducted within the ESA's project indicated the need of further investigation concerning active electronic corner reflectors performance, calibration of instruments and SAR positioning.

Accepted Article

Author contributions

Conceptualization: J.K., P.D., W.G., M.S.; original draft preparation: J.K., P.D., W.G., M.S.

Data availability statement

No datasets were used in this research.

Acknowledgements

The review paper was elaborated in the framework of the statutory project "Problems of geodesy and geodynamics" of IGiK, financially supported by the Polish Ministry of Education and Science as well as the activities of the Section of Geodesy and Geodynamics of the Committee on Geodesy of the Polish Academy of Sciences. Valuable help was provided by Kamila Karkowska, Marcin Sekowski, and Monika Wilde-Piorko.

References

[1]Banasik, P., Bujakowski, K., Kudrys, J. et al. (2020). Development of a precise local quasigeoid model for the city of Krakow – QuasigeoidKR2019. *Reports on Geodesy and Geoinformatics*, 109, 25–31. DOI: 10.2478/rgg-2020-0004.
[2]Belay, E.Y., Godah, W., Szelachowska, M. et al. (2021). ETH–GM21: A New Gravimetric Geoid Model over Ethiopia Developed Using the Least Square Collocation. *J. African Earth Sci.*, 183, 104313. DOI: 10.1016/j.jafrearsci.2021.104313.

[3]Belay, E.Y., Godah, W., Szelachowska, M. et al. (2022). ETH-GQS: An Estimation of Geoid-to-Quasigeoid Separation over Ethiopia. *Geod. Geodyn.*, 13(1), 31–37. DOI: 10.1016/j.geog.2021.09.006.
[4]Birylo, M., and Rzepecka, Z. (2021). An Analysis of Total Water Storage Changes Obtained from GRACE FO Observations over the Venezia Islands Area Supported with Additional Data. *Geomat. Environ. Eng.*, 15(2), 17-31. DOI: 10.7494/geom.2021.15.2.17.
[5]Dykowski, P., Sekowski, M., and Krynski, J. (2018a). Superconducting Gravimeter Data from Borowa Gora - Level 1. GFZ Data Services, http://doi.org/10.5880/igets.bg.l1.001.
[6]Dykowski, P., Sekowski, M., Krynski, J. (2018b). Superconducting Gravimeter Data from Borowa Gora - Level 2. GFZ Data Services, http://doi.org/10.5880/igets.bg.l2.001.
[7]Dykowski, P., Sekowski, M., Krynski, J. et al.. (2019). Gravity, GNSS, InSAR combination for monitoring deformation related to industrial activity on Multidisciplinary Upper Silesian Episode within the EPOS-PL project. In 5th IAG Symposium on Terrestrial Gravimetry: Static and Mobile Measurements TG-SMM, 1–4 October 2019, St. Petersburg, Russia.
[8]Dykowski, P., Sekowski, M., Wilde-Piorko, M. et al. (2021a). Development of tidal gravity records in Poland within the framework of the EPOS-PL project. In EUREF Symposium, 26-28 May 2021, Slovenia, Ljubljana.
[9]Dykowski, P., Krynski, J., Sekowski, M. et al. (2021b). Evaluation of the gravity reference function at the Borowa Gora Observatory. In IAG Scientific Assembly 2021, 28 June – 2 July, Beijing, online.
[10]Dykowski, P., Krynski, J., and Olszak, T. (2022a). Modernization and current status of the Polish Gravity Control. In IGRF Workshop 2022, 11–13 April, Leipzig, Germany.
[11]Dykowski, P., Arnal, M., Menoret, V. et al. (2022b). First results from the AQG-B07 absolute quantum gravimeter. In EGU General Assembly 2022, 23–27 May, Vienna, Austria.
[12]Dykowski, P., Arnal, M., Menoret V. et al. (2022c). Testing the capabilities of the AQG-B07 absolute quantum gravimeter. In Gravity Geoid and Height Systems 2022, 12–14 September 2022, Austin, USA.
[13]Falk, R., Pálinkáš, V., Wziontek, H. et al. (2020). Final report of EURAMET.M.G-K3 regional comparison of absolute gravimeters. *Metrologia*, 57(1A), 07019. DOI: 10.1088/0026-1394/57/1A/07019.
[14]Godah, W. (2019). IGiK–TVGMF: A MATLAB package for computing and analysing temporal variations of gravity/mass functionals from GRACE satellite based global geopotential models. *Comput. Geosci.*, 123, 47–58. DOI: 10.1016/j.cageo.2018.11.008.
[15]Godah, W., Gedamu, A.A., and Bedada, T.B. (2019a). On the contribution of dedicated gravity satellite mission to the modelling of the Earth gravity field over East Africa. In 27th IUGG General Assembly, 8–18 July, 2019, Montréal, Canada.
[16]Godah, W., Szelachowska, M., and Krynski, J. (2019b). On the recovery of temporal variations of geoid heights determined with the use of GGMs based on SST-hl data from non-dedicated gravity satellite missions. *Bull. Geod. Sci.*, 25(3), e2019017. DOI: 10.1590/s1982-21702019000300017.
[17]Godah, W., Szelachowska, M., Ray, J.D. et al. (2020a). Comparison of vertical deformations of the Earth's surface obtained using GRACE-based GGMs and GNSS data – A case study of Poland. *Acta Geodyn. et Geomater.*, 17, 169–176. DOI: 10.13168/AGG.2020.0012.
[18]Godah, W., Ray, J.D., Szelachowska, M. et al. (2020b). The Use of National CORS Networks for Determining Temporal Mass Variations within the Earth's System and for Improving GRACE/GRACE-FO Solutions. *Remote Sens.*, 12(20), 3359. DOI: 10.3390/rs12203359.

Accepted Article

[19]Godah, W., Szelachowska, M., Krynski, J. et al. (2020c). Assessment of Temporal Variations of Orthometric/Normal Heights Induced by Hydrological Mass Variations over Large River Basins Using GRACE Mission Data. *Remote Sens.*, 12(18), 3070. DOI: 10.3390/rs12183070.
[20]Gruber, T., Ågren, J., Angermann, D. et al. (2022). Geodetic SAR for Height System Unification and Sea Level Research – Results in the Baltic Sea Test Network. *Remote Sens.*, 14(14), 3250. DOI: 10.3390/rs14143250.
[21]GUGiK (2022) Information guide of Head Office of Geodesy and Cartography. Retrieved November 2022 from https://www.gov.pl/web/gugik/wydanie-2---listopad-2022.
[22]Jarmolowski, W. (2019). On the relations between signal spectral range and noise variance in least-squares collocation and simple kriging: example of gravity reduced by EGM2008 signal. *Bull. Geophys. Oceanography*, 60(3), 457–474. DOI: 10.4430/bgta0265.
[23]Karkowska, K., Wilde-Piorko, M., Dykowski, P. et al. (2021). Determination of the Earth's mantle structure based on a joint analysis of gravimetric and seismometric earthquake recordings at the Borowa Gora Geodetic-Geophysical Observatory. In IAG Scientific Assembly 2021, June 28 – July 2, Beijing, China, on-line.
[24]Karkowska, K., Wilde-Piorko, M., and Dykowski, P. (2022a). Analysis of earthquakes recordings of tidal gravimeters in the period range of 10-1000 s. *Acta Geodyn. et Geomater.*, 19, 1(205), 79–92. DOI: 10.13168/AGG.2021.004.3
[25]Karkowska, K., Wilde-Piorko, M., Dykowski, P. et al. (2022b). Exploring the Earth's mantle structure based on joint gravimetric and seismometric group-velocity dispersion curves of Rayleigh waves. In EGU General Assembly 2022, 23–27 May Vienna, Austria.
[26]Kotyrba, A., Frolik, A., Kortas, L. et al. (2020). Grawimetryczno-hydrometryczny system monitoringu wstrząsów górniczych na Górnym Śląsku. *Przegląd Geologiczny*, 68(11), 833–842. DOI: 10.7306/2020.35.
[27]Krynski, J., Dykowski, P., and Olszak, T. (2019). Research on gravity field modelling and gravimetry in Poland in 2015–2018. *Geod. Cartogr.*, 68(1), 31-63. DOI: 10.24425/gac.2019.126096.
[28]Krynski, J., and Rogowski, J.B. (2021). National Report of Poland to EUREF 2020/2021. In Symposium of the IAG Subcommission for Europe (EUREF), 26–28 May 2021, Ljubljana, Slovenia.
[29]Krynski, J., and Liwosz, T. (2023). Research on reference frames and reference networks in Poland in 2019-2022. *Adv. Geod. Geoinf.*, 72(2), e44. DOI: 10.24425/agg.2023.146156.
[30]Lenczuk, A., Leszczuk, G., Klos, A. et al. (2020). Comparing variance of signal contained in the most recent GRACE Solutions. *Geod. Cartogr.*, 69(1). 19-37. DOI: 10.24425/gac.2020.131084.
[31]Ligas, M., Lucki, B., and Banasik, P. (2022). A cross validation-based comparison of kriging and IDW in local GNSS/levelling quasigeoid modelling. *Reports on Geodesy and Geoinformatics*, 114(1), 1–7. DOI: 10.2478/rgg-2022-0004.
[32]Lyszkowicz, A., Nastula, J., Zielinski, J.B. et al. (2021). A New Model of Quasigeoid for the Baltic Sea Area. *Remote Sens.*, 13(13), 2580. DOI: 10.3390/rs13132580.
[33]Marjanska, D., Olszak, T., and Pietka, D. (2019). Validation of European Gravimetric Geoid models in context of realization of EVRS system in Poland. *Geod. Cartogr.*, 68(2), 329–347. DOI: 10.24425/gac.2019.128461.
[34]Marjanska, D. (2022). Aeronautical data requirements and geodetic data – a case study on regulations in Poland. *Aircraft Engineering and Aerospace Technology*, 94(5), 770-780. DOI: 10.1108/AEAT-09-2021-0276.

Accepted Article

[35]Ménoret, V., Vermeulen, P., Le Moigne, N. et al. (2018). Gravity measurements below 10−9 g with a transportable absolute quantum gravimeter. *Sci. Rep.*, 8, 12300. DOI: 10.1038/s41598-018-30608-1.
[36]Meyer, U., Sosnica, K., Arnold, D. et al. (2019). SLR, GRACE and Swarm Gravity Field Determination and Combination. *Remote Sens.*, 11 (8), 956. DOI: 10.3390/rs11080956.
[37]Nastula, J., Nawrocki, J., Pietrzak, J. et al. (2022). gPhoneX Stationary Tidal Gravimeter in AOS Borowiec. In Gravity Geoid and Height Systems 2022, 12–14 September 2022, Austin, USA.
[38]Öztürk, E.Z., Godah, W., and Abbak, R.A. (2020). Estimation of Physical Height Changes from GRACE Satellite Mission Data over Turkey. *Acta Geodaet. et Geophys.*, 55(2), 301–317. DOI: 10.1007/s40328-020-00294-5.
[39]Pyrchla, K., Pajak, M., Pyrchla, J. et al. (2020). Analysis of free-air anomalies on the seaway of the Gulf of Gdansk: A case study. *Earth Space Sci.*, 7, e2019EA000983 DOI: 10.1029/2019EA000983.
[40]Richter, H.M.P., Lück, C., Klos, A. et al. (2021). Reconstructing GRACE-type time-variable gravity from the Swarm satellites. *Sci. Rep.*, 11, 1117. DOI: 10.1038/s41598-020-80752-w.
[41]Rzepecka, Z., and Birylo, M. (2020). Groundwater storage changes derived from GRACE and GLDAS on smaller river basin – A case study in Poland. *Geosci.*, 10(4), 124. DOI: 10.3390/geosciences10040124.
[42]Strugarek, D., Sosnica, K., and Jäggi, A. (2019). Characteristics of GOCE orbits based on Satellite Laser Ranging. *Adv. Space Res.*, 63(1), 417-431. DOI: 10.1016/j.asr.2018.08.033.
[43]Szabó, V., and Marjanska, D. (2020). Accuracy analysis of gravity field changes from GRACE RL06 and RL05 data compared to in situ gravimetric measurements in the context of choosing optimal filtering type. *Artificial Satellites: Journal of Planetary Geodesy*, 55(3), 100-117. DOI: 10.2478/arsa-2020-0008.
[44]Szelachowska, M., Godah, W., and Krynski, J. (2022). Contribution of GRACE satellite mission to the determination of orthometric/normal heights corrected for their dynamics – A case study of Poland. *Remote Sens.*, 14(17), 4271. DOI: 10.3390/rs14174271.
[45]Sliwinska, J., Birylo, M., Rzepecka, Z. et al. (2019). Analysis of groundwater and total water storage changes in Poland using GRACE observations, in-situ data, and various assimilation and climate models. *Remote Sens.*, 11(24), 2949. DOI: 10.3390/rs11242949.
[46]Trojanowicz, M. (2019). Local Disturbing Potential Model with the Use of Geophysical Gravity Data Inversion Case Study in the Area of Poland. *Acta Geodyn. et Geomater.*, 16(3(195)), 293–299. DOI: 10.13168/AGG.2019.0025.
[47]Trojanowicz, M., Osada, E., and Karsznia, K. (2020a). Precise local quasigeoid modelling using GNSS/levelling height anomalies and gravity data. *Surv. Rev.*, 52(370), 76-83. DOI: 10.1080/00396265.2018.1525981.
[48]Trojanowicz, M., Pospíšil, L., and Jamroz, O. (2020b). Use of the UNB_TOPODENS model for local modelling of chosen gravity field parameters in the Western Carpathians. *Acta Geodyn. et Geomater.*, 17, 1(197), 113-118. DOI: 10.13168/AGG.2020.0008.
[49]Trojanowicz, M., Owczarek-Wesolowska, M., Wang, Y.M. et al. (2021). Quasi Geoid and Geoid Modeling with the Use of Terrestrial and Airborne Gravity Data by the GGI Method—A Case Study in the Mountainous Area of Colorado. *Remote Sens*., 13, 4217. DOI: 10.3390/rs13214217.
[50]Wziontek, H., Bonvalot, S., Falk, R. et al. (2021). Status of the International Gravity Reference System and Frame. *J. Geod.*, 95, 7. DOI: 10.1007/s00190-020-01438-9.
[51]Zhong, L., Sosnica, K., Weigelt, M. et al. (2021). Time-Variable Gravity Field from the Combination of HLSST and SLR. *Remote Sens.*, 13 (17), 3491. DOI: 10.3390/rs13173491.

Accepted Article

Research on Earth rotation and geodynamics in Poland in 2019-2022

Janusz Bogusz[1]*, Aleksander Brzezinski[2,3], Walyeldeen Godah[4], Jolanta Nastula[3]

[1]Military University of Technology, Warsaw, Poland,
[2]Warsaw University of Technology, Warsaw, Poland,
[3]Space Research Centre, Polish Academy of Sciences, Warsaw, Poland,
[4]Institute of Geodesy and Cartography, Centre of Geodesy and Geodynamics, Warsaw, Poland,
*Corresponding author: Janusz Bogusz, e-mail: janusz.bogusz@wat.edu.pl

Abstract: This paper summarizes the activity of the chosen Polish geodetic research teams in 2019-2022 in the fields of the Earth rotation and geodynamics. This publication has been prepared for the needs of the presentation of Polish scientists' activities on the 28th International Union of Geodesy and Geodynamics General Assembly, Berlin, Germany. The part concerning Earth rotation is mostly focused on the estimation of the geophysical excitation of polar motion using data from Gravity Recovery and Climate Experiment (GRACE) and its follow-on (GRACE-FO) missions, and on the improvement of the determination of Earth rotation parameters based on the Satellite Laser Ranging (SLR), Doppler Orbitography and Radiopositioning Integrated by Satellite (DORIS), and Global Navigation Satellite System (GNSS) satellite techniques. The part concerning geodynamics is focused on geodetic time series analysis for geodynamical purposes and monitoring of the vertical ground movements induced by mass transport within the Earth's system, monitoring of the crustal movements using GNSS and newly applied Interferometric Synthetic Aperture Radar (InSAR), discussing the changes of the landslides and its monitoring using geodetic methods as well as investigations of seismic events and sea-level changes with geodetic methods. Finally, the recent research activities carried out by Polish scientists in the international projects is presented.

Keywords: time series analysis, deformation, Earth rotation, geodynamics, seismic events

1. Introduction

In the research concerning Earth rotation and geodynamics carried out by Polish scientists in a period of 2019-2022 many research institutions were involved, namely (in the alphabetical order):

- AGH University of Science and Technology, Faculty of Mining Surveying and Environmental Engineering and Faculty of Geo-Data Science, Geodesy, and Environmental Engineering;
- Institute of Geophysics, Polish Academy of Sciences;
- Koszalin University of Technology, Faculty of Civil Engineering, Environmental and Geodetic Sciences;
- Military University of Technology, Faculty of Civil Engineering and Geodesy;
- Polish Air Force University;
- Polish Geological Institute – National Research Institute;

This article has been accepted for publication in the journal Advances in Geodesy and Geoinformation, issue 72/2, 2023. It has not yet undergone the process of copyediting, typesetting, pagination and proofreading. This may lead to differences between this version and the final published version. The article may be cited as DOI: 10.24425/agg.2023.144593.

Accepted Article

- Space Research Centre, Polish Academy of Sciences;
- University of Warmia and Mazury in Olsztyn, Faculty of Geoengineering;
- Warsaw University of Technology, Faculty of Civil Engineering and Faculty of Geodesy and Cartography;
- Wroclaw University of Environmental and Life Sciences, Faculty of Environmental Engineering and Geodesy;
- Wroclaw University of Science and Technology, Faculty of Geoengineering, Mining and Geology.

The main concern of the research related to the Earth rotation was the improvement of the geophysical excitation balance of the observed polar motion by the extensive use of different data products from Gravity Recovery and Climate Experiment (GRACE) and GRACE Follow-On (GRACE-FO) missions. Another important field of research was the estimation of global geodetic parameters, including those of Earth rotation and geocenter coordinates, from the analysis of observations from the satellite techniques.

The main concern of the research related to geodynamics was determination of the land motion with geodetic methods. The geodetic methods mainly used for these purposes were GNSS and InSAR with a focus of vertical land motion for determination of the relative sea-level changes as well as landslides and ground deformations caused by seismic tremors. Moreover, geodetic time series related to dynamic effects were carried out, paying attention to environmental loading sensed by GNSS and geocenter motion derived using SLR.

2. Earth rotation

In the period of 2019-2022 Polish researchers involved in the studies on Earth rotation took an active part in the programs of the international scientific organizations, such as the International Association of Geodesy (IAG), International Astronomical Union (IAU) and its Commission A2 Rotation of the Earth ([72]Malkin et al., 2019), International Earth Rotation and Reference Systems Service (IERS). In particular, they made contributions to the activity of the IAU/IAG Joint Working Group on Theory of Earth Rotation and Validation ([18]Ferrandiz et al., 2020), the IAG Inter-Commission Committee on "Geodesy for Climate Research" and its Joint Working Group C.1: Climate Signatures in Earth Orientation Parameters (http://iccc.iag-aig.org/joint-work-groups/215/), the IAU Division A Working Group on Time Metrology Standards (https://www.iau.org/science/scientific_bodies/working_groups/304/), and the IERS Working Group on the 2nd Earth Orientation Parameter (EOP) Prediction Comparison Campaign (https://www.iers.org/IERS/EN/Organization/WorkingGroups/PredictionComparison/predictionComparison.html). The 2nd EOP Prediction Comparison Campaign, originally scheduled for 2021-2023, has been implemented and maintained by the Space Research Centre of PAS in Warsaw. A comprehensive summary of the research on Earth rotation will be given below.

2.1 Geophysical excitation of Earth rotation

The influence of continental water storage and cryosphere on polar motion (PM) excitation was investigated using different data products from GRACE and GRACE-FO missions. Such contribution was assessed by analysis of time series of GRACE/GRACE-FO-based hydrological and cryospheric angular momentum (HAM/CAM) ([79]Nastula et al. 2019; [80]Nastula and Sliwinska 2020; [105]Sliwinska et al. 2020a, [106]2020b, [107]2021a, [108]2021b, [109]2022a; [111]Sliwinska, 2022).

Accepted Article

The achievements of 15 years of HAM/CAM research based on GRACE mission data were summarized in [79]Nastula et al. (2019). HAM/CAM determined using GRACE solutions delivered by seven data centers were compared with hydrological angular momentum (HAM) estimates from hydrological models and climate data, and validated with time series of geodetic residuals GAO (sum of hydrological and cryospheric signal in observed PM excitation) taken as a reference.. Special emphasis was placed on the analysis of non-seasonal changes in PM excitation. A high correlation between GRACE-based HAM/CAM and the corresponding GAO series in this spectral band was found. The lack of realistic information about the ice cover may have contributed to the fact that the HAM series from hydrological and climate models were characterized by a much weaker correlation with the GAO than the series determined from gravimetric data.

HAM/CAM from the two most recent releases (RL05 and RL06) of the GRACE monthly solutions were compared by [80]Nastula and Sliwinska (2020). The prograde and retrograde circular components in gravimetric excitation series were determined by applying complex Fourier transform, and analyzed in seasonal, non-seasonal short-term and non-seasonal long-term spectral bands. GRACE has been shown to be equally accurate in identifying prograde and retrograde oscillations in HAM/CAM. The highest correlation between HAM/CAM and GAO was found for seasonal and non-seasonal long-term oscillations.

A comprehensive assessment of HAM/CAM determined from the newest GRACE Level-2 solutions (degree-2 order-1 coefficients of geopotential, $\Delta C21$, $\Delta S21$) delivered by different data centers was conducted by [105]Sliwinska et al. (2020a). Analysis of HAM/CAM in various spectral bands (oscillations with periods of 1000-3000, 450-1000, 100-450, and 60-100 days) and for several periods of GRACE measurements (data from the beginning, middle and end of experiment activity) showed that exploiting data from the University of Texas at Austin Center for Space Research (CSR) and the Institute of Geodesy of the Technical University Graz, Austria (ITSG) enables the greatest compatibility between HAM/CAM and GAO.

First estimates of HAM/CAM based on data from the novel GRACE-FO mission were analyzed and juxtaposed with GRACE results by [106]Sliwinska et al. (2020b). The study showed that during the initial 19-month period of GRACE-FO measurements, the compatibility between HAM/CAM and GAO was in line with the accord achieved during the initial stage of GRACE activity, and superior to the corresponding compatibility achieved during the final months of GRACE operation. A detailed comparative analysis of HAM/CAM derived from three kinds of data from GRACE/GRACE-FO missions, i.e. $\Delta C21$, $\Delta S21$ geopotential coefficients, terrestrial water storage (TWS) maps based on coefficients of geopotential, and TWS maps obtained from mascon solutions, was conducted. These studies were continued in the subsequent paper ([107]Sliwinska et al., 2021a), where the analysis was extended to include trends, seasonal and non-seasonal changes. A comparison with results from satellite laser ranging (SLR) was also provided. It was demonstrated that HAM/CAM series computed from GRACE/GRACE-FO mascon solutions were in higher consistency with GAO than the same series based on data from other types, particularly with regards to seasonal fluctuations. A detailed analysis of PM excitation derived from mascon data provided by different data centers proved that the choice of mascon solution has no noticeable impact on the level of compliance between HAM/CAM and GAO ([108]Sliwinska et al., 2021b; [111]Sliwinska, 2022). A summary of the research on the use of different types of GRACE and GRACE-FO data products to determine HAM/CAM was included in the PhD thesis of Justyna Sliwinska ([111]Sliwinska, 2022). The thesis was defended with honors in April 2022.

In [111]Sliwinska et al. (2022), several combined HAM/CAM series were computed from GRACE and GRACE-FO solutions using the three cornered hat (TCH) method, which allowed to minimize the noise in the combined series. Individual combined series were calculated as a

Accepted Article

weighted average of single solutions, in which the determined noise had an inverse relationship with the weights. A validation of combined series with the GAO as a reference showed that the proposed approach allows for increased compliance with GAO compared to exploiting single GRACE/GRACE-FO solutions.

The coefficients ΔC21, ΔS21 from temporal gravity field models based on kinematic orbits of several low-Earth-orbit satellites were exploited in ([104]Sliwinska and Nastula, 2019) to determine HAM/CAM. The study revealed that the quality of HAM/CAM computed from data of this type is highly dependent on orbital altitude and inclination of satellite used. Models based on Swarm data were proved to be the most appropriate for analysis of PM excitation.

Historical simulations from the sixth phase of the Coupled Model Intercomparison Project (CMIP6) were utilized to verify whether climate models offer plausible data for determining HAM ([82]Nastula et al., 2022). Climate-based HAM series were compared with GAO, GRACE-based HAM/CAM and HAM obtained from the Land Surface Discharge Model (LSDM). Overall, the agreement between GAO and HAM derived from CMIP6 was less than the previous agreement established with the GRACE scores, and the level of consistency varied depending on the model and oscillations considered. Nevertheless, some CMIP6 models may produce reliable HAM data, especially for annual variations.

Various datasets were used by [126]Winska and Sliwinska (2019) and [127]Winska (2022) to determine the geophysical excitation of PM. [127]Winska (2022) focused on interannual oscillations in PM excitation calculated using different atmospheric and ocean models, GRACE/GRACE-FO data, and LSDM. Interannual oscillations in PM excitation were retained using the Multi Singular Spectrum Analysis method. The primary finding of the research indicates that adding hydrological considerations to the coupling of atmospheric and oceanic excitations enhances the consistency between geophysical and geodetic excitation in the interannual spectral band. However, the models still need some amelioration to reduce non-negligible differences between geodetic and geophysical estimates of PM excitation. [126]Winska and Sliwinska (2019) focused on various estimates of GAO computed as differences between geodetic and joint atmospheric and oceanic excitation. It was shown that the choice of atmospheric and oceanic models has a considerable influence on amplitudes of GAO but affects the GAO phases to a much lesser extent.

Celestial pole offsets (CPO) predictions developed at the Jet Propulsion Laboratory (JPL) with the use of Kalman filter and smoother were evaluated by [81]Nastula et al. (2020) for 90-day forecast horizon. The JPL predictions were compared with corresponding forecasts delivered by the IERS and with IERS observational data. JPL prediction errors have been shown to increase less rapidly with prediction day than errors of forecasts processed at IERS. When JPL predictions were employed instead of IERS predictions, the root mean square differences between forecasted and observed celestial pole offsets (CPOs) were reduced by 43% for dX and 33% for dY at 90th day of prediction.

2.2 Research on the methods of monitoring Earth rotation

Polish scientists contributed during 2019-2022 to the investigations concerning the methods of determination of global geodetic parameters including Earth rotation parameters and coordinates of the geocenter based on the satellite techniques: Satellite Laser Ranging (SLR), Global Navigation Satellite Systems (GNSS) and Doppler Orbitography and Radiopositioning Integrated by Satellite (DORIS).

[52]Kosek et al. (2020) reported results of the determination and analysis of the common signals in the geocenter motion determined by GNSS, SLR, DORIS, and GRACE, with particular attention paid to seasonal components. The amplitude of the annual term was estimated at the level of 2 mm for the X coordinate, 2.4 to 3.6 mm for the Y coordinate and 2.8

Accepted Article

to 5.6 mm for the Z coordinate components, while the semiannual term was found about 2 times smaller than the annual one. Detailed analysis revealed that the seasonal signals computed in the study were not stable in time and there were considerable divergences between the outcomes derived from various techniques.

The paper by [131]Zajdel et al. (2020) discussed estimation of polar motion (PM) coordinates, rates of the pole coordinates, and Length-of-Day, commonly referred to as Earth Rotation Parameters (ERP). The GPS, GLONASS, and Galileo daily estimates of ERP have been evaluated with a detailed search for system-specific signals. The ERP estimates have been compared to the IERS-C04 series and the products of IGS analysis centers. [132]Zajdel et al. (2021a) derived the sub-daily polar motion series based on GPS, GLONASS and Galileo observations. The first empirical models of sub-daily PM have been developed with 38 main tidal harmonics, separately for each participating GNSS system and multi-GNSS solution. The solutions have been compared to other available sub-daily models, the Desai-Sibois model (based on hydrology), IERS 2010 Conventions model (mixed) and the Gipson model (from VLBI).

[128]Yu et al. (2021) recomputed weekly time series of geocenter motion determined using SLR data. Observations from LAGEOS 1/2 satellites covering the period from 1994 to 2020 were processed with Bernese GNSS Software 5.2. For computing the GCM (Geocenter Motion) time-series, the network shift approach was used. To separate and research on the geophysical signal inside the series, the SSA method was applied. First two Principal Components (PCs) with large w-correlation were regarded as one periodic signal pair. With this method the substantial annual signal in X, Y and Z components were detected. Moreover, semi-annual oscillations were found to be significant in X and Z components. Moreover, other periodic signals were identified and explained by draconitic effects or/and aliasing of K1/O1, T2, and Mm tides. However, overlapping effects of the ground-track repeatability of SLR satellites data should also be considered. Systematic differences in X and Z components suggest a better distribution of SLR stations for recover the GCM in Y component.

[133]Zajdel et al. (2021b) searched for common patterns in geocenter coordinates derived from GPS, GLONASS, and Galileo observations. Three years of data collected at the globally distributed stations were considered. They tested all individual solutions as well as combinations of data from the aforementioned GNSS constellations. They proved that using a box-wing model a priori information on forces related to the solar radiation pressure (SRP) acting on satellites mitigates most of the spurious signals in geocenter coordinates originated from the different navigation satellite systems. They concluded, that combination of Galileo and GPS solutions take the lead to the best geocenter estimates.

[14]Drozdzewski et al. (2019) investigated the problem of how modeling of horizontal gradients in the SLR technique influences the determination of PM coordinates and Length-of-Day. So far, SLR was the only satellite geodesy technique in which the asymmetry of the atmosphere has been not accounted for in modeling the tropospheric delay. The model of horizontal gradients, developed in the paper, improves the consistency of SLR-derived and the IERS C04 PM series by reducing the offset for the pole coordinates by about 20 microarcseconds (μas).

The paper by [115]Strugarek et al. (2019) discusses the determination of global geodetic parameters, including pole coordinates and UT1-UTC from the laser ranging to LEO satellites, Sentinel-3A and 3B as well as from the combined LAGEOS-1/2 and Sentinel-3A/B solutions. [113]Sosnica et al. (2019) considered the estimation of global geodetic parameters including pole coordinates and Length-of-Day by the use of SLR observations to Galileo, GLONASS, BeiDou, GPS, and QZSS. The ERPs were derived by applying the approaches with the orbits based on the SLR observations and with orbits based on microwave GNSS observations.

Accepted Article

Finally, the ERP solutions based on the observations of LAGEOS-1/2 were compared to the GNSS-only solutions.

[10]Bury et al. (2021a) applied the combination of SLR and GNSS observations for the determination of precise Galileo orbits and geodetic parameters including the Length-of-Day. The secular drift which is present in cumulated Length-of-Day series from GNSS-only solutions could be significantly reduced when using the combined GNSS-SLR solution with an equal weighting of GNSS and SLR observations. In the paper [11]Bury et al. (2021b) the integration of SLR and GNSS techniques onboard the Galileo and GLONASS satellites was used for different realizations of the terrestrial reference frame. The paper investigated how the minimum no-net-rotation and no-net-translation network constraints influence the estimation of station coordinates and Earth rotation parameters including Length-of-Day variation.

[129]Zajdel et al. (2019a) investigated the so-called GNSS network effect, the question of how the inhomogeneous distribution of GNSS stations influences the estimation of global geodetic parameters. In addition, the authors verified the influence of the network constraints and the realization of the origin of the terrestrial frame on the estimation of the pole coordinates and Length-of-Day variation. When accounting for the geocenter motion in GNSS solutions, the pole coordinates are changed by about 12 μas (in a sense of Weighed Root Mean Square – WRMS) and Length-of-Day by 1-2 μs. [130]Zajdel et al. (2019b) addressed the problem of how the selection of SLR stations for the realization of no-net-rotation constraints influences the accuracy of estimation of the pole coordinates and Length-of-Day variation in the solutions based on the SLR observations to LAGEOS-1/2.

Polish researchers continued during 2019-2022 investigations on the application of the large Ring Laser Gyroscope (RLG) for continuous monitoring of variations in Earth rotation. [123]Tercjak et al. (2020) studied in detail the impact of solid Earth tides, ocean tidal loading and non-tidal loading phenomena (influences of the atmosphere and continental hydrosphere) on the main RLG observable, the Sagnac frequency. They also discussed potential causes of existing discrepancies between the data reduced with the use of tiltmeter measurements and the data reduced with model-based signal. Recently, a four-component, tetrahedral laser gyroscope array ROMY has been constructed at the Geophysical Observatory Fuerstenfeldbruck near Munich ([20]Gebauer et al., 2020). Preliminary analysis of the initial measurements of ROMY (ibid.) demonstrated that reconstruction of all coordinates of the Earth rotation vector over the period of six weeks and the sub-arcsecond spatial resolution is possible. [124]Tercjak (2021) concluded research on the interpretation of RLG observations by defending her PhD Thesis with excellent note.

2.3 The second Earth Orientation Parameters prediction comparison campaign

Predictions of EOP are needed for different operational activities like navigation of deep-space satellite missions or global satellite positioning and navigation systems. The first EOP Prediction Comparison Campaign (EOP PCC), run by Vienna University of Technology and Space Research Centre PAS in Warsaw (Kalarus et al., 2010, https://doi.org/10.1007/s00190-010-0387-1), considerably contributed to the assessment of different EOP prediction capabilities. The current need for improved EOP predictions prompted the establishment of the second EOP PCC under the auspices of the IERS. As in case of the 1st EOP PCC, the current campaign is again managed by SRC PAS with support from the GFZ Potsdam. So far, 28 institutions from 9 countries registered to the 2nd EOP PCC, and over 60 researchers have been delivering EOP predictions. The paper by [111]Sliwinska et al. (2022) provided overview of the 2nd EOP PCC, including preliminary comparison of the IERS 14 C04 EOP reference series and selected EOP prediction solutions; see also the official campaign website https://eoppcc.cbk.waw.pl/ (accessed 29.03.2023). A more detailed validation of selected short-

Accepted Article

term forecasts of the universal time UT1-UTC and the length-of-day LOD collected by the EOP PCC was reported by [61]Kur et al. (2022). Particular attention in this evaluation is paid to the forecasting methods based on the Effective Angular Momentum predictions.
One Polish research group from the AGH University of Science and Technology, Krakow, has been delivering EOP predictions to the 2nd EOP PCC. [75]Michalczak et al. (2022) computed the ultra-short-term and short-term (up to 15 and 30 days into the future, respectively) predictions of polar motion coordinates (PMx, PMy) and LOD using geostatistical method of kriging and autoregressive integrated moving-average (ARIMA) method. Detailed description of the kriging-based predictions of polar motion can be found in [73]Michalczak and Ligas (2021), while the application of kriging for LOD predictions was discussed by [74]Michalczak and Ligas (2022). The authors concluded that the kriging-based short and ultra-short term prediction applied to both PM and LOD may compete with other existing prediction algorithms. [75]Michalczak et al. (2022) stated also that ARIMA-based prediction is more accurate than kriging-based one for very short term prediction.

3. Geodynamics

3.1 Geodetic time series analysis

The main task of geodetic time series analysis is to discover significant and/or unknown oscillations inside the series, as well as to study the noise of the residuals after the deterministic model is taken into account.

[49]Klos et al. (2020a) compared 6 different approaches to extract seasonal signals from the GPS-derived position time series. They analyzed results obtained using commonly applied Least Squares Estimation (LSE), Wavelet Decomposition (WD), Moving Ordinary Least-Squares (MOLS), Kalman Filter (KF), Singular Spectrum Analysis (SSA), and newly applied Adaptive Wiener Filter (AWF). The advantages or disadvantages of each method were described with an emphasis on Power Spectral Density (PSD) appearance after the extraction. First, the tests were performed on the synthetic database, created upon certain assumptions concerning seasonal signals, then real displacement time series reduced by environmental loadings were analyzed. The studies were followed by noise analysis using Hector software because the main purpose of the study was to investigate the use of such a method of eliminating seasonal curves that changes the nature of stochastic part of the series as minimum as possible. The SSA and AWF were found as appropriate methods that meet this condition to the greatest extent.

[50]Klos et al. (2020b) adopted the GRACE-assimilating land surface model (CLM-DA) for separating the deterministic part of GPS (Global Positioning System) derived position time series from noise. They used data from 221 continuously operating stations of the EUREF (European Reference Frame) Permanent GNSS Network (EPN) located in Europe. The navigational data were processed at the ASI (Italian Space Agency) using the Precise Point Positioning (PPP). They confirmed, that a reduction of up to 60% of annual and semiannual amplitudes in position time series reduced by atmospheric and non-tidal loading comes from considering CLM-DA model in the series. The remaining part may come from draconitics or aliasing, being the systematic errors of GPS. They compared the results obtained to those recovered from the classical approach using harmonic functions, however, the latter cannot provide physical interpretations of the results since it was difficult to decouple each individual physical process that contributed to seasonal changes. Insufficient consideration of seasonal signals may induce an artificial change of the stochastic parts of the series, and resulting in mis-determinations of uncertainties of determined trends or amplitudes of seasonal signals. They

Accepted Article

concluded, that in the view of current and future International Terrestrial Reference Frames (ITRFs), including loading effects based on the GRACE data may contribute to a better realization.

[51]Klos et al. (2021) examined the sensitivity of the GPS for environmental loadings. They used vertical displacements from 100 permanent stations being processed at the Nevada Geodetic Laboratory in the PPP mode. All selected stations were located in continental Eurasia with a minimal time span of 5 years each. Non-tidal loading models were delivered by the Earth-System-Modeling Group of Deutsches Geo-ForschungsZentrum (ESMGFZ). Non-tidal atmospheric (NTAL), non-tidal ocean (NTOL), hydrological loadings (HYDL), and barystatic sea-level changes (SLEL) were interpolated to GPS positions from the gridded crustal displacements using bicubic interpolation method. They used Wavelet Decomposition (WD) with a Meyer wavelet which enables signals to be acquired at various temporal resolutions. The analyzed data allowed the extraction of nine levels of details, and the final approximation. Using Pearson correlation coefficients between GPS-derived vertical displacements and displacements predicted from environmental models for different levels of decomposition concluded that improper recognition of the loading impact may significantly bias the determination of the velocities and amplitudes of the seasonal signals. Finally, they studied the impact of non-tidal loading on character of the GPS noise, noting that different loading effects have different impacts on the stochastic parts of the GPS-derived position time series.

[42]Kaczmarek (2019) focused on the analysis of geophysical signal, in particular, the crustal deformation of the Earth induced by HYDRO, NTAL, and NTOL (non-tidal ocean) loads as well as the influence of these geophysical signal on the coordinate of permanent GNSS stations in Central Europe. The author analyzed time series of coordinates from BOR1, LAMA, WROC, PENC, GRAZ, GOPE, POTS, and JOZ2 permanent GNSS stations obtained from the CODE (Center for Orbit Determination in Europe). In order to identify whether deformations from geophysical signal on these stations are globally- or locally-related, he analyzed the correlation between GNSS time series coordinates of station selected and the Earth's surface deformations resulted from the aforementioned geophysical signal. Moreover, the author performed a coherence analysis to investigate whether similar seasonal deformations are observable within the GNSS time series coordinates of the GNSS stations investigated. He concluded that the crustal deformations of the Earth induced by NTAL have the major impact on temporal variations of GNSS time series coordinates. On a global scale, geophysical signal exhibited a clear impact on the Up component of GNSS time series coordinates analyzed. The horizontal components of GNSS coordinates may substantially be affected by local conditions surrounding the GNSS station, rather than geophysical signal. On the basis of coherence analysis, he found totally various seasonality in the North, East and Up components of GNSS stations investigated.

[46]Karkowska and Wilde-Piorko (2022) presented a new concept of using the recordings of tidal gravimetric for, reliably, determining the Earth's structure in a regional scale. This concept is based on measuring and inversing the dispersion's curve of Rayleigh Surface Waves (RSW) of intermediate-periods (i.e. period 10-180 s). They analyzed time series data from tidal gravimeters and co-located broadband seismometers. These data were obtained from three gravimetric stations (two in Belgium and one in Germany) with estimated transfer functions (TF) and co-located with seismic stations. They proposed the deconvolution of the TF for pre-processing of gravimetric data. They also determine group velocities of fundamental-mode of RSW recorded by tidal gravimeters and co-located seismometers. They also applied a linear inversion algorithm to retrieve S-wave velocity models for Central and Southern Europe. As a conclusion, they reported that tidal gravimeters provide very reliable recordings of period 10-180 s surface waves, as good agreement between the outcomes from gravimeters and

Accepted Article

seismometers can be obtained. They also illustrated the potential of gravimeters, especially the superconducting ones, and seismometers for the determination of the Earth's structure on a regional scale.

[47]Karkowska et al. (2022) analyzed the earthquake's tidal gravimeters recordings in the period of 10-1000 s. Three observatories, namely Membach and Rochefort in Belgium as well as Black Forest in Germany, in Western and Central Europe were chosen as a case study. They investigated over 10,000 traces of worldwide earthquakes recorded by tidal gravimeters and co-located very broad-band and very broad-band seismometers. The results obtained by them indicated that earthquakes' gravimetric recordings in the period of 10-1000 s and the corresponding ones from seismic data agree very well. The coefficient of correlations between the results obtained from seismometric and gravimetric data are ranging from –0.67 to –0.86. After elaborating the transfer function scheme, those coefficients of correlations became –0.9975±0.0005. Moreover, they illustrated that for determining the greater depths of Earth's mantle structure, the recording of tidal gravimeters provides complementary information to their respective ones obtained from seismometers.

[102]Rosat et al. (2020) compared time series of vertical displacements determined from GPS observations and gravity changes from superconducting gravimeters (SG). Due to the similar driving mechanism combining vertical and gravity changes, the transfer function of the Earth related to its rheological properties at various time-scales was able to be determined. The navigational data from 117 globally distributed permanent GPS stations were processed using GAMIT/GLOBK software including non-tidal atmospheric and oceanic effects with 9 of them being selected to the final analysis. Concerning SG observations, they used Level-3 products from the International Centre for Earth Tides (IGETS) cleaned from gaps, spikes and significant steps. For consistency, the same corrections for geophysical effects as in the case of GPS were implemented. With the use of these data, they determined the spectral coherency as well as gravity-to-height ratio, which is a real part of the transfer function between gravity reduced to the Earth's surface and height changes. They concluded that this ratio varies between analyzed stations significantly (from –5 to +1.1), which indicates a strong dependence on local mass fluctuations.

[101]Ray et al. (2021) analyzed the correspondences between the annual oscillations of deformations determined with GPS and GRACE data. As a case study, they chose Nepal Himalaya and North-East India. This region is subjected to significant annual changes due to the monsoons. Thirty six GPS permanent stations as well as release 05 (RL05) GRACE-based Global Geopotential Models (GGMs) were chosen. Daily position time series expressed in ITRF2008 were obtained from navigational data processed using GAMIT/GLOBK software. The temporal variations of Equivalent Water Heights (*EWH*) were provided by the NASA MEaSUREs (Making Earth Science Data Records for Use in Research Environments) program with a root data in the form of spherical harmonics coefficients of RL05 GRACE-based GGMs. The seasonal deformations were determined using the CATS (Create and Analyse Time Series) software. Their results showed that almost 90% of the analyses series revealed positive correlation between seasonal deformations determined using both satellite methods in North component. Finally, they estimated the median value of Nash-Sutcliffe model Efficiency (NSE) to –0.01 and +0.28 for East and North components, respectively. This research confirmed, that seasonal horizontal deformations in the investigated area were mostly driven by local tectonics.

[83]Nistor et al. (2021) investigated the seasonal signals, i.e. annual and semiannual oscillations, within the GNSS position time series. They considered the correlations between different types of geophysical events, namely volcanic activity, landslides, and earthquakes. The main aim of the research was to explore variation in amplitudes of the mentioned seasonal signals. The overlapping Hadamard variance (OHVAR) was applied to search for the presence

Accepted Article

of random walk and flicker noise. Moreover, the non-stationarity of the GNSS position time series was performed using continuous wavelet transform (CWT).

[65]Lyszkowicz et al. (2021a) used the GipsyX software to investigate the position time series of the GNSS permanent network in Poland. They selected the time span of GNSS data used, covering the period from 2011 to 2018. They concluded that the velocities of the Polish permanent GNSS stations can be determined with an accuracy of 0.01 mm/yr.

[3]Baselga and Najder (2019) presented an automated algorithm for the analysis of the position time series of the EPN stations neighboring an earthquake epicenter. This tool was named ADDquake (Automated Detection of Discontinuities in EPN stations due to earthquake events) which was developed using App Designer tool of Matlab release 2020b. Earthquakes data from the U.S. Geological Survey and GNSS time series coordinates provided for EPN stations were used as input for the ADDquake. As examples, the authors considered two significant earthquakes that occurred in Europe: L'Aquila (Mw 6.3) and Lorca (Mw 5.1) which took place on 6 April 2009 and on 11 May 2011, respectively. With the use of the ADDquak, they presented the analysis of time series of GNSS coordinates from ALBA, ALAC, and ALME permanent GNSS stations covering the period before and after these earthquakes. The authors made the ADDquak freely available for users via the website.

On the basis of SLR, DORIS and VLBI (Very Long Baseline Interferometry) station positions and velocities in ITRF2008, [37]Jagoda et al. (2020a) determined the motion parameters of six chosen tectonic plates, i.e. the position of pole rotation (Φ, Λ) and the angular rotation velocity (ω). The least squares sequential adjustment approach was implemented to analyze the data from each technique (i.e. SLR, DORIS and VLBI) separately. The agreement between Φ, Λ and ω determined by them and the corresponding ones from the APKIM2005 (Actual Plate Kinematic and Crustal Deformation Model 2005) IGN (Institute of National Geography, France) model was at the level of 2° or better. However, they reported that the location of SLR, DORIS and VLBI stations is essential for the reliable resolve of Φ, Λ and ω.

[35]Jagoda and Rutkowska (2020a) estimated and analyzed Eurasian plate motion and its parameters, i.e. Φ, Λ and ω, using ITRF2014 velocities and positions of 120 GNSS stations. For this purpose, four scenarios, with 30 GNSS stations each, were created considering the stable region and the boundary of the Eurasian plate. The results obtained revealed good agreement between estimated values of Φ, Λ and ω from these four scenarios, as for Φ and Λ the maximum differences were at the level of 0.31° and 0.24°, respectively, while there were no differences for ω. When analyzing all selected GNSS stations (i.e. 120 GNSS stations), they found that the estimated Eurasian plate motion parameters were 54.81°±0.37° for Φ, 261.04°±0.48° for Λ, and 0.2585°/Ma±0.0025°/Ma for ω which is consistent with the corresponding values published in the literature, e.g. the APKIM2005 IGN model.

[36]Jagoda and Rutkowska (2020b) investigated the use of VLBI measurements for resolving of Φ, Λ and ω. For this purpose, velocities of positions in the ITRF2008 for VLBI stations distributed within six tectonic plates, i.e. EUAS, AFR, AUS, North NOAM, PACF and ANTC, were analyzed using sequential least squares adjustment procedure. The values Φ, Λ and ω determined from VLBI measurements were compared with those obtained from the APKIM2005 model. Overall, despite the inhomogeneous distribution of VLBI stations within major tectonic plates investigated, they found good consistency (i.e. discrepancies were within the level of 2°) between Φ, Λ and ω obtained from VLBI and APKIM2005 model.

[39]Jagoda (2021) focused on the determination and analysis of Φ, Λ and ω of five selected tectonic plates. The author determined Φ, Λ and ω using ITRF2014 GNSS velocities stations positions. The author also proposed and applied the sequential least squares adjustment method to estimate Φ, Λ and ω. Then, those Φ, Λ and ω were compared with those from the No-net-rotation model of geologically current plate motions (i.e. NNR-MORVEL56) and the

Accepted Article

ITRF2014-PMM geodetic model. The results obtained indicated that the difference between parameters of the plate motion (i.e. Φ, Λ and ω) determined using the sequential least squares adjustment method and the corresponding ones obtained from the NNR-MORVEL56 and/or ITRF2014-PMM do not exceed the level of ±3.88° for Φ, ±6.95° for Λ, and ±0.022°/Ma for ω. The sequential method proposed by the author was beneficial to optimize the data volume required to obtain a stable solution as well as to identify stations that can corrupt the solution's quality and amplify the errors of the Φ, Λ and ω estimated.

With the use of SLR data from LAGEOS-1/2 satellites, [32]Jagoda and Rutkowska (2019a) estimated the values of Love and Shida numbers (h_2 and l_2) which are connected to the tidal variations at the Polish SLR station located in Borowiec. These SLR data covered the period from January 1, 1999 to January 1, 2019. The sequential adjustment method was applied to estimate h_2 and l_2. They found that the values of h_2 and l_2 were equal to 0.7308±0.0008 and 0.1226±0.0003, respectively, which were significantly different (i.e. the difference reach up to 0.1230 (ca. 20%) for h_2 and 0.0379 (ca. 44%) for l_2) with the respective ones from the International Earth Rotation and Reference Systems Service (IERS) and from the previous research conducted by other scholars as well. The authors ascribed these differences to the length of data used in previous research (i.e. 2 years of SLR data) and the one used by them. Moreover, the coordinates of Borowiec station were determined using two sets of h_2 and l_2: (1) from [32]Jagoda and Rutkowska (2019a) and (2) from the IERS. The authors found that the differences between *X, Y, Z* components determined using these different sets of h_2 and l_2 were 3.5, 3.3 and 4.2 mm, respectively. Furthermore, following the same procedure presented in [32]Jagoda and Rutkowska (2019a), h_2 and l_2 for Riga SLR station were estimated using LAGEOS-1 and LAGEOS-2 satellite data covering the period of 01.01.2004-01.01.2019 ([33]Jagoda and Rutkowska, 2019b). The results obtained by them revealed that the values of h_2 and l_2 for Riga SLR station were 0.6891±0.0009 and 0.1043±0.0004, respectively, which were differ by 0.0813 for h_2 and 0.0196 for l_2 from the values provided by the IERS. The differences between *X, Y, Z* coordinates determined with the use of h_2 and l_2 obtained by them and corresponding coordinates obtained from the ITRF2014 were 4.4, 4.7 and 6.9 mm, respectively.

[34]Jagoda et al. (2019) assessed the effect of using different values of h_2 and l_2 on the determination of the coordinates of the selected SLR stations. With the use of SLR data from LAGEOS-1 and LAGEOS-2 satellites covering the period January 01, 2008- January 01, 2018, they estimated the values of h_2 and l_2 at these selected SLR stations. Then, on the basis of ITRF2014, the coordinates of SLR stations investigated were determined using the h_2 and l_2 estimated by them and the respective ones from the IERS. The comparison between the determined coordinates indicated that the use of different values of h_2 and l_2 can result in coordinate differences from –2.3 to 3.3 mm for *X*, from –2.7 to 4.1 mm for *Y*, and from –3.2 to 4.9 mm for *Z* coordinate.

[38]Jagoda et al. (2020b) focused on the determination and analysis of local h_2 and l_2 values for Mount Stromlo and Yarragadee SLR stations. Data from LAGEOS-1, LAGEOS-2, STARLETTE, and STELLA covering the period January 01, 2014-January 01, 2019, were used. The authors implemented the sequential method to determine h_2 and l_2. Thereafter, the authors compared these h_2 and l_2 determined with the corresponding ones from the IERS. They reported that l_2 cannot be reliably determined from STARLETTE and STELLA satellites data. On the biases of the combination of LAGEOS-1/2 satellites data, they found that for station Yarragadee were 0.5756±0.0005 for h_2, and 0.0751±0.0002 for l_2, which were differed by 5% and 11% from the corresponding values from the IERS, respectively. The combination of STELLA and STARLETTE satellites data indicated that h_2 was equal to 0.5742±0.0015, and it differed by 6% from h_2 provided by the IERS. For station Mount Stromlo, the h_2 obtained by

Accepted Article

combining STELLA and STARLETTE satellites data was 0.5618±0.0017, and it differed by 7% from the respective one of the IERS, while local h_2 and l_2 determined by combing LAGEOS-1/2 satellites data were 0.5601±0.0006 and 0.0637±0.0003, respectively, and there were differed by 8% for h_2 and 0.021 25% for l_2 from the respective ones given by the IERS. Moreover, they compared the coordinates (*X, Y, Z*) of Mount Stromlo and Yarragadee sites determined with the use of these local and IERS h_2 and l_2. The results of these comparisons indicated that using different estimates of Love and Shida numbers can induce coordinates discrepancies of approx. –3.5±0.3 mm, 4.5±0.5 mm and 5.3±0.2 mm for *X*, Y and *Z* coordinates, respectively.

[12]Cegla et al. (2020) investigated the use of a simplified approach based on: GNSS data and weather data from a numerical model and in-situ observations, to detect the volcanic plume over the area of Sakurajima volcano in Japan. Within the activity period of the volcano (i.e. during October 2014), zenith tropospheric delays (ZTD) were estimated using GNSS data from the a network in Sakurajima area. Moreover, ERA5 atmospheric data as well as eruption information and weather observations were utilized. They found that semblance analysis (i.e. time series analysis) of ZTDs from GNSS, ray-traced ERA5 and weather data were appropriate to reveal the effect of volcanic plumes. In a conclusion, the analytic approach implemented by them can reliably determine the volcanic plume activity over the area of Sakurajima.

[22]Godah (2019) developed an open source scientific software, named IGiK-TVGMF, for the determination of temporal variations of gravity/mass functionals (TVGMFs) in the Earth's system using GRACE data as well as for analyzing and modelling TVGMF. This software was developed within the project entitled (European Plate Observing System-Poland)- task Gravimetric Observations Research Infrastructure Centre). The IGiK-TVGMF software was developed using the MATLAB R2017a App Designer. With the use of this software, thirteen TVGMFs can be computed using monthly RL05 GRACE-based GGMs developed by seven different computation centers. The results obtained from IGiK-TVGMF software were validated using the corresponding ones from the ICGEM (International Centre for Global Earth Models) interactive online tool and GRAVSOFT scientific software. This validation indicated good agreement, e.g. sub-mm in terms of temporal variations of geoid height, between TVGMFs values from IGiK-TVGMF software and the respective ones from GRAVSOFT and ICGEM interactive online tool.

3.2 Monitoring of the crustal movement with geodetic methods

For more than 20 years, GPS technology has been used effectively to investigate the dynamics of the Earth. Lately, the InSAR (Interferometric Synthetic Aperture Radar) technique has also been a prominent source of information to investigate the deformations of both the Earth's surface and man-made structures.

[9]Bogusz et al. (2019) proposed a set of recommendations concerning GNSS-derived position time series to properly investigate dynamic effects of the Earth's crust. They perform a complex analysis of 469 European GPS vertical position time series from the Nevada Geodetic Laboratory (NGL) obtained through the PPP method. Sixty two of them were identified to have significant non-linearities, as a consequence the polynomial trend model (PTM) has been applied to properly describe the deterministic part. The ICE-6G_C (VM5a) and ICE-5G (VM2) models of Glacial Isostatic Adjustment (GIA) were used for comparison purposes. The vertical time series were then analyzed using Maximum Likelihood Estimation (MLE) method. For the stochastic part, the combination of white and power-law noise was assumed as optimal. Spectral indices were found to vary between –1.2 and –0.3, while maximum amplitude of the power-law noise was equal to 28.0 mm/yr$^{-k/4}$. Owing to this 297 out

Accepted Article

of 469 stations were found to have significant vertical rates and further analysis might be required. Comparison with present-day uplift predicted by the GIA models showed the differences reached 0.5 mm/yr on average. The assumptions they proposed should be employed to perform the GIA-oriented comparison, however, method is universal and applicable to the series recorded at each locations with strong geodynamical effects.

In recent years, the Military University of Technology (MUT) and Polish Geological Institute – National Research Institute (PGI-NRI) continued research on the neotectonics of Poland. [40]Jarosinski et al. (2022) investigated the possibility of using geodetic satellite measurements to assess the magnitude of contemporary stress in an area of northern Poland. This is a relatively stable area, located on the East European Platform, the Paleozoic Platform and the Teisseyre-Tornquist Zone separating them. This study used GPS data from 63 stations of the ASG-EUPOS (Active Geodetic Network of the European Position Determination System) network, of which 35 remained after filtering. The strain rate was estimated using the least square collocation (LSC) method. The results published in this paper illustrated a high correspondence between the directions of the main strain rate and the stress directions determined from the boreholes. The main problem that arose in the study was the accuracy of the estimated strain rate. The strain rates obtained, ranging from $4.3x10^{-17}$/s to $8.7x10^{-17}$/s, are generally consistent with the strength of the lithosphere for each block. Unfortunately, the estimated strain rate error was between $4x10^{-17}$/s and $10x10^{-17}$/s, depending on the local density of ASG-EUPOS stations. Thus, it may seem that the estimated deformations are not reliable. However, they were consistent with stress directions as well as strain magnitudes from other works, tectonic history and the current stress regime for considered area. The authors hypothesized that if station velocities exhibit some random residual instability, but are limited due to the prior filtering used, then with a model smoothing method (such as LSC method), this randomness can sufficiently be reduced which leads to a clear illustration of the tectonic signal.

[62]Ligas et al. (2019) presented a method for approximating the planar deformation that consists of components of rotation and tensor. This method was based on the distance-weighted affine transformation model performed on regular and irregular grids generated with the use of the Swirl-like and Barrel-Pincushion deformations. The grid's area size selected was 500 m^2. The outcomes of this method were compared with the corresponding ones obtained using a simplified decomposition method. The results obtained by them indicated a good performance of the proposed method. For example, for ca. ≥90% of the grid's points, good agreements (e.g. measurements error range from zero to ca. ±0.0002, and correlation coefficients range from 0.82977 to 0.99925) between true and estimated strain components were obtained. However, the authors reported that unreliable results can be obtained from this simple method when there were small strain tensors and non-negligible rotation components.

[41]Jozkow et al. (2021) assessed the prospect of Unmanned Aerial Systems (UAS) data: aerial photos and Light Detection and Ranging (LiDAR), for monitoring the terrain vertical deformations caused by underground mining in the Upper Silesia region. The UAS data used in their research were collected via three campaigns conducted with the period 2018-2019. Methods based on point cloud analysis and DTM of Difference (DoD) were implemented to handle these data. The terrain vertical deformations from ALS (Airborne Laser Scanning) data acquired in 2011 were also evaluated. They found a subsidence of 33 cm for the period 2011-2018, which results in a subsidence of ca. 5 cm/yr. For the period 2018-2019, depending on the investigated area within the Upper Silesia region, a subsidence of ca. 5 to 15 cm can be obtained.

Vertical deformations of the Earth's surface (VDES) at 25 sites of ASG-EUPOS in south-eastern Poland were studied by [23]Godah et al. (2020a). For the period 2008-2013, monthly VDES were compued from: (1) release 06 (RL06) GRACE-based GGMs using the IGiK-

Accepted Article

TVGMF software, and (2) daily GNSS data processed with the GAMIT/GLOBK software. Then, comparisons between those monthly vertical deformations were conducted. The results obtained revealed good agreement between monthly VDES determined from GRACE data and the corresponding ones from GNSS data. Standard deviations of differences between these VDES are in ranging from 2.6 to 5.7 mm, while they are correlated to each other with corr. coef. range from 0.60 to 0.90.

[24]Godah et al. (2020b) investigated the orthometric/normal heights change ($\Delta H/\Delta H^*$) over 24 large river basins using GRACE data. These $\Delta H/\Delta H^*$ were computed by combining time-varying of geoid/quasigeoid heights and ellipsoidal height changes estimated using the RL06 of monthly GRACE-based GGMs, load Love numbers based on PREM (Preliminary Reference Earth Model), and the IGiK-TVGMF software. The authors found that for the Amazon basin, $\Delta H/\Delta H^*$ reach 8 cm, while $\Delta H/\Delta H^*$ do not exceed ±1 cm in the case of the Orange basin. They also investigated the relation between the time-varying of equivalent water thickness (ΔEWT) and $\Delta H/\Delta H^*$ over those 24 large river basins. They found that strong correlations between $\Delta H/\Delta H^*$ and ΔEWT in 87% of river basin areas investigated with 45% reveal corr. coef. range from −0.97 to −0.70. Furthermore, they analyzed $\Delta H/\Delta H^*$ determined over Amazon and Orange using the PCA/EOF (Principal Component Analysis/Empirical Orthogonal Function) method. The results of this analysis indicate substantial differences for $\Delta H/\Delta H^*$ within subareas of the same river basin (e.g., ±2 cm in the Amazon basin). These substantial differences are highly dependent on different spatio-temporal hydrological phenomena (e.g. the precipitation, rainfall seasonality floods, and droughts, as well as the location of the downstream and upstream areas of the river basin,) of the entire river basin.

[116]Szafarczyk (2019a) discussed the landslides on the slopes of the Swinna Poreba dam reservoir in Poland. The author reported that heavy rainfall in May 2010 was one of the main reasons for the ongoing landslide that affected an area of 0.3 hectares. The magnitudes of landslides on the main slopes were estimated to 0.5-1.5 m, and do not exceed 0.5 m within the area of headwaters. In general, these landslides were located on the eastern side of the stream. The geological structure, erosional properties of the stream, and slope of the valley in addition to the rainwater were also contributed significantly to landslides on the slopes of the Swinna Poreba dam. Overall, she emphasized the need for ensuring the entire slopes of the stream in the area of the Swinna Poreba dam and their impedance for mass transport within the area of this dam.

[117]Szafarczyk (2019b) focused on the use of GPS and GBInSAR (ground-based radar interferometry) technology for investigating the impact of kinematic mass variations on the determination of landslides. The author aimed to study the landslides placed in the selected open-pit mining area in Poland. She utilized 38 radarograms from GBInSAR data, as well as seventeen positions of points obtained using GPS RTK (real-time kinematic) technologies and total stations. The author illustrated that the determination of the landslide trend can be improved by eliminating the non-linear landslide in a 24-hour period. She also reported the advantage of GBInSAR technology for mentoring landslides, particularly, over inaccessible areas.

[118]Szafarczyk et al. (2019) focused on the application of measurements using gyroscope in underground mining, in particular, the mines of Zofiowka and Borynia in Katwit. The orientations between these two mines as well as between each individual mine with respect to two GPS stations of the ASG-EUPOS network were obtained using the Sokkia model SX1 gyroscope. For this purpose, also angular-linear measurements as well as static GPS measurements and spirit levelling were also used. The authors compared the topographic azimuths of basic orientation obtained from strict levelling and the corresponding ones measured by the gyroscope. The results of these comparisons indicated that the differences

Accepted Article

between these topographic azimuths were in the range from -14^{cc} to 5^{cc}. Overall, they concluded that first results obtained from the application of gyroscope measurements in Zofiowka and Borynia in Katwit mines were very promising.

[6]Blachowski et al. (2019) concentrated on the determination of the surface deformations for the period 1995-2010 over the Walbrzych Coal Basin (WCB) in south-west Poland. They used the European Remote Sensing satellite 1/2 (ERS 1/2) and Environmental Satellite (Envisat) radar data and the persistent scatterer InSAR (PSInSAR) method. They also analyzed the ground deformations induced by hydrogeological change. They utilized geological and mining data over this coal basin. The results obtained indicated a surface uplift of can reach +8 mm/yr for the period until 2002. This uplift can be caused by the process of the underground water table within the basins associated with the three adjacent coal fields. From 2002-2010 when the underground water table is stabilized, the ground deformations reach ±5 mm/yr, over WCB. These ground deformation activities are associated with the ground reaction to long-term shallow and deep mining. Overall, the results obtained by them illustrated the processes complication of ground deformations in post-mining areas. They emphasized the usefulness of SAR techniques to gain valuable historical information about ground deformation over mining areas and their relation with hydrological mass change.

Becek et al. (2021) focused on the use of freely available global digital elevation models (DEMs) and a simplified statistical method for determining the land deformations that resulted from mining and geodynamic processes over the central northern part of Turkey. They implemented the SBAS (small baseline subset) InSAR method to determine mining-induced land deformation, as well as to split the deformation and no-deformation over the region investigated. Moreover, they computed the difference between elevations from the recent Shuttle Radar Topography Mission (SRTM) and TanDEM-X DEMs. The results obtained reveal constant estimates of land subsidence from the SBAS InSAR method (−0.041 m/yr) with the one obtained from the differences between SRTM and TanDEM-X DEMs (−0.034 m/yr). They concluded that the approach based on the differences between DEMs of high accuracy can sufficiently be used to recognize land deformation caused by mining activities from the ones induced by geodynamic processes.

In order to analyze the transportation of rock raw materials and its effect on regional planning and development over the Lower Silesia, [7]Blachowski and Buczynska (2020) assessed the scale of rails and roads used to transport the rock raw materials. They also proposed and applied multi-criteria scoring scheme to identify and select the operations related to the transport of the rock raw material that required to change road to rail or combined road and rail forms of transport. They reported that 70% of active mine productions were transported via road transports, which put substantial pressure on the road infrastructure condition, transport safety, as well as the environment surrounding these roads.

To identify the weaker areas that are susceptive to secondary land deformation and mine collapse, [8]Blachowski et al. (2022) created a digital inventory of post-mining workings and mapped the underground rock mass. As a unique postglacial environment, the Friendship of Nations-Babina coal mine in western Poland was selected as a study area. With the use of GIS (Geographic Information System) data, a three-dimensional underground workings database from available historical mining documentations, ware developed. Furthermore, ERT (electrical resistivity tomography) geophysical measurements were performed. The primary outcomes obtained by them confirmed the fact that in complex and complicated glaciotectonic conditions, the coal mining of multi-level deposits can induce discontinuous of ground deformations.

To investigate landslide morphology and identify landslide features [88]Pawluszek (2019) applied the high-resolution digital elevation model (HRDEM). She proposed a new method of

Accepted Article

identification of landslide feature mapping of the morphology with computer-aided techniques to enhance the interpretation of the elevation model. Morphological signatures of landslides were identified using the PCA on the basis of two landslides located in the South of Poland (namely, Roznow Lake and Grodek nad Dunajcem). Seven different derivatives of the HRDEM were applied to maximize the morphological information and to perform an enhancement of the visual interpretation. The proposed method is very promising since the conventional geodetic methods are time-consuming, however, this technique has its limitations which were also discussed in the paper.

[89]Pawluszek et al. (2019) studied the possible detection of landslides with the use of object-based image analysis (OBIA) and data derived from LiDAR. Forested and agricultural areas located in the south of Poland (Outer Carpathians) were chosen for research, which are characterized by the specifically degraded landslide geomorphology. They considered the different aspects of degradation of OBIA accuracy, i.e. resolution of the applied Digital Elevation Model (DEM), feature selection, and scale of segmentation. The efficiency of this approach was presented with the use of 85% of overall accuracy and Kappa's index (KIA) reaching 0.6. Finally, they discussed the challenges and advantages of automatic approaches for detecting landslides.

[92]Pawluszek-Filipiak et al. (2020) investigated landslides of two adjacent regions located in the south of Poland, namely "Lososina" and "Grodek", separated by the Roznow Lake and Dunajec River in order to develop an optimal method for mapping landslide susceptibility mapping (LSM). They performed a cross-modelling by creating various hydrological topographical, environmental, and geological landslide-conditioning factors (LCFs). Sentinel-2A data, DEMs, geological information as well as lake shapefile have been used for LCFs' generation. Then, the Seed Cell Area Index (SCAI) and Relative Landslide Density Index (RLDI) were used for checking and validating of the model. The applied methodology confirmed that with a lack of landslide inventory in the considered area, landslide susceptibility can be described based on inventory available for the adjacent area. Since landslide inventory is an expensive activity, this approach can be successfully used as an alternative.

[90]Pawluszek-Filipiak and Borkowski (2020a) compared two approaches, namely PSI (Persistent Scatterer Interferometry) and DInSAR (Differential Interferometric Synthetic Aperture Radar) in order to assess their suitability for monitoring the subsidence caused by exploitation in the coal mining. Their case study was conducted upon the Rydultowy mine situated in the Upper Silesian Coal Basin (USCB) in SW Poland. The data used covered 62 ascending Sentinel-1 images. The comparison involved 6-day time-series deformation maps. They concluded that the results of DInSAR processing provide better information exposure comparing to PSI results because of the temporal baseline being always (with just few exceptions equal to 6 days). In addition, due to the deformation model used, the PSI could not cope with estimating displacements of more than 12 cm/yr, while the deformations in the case area reached even 1 m per year.

[91]Pawluszek-Filipiak and Borkowski (2020b) used the same case area, but with the use of DInSAR and SBAS (Small BAseline Subset) techniques. The latter method requires a predefined deformation model, which is its disadvantage. However, the DInSAR accuracy is limited by correlations, either spatial or temporal, signal delays from atmosphere, and topographic or orbital errors. Therefore, they proposed to integrate those two techniques based on the geostatistical kriging prediction model to obtain the complete deformation pattern over the area of study. Moreover, they validated the proposed approaches with levelling data. Based on this validation the obtained minimum and maximum of the RMSE between displacements determined using DInSAR and levelling profiles were 0.9 and 3.2 cm, respectively. Unfortunately, SBAS processing is not suitable to monitor the subsidence in the area of

Accepted Article

maximum deformation rate. The final conclusion of the conducted research was that DInSAR is not the ideal technique when applied standalone and has to be supported by other geodetic measurements like GPS, LiDAR (Light Detection and Ranging) or classical spirit levelling.

[93]Pawluszek-Filipiak and Borkowski (2021a) used a combination of classical PSInSAR approach and conventional consecutive DInSAR for investigating the deformation rates in the Rydultowy Mining located in the South-West part of Poland. This allows measuring very significant subsidence of even 1 m per year. The time span of used data covers the period from March 2018 to March 2019. The developed methodology made it possible to determine a complete deformation model, which was compared with the results of precise levelling. The RMSE of 22 mm with a maximum subsidence rate reaching 1.05 m per year confirmed the validity of the methodology used.

[94]Pawluszek-Filipiak and Borkowski (2021b) applied the Object-Oriented Approach (OOA) and Digital Elevation Model (DEM) determined with the use of the Airborne Laser Scanning (ALS) data for the detection of landslides. Classical methods based on historical observations (e.g. precise levelling) are costly and time-consuming, so the future belongs to automatic methods. The vicinity of Roznow Lake (south of Poland) was taken as the study area. They concluded that even though some difficulties related to the smoothing of typical landslide features, automatic approaches are already very often used for these purposes, although as of today they are not yet fully able to replace the classical methods.

[95]Pawluszek-Filipiak and Borkowski (2021c) used the PSI technique to update the intensity of the landslide in the area of Roznow Lake in Poland. Observations made with Sentinel-1 A and B satellites covering 2017 were used for this purpose. The PSI-based matrix approach was applied to assess the landslide state. A total number of 205 landslides were assessed for their activity demonstrating that the majority of them were evaluated as active.

[97]Pawluszek-Filipiak et al. (2021) applied the PSI to verify the landslides in terms of their activity. Their test area covered Polish Flysch Carpathians (SE Poland). ALOS (Advanced Land Observing Satellite) PALSAR (Phased Array L-band Synthetic Aperture Radar) and Sentinel 1A/B data with different acquisition geometries were used. Line-Of-Sight (LOS) measurements were projected to the steepest slope to obtain the landslide intensity and expected maps of damages were created during field investigations. Forty-three of a total number of 50 investigated landslides were proved to be active, which was confirmed by in-situ measurements that have proved the applicability of the applied method for the assessment of landslide activity.

[76]Milczarek (2019a) applied a Small Baseline Subset (SBAS) method to study the deformation of the Earth's surface caused by underground mining. Two large SAR datasets from Sentinel 1A/B satellites have been applied. For calculations, they determined atmospheric delay using Tymofyeyeva and Fialko empirical method and the Mogi model, which allowed simulation of underground mining exploitation as well as induced tremors. The observational data covered underground copper ore extraction in SW Poland. They concluded that this method is very useful, but only for regions where mining system produces displacements being relatively time-constant. Moreover, induced seismic events may be effectively monitored with this approach.

[27]Grzempowski et al. (2020) investigated the Earth's surface deformations within the period 1995-2019 over Wroclaw as well as the potential factors causing these displacements. For this purpose, they used the PSI technique and data from ERS-2, Envisat, and Sentinel-1 satellites. The results obtained revealed that vertical and horizontal velocities over the area investigated reach up to 3 and 1 mm/yr, respectively. These results confirmed the linearity of Earth's surface deformations documented in historical geodetic data. They concluded that these displacements have a periodic subsidence pattern of 4-5 years and 2-3 years of stabilization or

Accepted Article

uplift. They reported that the area of Wroclaw is progressively decline in relation to the reference area, i.e. the area of the Fore-Sudetic Block.

[30]Ilieva et al. (2019a) concentrated on the life cycle of the Earth's surface deformations resulted from extracting the coal over the area of Upper Silesian Coal Basin (USCB). They utilized InSAR data from Sentinel-1 satellite and the DInSAR method. The Earth's surface deformation results obtained from InSAR data and the DInSAR method were validated using levelling data from a local geodetic levelling network that was semiannually re-measured. They concluded that the Earth's surface deformation results obtained from InSAR data are sufficient enough for monitoring the subsidence induced by mine processes that can reach up to −1.65 m over one year. The standard deviation of the difference and the bias between these results and corresponding ones from levelling data are 18.3 cm and −4 cm, respectively. They revealed good agreement between the detected surface vertical change and the amount of the material extracted. For the following eight months of the extraction, the corr. coef. between detected surface vertical change and the material extracted can reach up to 90%.

[4]Bazanowski et al. (2019) performed the study of the GNSS session durations to achieve the accuracy of several millimeters with 95% confidence level to monitor the subsidence of the Earth's surface due to mining of underground minerals. Their study area covered sylvinite mine in New Brunswick (East of Canada). Geodetic monitoring of the deformations contains GNSS measurements as well as precise levelling. The GPS observations have been carried out over the time of 18 days with 24-hour sessions. One baseline was selected for tests, the analysis of 58 3-hour long sessions indicated the accuracy in horizontal plane of 6 and 8 mm in Northing and Easting, respectively. Height component was determined with the accuracy of 8 mm. They concluded that to obtain several-mm accuracy of GNSS measurements for monitoring of the deformations in mines, the sessions should be at least 12-hour long.

[100]Przylucka et al. (2022) monitored the subsidence of the mining area located in the Upper Silesian Coal Basin (USCB) (South Poland) using the PSI and DInSAR techniques. They combined 8 different data sets, derived using two different methods, from various sensors and the 12-year period (1992-2012). The map of subsidence of an area of 3045 km^2 was obtained using 81 different interferograms. Moreover, the change (development) of the subsidence of the area of study was determined. They concluded that combining different InSAR datasets may provide reliable large-scale and long-term information about negative impact of mining activities in SW Poland.

[15]Dwornik et al. (2021) proposed an automatic procedure for the subsidence detection based on SAR interferograms. It makes use of analysis of spatial distribution of the interferogram phase, as well as its entropy and coherence. Sentinel-1 images were tested with the chosen mining areas located in south Poland that were considered as the test fields. The results were compared to those recovered with the use of circular Gabor filters. A significant improvement (34-83% of detection rate in comparison to 30-53%) has been observed, however, different numbers of false alarms for both methods were registered.

[2]Bala et al. (2021) applied the circlet transform for automatic detection of subsidence areas. Advantage of the newly proposed method is the consideration of the finite data frequency. Additionally, the search shape is not restricted to the circle. The transformation does not require further edge detection or a binary segmentation as it operates directly on the image gradient. Sentinel-1A data were taken for testing over the Upper Silesian Coal Basing that was chosen as a test field. The study have shown a 20% improvement in the method's effectiveness.

[69]Malinowska et al. (2019) used Envisat SAR images acquired between 2003 and 2010 to investigate the sinkholes caused by shallow submerged voids. They investigated an area in Upper Silesia (Poland) with 345 sinkholes that were identified between 1992 and 2013. The

Accepted Article

findings proved that the PSI technique is able to support the identification of zones with sinkholes and detect accelerated movements of the ground within 100 m of a single sinkhole.

[70]Malinowska et al. (2020a) applied the PSInSAR method to determine the ground movement in the area of one of the copper ore and anhydrite mines in Poland. The main aim of this study was to develop a new methodology for uplift prediction using satellite data and correlate them with hydrogeological conditions and mine life. The results showed that the uplift will reach up to 12 mm/yr in the next 6 years.

[71]Malinowska et al. (2020b) developed a new method for predicting surface deformations, generalized for the exploitation of various types of deposits. They presented a novel modification of the influence function method obtaining much more precise modelling of the ground movement for different types of minerals. They concluded, that each ground movements caused by different type of mineral reservoir exploitation can be predicted with this method.

[28]Guzy and Malinowska (2020) performed an inclusive review of models used to predict displacements caused by aquifer drainage with recent advances. They also gave a summary of implementations of InSAR technique to support the process of modelling of the aquifer compaction.

[63]Liu et al. (2019) described the capability of up-to-date ALOS-2 PALSAR data in observing the movement of the landslide of the test area in south China. According to the Authors either fast of slow movements can be captured, with different spatial or temporal baseline combination. The obtained results show that the L-band SAR data has its benefits in observing the landslide movements, especially in cloudy and rainy areas or in low latitudes.

[120]Szczerbowski (2020) studied the problem of deformations of ground surface in the area of the Bochnia Salt Mine (SW Poland). Deformations observed by geodetic methods are of two origins, namely natural (Carpathian push) and anthropogenic (past mining activity). He recognized the abnormal zones of subsidence basins, since the long-term vertical displacement distribution revealed atypical geometry. The analysis of lines of constant vertical displacement rate revealed some additional driving mechanisms of the deformation processes in the considered area. He proposed polynomial approximation to determine and describe the anomalous areas. [121]Szczerbowski and Gawalkiewicz (2020) applied geodetic methods to investigate the area of Inowroclaw town experienced by the halotectonic movement of salt diapir. They research on the vertical displacement of the set of benchmarks, which showed different characteristics depending on the distance from the reference benchmarks. As a result of the new approach, the points considered as reference were recognized as unstable, which is very important in the further study of the considered area. [122]Szczerbowski and Niedbalski (2021) applied a combination of sonic probe extensometer in intact rocks surrounding the gallery of the Bochnia Salt Mine. The gallery has been in use for more than 800 years. They also provided the real accuracy of the applied instrument. Their study presents the process of rock salt flow into the gallery observed over a period of 3 years revealing of a specific distribution of strain over the gallery, not discovered before. They proved, that the additional tectonic push of the Carpathians provides a tectonic stress and causes the tectonic activity in the underground movements.

[68]Maciuk et al. (2021) focused on the dynamics of European plate to assess their influence to the land boundaries. They analyzed the velocities of the selected permanent GNSS stations established in Poland and showed the differences in the velocities determined in IGS and ETRF (European Terrestrial Reference Frame) reference frames. They found, that within the next 25 years, the marks indicating borders may be shifted by 0.13 m due to tectonic movements and recommended verifications of cadastral data in Poland to be performed at least once every 15 years.

Accepted Article

[67]Maciuk (2021) summarized the practical research results from GNSS data for non-anthropogenic crustal deformations such as earthquakes, landslides, and tectonics. He described several measurement techniques. They were: real-time and post-processing of satellite navigation data in the absolute and relative positioning. At the end, he described the challenges related to the use of GNSS in future studies related to investigation of natural phenomena.

[125]Wajs et al. (2021) proposed an active remote sensing based solution for fast and accurate inventory of open-pit Mines. As a case study, the authors selected the Mikoszow Granite Mine located in Lower Silesia, south-west Poland. Mobile LiDAR System (MLS) with a mobile mapping platform equipped with DMI (Distance Measurement Indicator) and IMU (Inertial Measurement Unit) sensors as well as GNSS and mobile laser scanners mounted on a vehicle. For data acquisition and localization, the Simultaneous Localization and Mapping (SLAM) approach was applied. Point clouds and positions over the whole area of the Mikoszow mine and its vicinity were recorded. The final results obtained by the MSL contained a set of 1,968,367 point clouds which can be post-processed in approx. 30 minutes. The accuracy of positions obtained from these MSL results was similar to RTK GNSS accuracy. They reported that the proposed solution based on MLS and SLAM approach can successfully be applied to the open-pit mine entire life cycle.

[58]Kowalski et al. (2019) focused on studying the structural control of mass movements on slopes formed of magmatic and metamorphic rocks. The authors investigated the mechanisms and formation of landslides on the northern slopes of the dome-shaped, rhyolitic Wielislawka Mt. located in the Kaczawa Foothills of the Western Sudetes, south-west Poland. A multidisciplinary approach based on data from geological and geomorphological field studies, terrestrial laser scanning (TLS) and LiDAR-based DEMs, for old adits and shafts in the landslide area, was applied. This multidisciplinary approach allowed the determination of the recent extent and origin of the landslides over the area investigated. The use of these data indicated that the observed initial stages of mass changes in the excavations, in particular, the area characterized by cover rocks of the rhyolitic massif, the old adits and shafts, were unique areas to study the landslide processes. The results obtained by them revealed that existing discontinuity surfaces within the rock massif have an essential contribution to the intensity, development and potential future evolution of the slope failures on Wielislawka Mt. Concerning the northern slopes of Wielislawka Mt., the morphology and further development of landslides were associated directly to riverine erosion and the formation of the deeper part of Kaczawa River. The authors reported that structural anisotropy and lithological of the massif have an essential impact on slope failure development.

[55]Kowalczyk et al. (2020) evaluated the use of the co-kriging method to model the vertical deformations over Poland. They analyzed vertical movements of the Earth's crust from: (1) four precision levelling campaigns carried out in Poland within the period 1926-1937, 1953-1955, 1974-1982, and 1997-2003, respectively, (2) permanent GNSS stations data, and (3) the first alignment of vertical motion networks in Poland that include levelling (222 points) and GNSS (123 points) data. To process these data, methods based on variograms (semivariograms) were applied. The results obtained by them revealed that vertical deformations over Poland based on levelling data were anisotropic. They also indicated that vertical movements from GNSS data disagree with the respective ones from levelling data. This disagreement can be ascribed to data errors or external influences such as anthropogenic or geophysical factors. They concluded that co-kriging method allows the combination of numerous datasets, but the final model is considerably effected by initial dataset. This method is independent from the volume of data. They also confirm that co-kriging method is a numerically non-unique method, as the same input datasets can result in different models.

Accepted Article

[56]Kowalczyk et al. (2021a) focused on the need of creating a unified levelling network based on data from consistently campaigns of levelling measurements and permanent GNSS observations to increase the resolution of geodynamics models, in particular, the models of VDES, in space domain. For this purpose, they examined the scale-free network theory to obtain the most relevant common points in hybrid networks using the Euclidean's distance between points as a criterion. They utilized data from the UELN (United European Levelling Network) and EPN (European Permanent Network) networks. They identified 18 pseudo-nodal points with the highest number of links in this hybrid network. The Euclidean distance of 10 km was found as an appropriate criterion to identify these pseudo-nodal points as common points. Overall, they concluded that relative VDES can be estimated by aligning a hybrid network (UELN+EPN) using the scale-free network theory.

[16]Fan et al. (2019) estimated the glacier displacement with the use of SAR image intensity information. They used six COSMO-SkyMed (COnstellation of small Satellites for the Mediterranean basin Observation) images obtained between July and December 2016 to study the movements of five glaciers. They are located in the central Himalayas. Their research provided evidence of the reliability of the measurements of the SAR data in addition to the analyses of RMSE of the velocity residuals in non-glacial zones. They compared the results with those obtained by terrestrial laser scanning and concluded that merging of those techniques should provide better information concerning the monitoring of the glaciers.

[21]Glowacki and Kasza (2021) assessed the morphology change of the Werenskiold Glacier, south-west Spitsbergen and its end moraine. For this purpose, DEMs developed from aerial photogrammetry measurements for 1936, 1960, 1990, and 2011 as well as InSAR and GNSS data from GNSS RTK measurements for 2015 were utilized. The long-term analysis based on DEMs and with direct GNSS RTK survey revealed that the loss of rock and ice material disappeared from the end moraine of the glacier was about 200,000 m^3/yr. The short-term analysis of InSAR data covering the period between 2 August and 6 November 2015 indicated that this loss is at the level of 2000 m^3/day. They reported that the most essential morphology change was observed in the northern part of Werenskiold Glacier.

3.3 Investigation of seismic events

The progress in GNSS receiving equipment and processing of navigational data as well as new InSAR technology has led to considering these measurement techniques as very useful tools for the detection of co-seismic displacements and a source of information concerning the propagation of seismic waves.

[98]Paziewski et al. (2020) validated the algorithms for automatic Galileo+GPS high-rate signals processing at medium and long-range baselines for seismic events' characterization. They used the Galileo foR Seismography System (GRaSS) which was elaborated previously for near real-time monitoring of anthropogenic seismic events at the area of a copper mine in SW Poland. This system contains 4 modules liable for automatic processing of high-rate navigation measurements and presenting the results. In their results, they used the relative geometry-based model, which was recognized to provide the most precise coordinate estimates with GNSS signals. They tested the elaborated algorithm on the case study of M3.8 seismic event which took place in January 2019 in the SW of Poland. GNSS permanent stations were located 1.2 and 4.0 km, respectively. In addition, they used accelerometer observations for comparison purposes by performing the integration of the obtaining position displacement. They found a very similar shape of the seismic waves, however, the displacements derived by accelerometer were two times lower than GNSS-derived ones. Moreover, they demonstrated an agreement in a frequency domain with the use of Fast Fourier Transformation (FFT) with the dominant frequency of 0.3 and 0.7 Hz in the north direction and 0.3 Hz in the east one.

Accepted Article

Finally, they validated the measuring system on the specially constructed shake table with simulated dynamic displacement. The validation results obtained indicated that maximal differences between GNSS-derived mean amplitude and the benchmark values were at the range of 0.2-1.9 mm.

[59]Kudlacik et al. (2019) applied high-rate GPS PPP technique with a sampling frequency of 5 and 10 Hz to investigate the motion determined by GPS technique at permanent stations during three earthquakes. The seismic events took place in Nepal (Gorkha earthquake) and Italy (Visso and Norcia). The first one took place in April 2015 being a result of the thrust faulting and was successfully recorded by eight GPS permanent stations. The second and third events took place in October 2016 in the Apennines recorded by seven nearby permanent stations. First, the high-rate GPS data were processed with the RTKlib software in the kinematic PPP mode obtaining GPS-derived position time series. Then, tests of variuos types of digital filters were performed, with the conclusion that the 2nd order Butterworth band-pass filter adapted to each GPS station separately is an optimal filter for this study. They compared the GPS-derived results with those obtained using strong motion instruments (SM) obtaining GPS-SM absolute value of the average difference is 6 mm with GPS-SM distances within the range of 0.05 to 2.14 km although different measuring ideas (GNSS-derived displacement is absolute, while SM – relative). At the end, they found a significant relationship between those two types of data with correlation coefficients of 0.83 for the east, 0.95 for the north and 0.98 for up components, confirming the ability of GNSS for determining of the fault plane solution for earthquakes with magnitudes over 6. A similar methodology was applied by [60]Kudlacik et al. (2021), but to a much less energetic (M3.7) event that occurred in January 2019 in the area of Legnica-Glogow Copper District (SW Poland). That was one of the first analysis of mining tremor using high-rate GNSS positioning. GNSS position time series were derived using either double differencing (DD) or PPP methods. Seismological data (accelerations and velocities integrated into displacements) served as the reference for validation. They found that the peak ground displacements (PGDs) calculated for two GNSS stations with the PPP-approach were very close to the same PGDs calculated on the basis of seismological data recorded at the stations co-located with GNSS ones. Coherence analysis was used to confirm the consistency of two types of data in the frequency domain. They concluded that with this methodology and instrumentation not only significant natural earthquakes may be sensed and analyzed, but also events of smaller magnitudes might be recorded when the epicentral distance is quite small.

[119]Szczerbowski (2019) discussed the problem concerning the relations between seismic events of high-energy and regional scale deformations of the terrain surface. His test area covered the Legnica-Glogow Copper District (LGCD). He used position time series gathered from the GNSS stations of the ASG-EUPOS network that were located at the LGCD and adjacent areas were chosen. He investigated the temporal variation of distances between the chosen stations and evaluated the apparent strain, which was compared to the occurrence of tremors of high-energy, finding a significant correlation.

[45]Kaczorowski et al. (2022) focused on geodynamic harmonic signals of the range 10^{-3}-10^{-4} Hz recorded by water-tube (WT) tiltmeters installed in the Space Research Center, Geodynamic Laboratory (GL) in Ksiaz, south-west Poland. The authors reported that the main components of these geodynamic harmonic signals resulted from post-seismic Earth's solid-body free oscillations and atmospheric pressure microvibrations. The period 2004-2012 was selected to study the viscoelastic vibrations of the solid Earth. Within this period, two significant earthquakes: the Sumatra-Andaman on 26.12.2004 with a magnitude of M8.1, and the Tohoku-Oki on 11.03.2011 with a magnitude of M9.0, were occurred. To investigate harmonic signals induced by low-frequency atmospheric pressure microvibrations, different periods (e.g. June 6-21, 2010, February 2 to March 3, 2012) were considered. The authors found

Accepted Article

that amplitudes of air pressure microvibrations were in the range from ca. 0.15 to 0.50 mas. Overall, they concluded that amplitudes of harmonic signals induced by air pressure microvibrations were strongly dependent on the location of WT tiltmeters within the underground GL Ksiaz. For the harmonic signals generated by post-seismic free oscillations of the Earth, the location of WT tiltimeters did not play a significant role.

[99]Przylibski et al. (2020) focused on the relationships between variation in activity concentrations of radon ^{222}Rn and seismic events recorded using WT tltimeters of the GL Ksiaz. The change of ^{222}Rn activity concentration in the underground tunnels at GL Ksiaz was obtained using 5 semiconductor SRDN-3 detectors operated within the period from May 18, 2014 to January 18, 2016, and one ionisation chamber of the AlphaGUARD instrument operated for the period March 21–28, 2014. Tectonic and seismic activities of the orogen at the GL at Ksiaz were measured for the same period of radon activity concentration changes using two WT tiltmeters. The comparison between changes of radon activity concentration and WT tiltmeters illustrated that radon data sinusoidal oscillations with an amplitude range from 1000 to 1500 Bq/m^3 and a phase of 12 months. The results obtained indicated that the coefficients of correlation between ^{222}Rn activity concentration and seismic events were within the range from 0.38 to 0.43. They reported that a vital conclusion concerning the relationships between the change of ^{222}Rn activity concentration and seismic events observed at GL Ksiaz can be drawn from the preliminary analysis of approximately two years of ^{222}Rn activity concentration observations.

[43]Kaczorowski et al. (2019, [44]2021) focused on the deformation of the Swiebodzice Depression (SD) unit, which provide information concerning the deformation of the Fore-Sudetic Monocline (FSM). In particular, they concentrated on temporal variations of strong seismic events (i.e. magnitude ≥3.6) in the FSM using harmonic signals registered by WT tiltimeters in GL Ksiaz. [43]Kaczorowski et al. (2019) concentrated, mainly, on strong seismic events that take place in 2016, while [44]Kaczorowski et al. (2021) considered all strong seismic events occurred within the period 2013-2017. Either [43]Kaczorowski et al. (2019) or [44]Kaczorowski et al. (2021) reported that the comparison between the phases of tectonic activity of the SD orogeny and temporal variations of seismic events exhibited the presence of temporal dependency between these seismic events and the derivative of the tectonic activity (VTAF).

[13]Chrapkiewicz et al. (2020) conducted intensive research concerning the inversion of the surface wave dispersion and teleseismic receiver functions data required to investigate the S-wave structure at a craton margin. They proposed a linearized method with a full solution to the inverse problem. In this method an ensemble of starting models covering the entire space of acceptable solutions was used. Rayleigh wave phase velocity dispersion and P-wave receiver function data from the so-called 13 BB Star (i.e. the passive seismic experiment in north-western Poland) were integrated into the inversion solution. They developed a workflow of multistep for the linearized inversion to obtain reliable models of S-wave velocity down to 300 km using receiver function and surface wave dispersion data. The results obtained by them revealed a very good fit between S-wave velocity data and their final models developed. This may indicate that using correct parameter optimization can, successfully, mitigate the ill-posed problem of the inverse problem. Moreover, they found a similar mantle over the area investigated, but rather high-velocity values (ca. 4.80 km/s) which are larger by 0.1-0.2 km/s compared to those estimated for other cratons. This may indicate that further investigations would be required to explain whether such high-velocity values are due to a local anomaly associated with the Earth's structure, or if they are a consequence of the simplification of the assumptions applied in the modelling procedures.

Accepted Article

In order to assess the rapid response to the Samos M7.0 earthquake, [19]Foumelis et al. (2021) combined historical seismicity of rupture areas with seismological and geodetic, e.g. GNSS and InSAR data as well as in-situ observation. They demonstrated that such a combination is very valuable to specify the rapid response requirements for assessing and preliminary interpreting the earthquake activity, even within the first 24 hours that proceeding the time of the earthquake. They also exhibited that in a period of less than a week, several constraints concerning the accessibility of data as well as the drawbacks of the techniques used can partially be recovered to provide more reliable results and interpretation. Furthermore, they highlighted the preparedness level of the rapid seismological solutions, systematic availability of open access Earth Observations (EO) data and on-demand online processing of both EO and GNSS data that were considerably improved over the past years.

[84]Owczarz and Blachowski (2020a) investigated induced seismicity from anthropogenic activities in the mining areas of Poland. They analyzed surface displacements caused by eight induced tremors the area of Rudna copper mine (SW Poland). It is a region of moderate seismicity with no more than 100 induced shocks per year, mostly not felt by people. They used the DInSAR method with Sentinel-1 satellite imagery along with the geographic information system (GIS). They studied the vertical displacements derived from 37 calculated interferograms with 68 pairs of images being processed from November 2016 to February 2020 with eight events of magnitude greater than 2.7. They found that in the investigated region the average values of maximum vertical subsidence ranged from –44 to –119 mm depending on the induced shock with all analyzed vertical profile lines showing comparable subsidence properties. They also assessed the potential relations between maximum vertical displacements and the energy of tremors induced by underground mining activity, as well as energy and their spatial ranges in West-East and North-South directions with a strong positive relationship. In the paper by [85]Owczarz and Blachowski (2020b) results of similar investigations were published, but for seismic events occurred between December 2016 and September 2018 for the same area. As the results, maps of the deformation resulting from the consecutive seismic events were shown and discussed in detail.

[96]Pawluszek-Filipiak and Borkowski (2021d) investigated correlations between DInSAR-estimated deformations and mining tremors with the biggest amplitudes. For this purpose, they used data from Sentinel 1A and 1B ascending images. Fifty-one different interferograms in total have been processed. For correlation analyses, either time series in the center of subsidence basins or deformation profiles were taken. The result of their analysis was negative. For the earthquakes under consideration, they did not find correlations to attribute the deformation of the Earth's surface to a specific seismic event, probably due to the small magnitude (maximum 2.8) or the depth of extraction (1 km).

[77]Milczarek (2019b) used SAR interferometry to determine the deformation of the Earth’s surface due to the anthropogenic-induced earthquake. The area of study was located at the Legnica-Glogow Copper Belt (L-GCB) which reveals the highest level of seismic activity in SW Poland. Additionally, L-GCB is located at the FSM, which increases the likelihood of earthquakes. A total number of more than 1500 induced seismic events between 2000 and 2016 were recorded there. Data from Sentinel 1A and 1B satellites processed using DInSAR differential method covering 5 interferograms were used. Additionally, calculations using the SBAS time series method were also performed. Tremor that occurred in November 2016 was analyzed in detail. The displacements up to –80 mm in the radar Line-Of-Sight direction, were observed. They confirmed the ability of detecting surface displacement with small dimensions (few kilometers). Due to the lack of other geodetic observations within the period investigated, performing a comparative analysis was not possible.

Accepted Article

[31]Ilieva et al. (2019b) presented a combined seismological and geodetic study concerning the relationship between collapses resulted from mine processes and the ground response to seismic activities. They focused on the strongest seismic event that took place on 29 January 2019, in the area of Rudna Mine, Poland that is denoted as the M4.6 collapse. Seismic signal from the Legnica-Glogow Underground Mining INduced Earthquake Observing System (LUMINEOS) surface local seismic network, GNSS position time series as well as InSAR data from Sentinel-1 satellite mission were used. Daily-coordinates of high accuracy for the period of three months before and three months after the event, as well as oscillations of high-frequency in the horizontal and vertical coordinates, observed during the M4.6 collapse, were determined by processing GNSS observations collected at 10 Hz. In order to obtain surface deformation using InSAR data, a SBAS method for the slow-rate deformations and a conventional DInSAR method for fast-motion monitoring around the epicenter were elaborated. Through the analysis of GNSS and InSAR data, they confirmed the rapid decline of the ground. The analysis of InSAR data revealed that preceding the collapse by six days, a post-event rate of subsidence over an area of two km^2 was an increased. Overall, they concluded that in a very short time, shallow-induced seismic events with magnitudes of greater than M4 can result in a significant surface deformation.

[103]Rudzinski et al. (2019) investigated the M4.0 earthquake in Wujek/Slask underground coal mine in Poland which was held on April 17, 2015. They used Sentinel 1-A data with a 12-day revisit time. To study the deformation before, during and after the earthquake they took three pairs of SAR images obtaining the subsidence pattern showing one cycle of deformation corresponding to approximately 2.8 cm of subsidence. Then, they compared the results of obtained deformations with the estimated source mechanism as a full moment tensor (MT) solution. The full MT inversions were performed with respect to the signals filtered between 0.13 and 0.16 Hz. They concluded that linkage of data from geodetic techniques with results of analysis of seismological information is able to provide very important insight into mine collapses.

[29]Hejmanowski et al. (2019) discussed the effects of severe nearby mining-induced M4.7 and M4.8 earthquakes which took place in 2017 with 1.6 km distance between hypocenters. They applied InSAR technique to monitor the ground deformations caused by those two tremors. The earthquakes occurred in the area of "Rudna" Copper Ore Mine (SW Poland). A high level of seismicity in this region is caused not only by anthropogenic reasons, but also due to complex geological conditions. The ground movement was analyzed using Sentinel-1 data obtained from both, descending and ascending satellite orbits. The DInSAR method was applied for processing of the radar images with successful detection of the local dynamic subsidence troughs of a regular shape and a range of about 2 km induced by these tremors. They obtained the maximum vertical displacements of –84 and –116 millimeters depending on the tremor. The area affected by the earthquakes has reached the dimension of 1.2 km per 4.2 km. Finally, they found a very significant relationship between the magnitude of the mining-induced tremors and determined surface displacement.

[112]Sopata et al. (2020) investigated the change in the shape of land surface after series of seven rock mass tremors of 2.3 to 2.7 magnitude which took place during the Spring of 2017 in the Upper Silesian Coal Basin (Poland). Using DInSAR method, the authors focused on vertical changes showing the applicability of the proposed methodology to study the deformations in large-scale areas.

3.4 Investigation of sea level changes

For decades, the study of sea level changes has been one of the important components of monitoring climate change in the Earth system. [17]Fenoglio et al. (2019) investigated new

Accepted Article

altimeter missions equipped with Synthetic Aperture Radar (SAR) mode, which is to provide more accurate information about sea level heights. They used data from 2010 to 2018 gathered by CryoSat-2 and Sentinel-3A satellites, with the region of interest covering French and British Atlantic coasts as well as the coast of the North Sea. The results were compared to the in-situ measurements, by means of tide-gauges at 17 stations and 38 GPS stations located along the German coasts. In their research, they used two ocean models (operational model BSHcmod of the German Federal Maritime and Hydrographic Agency – BSH as well as NEMO-WAM being a part of the Geesthacht Coupled cOAstal model SysTem – GCOAST). The altimetry-derived sea level heights were referred to the WGS84 (World Geodetic System 1984) ellipsoid. Two GNSS solutions were taken, network solution processed in Bernese software in IGb08 (IGS Reference Frames 2008) reference frame and PPP solution from the Nevada Geodetic Laboratory. GNSS-derived velocities with realistic uncertainties were determined using CATS software. This comparison showed that the differences between altimetric and in-situ sea level determinations agree with GNSS-derived rates within 1.5 mm/yr at half of the investigated sites, with the uncertainty being larger than the error of the GPS rate by a factor bigger than two and more. The proposed methodology improved detection of the coastal sea level variability in the last 10 km from the coast.

The Mean Sea level (MSL) changes on the southern Baltic Sea coast were determined using data from five tide gauges (TGs) stations ([53]Kowalczyk, 2019). Time series of MSL data from station Swinoujscie covering the period 1811-2015 were used, while for the remaining four TG stations data for the period 1951-2016 were utilized. In order to analyze vertical bias in time series that caused by using inconsistent reference levels, he used additional data from Stolpmunde and Gdynia TG stations. Furthermore, the author's own algorithm called Vertical Switching Edge Detection was utilized to reduce the MSL time series into a common reference level. For the determination of MSL change, methods based on linear regression, index decomposition, and Fourier function were implemented. He found slight increases in the MSL on the Polish coast of the Baltic Sea. These increases in MSL range from +0.8 to +2.4 mm/yr.

[54]Kowalczyk et al. (2019) studied the vertical crustal motions (VCM) of the Polish coast of the Baltic Sea. They estimated secular variations of MSL using monthly average sea levels data from five TGs stations covering the periods of 1951-2017 and 1993-2017 as well as satellite altimetry (SA) data. Furthermore, for the period 2004-2018, they estimated the VCM at twelve permanent GNSS stations located in the north of Poland using the IGS08 (International GNSS Service 2008) reference frame. The results obtained by them indicated that the absolute VCM of the Polish coast determined from TG and SA data for the period 1951-2017 range from +2.20±0.42 mm/yr to +2.68±0.31 mm/yr. They found that the absolute vertical movements based on GNSS data range from zero to +1.30 mm/yr, which do not agree well with the corresponding absolute vertical motions obtained from TG and SA data. They ascribed this disagreement to several factors such as the time span and the continuity of the time series investigated, local movement of TG stations, anthropogenic activities, geophysical, geological and hydrological factors, the method elaborated to estimate the VCMs, as well as other unidentified movements of GNSS stations.

[57]Kowalczyk et al. (2021b) analyzed the accuracy of VCM along the European coast estimated from SA, TG, GNSS and radar interferometry. Time series of daily and monthly MSL at 27 TG sites were obtained from SA and TG data. Moreover, daily VCM were acquired from GNSS data of permanent GNSS stations that co-locate with these TG sites. With the use of Sentinel-1A/B data from the Copernicus Open Access Hub, mean deformation velocity maps covering the locations of TG sites investigated were obtained. The time series of VCMs were decomposed. As a consequence of this decomposition, linear trends of VCM together with their standard errors were determined at all TG and GNSS sites investigated. For this purpose, they

Accepted Article

used the linear regression method and Fourier analysis. They reported that accuracies of VCMs estimated from TG, SA, GNSS and SAR data are different. In terms of the standard error of these VCMs from TG and SA data ranged from ±0.06 to ±0.21 mm/yr at a long-time span (i.e. TG data from 1856 to 2018) and from ±0.31 to ±1.59 mm/yr at a short-time span (i.e. TG data from 1993 to 2018). These standard errors are in the range from ±0.20 to ±0.49 mm/yr for SAR data, and from ±0.04 to ±1.92 mm/yr for GNSS data.

[86]Pajak and Kowalczyk (2019) investigated seasonal variations of Baltic Sea level determined from altimetry and tide-gauge observations. They examined data between 1993 and 2015 with the aim of annual and semi-annual amplitudes comparison. They used the gridded (resolution of 0.25° per 0.25°)) daily sea level anomalies obtained from the Copernicus Marine and Environment Monitoring Service (CMEMS) along with the five tide-gauge stations located at the coast of the South part of the Baltic Sea. For comparison purposes altimetric grid points closest to the tige-gages were taken. Their assumed deterministic model consisted of the in-phase and out-of-phase annual and semi-annual terms along with the linear trend determined with the Least Squares Estimation (LSE). The amplitude of the annual oscillation they calculated ranged from 2.86 at the West coast to 5.49 cm at the East coast. They also found that the maximum of the annual cycle at the Polish coastline is in November/December. Maximum difference between techniques was 1.5 cm with a mean correlation coefficient between the satellite altimetry and tide gauge data being equal to 0.92.

[87]Pajak et al. (2021) investigated vertical crustal movements with the use of differences between satellite altimetry (SA) and tide-gauge observations (TG) monthly sea level time series at each TG station along the Adriatic Sea coast. They used observational data from six tide-gauge stations co-located with nearby GNSS permanent stations. Satellite altimetry data were obtained from satellite multi-mission products in the form of the gridded (0.25° per 0.25°) sea level anomalies (SLA). To estimate trends in the MSL, they select two time periods. First, from 1993 to 2018 corresponded to the available satellite data. Second, from 1908 to 2018 based on the available tide-gauge records. They found the mean annual amplitude of +5.90±1.15 cm from satellite altimetry data and +4.32±0.90 cm from tide-gauge data. Finally, they used information about GNSS-derived displacements on permanent stations from the Nevada Geodetic Laboratory PPP solution to connect both types of sea level determinations. They concluded that in the area under study, quite coherent regional patterns of sea level change may be observed, with the trend +3.30±0.32 mm/yr from the satellite altimetry data.

[48]Klos et al. (2019) analyzed the relative and absolute sea level changes referenced to 38 tide-gauge stations located in the Western-North Pacific with the focus on a proper modelling of the Vertical Land Motion (VLM). A region with strong seismological effects was specifically taken to prove the thesis that stations affected by earthquakes still can be further useful for studying vertical changes of the Earth's crust. Therefore, they proposed a new mathematical description methodology for the nonlinear movement of GPS permanent stations with strong post-seismic deformations (PSDs). They also proposed, for the first time, the use of a combination of white and power-law noise for the determination of errors of linear trend and parameters of a nonlinear model determined in one run. Moreover, they analyzed differences in the pre- and post-seismic velocities (relaxation mode) finding very significant (of 15 mm/yr at maximum) differences. They concluded, that not accounting for non-linear vertical land motion in the tectonically unstable areas may lead to errors in estimating absolute sea level rise determined from tide-gauges of about 10 mm/yr. Finally, they found that altimetric determinations much better agree with tide-gauge data after the employment of the newly-proposed nonlinear VLM model.

[64]Lyszkowicz and Bernatowicz (2019) investigated the changes in the Baltic Sea at 6 Polish tide gauge stations. All of them belong to the SONEL (Coastal Water Level Observation

Accepted Article

System) network. Moreover, they applied the TSAnalyzer software to analyze the vertical position time series from the co-located GNSS permanent stations. Assumptions concerning the deterministic part included annual and semi-annual oscillations plus linear trends. They concluded that geocentric changes of the Baltic Sean along its southern coastlines are between +2.6 mm/yr and +3.5 mm/yr.

3.5 International projects

EPOS (European Plate Observation System) is an infrastructure project aimed at integration of data, data products, and facilities in Europe (https://www.epos-eu.org/about-epos). Within EPOS-PL (EPOS-Poland; https://epos-pl.eu/) the information and measurement system for investigating dynamic events in the Upper Silesian Coal Basin (USCB) in Poland was recently established ([78]Mutke et al., 2019). It's main aim is to carry out either continuous or periodic measurements in post mining and mining areas to show the relationships between underground mining, USCB geodynamics, surface flooding and subsidence, induced seismicity, and sinkholes. In situ observations include gravity monitoring, monitoring of seismicity by surface and underground stations, deformation of the Earth's crust by GNSS, groundwater table movements, as well as Earth's crust deformation monitoring using aerial and satellite (InSAR and PSI) observations. The research infrastructure within EPOS-PL is continuously extending. The proposed system is to investigate causal relations between mining and geodynamic processes taking place in Upper Silesia, but is universal and can be applied to any region of the world with increased anthropogenic seismicity.

In 2022, the construction of the GNSS Data Research Infrastructure Center was also completed, which included the start of a service providing access to GNSS data and products from the Polish GNSS observation infrastructure ([1]Araszkiewicz et al., 2022). The portal (http://www.gnss.wat.edu.pl/cibdg/) presents also analysis of GNSS data quality, stations displacement and zenith troposphere delays.

[114]Sousa et al. (2021) presented the report of the international Dragon 4 program project named "Landslide Identification, Movement Monitoring And Risk Assessment Using Advanced Earth Observation Techniques" (https://earth.esa.int/documents/163802/2550004/32365_PROJECT_SUMMARY.pdf) aimed at application of different geodetic techniques for wide application of remote sensing data, with special emphasis given to risk management, landslide hazard, and disaster prevention. They tested Multi-temporal InSAR, high-resolution image matching, SAR tomography, and data modelling with the aim to investigate the landslides and other geohazards. Moreover, the surface deformation of mountain slopes and glaciers, as well as subsidence, landslides and ground fissure were possible to be monitor with the use of the mentioned methods.

Space Research Centre of the Polish Academy of Sciences participates in the international project under the umbrella of European Space Agency "Geodetic SAR for Height System Unification and Sea Level Research" ([25]Gruber et al., 2020; [26]2022). The main aim of this project is providing an integrated sea level observing system including commonly applied geodetic methods as GNSS of tide gauges, and introducing the SAR positioning in the Baltic Sea area. Within this project a new model of gravimetric quasi-geoid for Baltic Sea has been proposed ([66]Lyszkowicz et al., 2021b). It has been calculated by applying Helmert condensation method with the use of high-quality dataset from Baltic countries including BNSS/levelling for verification.

4. Summary

Accepted Article

In this review article an outline of researches concerning Earth rotation and geodynamics carried out by scientists from Polish scientific institutions from 2019 to 2022 is given. The main concern of the research works on Earth rotation was the estimation of the excitation of polar motion by surficial geophysical fluids using available data from GRACE and GRACE-FO experiments. Another important task was improvement of the quality of Earth rotation parameters estimated from the satellite techniques SLR, GNSS and DORIS. The studies concerning geodynamics were focused on the determination of the ground motion with geodetic methods with several aims. One of them was to monitor landslides and ground deformations caused by mining and seismic tremors. Another, determination of the vertical land motion for sea-level studies (relative sea level). All the results show the high activity of Polish research groups, commitment to scientific cooperation and activity in cooperation with leading international scientific units, conducting research related to Earth rotation and geodynamics.

Author contributions

Conceptualization: J.B., A.B., W.G., J.N.; original draft preparation, editing and reviewing: J.B., A.B., W.G., J.N.

Data availability statement

No datasets were used in this research.

Acknowledgements

We thank the editors of Advances in Geodesy and Geoinformation and the anonymous reviewers for their valuable comments.

References

[1]Araszkiewicz, A., Całka, B., Kiliszek, D. et al. (2022). Geoportal Centrum Infrastruktury Badawczej Danych GNSS. *Roczniki Geomatyki*, XX, 1(96), 7-16 (in Polish).

[2]Bala, J., Dwornik, M., and Franczyk, A. (2021). Automatic subsidence troughs detection in SAR interferograms using circlet transform. *Sensors*, 21, 1706. DOI: 10.3390/s21051706.

[3]Baselga S., and Najder J. (2021). Automated detection of discontinuities in EUREF permanent GNSS network stations due to earthquake events. *Survey Rev.*, 54(386), 420-428. DOI: 10.1080/00396265.2021.1964230.

[4]Bazanowski, M., Szostak-Chrzanowski, A., and Chrzanowski, A. (2019). Determination of GPS session duration in ground deformation surveys in mining areas. *Sustainability*, 11, 6127. DOI: 10.3390/su11216127.

[5]Becek, K., Ibrahim, K., Bayik, C. et al. (2021). Identifying Land Subsidence Using Global Digital Elevation Models. *IEEE J. Sel. Top. Appl. Earth Obs. Remote Sens.*, 14, 8989-8998. DOI: 10.1109/JSTARS.2021.3110438.

[6]Blachowski, J., Kopec, A., Milczarek, W. et al. (2019). Evolution of Secondary Deformations Captured by Satellite Radar Interferometry: Case Study of an Abandoned Coal Basin in SW Poland. *Sustainability*, 11, 884. DOI: 10.3390/su11030884.

Accepted Article

[7]Blachowski, J., and Buczynska, A. (2020). Analysis of Rock Raw Materials Transport and its Implications for Regional Development and Planning. Case Study of Lower Silesia (Poland). *Sustainability*, 12(8), 3165. DOI: 10.3390/su12083165.
[8]Blachowski, J., Warchala, E., Kozma, J. et al. (2022). Geophysical Research of Secondary Deformations in the Post Mining Area of the Glaciotectonic Muskau Arch Geopark – Preliminary Results. *Appl. Sci*., 12(3), 1194. DOI: 10.3390/app12031194.
[9]Bogusz, J., Klos, A., and Pokonieczny, K. (2019). Optimal strategy of the GPS position time series analysis for the Post-Glacial Rebound investigation in Europe. *Remote Sens.*, 11, 1209. DOI: 10.3390/rs11101209.
[10]Bury, G., Sosnica, K., Zajdel, R. et al. (2021a). Determination of precise Galileo orbits using combined GNSS and SLR observations. GPS Solutions, 25(11), 1-13, doi:10.1007/s10291-020-01045-3.
[11]Bury, G., Sosnica, K., Zajdel, R. et al. (2021b). Geodetic datum realization using SLR-GNSS co-location onboard Galileo and GLONASS. Journal of Geophysical Research – Solid Earth, 126(10), 1-23, doi:10.1029/ 2021JB022211.
[12]Cegla, A., Rohm, W., Lasota, E. et al. (2022). Detecting volcanic plume signatures on GNSS signal, Based on the 2014 Sakurajima Eruption. *Adv. Space Res.*, 69(1), 292-307. DOI: 10.1016/j.asr.2021.08.034.
[13]Chrapkiewicz, K., Wilde-Piórko, M, Polkowski, M. et al. (2020). Reliable workflow for inversion of seismic receiver function and surface wave dispersion data: a "13 BB Star" case study. *J. Seismol.*, 24(1), 101-120. DOI: 10.1007/s10950-019-09888-1.
[14]Drozdzewski, M., Sosnica, K., Zus, F. et al. (2019). Troposphere delay modeling with horizontal gradients for satellite laser ranging. *J. Geod.*, 93(10), 1853-1866. DOI: 10.1007/s00190-019-01287-1.
[15]Dwornik, M., Porzycka-Strzelczyk, S., Strzelczyk, J. et al. (2021). Automatic Detection of Subsidence Troughs in SAR Interferograms Using Mathematical Morphology. *Energies*, 14(22), 7785. DOI: 10.3390/en14227785.
[16]Fan, J., Wang, Q., Liu, G. et al. (2019). Monitoring and Analyzing Mountain Glacier Surface Movement Using SAR Data and a Terrestrial Laser Scanner: A Case Study of the Himalayas North Slope Glacier Area. *Remote Sens.*, 11(6), 625. DOI: 10.3390/rs11060625.
[17]Fenoglio, L., Dinardo, S., Uebbing, B. et al. (2020). Advances in NE-Atlantic coastal sea level change monitoring by Delay Doppler altimetry. *Adv. Space Res.*, 68(2), 571-592. DOI: 10.1016/j.asr.2020.10.041.
[18]Ferrandiz, J.M., Gross, R.S., Escapa, A. et al. (2020). Report of the IAU/IAG Joint Working Group on Theory of Earth Rotation and Validation, IAG Symposia. DOI: 10.1007/1345_2020_103.
[19]Foumelis, M., Papazachos, C., Papadimitriou, E. et al. (2021). On rapid multidisciplinary response aspects for Samos 2020 M7.0 earthquake. *Acta Geophys.*, 69, 1025-1048. DOI: 10.1007/s11600-021-00578-6.
[20]Gebauer, A., Tercjak, M., Schreiber, K.U. et al. (2020). Reconstruction of the Instantaneous Earth Rotation Vector with Sub-Arcsecond Resolution Using a Large Scale Ring Laser Array. *Physic. Rev. Lett.*, 125:033605. DOI: 10.1103/PhysRevLett.125.033605.
[21]Glowacki, T., and Kasza, D. (2021). Assessment of morphology changes of the end moraine of the Werenskiold Glacier (SW Spitsbergen) using active and passive remote sensing techniques. *Remote Sens.*, 13(11), 2134. DOI: 10.3390/rs13112134.
[22]Godah, W. (2019). IGiK-TVGMF: A MATLAB package for computing and analysing temporal variations of gravity/mass functionals from GRACE satellite based global geopotential models. *Comput. Geosci.*, 123, 47-58. DOI: 10.1016/j.cageo.2018.11.008.

Accepted Article

[23]Godah, W., Szelachowska, M., Ray, J.D. et al. (2020a). Comparison of vertical deformations of the Earth's surface obtained using GRACE-based GGMs and GNSS data – A case study of Poland. *Acta Geodyn. Geomater.*, 17, 169-176. DOI: 10.13168/AGG.2020.0012.
[24]Godah, W., Szelachowska, M., Krynski, J. et al. (2020b). Assessment of Temporal Variations of Orthometric/Normal Heights Induced by Hydrological Mass Variations over Large River Basins Using GRACE Mission Data. *Remote* Sens., 12(18), 3070. DOI: 10.3390/rs12183070.
[25]Gruber, T., Ågren, J., Angermann, D. et al. (2020). Geodetic SAR for Height System Unification and Sea Level Research – Observation Concept and Preliminary Results in the Baltic Sea. *Remote Sens.*, 12, 3747. DOI: 10.3390/rs12223747.
[26]Gruber, T., Ågren, J., Angermann, D. et al. (2022). Geodetic SAR for Height System Unification and Sea Level Research – Results in the Baltic Sea Test Network. *Remote Sens.*, 14, 3250. DOI: 10.3390/rs14143250.
[27]Grzempowski, P., Badura, J., Milczarek W. et al. (2020). Determination of the Long-Term Ground Surface Displacements Using a PSI Technique – Case Study on Wroclaw (Poland). *Appl. Sci.*, 10(10), 3343. DOI: 10.3390/app10103343.
[28]Guzy, A., and Malinowska, A.A. (2020). State of the art and recent advancements in the modelling of land subsidence induced by groundwater withdrawal. *Water*, 12, 2051. DOI: 10.3390/w12072051.
[29]Hejmanowski, R., Malinowska, A.A., Witkowski, W.T. et al. (2019). An analysis applying InSAR of subsidence caused by nearby mining-induced earthquakes. *Geosci.*, 9, 490. DOI: 10.3390/geosciences9120490.
[30]Ilieva, M., Polanin, P., Borkowski, A. et al. (2019a). Mining Deformation Life Cycle in the Light of InSAR and Deformation Models. *Remote Sens.*, 11(7), 745. DOI: 10.3390/rs11070745.
[31]Ilieva, M., Rudzinski, L., Pawluszek-Filipiak, K. et al. (2019b). Combined Study of a Significant Mine Collapse Based on Seismological and Geodetic Data – 29 January 2019, Rudna Mine, Poland. *Remote Sens.*, 12(10). DOI: 10.3390/rs12101570.
[32]Jagoda, M., and Rutkowska, M. (2019a). Determination of the local tidal parameters for the borowiec station using satellite laser ranging data. *Studia Geophys. et Geod.*, 63, 509-519. DOI: 10.1007/s11200-019-0726-5.
[33]Jagoda, M., and Rutkowska, M. (2019b). Estimation of the local tidal parameters h2, l2 for the Riga satellite laser ranging station based on LAGEOS data. *Estonian J. Earth Sci.*, 68(4), 199-205. DOI: 10.3176/earth.2019.14.
[34]Jagoda, M., Rutkowska, M., Obuchovski, R. et al. (2019). Tidal Parameters as a Tool for the Determination of the Coordinates of the SLR Stations. *Artificial Satellites, Journal of Planetary Geodesy*, 54(4), 129-135. DOI: 10.2478/arsa-2019-0010.
[35]Jagoda, M., and Rutkowska, M. (2020a). An analysis of the Eurasian tectonic plate motion parameters based on GNSS stations positions in ITRF2014. *Sensors*, 20(21), 6065. DOI: 10.3390/s20216065.
[36]Jagoda, M., and Rutkowska, M. (2020b). Use of VLBI measurement technique for determination of motion parameters of the tectonic plates. *Metrol. Meas. Syst.*, 27(1), 151-165. DOI: 10.24425/mms.2020.131722.
[37]Jagoda, M., Rutkowska, M., Suchocki, C. et al. (2020a). Determination of the tectonic plates motion parameters based on SLR, DORIS and VLBI stations positions. *J. Appl. Geod.*, 14(2), 121-131. DOI: 10.1515/jag-2019-0053.

Accepted Article

[38]Jagoda, M., Rutkowska, M., Lejba, P. et al. (2020b). Satellite Laser Ranging for retrieval of the local values of the Love h2 and Shida l2 numbers for the Australian ILRS stations. *Sensors*, 20(23), 6851. DOI: 10.3390/s20236851.
[39]Jagoda, M. (2021). Determination of motion parameters of selected major tectonic plates based on GNSS station positions and velocities in the ITRF2014. *Sensors*, 21(16), 5342. DOI: 10.3390/s21165342.
[40]Jarosinski, M., Araszkiewicz, A., Bobek, K. et al. (2022). Contemporary state of stress in a stable plate interior (northern Poland): The integration of satellite geodesy, borehole and seismological data. T*ectonophys.*, 831, 229336. DOI: 10.1016/j.tecto.2022.229336.
[41]Jozkow, G., Walicka, A., and Borkowski, A. (2021). Monitoring terrain deformations caused by underground mining using UAV data. *Int. Arch. Photogramm. Remote Sens. Spatial Inf. Sci*., XLIII-B2-2021, 737-744. DOI: 10.5194/isprs-archives-XLIII-B2-2021-737-2021.
[42]Kaczmarek, A. (2019). Influence of Geophysical Signals on Coordinate Variations GNSS Permanent Stations in Central Europe. *Artificial Satellites, Journal of Planetary Geodesy*, 54(3), 57-71. DOI: 10.2478/arsa-2019-0006.
[43]Kaczorowski, M., Kasza, D., Zdunek, R. et al. (2019). Time dependencies between tectonic activity of Świebodzice Depression (SW Poland) and seismic activity in Poland and Czech mining regions. In E3S Web of Conferences, 105, 02001. DOI: 10.1051/e3sconf/201910502001.
[44]Kaczorowski, M., Kasza, D., Zdunek, R. et al. (2021). Time distribution of strong seismic events in the Fore-Sudetic Monocline in context of signals registered by water-tube gauges in Ksiaz Geodynamic Laboratory. *Sensors*, 21(5), 1603. DOI: 10.3390/s21051603.
[45]Kaczorowski, M., Kasza, D., Zdunek, R., Wronowski, R. (2022). Investigation of signals of the range 10-3 – 10-4 Hz registered by water-tube tiltmeters in the Underground Geodynamic Laboratory in Ksiaz (SW Poland). *Artificial Satellites, Journal of Planetary Geodesy*, 57(4), 210-236. DOI: 10.2478/arsa-2022-0011.
[46]Karkowska, K., and Wilde-Piorko, M. (2022). Determination of the Earth's structure based on intermediate-period surface wave recordings of tidal gravimeters: A case study. *Earth Planets Space*, 74(1), 1-14. DOI: 10.1186/s40623-022-01712-4.
[47]Karkowska, K., Wilde-Piorko M., and Dykowski, P. (2022). Analysis of earthquakes recordings of tidal gravimeters in the period range of 10–1000 s. *Acta Geodynyn. Geomater.*, 19(1), 79-92. DOI: 10.13168/AGG.2021.0043.
[48]Klos, A., Kusche, J., Fenoglio-Marc, L. et al. (2019). Introducing a vertical land motion model for improving estimates of sea level rates derived from tide gauge records affected by earthquakes. *GPS Solut.*, 23, 102. DOI: 10.1007/s10291-019-0896-1.
[49]Klos, A., Bogusz, J., Bos, M.S. et al. (2020a). *Modelling the GNSS time series: different approaches to extract seasonal signals*. In: Montillet J.-P. and Bos M. (eds.) Geodetic Time Series Analysis in Earth Sciences. Springer: Geophysics, 211-237. DOI: 10.1007/978-3-030-21718-1_7.
[50]Klos, A., Karegar, M.A., Kusche, J. et al.. (2020b). Quantifying Noise in Daily GPS Height Time Series: Harmonic Function Versus GRACE-Assimilating Modeling Approaches. *IEEE Geosci. Remote Sens. Lett.*, 18(4), 627-631. DOI: 10.1109/LGRS.2020.2983045.
[51]Klos, A., Dobslaw, H., Dill, R. et al. (2021). Identifying the sensitivity of GPS to non-tidal loadings at various time resolutions: examining vertical displacements from continental Eurasia. *GPS Solut.*, 25, 89. DOI: 10.1007/s10291-021-01135-w.
[52]Kosek, W., Popinski, W., Wnek, A. et al. (2020). Analysis of Systematic Errors in Geocenter Coordinates Determined From GNSS, SLR, DORIS, and GRACE. *Pure Appl. Geophys.*, 177, 867-888. DOI: 10.1007/s00024-019-02355-5.

Accepted Article

[53]Kowalczyk, K. (2019). Changes In Mean Sea Level On The Polish Coast Of The Baltic Sea Based On Tide Gauge Data From The Years 1811-2015. *Acta Geodyn. et Geomater.*, 16(2), 195-210. DOI: 10.13168/AGG.2019.0016.

[54]Kowalczyk, K., Pajak, K., and Naumowicz, B. (2019). Modern vertical crustal movements of the Southern Baltic coast from tide gauge, satellite altimetry and GNSS observations. *Acta Geodyn. et Geomater.*, 16(3), 245-253. DOI: 10.13168/AGG.2019.0020.

[55]Kowalczyk, K., Kowalczyk, A.M., and Chojka, A. (2020). Modeling of the vertical movements of the earth's crust in Poland with the co-kriging method based on various sources of data. *Appl. Sci.*, 10(9), 3004. DOI: 10.3390/app10093004.

[56]Kowalczyk, K., Kowalczyk, A.M., and Rapinski, J. (2021a). Identification of common points in hybrid geodetic networks to determine vertical movements of the Earth's crust. *J. Appl. Geod.*, 15(2), 153-167. DOI: 10.1515/jag-2021-0002.

[57]Kowalczyk, K., Pajak, K., Wieczorek, B. et al. (2021b). An Analysis of Vertical Crustal Movements along the European Coast from Satellite Altimetry, Tide Gauge, GNSS and Radar Interferometry. *Remote Sens.*, 13(11), 2173. DOI: 10.3390/rs13112173.

[58]Kowalski, A., Kasza, D., and Wajs, J. (2019). Structural control of mass movements on slopes formed of magmatic and metamorphic rocks: the case study of Wielisławka Mt. (SW Poland, Sudetes Mts.). *Geological Quarterly*, 63(3), 460-477. DOI: 10.7306/gq.1482.

[59]Kudlacik, I., Kaplon, J., Bosy, J. et al. (2019). Seismic phenomena in the light of high-rate GPS Precise Point Positioning results. *Acta Geodyn. et Geomater.*, 16(1(193)), 99-112. DOI: 10.13168/AGG.2019.0008.

[60]Kudlacik, I., Kaplon, J., Lizurek, G. et al. (2021). High-rate GPS positioning for tracing anthropogenic seismic activity: The 29 January 2019 mining tremor in Legnica-Glogów Copper District, Poland. *Measurement*, 168, 108396. DOI: 10.1016/j.measurement.2020.108396.

[61]Kur, T., Dobslaw, H., Sliwinska, J. et al. (2022). Evaluation of select-ed short term predictions of UT1 UTC and LOD collected in the second earth orientation parameters prediction comparison campaign. *Earth Planets Space*, 74(191). DOI: 10.1186/s40623-022-01753-9.

[62]Ligas, M., Banas, M., and Szafarczyk, A. (2019). A method for local approximation of a planar deformation field. *Rep. Geod. Geoinform.*, 108(1), 1-8. DOI: 10.2478/rgg-2019-0007.

[63]Liu, G., Guo, H., Perski, Z. et al. (2019). Landslide movement monitoring with ALOS-2 SAR data. *IOP Conf. Ser.: Earth Environ. Sci*., 227, 062015. DOI: 10.1088/1755-1315/227/6/062015.

[64]Lyszkowicz, A., and Bernatowicz, A. (2019). Geocentric Baltic Sea level changes along the southern coastline. *Adv. Space Res.*, 64, 1807-1815. DOI: 10.1016/j.asr.2019.07.040.

[65]Lyszkowicz, A., Pelc-Mieczkowska, R., Bernatowicz, A. et al. (2021a). First results of time series analysis of the permanent GNSS observations at Polish EPN stations using GipsyX software. *Artificial Satellites, Journal of Planetary Geodesy*, 56, (3). DOI: 10.2478/arsa-2021-0008.

[66]Lyszkowicz A., Nastula J., Zielinski J.B., Birylo M. (2021b). A New Model of Quasigeoid for the Baltic Sea Area. Remote Sensing, 13, 2580, doi:10.3390/rs13132580.

[67]Maciuk, K. (2021). *GNSS monitoring natural and anthropogenic phenomena*. In: George p. Petropoulos, Prashant K. Srivastava (eds) GPS and GNSS Technology in Geosciences. Elsevier, 177-197, ISBN 9780128186176, DOI: 10.1016/B978-0-12-818617-6.00007-X.

[68]Maciuk, K., Peska-Siwik, A., El-Mowafy, A. et al. (2021). Crustal Deformation Across and beyond Central Europe and Its Impact on Land Boundaries. *Resources*, 10, 15. DOI: 10.3390/resources10020015.

Accepted Article

[69]Malinowska, A.A., Witkowski, W.T., Hejmanowski, R. et al. (2019). Sinkhole Occurrence Monitoring Over Shallow Abandoned Coal Mines with Satellite-Based Persistent Scatterer Interferometry. *Eng. Geo.*, 262, 105336. DOI: 10.1016/j.enggeo.2019.105336.
[70]Malinowska, A.A., Witkowski, W.T., Guzy, A. et al. (2020a). Satellite-based monitoring and modeling of ground movements caused by water rebound. *Remote Sens.*, 12, 1786. DOI: 10.3390/rs12111786.
[71]Malinowska A.A., Hejmanowski, R., and Dai, H. (2020b). Ground Movements Modeling Applying Adjusted Influence Function. *Int. J. Mining Sci. Tech.*, 30, 243-249. DOI: 10.1016.j.ijmst.2020.01.007.
[72]Malkin, Z., Gross, R., McCarthy, D. et al. (2019). On the eve of the 100th anniversary of IAU Commission 19/A2 "Rotation of the Earth". Under One Sky: The IAU Centenary Symposium Proc. IAU Symposium No. 349, C. Sterken, J. Hearnshaw and D. Valls-Gabaud (eds.), 325-331. DOI: 10.1017/S1743921319000462.
[73]Michalczak, M., and Ligas, M. (2021). Kriging-based prediction of the Earth's pole coordinates. *J. Appl. Geod.*, 15(3), 233-241. DOI: 10.1515/jag-2021-0007.
[74]Michalczak, M., and Ligas, M. (2022). The (ultra) short term prediction of length-of-day us-ing kriging. *Adv. Space Res.*, 70(3), 610-620. DOI: 10.1016/ j.asr.2022. 05.007.
[75]Michalczak, M., Ligas, M., and Kudrys, J. (2022). Prediction of Earth Rotation Parameters with the use of Rapid Products from IGS, Code and GFZ Data Centres Using Arima and Kriging – A Comparison. *Artificial Satellites, Journal of Planetary Geodesy*, 57(s1), 275-289. DOI: 10.2478/ arsa-2022-0024.
[76]Milczarek, W. (2019a). Application of a small baseline subset time series method with atmospheric correction in monitoring results of mining activity on ground surface and in detecting induced seismic events. *Remote Sens.*, 11, 1008. DOI: 10.3390/rs11091008.
[77]Milczarek, W. (2019b). Investigation of post inducted seismic deformation of the 2016 MW 4.2 Tarnowek Poland mining tremor based on DinSAR and SBAS method. *Acta Geodyn. et Geomater.*, 16(2), 183-193. DOI: 10.13168/AGG.2019.0015.
[78]Mutke, G., Kotyrba, A., Lurka, A. et al. (2019). Upper Silesian Geophysical Observation System – A unit of the EPOS project. *J. Sustain. Min.*, 18(4), 198-20. DOI: 10.1016/j.jsm.2019.07.005.
[79]Nastula, J., Winska, M., Sliwinska, J. et al. (2019). Hydrological signals in polar motion excitation – Evidence after fifteen years of the GRACE mission. *J. Geodyn.*, 124, 119-132. DOI: 10.1016/j.jog.2019.01.014.
[80]Nastula, J., and Sliwinska, J. (2020). Prograde and Retrograde Terms of Gravimetric Polar Motion Excitation Estimates from the GRACE Monthly Gravity Field Models. Remote Sensing, 12(1), 1-29, doi:10.3390/rs12010138.
[81]Nastula, J., Chin, T.M., Gross, R. et al. (2020). Smoothing and pre-dicting celestial pole offsets using a Kalman filter and smoother. *J. Geod.*, 94(3). DOI: 10.1007/s00190-020-01349-9.
[82]Nastula, J., Sliwinska, J., Kur T. et al. (2022). Preliminary study on hydrological angular momentum determined from CMIP6 historical simulations. *Earth Planets Space*, 74, 1-26. DOI: 10.1186/s40623-022-01636-z.
[83]Nistor, S., Suba, N.-S., El-Mowafy, A. et al. (2021). Implication between Geophysical Events and the Variation of Seasonal Signal Determined in GNSS Position Time Series. *Remote Sens.*, 13, 3478. DOI: 10.3390/rs13173478.
[84]Owczarz, K., and Blachowski, J. (2020a). Application of DInSAR and Spatial Statistics Methods in Analysis of Surface Displacements Caused by Induced Tremors. *Appl. Sci.*, 10, 7660. DOI: 10.3390/app10217660.

Accepted Article

[85]Owczarz, K., and Blachowski, J. (2020b). Analysis of the geometry of surface deformations caused by induced tremors in the area of underground copper mining. *ISPRS Ann. Photogramm. Remote Sens. Spatial Inform. Sci.*, V-3-2020, 149-156. DOI: 10.5194/isprs-annals-V-3-2020-149-2020.
[86]Pajak, K., and Kowalczyk, K. (2019). A comparison of seasonal variations of sea level in the southern Baltic Sea from altimetry and tide gauge data. *Adv. Space Res.*, 63, 1768-1780. DOI: 10.1016/j.asr.2018.11.022.
[87]Pajak, K., Kowalczyk, K., Kaminski, J. et al. (2021). Studying the Sensitivity of Satellite Altimetry, Tide Gauge and GNSS Observations to Changes in Vertical Displacements. *Geomat. Environ. Eng.*, 15(4), 45-58. DOI: 10.7494/geom.2021.15.4.45.
[88]Pawluszek, K. (2019). Landslide features identification and morphology investigation using high-resolution DEM derivatives. *Nat. Hazards*, 96, 311-330. DOI: 10.1007/s11069-018-3543-1.
[89]Pawluszek, K., Marczak, S., Borkowski, A. et al. (2019). Multi-Aspect Analysis of Object-Oriented Landslide Detection Based on an Extended Set of LiDAR-Derived Terrain Features. *ISPRS Int. J. Geo-Inform.*, 8(8), 321. DOI: 10.3390/ijgi8080321.
[90]Pawluszek-Filipiak, K., and Borkowski, A. (2020a). Comparison of PSI and DInSAR approach for the subsidence monitoring caused by coal mining exploitation. *ISPRS Archiv. Photogramm., Remote Sens. Spatial Infor. Sci. (ISPRS Archives)*, XLIII-B3-2020, 333-337. DOI: 10.5194/isprs-archives-XLIII-B3-2020-333-2020.
[91]Pawluszek-Filipiak, K., and Borkowski, A. (2020b). Integration of DInSAR and SBAS Techniques to Determine Mining-Related Deformations Using Sentinel-1 Data: The Case Study of Rydultowy Mine in Poland. *Remote Sens.*, 12(2), 242. DOI: 10.3390/rs12020242.
[92]Pawluszek-Filipiak, K., Orenczak, N., and Pasternak, M. (2020). Investigating the Effect of Cross-Modeling in Landslide Susceptibility Mapping. *Appl. Sci.*, 10 (18), 6335. DOI: 10.3390/app10186335.
[93]Pawluszek-Filipiak, K., and Borkowski, A. (2021a). Monitoring mining-induced subsidence by integrating differential radar interferometry and persistent scatterer techniques. *European J. Remote Sens.*, 54(S1), 18-30. DOI: 10.1080/22797254.2020.1759455.
[94]Pawluszek-Filipiak, K., and Borkowski, A. (2021b). *Object-Oriented Automatic Landslide Detection from High Resolution Digital Elevation Model – Opportunities and Challenges Based on a Case Study in the Polish Carpathians*. In: Guzzetti, F., Mihalić Arbanas, S., Reichenbach, P., Sassa, K., Bobrowsky, P.T., Takara, K. (eds) Understanding and Reducing Landslide Disaster Risk. WLF 2020. ICL Contribution to Landslide Disaster Risk Reduction. Springer: Cham. DOI: 10.1007/978-3-030-60227-76.
[95]Pawluszek-Filipiak, K., and Borkowski, A. (2021c). *Updating Landslide Activity State and Intensity by Means of Persistent Scatterer Interferometry*. In: Guzzetti, F., Mihalić Arbanas, S., Reichenbach, P., Sassa, K., Bobrowsky, P.T., Takara, K. (eds) Understanding and Reducing Landslide Disaster Risk. WLF 2020. ICL Contribution to Landslide Disaster Risk Reduction. Springer: Cham. DOI: 10.1007/978-3-030-60227-7_12.
[96]Pawluszek-Filipiak, K., and Borkowski, A. (2021d). Mining-induced tremors in the light of deformations estimated by satellite SAR interferometry in the Upper Silesian Coal Basin, Poland. *Procedia Computer Science*, 181, 685-692. DOI: 10.1016/j.procs.2021.01.219.
[97]Pawluszek-Filipiak, K., Borkowski, A., and Motagh, M. (2021). Multi-temporal landslide activity investigation by spaceborne SAR interferometry: The case study of the Polish Carpathians. *Remote Sens. Applicat. Soc. Environ.*, 24, 100629. DOI: 10.1016/j.rsase.2021.100629.

Accepted Article

[98]Paziewski, J., Kurpinski, G., Wielgosz, P. et al. (2020). Towards Galileo + GPS seismology: Validation of high-rate GNSS based system for seismic events characterisation. *Measurement*, 166, 108236. DOI: 10.1016/j.measurement.2020.108236.
[99]Przylibski, T.A., Domin E., Gorecka J. et al. (2020). 222Rn concentration in groundwaters circulating in granitoid massifs of Poland. *Water*, 12(3), 748. DOI: 10.3390/w12030748.
[100]Przylucka, M., Kowalski, Z., and Perski, Z. (2022). Twenty years of coal mining-induced subsidence in the Upper Silesia in Poland identified using InSAR. *Int. J. Coal Sci. Tech.*, 9, 86. DOI: 10.1007/s40789-022-00541-w.
[101]Ray, J.D., Vijayan, M.S.M., and Godah, W. (2021). Seasonal Horizontal Deformations Obtained Using GPS and GRACE Data: Case Study of North-East India and Nepal Himalaya. *Acta Geod. Geophys*., 56, 61-76. DOI: 10.1007/s40328-020-00331-3.
[102]Rosat, S., Boy, J.-P., Bogusz J. et al. (2020). *Inter-Comparison of Ground Gravity and Vertical Height Measurements at Collocated IGETS Stations*. In: Freymueller, J.T., Sánchez, L. (eds) Beyond 100: The Next Century in Geodesy. International Association of Geodesy Symposia, 152, 113-120. DOI: 10.1007/1345_2020_117.
[103]Rudzinski, L., Mirek, K., and Mirek J. (2019). Rapid ground deformation corresponding to a mining-induced seismic event followed by a massive collapse. *Nat. Hazards*, 96(1), 461-471. DOI: 10.1007/s11069-018-3552-0.
[104]Sliwinska, J., and Nastula, J. (2019). Determining and evaluating the hydrological signal in polar motion excitation from gravity field models obtained from kinematic orbits of LEO satellites. *Remote Sens.*, 11(15), 1-19. DOI: 10.3390/rs11151784.
[105]Sliwinska, J., Nastula, J., Dobslaw H. et al.. (2020a). Evaluating gravimetric polar motion excitation estimates from the RL06 GRACE monthly-mean gravity field models. *Remote Sens.*, 12(6), 1-29. DOI: 10.3390/rs12060930.
[106]Sliwinska, J., Winska, M., and Nastula J. (2020b). Preliminary estimation and validation of polar motion excitation from different types of the GRACE and GRACE Follow-On missions data. *Remote Sens.*, 12(21), 1-28. DOI: 10.3390/rs12213490.
[107]Sliwinska, J., Nastula, J., and Winska, M. (2021a). Evaluation of hydrological and cryospheric angular momentum estimates based on GRACE, GRACE-FO and SLR data for their contri-butions to polar motion excitation. *Earth Planets Space*, 73(1). DOI: 10.1186/s40623-021-01393-5.
[108]Sliwinska, J., Winska, M., and Nastula, J. (2021b). Validation of GRACE and GRACE-FO Mascon Data for the Study of Polar Motion Excitation. *Remote Sens.*, 13(6), 1-22. DOI: 10.3390/rs13061152.
[109]Sliwinska, J., Winska, M., and Nastula, J. (2022a). Exploiting the Combined GRACE/GRACE-FO Solutions to Determine Gravimetric Excitations of Polar Motion. *Remote Sens.*, 14(24), 1-22. DOI: 10.3390/rs14246292.
[110]Sliwinska, J., Kur, T., Winska, M. et al.. (2022b). Second Earth Orientation Parameters Prediction Comparison Campaign (2nd EOP PCC): overview. *Artificial Satellites, Journal of Planetary Geodesy*, 57(S1), 237-253. DOI: 10.2478/arsa-2022-0021.
[111]Sliwinska, J. (2022). *Estimating and validating the hydrological and cryospheric signal in polar motion excitation determined from observations of the Gravity Recovery and Climate Experiment (GRACE) and GRACE Follow-On (GRACE-FO) satellite missions*. PhD Thesis, Space Research Centre PAS, Warsaw.
[112]Sopata, P., Stoch, T., Wojcik, A. et al. (2020). Land Surface Subsidence Due to Mining-Induced Tremors in the Upper Silesian Coal Basin (Poland) – Case Study. *Remote Sens.*, 12(23), 3923. DOI: 10.3390/rs12233923.

Accepted Article

[113]Sosnica, K., Bury, G., Zajdel, R. et al. (2019). Estimating global geodetic parameters using SLR observations to Galileo, GLONASS, Bei-Dou, GPS, and QZSS. *Earth Planets Space*, 71(20), 1-11. DOI: 10.1186/s40623-019-1000-3.
[114]Sousa, J.J., Liu, G., Fan, J. et al. (2021). Geohazards Monitoring and Assessment Using Multi-Source Earth Observation Techniques. *Remote Sens.*, 13, 4269. DOI: 10.3390/rs13214269.
[115]Strugarek, D., Sosnica, K., Arnold, D. et al. (2019). Determination of Global Geodetic Parameters Using Satellite Laser Ranging Meas-urements to Sentinel-3 Satellites. *Remote Sens.*, 11(19), 2282, 1-21. DOI: 10.3390/rs11192282.
[116]Szafarczyk, A. (2019a). Stages of geological documentation on the example of landslides located on the slopes of the dam reservoir "Swinna Poreba" (Poland). In IOP Conference Series: Earth and Environmental Science (Vol. 221, No. 1, p. 012037). IOP Publishing. DOI: 10.1088/1755-1315/221/1/012037.
[117]Szafarczyk, A. (2019b). Kinematics of mass phenomena on the example of an active landslide monitored using GPS and GBInSAR technology. *J. Appl. Eng. Sci.*, 17(2), 107-115. DOI: 10.5937/jaes17-18748.
[118]Szafarczyk, A., Skaba, A., and Sokalla, K. (2019). Implementation of gyroscope measurements in underground mines; focus on the mine of ruch (unit) „Borynia" in the Jastrzębie Coal Company. *Geoinformatica Polonica*, 18, 113-120. DOI: 10.4467/21995923GP.19.009.11576.
[119]Szczerbowski, Z. (2019). High-energy seismic events in Legnica–Głogów Copper District in light of ASG-EUPOS data. *Rep. Geod. Geoinform.*, 107(1), 25-40. DOI: 10.2478/rgg-2019-0004.
[120]Szczerbowski, Z. (2020). Irregularity of post mining deformations as indicator revealing effects of processes of unknown origin in area of Bochnia. *Geoinformatica Polonica*, 19, 7-18. DOI: 10.4467/21995923GP.20.008.13073.
[121]Szczerbowski, Z., and Gawalkiewicz, R. (2020). The apparent displacement method as a tool in leveling data processing applied for validated determination of ground deformation. *Geoinformatica Polonica*, 19, 95-105. DOI: 10.4467/21995923GP.20.009.13074.
[122]Szczerbowski, Z., and Niedbalski, Z. (2021). The Application of a Sonic Probe Extensometer for the Detection of Rock Salt Flow Field in Underground Convergence Monitoring. *Sensors*, 21(16), 5562. DOI: 10.3390/s21165562.
[123]Tercjak, M., Gebauer, A., Rajner, M. et al. (2020). On the Influence of Diurnal and Subdiurnal Signals in the Normal Vector on Large Ring Laser Gyroscope Ob-servations. *Pure Appl. Geophys.*, 177, 4217-4228. DOI: 10.1007/s00024-020-02484-2.
[124]Tercjak, M. (2021). Short period variations of Earth rotation from measurements made by Ring Laser Gyroscopes. PhD Thesis, Warsaw University of Technology, Faculty of Geodesy and Cartography.
[125]Wajs, J., Trybala, P., Gorniak-Zimroz, J. et al. (2021). Modern solution for fast and accurate inventorization of open-pit mines by the active remote sensing technique – case study of Mikoszów granite mine (Lower Silesia, SW Poland). *Energies*, 14(20), 6853. DOI: 10.3390/en14206853.
[126]Winska, M., and Sliwinska, J. (2019). Assessing hydrological signal in polar motion from observations and geophysical models. *Studia Geophys. Geod.*, 63(1), 95-117. DOI: 10.1007/s11200-018-1028-z.
[127]Winska M. (2022). A comparative study of interannual oscillation models for determining geophysical polar motion excitations. Remote Sensing, 14(1), 147, doi:10.3390/rs14010147.

Accepted Article

[128]Yu, H., Sosnica, K., and Shen, Y. (2021) Separation of Geophysical Signals in the LAGEOS Geocenter Motion based on Singular Spectrum Analysis. *Geophys. J. Int.*, 225(3), 1755-1770. DOI: 10.1093/gji/ggab063.

[129]Zajdel, R., Sosnica, K., Dach, R. et al. (2019a). Network effects and handling of the geocenter motion in multi-GNSS processing. *J. Geophys. Res. Solid Earth*, 124(6), 5970-5989. DOI: 10.1029/2019JB017443.

[130]Zajdel, R., Sosnica, K., Drozdzewski, M. et al. (2019b). Impact of network constraining on the terrestrial reference frame realization based on SLR observations to LAGEOS. *J. Geod.*, 93(11), 2293-2313. DOI: 10.1007/ s00190-019-01307-0.

[131]Zajdel, R., Sosnica, K., Bury, G. et al. (2020). System-specific systematic errors in earth rotation parameters derived from GPS, GLONASS, and Galileo. *GPS Solut.*, 24(74), 1-15. DOI: 10.1007/s10291-020-00989-w.

[132]Zajdel, R., Sosnica, K., Bury, G. et al. (2021a). Sub-daily polar motion from GPS, GLONASS, and Galileo. *J. Geod.*, 95(3), 1-27. DOI: 10.1007/s00190-020-01453-w.

[133]Zajdel, R., Sosnica, K., and Bury, G. (2021b). Geocenter coordinates derived from multi-GNSS: a look into the role of solar radiation pressure modeling. *GPS Solut.*, 25, 1. DOI: 10.1007/s10291-020-01037-3.

Accepted Article

Research on GNSS positioning and applications in Poland in 2019-2022

Jacek Paziewski[1]*, Tomasz Hadas[2], Witold Rohm[2], Pawel Wielgosz[1]

[1]University of Warmia and Mazury, Olsztyn, Poland,
[2]Wroclaw University of Environmental and Life Sciences, Wroclaw, Poland,
*Corresponding author: Jacek Paziewski, e-mail: jacek.paziewski@uwm.edu.pl

Abstract: This paper reviews the key studies concerning GNSS positioning and applications conducted at leading Polish research institutions from 2019 until 2022. The review also constitutes a contribution to the national report of Poland for the International Union of Geodesy and Geodynamics (IUGG) presented at the 28th General Assembly of IUGG held in 2023 in Berlin, Germany. In particular, we discuss the advances in theory and applications of relative and absolute positioning, troposphere and ionosphere sounding, smartphone and low-cost GNSS data processing, and other specific studies such as those on satellite antenna calibration and clock stability. In light of these recent advances by the Polish scientific community, continuous progress in GNSS theory and processing algorithms is thought to be maintained in the future, and GNSS applications are expected to continue to proliferate.

Keywords: GNSS, positioning, geodesy, troposphere, ionosphere

1. Introduction

GNSS now plays a vital role in providing position-related information and in Earth and environmental studies by exploiting advances in theories and cutting-edge processing algorithms, satellite deployment, the precision of new signals, and multi-sensor fusion. This progress has led to a significant spread of GNSS to new fields of science and industry, bringing further benefit to society. As a result, with GNSS, it is now feasible to support a broad scope of applications ranging from personal and vehicle navigation through geodesy and surveying to geohazard and atmosphere monitoring.

This paper offers a review of the recent advancements by the Polish geodetic community in GNSS positioning and applications and an outline of possible future developments. This review also constitutes a contribution to the national report of Poland for the International Union of Geodesy and Geodynamics (IUGG) covering the period of 2019-2022 and presented at the 28th General Assembly of the IUGG held in 2023 in Berlin, Germany. In particular, we give credit to the most important and latest articles by Polish research institutions, which approach a wide range of GNSS studies, such as enhancing functional, stochastic, and correction models of positioning, structural health and seismicity monitoring, troposphere and ionosphere sounding, and geodynamics studies (Fig. 1). All the commented articles exhibited high novelty and research standards and were published in leading scientific journals in the field. Therefore, we anticipate they will foster meaningful scientific and technological progress and outreach geodetic-related studies.

Accepted Article

This article has been accepted for publication in the journal Advances in Geodesy and Geoinformation, issue 72/2, 2023. It has not yet undergone the process of copyediting, typesetting, pagination and proofreading. This may lead to differences between this version and the final published version. The article may be cited as DOI: 10.24425/agg.2023.144595.

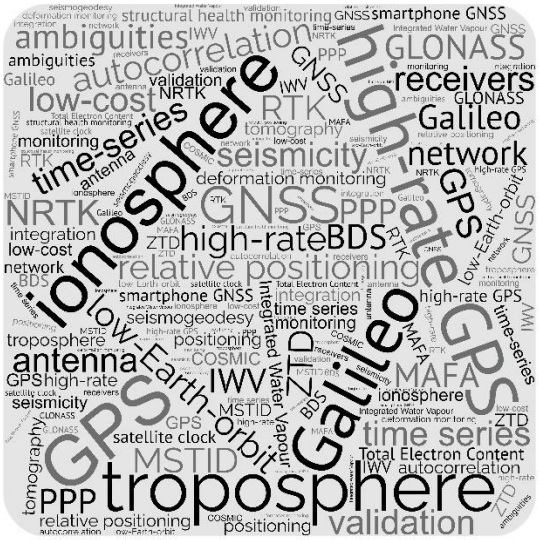

Fig. 1. Word cloud of the topics discussed in this review paper

2. Advances in GNSS positioning

The Polish geodetic research community has recognizable achievements in developing, assessing, and applying precise positioning methods based on GNSS systems. In this regard, we distinguish the studies taking the employed positioning technique as a criterion. Consequently, below, we report the recent progress in relative positioning, including Real Time Kinematics (RTK) and Precise Point Positioning (PPP) modes.

2.1 Progress in relative positioning

Relative positioning has proved its exceptional accuracy and reliability among GNSS positioning techniques. Despite its high performance, still, noticeable progress has been recently made. This section discusses the studies on Integer Ambiguity Resolution (IAR) algorithms, correction, stochastic and functional models of relative positioning, which foster further development in the field.

Studies on integer ambiguity resolution and validation

MAFA is the method for IAR developed at the University of Warmia and Mazury in Olsztyn (UWM). Recently, a few noticeable advances in this regard have been introduced. A search procedure has been improved by optimizing a search step. In [11]Cellmer et al. (2022a), the authors analytically derived the search step's length for a given satellite configuration. The upper limit of the search step's size is individual for each satellite configuration. This improvement reduces the number of necessary candidates needed to find the correct solution compared to the case with fixed search steps used to date. The authors described their method using a concept of the Voronoi cells in three-dimensional space.

A reduction based on decorrelation was, in turn, proposed in [12]Cellmer et al. (2022b) to improve the MAFA method further. The reduction process transforms the original math model into an equivalent one in the sense of obtaining the same solution. Such a reduction aims to increase the efficiency of searching for some parameters, i.e., integer ambiguities. Experiment results show a positive impact on search process efficiency, as computational time is reduced by more than 40% when processing short sessions.

Accepted Article

Further advances were related to enhancing IAR in instantaneous relative GNSS positioning. The iterative Tikhonov regularization for single-epoch positioning was demonstrated in [18]Fischer et al. (2022). This approach considers a single regularization parameter that regularizes baseline components and ambiguities. The precision of float solutions was improved at the cost of a small amount of regularized bias. Therefore, the overall accuracy was superior in the sense of mean-squared error. Due to the better accuracy properties of the float solution, the success probability of correct integer ambiguity estimation was higher. As a result, instantaneous precise relative positioning was more frequently guaranteed.

Despite the abovementioned progress in integer ambiguity resolution methods, a reliable validation of this step is still an issue. This task is typically accomplished with the use of hypothesis testing. From the statistical point of view, however, this approach is not rigorous in the case of multiple outliers, as it suffers from statistical dependencies between test statistics, especially in the case of baseline GNSS observations which are strongly correlated. A particular problem of the model validation using a hypothesis testing approach is the arbitrary choice of significance level - false alarm rate. In the paper by [56]Nowel et al. (2021), a new approach that overcomes the hypothesis testing issues was presented. It uses combinatorics and information criteria (IC) from information theory. The experiments revealed that the hypothesis testing approach achieved the highest success rates of model validation when no outlier existed. However, as the number of outliers increased, the IC approach achieved the highest success rates. The validation of relative GNSS observation models using the suggested IC approach turned out to be a valuable alternative to the conventional hypothesis testing approach and, thus, deserves further investigation.

Enhancing functional, stochastic, and correction models of relative positioning

Ionospheric disturbances imply precise positioning performance to a great extent. Even in the case of Network RTK (NRTK) positioning, this unfavorable effect cannot be fully mitigated by providing network ionospheric corrections. Under disturbed ionospheric conditions, the corrections suffer from poor accuracy and the presence of outliers. These effects are driven by a failure of a spatial interpolation process. RTK positioning becomes even more challenging in the case of a long-range scenario when baselines often exceed 100 km.

In [62]Paziewski and Sieradzki (2020a), the authors proposed and examined the method allowing for precise wide-area rapid static and RTK positioning under severe ionospheric conditions. The method enhances the relative positioning model by combining multi-constellation network ionospheric corrections and a new algorithm eliminating the changes of the ionospheric delays in time. The method's performance was validated using GPS, BDS, and Galileo observations collected at high latitudes during the ionospheric storm on August 25-26, 2018. As expected, the poor accuracy of the network ionospheric corrections and, consequently, a decline in RTK performance with routine relative positioning model were confirmed. On the contrary, with the novel method, it was feasible to achieve a remarkable improvement in the ambiguity resolution domain, which reached even over 20% compared to the benchmark models.

The studies on enhancing Network RTK positioning were also conducted at the Department of Geodesy and Geodetic Astronomy Warsaw University of Technology (WUT). In [71]Prochniewicz et al. (2020), the authors comprehensively analyze the performance of all RTK services provided by Poland's nationwide networks of Continuous Operating Reference Stations (CORS). The tests covered 15 Network RTK services and 7 RTK services from the ASG-EUPOS, SmartNet, TPI NetPro, VRSNet, and NadowskiNet networks. The accuracy and reliability of positioning performance, time to first fix, correction average age, and compliance of the reference frame realization were investigated. Table 1 exhibits position accuracy with

Accepted Article

Root Mean Square Error (RMSE) and standard deviation (STD) for tested services as an average value for each network. The results revealed that accuracy and precision for all NRTK and RTK services for the horizontal component were at very similar levels of 1 cm for RMSE and up to 1 mm for STD. The only exception is the NadowskiNet network, for which the RMSE for the NRTK service reached 2 cm. Regarding the height component, the accuracy of NRTK and RTK ASG-EUPOS services are two to three times less accurate than other networks with an RMSE of 4 cm.

Table 1. Mean positioning accuracy and precision reflected in RMSEs and STDs for tested networks ([71]Prochniewicz et al., 2020)

Method	Network	RMSE [m]		STD [mm]		
		Hor.	Vert.	North	East	Height
NRTK	ASG-EUPOS	0.010	0.027	0.61	0.44	1.12
	SmartNet	0.009	0.009	0.61	0.42	0.96
	TPI NetPro	0.012	0.018	0.53	0.35	1.21
	VRSNet	0.012	0.017	0.63	0.44	1.21
	NadowskiNet	0.022	0.009	0.52	0.37	0.86
RTK	ASG-EUPOS	0.011	0.036	0.76	0.57	1.29
	SmartNet	0.011	0.012	1.11	0.61	1.82
	TPI NetPro	0.011	0.021	0.68	0.45	1.30
	VRSNet	0.011	0.018	0.65	0.47	1.78

Much attention has also been paid to refining the stochastic models of GNSS positioning. A new multi-constellation and multi-signal empirical stochastic model was proposed as a fully populated variance-covariance (VC) matrix. The model considers the Carrier-to-Noise density Ratio (C/N0)-dependent variance function and the cross- and time-correlations between the observations ([73]Prochniewicz et al., 2021). The validation of the novel stochastic model against the common elevation-dependent one showed that the former increases both the positioning accuracy and the efficiency of ambiguity resolution. Figure 2 summarizes the position error of two comparative weighting methods: the elevation-dependent model and the C/N0 model, with the individual empirical model for each satellite block taking into account the correlation parameters. The 3D position error statistics are shown as a box whisker plot with the 75th, 50th, and 25th percentiles of errors and most extreme values. In addition, a red dot marks the maximum position error for each scenario. These statistics confirmed the effectiveness of the C/N0 model in reducing errors, for which the optimal solution was obtained for the multi-GNSS model (GREC) with a median error of 4.3 mm and the lowest maximum error of 15.2 mm.

Accepted Article

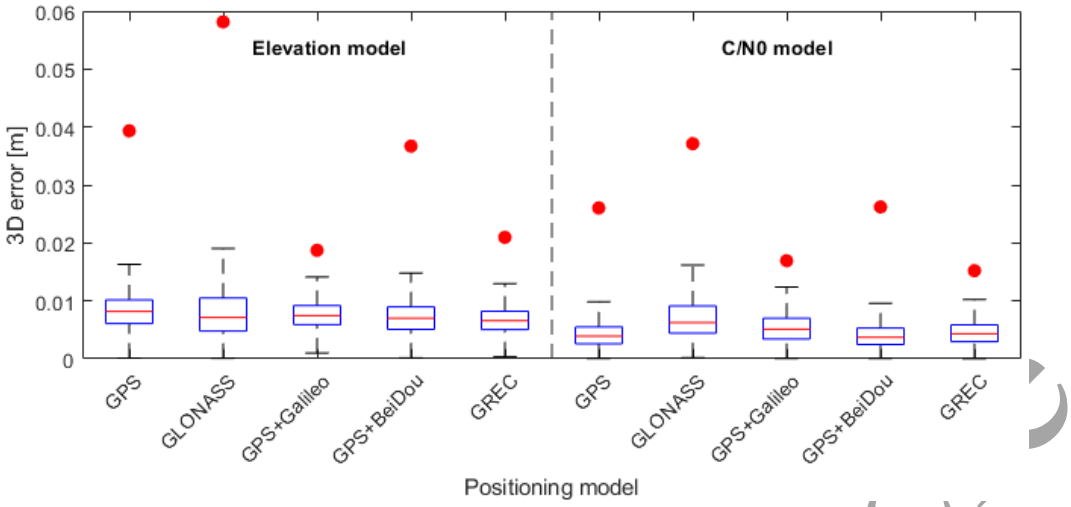

Fig. 2. Positioning error statistics for different stochastic models and system combinations

Research on stochastic properties of GNSS signals also included a complex analysis of the noise type in double-differenced GNSS observations using three statistical tools: Autocorrelation Function (ACF) method, the Lomb-Scargle (L-S) periodogram method, and the Allan variance (AVAR) method ([74]Prochniewicz et al., 2022). The methods allow identifying different noise characteristics for different types of observations. As experiment results revealed, the lowest noise of code measurements characterized the GPS C5Q and Galileo C7Q/C8Q observations, with an STD of about 10 cm. The noisiest were the GLONASS C1C and C2C signals, with 90 cm and 45 cm STDs, respectively. The carrier-phase observations, in turn, were characterized by a comparable noise of 1-3 mm. The ACF analysis showed that the double-differenced carrier-phase observations could be considered uncorrelated for the 1-second interval data, while for the code observations, this interval increases to 20 seconds. Based on the Modified Allan deviation method, the noise type for GPS and Galileo carrier-phase observations was identified as a white phase modulation one. In contrast, a white or flicker noise was found for the GLONASS signals depending on the integration step.

The following studies considered the multipath impact on GPS and Galileo code and phase observations. The analysis was performed using code and carrier-phase observations combination, double differences of carrier-phase observations, and wavelet transform ([72]Prochniewicz and Grzymala, 2021). It was shown that Galileo code observations are more resistant to multipath and measurement noise than GPS ones (Fig. 3). The maximum impact of multipath on code observations was even a meter higher for the GPS C/A code than the E1 civil code of Galileo. The impact of multipath on phase measurements was similar for both systems, at a few millimeters.

Accepted Article

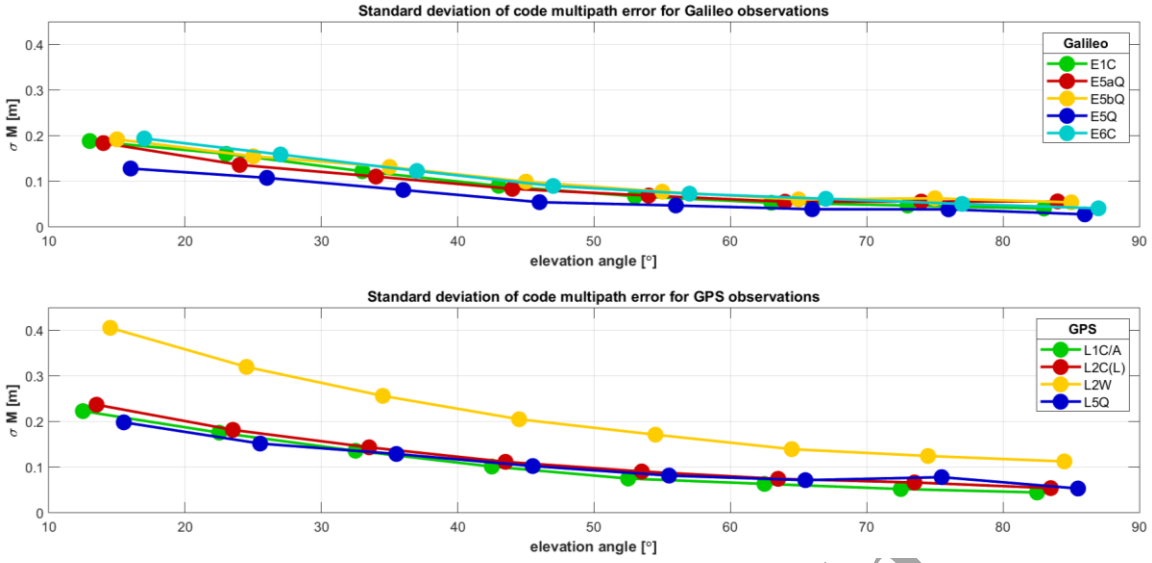

Fig. 3. Multipath error for code observation: Galileo (top) and GPS (bottom)

2.2 Progress in Precise Point Positioning

The studies by the Polish scientific community related to the Precise Point Positioning technique considered, among other topics, the impact of emerging GNSS, such as Galileo and BeiDou, the monitoring of orbit and clock products, including real-time corrections, refining functional and stochastic models of positioning, and the analysis of static and kinematic positioning in various applications.

[19]Hadas et al. (2019) analyzed the performance of absolute positioning with the fully serviceable Galileo constellation. It was noticed that despite two empty slots in the Galileo constellation, the maturity of the Galileo space segment already allowed for the worldwide Galileo-only positioning. It was demonstrated that few-decimeter horizontal accuracy is achievable by processing Galileo pseudoranges and broadcast ephemeris in a static mode, which is superior to the corresponding GPS standard positioning service (SPP). A sub-decimeter horizontal accuracy for both GNSS was achieved when broadcast ephemeris was replaced with real-time products from the Centre National d'Études Spatiales (CNES). It was noticed that the high stability of the Galileo onboard clocks allows performing PPP with broadcast ephemeris leading to remarkable accuracy in the daily static solution, i.e., RMSE of 0.07 m and 0.10 m for the horizontal and vertical components, respectively. Compared to GPS-only positioning, this improved by a factor of 3 and 2, respectively. In the kinematic mode, the improvement with respect to GPS was 15% and 4%, respectively.

The impact of the GNSS constellation development on the PPP performance was also investigated at the Military University of Technology in Warsaw (MUT). In [36]Kiliszek and Kroszczynski (2020), the authors used GPS, GLONASS, and Galileo measurements from one week of consecutive years, i.e., 2017, 2018, and 2019. In the following years, the increasing influence of the Galileo system was noticed, where already in 2019, positioning using only this system was possible. In addition, Galileo-only positioning precision obtained a 50% improvement in 2019 compared to 2017. The best results were obtained for GPS+GLONASS+Galileo in 2019, which was strongly influenced by the development of the Galileo system, but the use of GPS still had the most significant impact. GPS-based PPP performance still outperformed GLONASS-only and Galileo-only, and even than GLONASS+Galileo. A triple-system solution allowed for achieving high accuracy with 90% availability even with an elevation angle of 40º.

Accepted Article

In [94]Zajdel et al. (2022), the authors compared GNSS station coordinates' precision and spectral content determined using GPS, GLONASS, and Galileo constellations. The recent development of the Galileo, GLONASS, and BeiDou systems allowed for evaluating incompatibilities resulting from using different constellations and highlighted the benefits and consequences of using individual GNSS and multi-constellation observations. It was found that each system introduces significant changes to the measured coordinates, with magnitudes of up to several centimeters. The researchers identified a particular group of signals unique to each GNSS system, called the orbital artifact group, which causes inconsistencies in station coordinate series. These signals were demonstrated by analyzing 2-year data from fifteen globally distributed stations using the PPP technique. Galileo has the most dominant orbital artifacts with periods of 14.08 h, 17.09 h, 34.20 h, 2.49 d, and approximately 3.4 d, while GLONASS has analogous signals with periods of 5.63 h, 7.36 h, 10.64 h, 21.26 h, 3.99 d, and about 8 d. GPS orbital signals appear with periods that correspond to the satellite ground track repeat period and its harmonics. These harmonics coincide with the solar tide K1 (23.93h), resulting in inconsistencies between GPS-based analyses and tidal geophysical models, which can reach an average of 12 mm for the ocean tide K2 (12.97h) in the height component of station coordinates. Finally, the authors outlined that the amplitude of the orbital signals varies for different station locations and depends on the geometry of GNSS observations and the dominant direction of satellite overflights. Using a combination of GPS and Galileo provides a 10% increase in station coordinate precision compared to using the best-case single system solution based on Galileo observations.

Due to the increasing interest and utilization of real-time PPP services, much attention was paid to analyzing the quality of real-time corrections. [35]Kazmierski et al. (2020) investigated the quality of real-time quad-system orbit and clock corrections provided by CNES over three years (2017-2019). The reported availability of corrections increased to 95% during 2019, with some issues related to individual GLONASS and Galileo satellites, as well as to geostationary BeiDou satellites. The accuracy of products was assessed with respect to CODE final products and expressed in terms of the Signal In Space Range Error (SISRE). For GPS and GLONASS, SISRE usually remained below 2 cm and 10 cm, respectively, over the entire test period. A clear evolution of Galileo products was noticed, and since 2019, they occurred to be superior even to GPS products. For BeiDou, the SISRE also changed over time, but since 2019 it has remained at the 5 cm level. It was shown that the accuracy of real-time products depends on the GNSS, satellite block, onboard atomic clock, and sun elevation above the orbital plane. Finally, independent validation of real-time orbits was performed with satellite laser ranging (SLR). The number of outliers in the real-time products was found, thus indicating that despite the high quality, these products are still not as robust as expected.

[69]Pelc-Mieczkowska and Tomaszewski (2020), in turn, evaluated real-time products from four different analysis centers, aiming at the representative evaluation of state-space representation (SSR) products. It was noted that the magnitude of the orbital residuals with respect to a reference orbit was similar for each real-time product. Still, streams performed differently over time due to various strategies applied in the processing software. More significant differences between SSR products were noticed in the clock accuracy, from 2 cm to over 10 cm. To evaluate the impact of these products on positioning performance, PPP and SPP results were derived from GPS data. Two streams, i.e. CLK90 and CLK50 were identified as those providing the highest accuracy in the PPP mode, i.e. 5 cm, 7 cm, and 11 cm for the North, East, and Up components, respectively. All SSR products improved the accuracy of code-only positioning by a factor of 3.5.

The following studies were aimed at enhancing the stochastic models of PPP. In this regard [37]Kiliszek et al. (2022) analyzed the impact of using various weighting functions of GPS and

Accepted Article

Galileo observations. Calculations were made for GPS-only, Galileo-only, and GPS+Galileo using eight different weighting functions. For GPS-only, the best results were obtained for a different function than for Galileo-only. In contrast, the best function for Galileo-only was the one for which the observations at lower elevation angles assumed higher weights than for GPS. The best results for the GPS+Galileo solution were obtained using two different weighing functions depending on the constellation. It was noticed that the choice of the weighting function had a particular impact on the Up coordinate component and a significant impact on the tropospheric delay and the convergence time.

As the ionosphere remains the primary error source in absolute GNSS positioning, it must be handled carefully in PPP. The first-order ionosphere delay is typically eliminated by forming an ionosphere-free linear combination. Alternatively, ionospheric delays can be parametrized and estimated when undifferenced and uncombined observations are processed. [63]Paziewski and Sieradzki (2020b) investigated both functional models of PPP and concluded their equivalent performance, providing that corresponding stochastic models are also applied. Furthermore, [70]Poniatowski and Nykiel (2020) investigated the impact of Medium-Scale Traveling Ionosphere Disturbances (MSTIDs) on the kinematic PPP. This case study considered the strongest geomagnetic storm of the 24th solar cycle, with the geomagnetic activity index reaching -223 nT. The MSTIDs caused numerous cycle slips, which reduced the number of satellites considered in positioning. As a result, significant accuracy degradation was noticed at all analyzed stations, and for some epochs, the number of available satellites was insufficient to determine the position. The authors claimed that receivers struggle with correct phase tracking during an MSTID.

The worth-mentioning results were also achieved in the field of geodynamic applications of PPP. [68]Pelc-Mieczkowska (2020) aimed to determine the uncorrelated trends in the coordinate time series derived with PPP. Seven-year long time series of daily solutions of nine permanent stations were considered. The accuracies of the obtained trends were better than 0.1 mm, thus legitimating the PPP technique for geodynamic studies. [14]Dawidowicz (2019) in turn, analyzed position determination accuracy from 30-minute GPS and GLONASS observation sessions using the PPP technique. Previous research in this area has mainly focused on more extended time frames, where observation sessions ranged from 1 to 8 hours. The analysis was based on 30 days of GNSS observations recorded at eight permanent stations of the ASG-EUPOS system in Poland. Post-processing was performed in the NAvigation Package for Earth Orbiting Satellites (NAPEOS) software in five scenarios considering single-GNSS and dual-GNSS processing and a float or fixed ambiguity resolution for GPS. Individual antenna phase center corrections (PCC) values were used to correct observations. It was revealed that the sub-hourly PPP technique could provide an accuracy of 0.5 cm for the horizontal position components and 1 cm for the vertical position component. Such accuracy characterized the solutions where GPS and GLONASS observations were used in the multi-station PPP approach (fixed ambiguity solution). Similar results were also obtained for two other scenarios: GPS-only with ambiguity fixing and the GPS/GLONASS scenario with float ambiguity solution. GPS-only and GLONASS-only with float ambiguities resulted in an accuracy of 1 cm and 2 cm for horizontal and vertical components, respectively.

Finally, a practical application of PPP was reported in ([39]Krasuski and Wierzbicki, 2021). The authors developed a method of determining an aircraft's position based on the PPP technique that uses a weighted mean of positions determined with GPS-only and GLONASS-only processing. An airborne experiment was carried out with a dual-frequency GNSS receiver on board, and the online CSRS-PPP software was used for the processing. Obtained positions were validated against the RTK solution. An improvement of 11% to 87% was obtained by

Accepted Article

weighting the single-GNSS solutions. The model was also implemented in the RTKLib software, and the corresponding improvement varied from 45% to 82%.

3. Troposphere studies with GNSS

Between 2018 and 2022, a significant number of articles were published by Polish research teams, some in collaboration with international researchers affiliated to institutions in countries such as Luxembourg, Bulgaria, Italy, France, Germany, Netherlands, Portugal, Belgium, Czechia, Austria, Switzerland, Taiwan, USA, China, Iran, and Australia. These papers were published in internationally recognized journals thematically linked with remote sensing, GNSS processing and applications, geophysics, the Earth system and the atmosphere.
The literature review revealed that topics that are of interest to the Polish GNSS remote sensing research community are related to: increasing the capabilities and capacities of ground-based GNSS products, developing space-based GNSS products, advancing GNSS tomography, monitoring and investigating climate change using GNSS sensors, investigating severe weather case studies with GNSS, moving even further by using GNSS observations in numerical weather models and nowcasting.

3.1 Ground-based GNSS products

Within this topic, the authors studied the GNSS troposphere products using post-processing ([82]Stepniak et al., 2022), near real-time ([84]Tondas et al., 2020) and real-time mode ([20]Hadas et al., 2020; [21]Hadas and Hobiger, 2021) with both relative and Precise Point Positioning approaches.
[82]Stepniak et al. (2022) evaluated the performance of GNSS tropospheric post-processing estimates derived from IF PPP and the relative mode. The study also aimed to evaluate the impact of some GNSS data processing aspects on the quality of the derived ZTD series for climate applications. Three following scientific questions were discussed in this research: 1) Does the PPP technique generate fewer outliers than DD processing? 2) What is the impact of orbit & clock products on the accuracy of ZTD estimates using the PPP technique? 3) How does ambiguity resolution impact ZTD estimates in the PPP solution? The results showed that the ZTD time series obtained from DD solutions contained more outliers with larger magnitudes than estimates from PPP solutions. The sensitivity tests of ZTD estimates to the satellite products, the ambiguity resolution, and the mapping functions indicated that PPP solutions were superior to the DD results. The latter showed larger biases and excessive noise, partly due to datum effects, compared to ERA5 reanalysis. It was demonstrated that changing the mapping function has a significant impact, with VMF1 being superior to GMF, mainly found at a time scale longer than one day, which is not adequately represented in GMF. The impact of ambiguity resolution on the ZTD estimates in PPP mode was found to be small, mainly because the satellite products are determined from ambiguity-fixed processing of the global IGS network, transferring the information to the PPP solution.
Over the past decades, the Near Real-Time (NRT) processing of GNSS troposphere estimates has been continuously improved; however, the standard processing strategy was based on an hourly calculation interval. [84]Tondas et al. (2020) investigated a new ultra-fast GPS data processing (NRT UF) service to obtain troposphere parameters and coordinates with a 15-minute latency (Fig. 4). The NRT UF system was designed to collect the GNSS observations and products in the first minute of each quarter hour. The remaining 14 minutes were dedicated to the estimation process in Bernese GNSS Software v. 5.2. To assess the quality of the NRT

Accepted Article

UF solution, the independent GNSS post-processing service, the official EUREF solution, and radiosonde observations were used. The quality analyses demonstrated that the standard deviation of the zenith total delay (ZTD) was at level 5-10 mm for co-located GNSS and radiosonde locations. An evaluation of the coordinates obtained from the 15-minute NRT UF processing indicated the RMSE of the Helmert transformation of 2.2 mm with respect to the post-processing data sets. The newly investigated methodology of the NRT UF service may be applied for short-term weather forecasts and ground deformation monitoring.

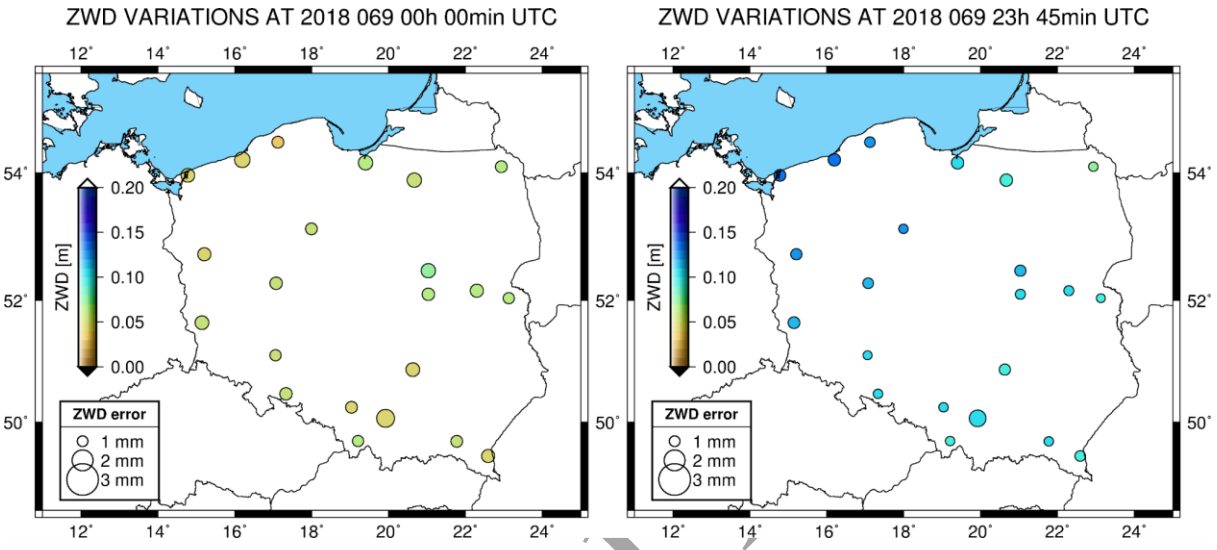

Fig. 4. Zenith Wet Delay values and errors estimated by NRT UF service from 069 DOY 2018 at 00:00 UTC and 23:45 UTC

[20]Hadas et al. (2020) investigated various strategies for real-time ZTD estimation and the impact of processing parameters on the accuracy of troposphere products, including horizontal gradients. The following aspects were considered: PPP functional model, GNSS selection and combination, inter-system weighting, elevation-dependent weighting function, and gradient estimation. A cosine-type elevation-dependent weighting function was proposed. An advanced strategy dedicated to real-time GNSS meteorology was defined as follows: multi-GNSS undifferenced and uncombined processing with inter-system weighting using SISRE ([34]Kazmierski et al., 2018) and gradient estimation. It allowed estimating ZTD with accuracy ranging from 5 to 10 mm. Compared to the common approach in real-time GNSS meteorology, i.e., GPS-only processing using ionosphere-free linear combinations, the advanced strategy improved the accuracy of ZTD by 17% and its uncertainty by over 40%. Moreover, it was demonstrated that the maturity of all four GNSS and corresponding real-time orbit and clock products allowed for providing single-system GNSS ZTD, but with varying accuracy. Further studies analyzed the benefits of the fully serviceable Galileo constellation for real-time meteorology ([21]Hadas and Hobiger, 2021). Although Galileo and supporting services were already reliable, and Galileo has many advantages over other GNSS, including GPS, the Galileo-only real-time ZTDs were less accurate than GPS only-products. The superior results were obtained by combining both GNSS, which led to improved accuracy with respect to IGS and EPN products by up to 8.5%. For EPN stations, the 5 mm accuracy of ZTD was achieved (Fig. 5). Moreover, GPS+Galileo solutions were free from orbit-related artificial signals of high frequency. The abovementioned achievements legitimate real-time ZTD products for assimilation in numerical weather prediction (NWP) models.

Accepted

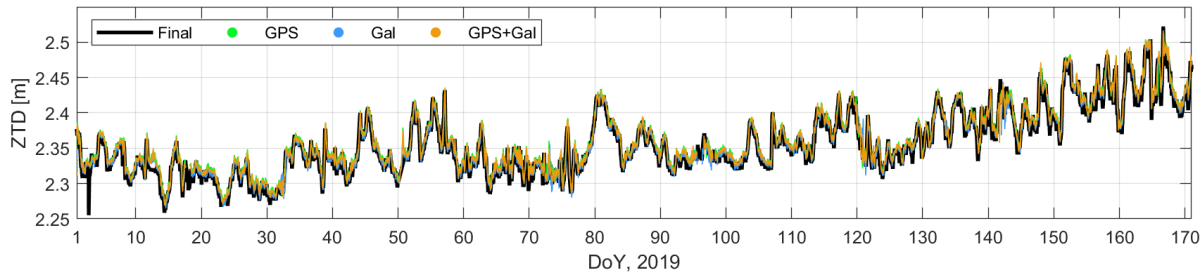

Fig. 5. Time series of real-time ZTD from GPS, Galileo, and GPS+Galileo solutions compared to the IGS Final products; station WROC, DoY 1-170, 2019

Further developments of GNSS real-time troposphere monitoring capabilities for small-scale atmosphere variability were discussed in [53]Marut et al. (2022). Authors used in-house developed low-cost dual-frequency GNSS receivers and validated the possibility of observing changes in integrated water vapor (IWV) content in the atmosphere on the local scale. For this purpose, they recorded two weeks of multi-GNSS data with a low-cost station and compared results with the co-located IGS station WROC and the water vapor radiometer. Analysis showed that standard deviations of IWV differences were 1.0 kg/m^2 and 1.5 kg/m^2 for post-processing and real-time products, respectively. Moreover, the authors set up a city-scale network of 16 low-cost receivers in and around Wroclaw, Poland. It was noticed that the IWV time series among stations were relatively consistent. The standard deviation of IWV differences between low-cost GNSS and other sources remained below 1.5 kg/m^2. Still, significant inter-station differences up to 16 kg/m2 were observed, as well as temporal disagreements with the high-resolution numerical weather model WRF ranging from -12 to +11 kg/m^2 (Fig. 6). Therefore, local-scale IWV dynamics were captured for the first time using in-situ measurements, i.e., the network of low-cost GNSS receivers.

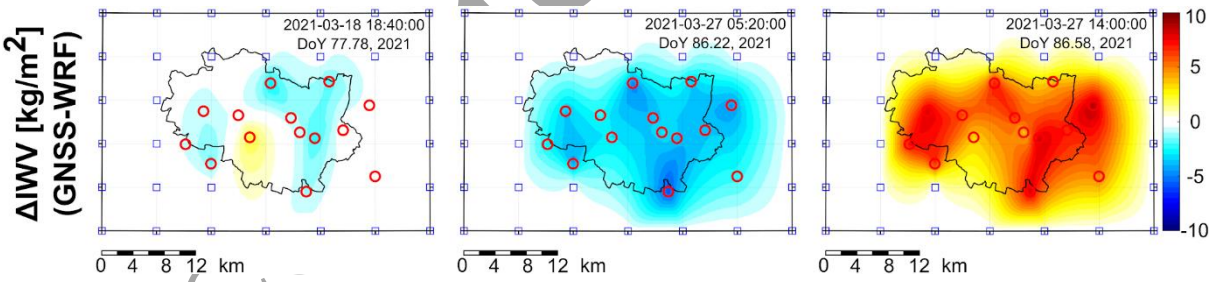

Fig. 6. Small-scale IWV variations with respect to the WRF model

3.2 Space-based GNSS products

The space-based neutral atmosphere GNSS processing capabilities were developed by [26]Hordyniec et al. (2019). Authors developed in-house radio occultation (RO) processing software to process the level-1 excess phase delay data from most satellite-based GNSS receivers such as Constellation Observing System for Meteorology, Ionosphere and Climate (COSMIC-1 or 2). The full processing cycle was established from excess phase observations to refractivity, temperature, and water vapor profiles. The comparison between retrieved refractivity profiles and radiosonde profiles shows discrepancies up to 5% of root mean square error. The results were also validated with official products processed at COSMIC Data Analysis and Archive Center (CDAAC), showing only slightly worse performance.

Further use of space-based RO profiles was investigated in [45]Lasota (2021). The author followed a trend to exploit artificial intelligence in GNSS space-based meteorology. In the

Accepted Article

usual approach, refractivity profiles are combined with the external information from weather models through a one-dimensional variational scheme to determine a one-dimensional tropospheric state in a statistically optimal way. To overcome the dependency on the auxiliary meteorological parameters, the author trained four different models, namely artificial neural network and random forest algorithms accepting refractivity or bending angle as an input to obtain vertical profiles of temperature, pressure, and water vapor. The tests agreed well with the background ERA5 information and the official wetPf2 of the COSMIC Data Analysis and Archive Center. The vertically averaged RMSEs were around 1.7 K for the temperature, 1.4 and 0.45 hPa for total and water vapor pressure, respectively. Further validation with the radiosondes revealed slightly worse results, with the largest discrepancies visible in the lower troposphere below 5 km altitude.

3.3 GNSS tomography

Polish research teams have been intensively investigating GNSS tomography models (Fig. 7) since the initial research nearly 15 years ago ([77]Rohm and Bosy, 2009). One of the cornerstone papers was published by [10]Brenot et al. (2019), who summarised the efforts of the IAG's Working Group on GNSS tomography. This study aimed to revise and compare the methodology of GNSS tomography by using GPS data from the Australian CORS network during a severe weather event. Sensitivity tests and statistical cross-comparisons of tomography retrievals with independent observations from radiosonde and radio-occultation profiles demonstrated the effectiveness of the presented methodology. The initial conditions and the use of data stacking and pseudo-slant observations are critical to GNSS tomography. The best strategy can reduce the normalized RMSE of the tomography solution by more than three compared to radiosonde estimates. Data stacking and pseudo-slant observations can also significantly improve tomography retrievals, resulting in a normalized RMSE improvement up to 17% in the 0-8 km layer. The study highlights the importance of evaluating tomography retrievals against independent measurements and estimating the quality of weather forecasts. Finally, a comparison of multi-model tomography with NWP demonstrates the potential of tomography retrievals for enhancing our understanding of severe weather conditions.

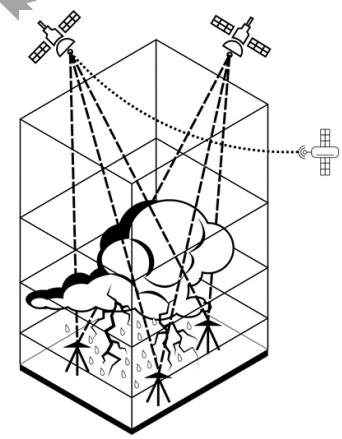

Fig. 7. Concept of GNSS tomography model that is sensing severe weather events using intersecting GNSS signals

GNSS tomography domain optimization and apriori data were identified in [23]Haji-Aghajany et al. (2020) as two of the most promising advancements. This study proposed a new tomography approach that optimized the number of voxels and incorporated constraints to improve the spatial resolution of tomography. The accuracy of the obtained water vapor

Accepted Article

estimates was validated using radiosonde observations and GPS positioning results. Comparing the results with radiosonde observations, it was found that incorporating the WRF model outputs and topography information reduces the RMSE by 0.803 gr/m^3. Furthermore, the validation using GPS positioning data shows that under wet weather conditions, incorporating WRF model outputs and topography information reduces the RMSE of the east, north, and up components by approximately 17.4, 10.5, and 20.0 mm, respectively, which corresponds to reductions of 46%, 36%, and 54%. A similar study was performed by [1]Adavi et al. (2020). The authors claimed that the parameterization method used for computing the design matrix could affect the accuracy of the resulting model. This paper examined the impact of two different methods, the straight-line and ray-tracing methods, on the accuracy of computed ray lengths passing through model elements. Additionally, the effect of including topography in the tomography model was investigated. Radiosonde measurements from the COST benchmark dataset were used to validate the model's accuracy. The results indicated that the Eikonal ray-tracing method, with or without topography, produces more accurate wet refractivity estimates than other methods. The mean RMSE values for wet refractivity estimates using the Eikonal ray-tracing method were 1.313 and 1.766 ppm, respectively, for models with and without topography compared to radiosonde profiles.

To further investigate the preconditions to the final GNSS tomography retrieval quality, [2]Adavi et al. (2022) proposed using the concept of matrix resolution spread. The authors tested this method on two synthetic and one real dataset covering overlapping periods in Germany and Czechia in 2013. Results showed a strong correlation between the spread and the standard deviation of the reconstructed wet refractivity and a significant correlation with the bias of the retrieved field. Thus, the spread of the resolution matrix can serve as a proxy for the accuracy of the tomography reconstruction field based on the quality of the observations, the initial field, and the design matrix.

The introduction of real-time and near real-time high-quality troposphere products motivated the researchers to look into real-time GNSS tomography retrievals. [79]Sá et al. (2021) introduced a new tomographic system called SEGAL GNSS Water Vapour Reconstruction Image Software (SWART). The method utilizes parallelized algebraic reconstruction techniques (ARTs). It is faster than other implementations, making it possible to estimate water vapor for larger GNSS networks and for near real-time weather predictions. The potential of SWART was demonstrated using data from 26 stations in Poland over 56 days. The estimated water vapor from SWART showed good agreement with radiosonde solutions, with a mean RMS of 1.5 g/m^3 for lower layers and an overall improvement of 5% until the layer 6750 m compared to the WRF atmospheric model. Additionally, rapid and strong variations in water vapor observed by radiosondes were detected by GPS tomography but not modeled by the WRF.

Another exciting use of GNSS tomography was demonstrated by [24]Haji-Aghajany et al. (2021), who, for the first time, introduced the GNSS tomography model in positioning. This study used GNSS stations under different weather conditions to investigate the effect of function-based and voxel-based tropospheric tomography methods on positioning accuracy in static and kinematic modes. After validating the results of tomography methods using radiosonde observations, the tomography-based positioning solutions were compared with the positions obtained using tropospheric models. Results showed that the accuracy increases when applying tomography approaches, particularly with the use of function-based tropospheric tomography. The function-based method can improve the up component of the static and kinematic modes by approximately 0.4 and 0.8 cm, respectively, compared to the voxel-based method. Moreover, the function-based tropospheric tomography reduces the convergence time of the kinematic PPP solution.

Accepted Article

3.4 GNSS troposphere estimates in climate change

The GNSS observations are stable over long periods, with little to no calibration and verification needed. Therefore a clear interest in climate research was also identified in the publications authored or coauthored by Polish researchers. One of the fundamental studies related to the usability of the GNSS troposphere time series was published by [93]Yuan et al. (2021). The authors evaluated the use of the newly published dataset from the fifth-generation European Centre for Medium-Range Weather Forecasts (ECMWF) atmospheric reanalysis (ERA5) to analyze climate change in Europe. For this purpose, they determined time series trends of IWV values and compared them with IWV trends determined from GPS observations for 109 permanent stations operating in the period 1994-2019. The authors showed that the commonly used nature of the series that does not consider the internal temporal correlation is unsuitable for describing the above series. Consequently, the appropriate model to reliably describe the nature is the ARMA(1,1) model. Using the erroneous nature of the series leads to an underestimation of the error values of the determined IWV trends and thus affects the interpretations in terms of climate.

Another study that looked at the GNSS time series was the one published by [87]Van Malderen et al. (2020). The authors tested the effectiveness of algorithms commonly used to homogenize tropospheric time series. They used three training data sets for this purpose, named easy, moderate, and complex, each consisting of 120 time series that differed in the nature of the series and the number of jumps. Participants in the experiment did not know the true epochs of the jumps. The investigation showed that most methods underestimate the number of breaks and have a significant number of false detections, which can significantly affect the trend values determined from tropospheric series and thus lead to erroneous climate interpretations.

Both studies ([87]Van Malderen et al., 2020; [93]Yuan et al., 2021) highlighted a need for careful investigation of GNSS troposphere estimates before use in climate trend estimation. Such successful trend investigations were performed for the global tropics ([8]Baldysz et al., 2021) and Poland ([6]Araszkiewicz et al., 2021). [8]Baldysz et al. (2021) have investigated the possibility of using GNSS IWV time series to monitor atmospheric moisture variability related to the various climate modes. They have used 18 years of GNSS IWV time series from International GNSS Service (IGS) stations located in global tropics and applied singular spectrum analysis (SSA) to estimate non-linear trends. Results showed that climate modes on different time scales were visible in long-term GNSS IWV variability. Both global and regional climate patterns were reflected in the analyzed time series. The largest number of stations were correlated to the El Nino Southern Oscillation (ENSO), with a maximum cross-correlation coefficient between GNSS IWV and Multivariate Enso Index equal to 0.78. However, smaller scales (compared to the ENSO) climate phenomena, expressed by the, e.g. Dipole Mode Index, Hawaii index, Caribbean index, or North Pacific Gyro Oscillation index, were also clearly visible. The local sea surface temperature (SST), associated with mentioned climate patterns, was investigated as the main driver of integrated moisture variability over most stations. However, there were still cases of coastal stations that showed insignificant correlation to the local SST but statistically significant correlation to the e.g., ENSO, thus pointing to the strong influence of atmospheric teleconnections.

[6]Araszkiewicz et al. (2021), in turn, determined the ZTD from more than 150 stations in Poland and the surrounding area from 2008 to the end of 2020. The study aimed to analyze multi-year changes in atmospheric precipitable water (PW). For these purposes, the ZTD was converted to PW, and temporal and spatial changes were analyzed. The mean PW value for the entire period for the Polish area was 15.05 mm, which was consistent with previous studies using meteorological data. The distribution of the PW and their fluctuations illustrate the strong

Accepted Article

influence of the abrasion of two climatic zones. It was particularly evident in the annual PW fluctuations, where the northwestern part of Poland, tempered by the influence of the oceanic climate, showed smaller amplitudes of seasonal changes, while the continental climate influenced the eastern region. The paper also showed a positive trend of PW changes at all stations, confirmed by a systematic change in temperature in the area.

3.5 GNSS troposphere for severe weather case studies and modeling efforts

GNSS-derived ZTDs, horizontal gradients, and Precipitable/Integrated Water Vapour (PWV/IWV) are frequently employed for investigating signatures of severe weather events, such as tropical cyclones (aka hurricanes), severe storms with hail, and derechos. Moreover, some authors employ space-based GNSS profiles and raytracing to enhance understanding of severe weather phenomena. Tropical cyclones (TC) are synoptic-scale systems forming over warm oceans characterized by extremely strong winds and copious rainfalls. The potential financial losses they can cause and the risks to human safety underscore their significance. Although the correct prediction of TC tracks has improved over the years, our understanding of their structure and development remains limited. Radio Occultation (RO) meteorological profiles and GNSS ground-based observations serve as a valuable source of information about the atmosphere, improve weather forecasting, and help predict severe weather events such as tropical cyclones.

The GNSS products can also serve as an extra tool for validation, as presented in [44]Lasota et al. (2020b). The authors used the slant total delays (STD) from 28 GNSS stations uniformly distributed over Taiwan to verify the quality of NWP and atmospheric reanalysis during the passage of tropical cyclone Meranti, which was the strongest TC in 2016. For this purpose, the STDs were reconstructed from WRF, GFS, and ERA Interim using a 2D piecewise ray-tracing algorithm and compared to GNSS retrievals. The analysis showed good agreement between GNSS and ray-traced STD with the best results for the WRF model, where the mean difference and standard deviation equaled -0.5 mm and 29.4 mm. The highest discrepancy was found for ERA-Interim reanalysis, most likely due to coarse spatial and temporal resolutions. Furthermore, the impact of hydrometeors on propagating GNSS signal was evaluated and reached an average of 2.8 mm for the WRF model and contributed to the lower errors in most cases.

Another example of a tropical cyclones study is [17]Ejigu et al. (2021). The authors used ZTDs from 922 permanent GPS stations located on the east coast of the United States to monitor and predict the paths of two hurricanes, namely Hurricane Harvey and Irma occurred in 2017. For this purpose, ZTD values were converted to IWV values, which were then analyzed for maxima and modeled using a spaghetti plot. The authors showed that IWV values determined from GPS observations could facilitate the tracking and monitoring of hurricane activity at least several hours before the storm arrives. This is of great importance with the increasing number of hurricanes striking US coasts each year, given the incredible number of permanent GPS stations whose observations are available with little delay.

Next, [22]Hadas et al. (2021) estimated ZTD and horizontal gradients for 160 EPN stations during the category 5 Lorenzo hurricane from September 23 to October 4, 2019. Before the hurricane was formed and after it dissipated, the magnitudes of horizontal gradients mainly remained below 1 mm and did not reveal any predominant directions. However, starting from September 24, magnitudes of gradients exceeded 3 mm in central Europe, and consistent signatures in the gradient fields were observed. Therefore it was confirmed that horizontal gradients reflect meteorological situations during severe weather events. To further leverage TC studies, [43]Lasota et al. (2020a) comprised TC best tracks with the nearby RO profiles in the publicly available archive. The authors gathered 1822 TC best tracks and co-located them

with 48 313 RO profiles, which lied 500 km and occurred within a three hour window from the TC eye. The analysis showed that the repository covers all the TC intensities and basins, which was proved by the practical example.

The most common severe weather events in Europe are storms, which could produce a number of devastating weather phenomena such as hail, copious winds, and flash floods. Most of these events are fueled by vertical instability and an excessive amount of water vapor. Both can be sensed with GNSS signals on ground and space platforms. Densely distributed ground-based stations provide accurate but averaged information about the tropospheric state above the receiver, while RO profiles have high vertical resolution and accuracy; however, their location is quasi-random and sparse. Therefore, GNSS data fusion is crucial and can provide detailed insight into the atmospheric state as presented by [46]Lasota et al. (2022), who used combined ground-based GNSS and RO observations to study severe weather phenomena. The authors showed that two selected severe hail events, which occurred in 2014 and 2019 in Bulgaria, were characterized by a cold upper air-pool and large specific humidity anomaly between 2 and 6 km pronounced in the RO anomalies of bending angle, temperature, and humidity. Further inspection of the ERA5 integrated water vapor transport confirmed the elevated humidity in the form of the atmospheric river. The discrepancy was also visible in the ground-based observations, where the large fractional differences between GNSS and WRF tropospheric delays resulted most likely due to offset between RO and WRF humidity profiles.

Another example of using dense GNSS observation was demonstrated in [57]Nykiel et al. (2019). Specifically, The authors analyzed a derecho event in Poland on August 11, 2017. The investigation employed GPS and GLONASS observations from 278 GNSS reference stations in Poland. With the Bernese GNSS Software ver. 5.2, the authors estimated the ZTDs and tropospheric gradients at 5 and 15-minute intervals, respectively. By integrating meteorological data from synoptic stations, PWV was retrieved, providing information about the amount of water vapor in the atmosphere. PWV, rate of PWV (ROP), and tropospheric gradient maps facilitate monitoring the derecho event. Case studies on selected GNSS stations compared PWV, reflectivity, and microwave radiometer readings. During the primary phase of the event, the authors observed the maximum PWV value of 52.1 mm at 20:30 UTC. The analysis also revealed a high correlation between PWV/ROP maps and reflectivity data derived from meteorological radars regarding the direction, speed, time, and location of the derecho event.

The efforts to improve the consistency of IWV retrieval were reported in [7]Baldysz and Nykiel (2019). The authors developed a new model for dependency between water vapor weighted mean temperature and surface temperature (the Tm - Ts relationship) by studying long-time series of integrated water vapor (IWV) delivered from radio-soundings (RS) across Europe. Using 24 years of RS IWV data (1994-2018), they estimated various coefficients of the Tm - Ts relationship and established models based on various synoptic terms. The accuracy of all developed models was tested using 109 RS stations. Results showed that the best accuracy was achieved for the ETmPoly model (2.8 ± 0.3K). This model considers all synoptic terms for which there were more than 20 000 RS IWV observations and assumes a fifth-degree polynomial relation between them. More detailed analyses showed that the ETmPoly model performed better during winter (DJF) than summer (JJA) months, which was strongly related to the water vapor variability. The model's impact was also validated against the Bevis model and by comparing the ETmPoly to the conversion of GNSS ZTD to GNSS IWV. The differences obtained between these two approaches reached up to 0.8 mm.

Regional GNSS meteorology studies in Brazil were reported by [55]Mota et al. (2019). The authors evaluated the suitability and performance of the IWV estimates in the state of Rio de Janeiro in Amazonia. This region is characterized by high variability of temperature and relative humidity and high annual rainfall, ranging from about 2000 mm/year in the central part

to around 3000 mm/year in its coastal counterpart and in northwestern Amazonia. However, there is a low density of conventional/automatic stations and meteorological radars monitoring weather phenomena. [55]Mota et al. (2019) used one year of GNSS data from the Brazilian Continuous Monitoring Network (RBMC) and the International GNSS Monitoring and Assessment System (iGMAS) in Brazil to estimate GNSS IWV. GNSS estimates were analyzed and compared to retrievals from radiosonde and Moderate Resolution Imaging Spectroradiometer (MODIS). The research showed important differences in the spatiotemporal distribution of water vapor determined by the GNSS-, MODIS-, and radiosonde-derived IWV datasets. This work also confirmed a need to complete the GNSS network in Rio de Janeiro with the meteorological stations near each GNSS receiver. It is intended to improve local IWV estimates and serve as additional support for operational numerical assimilation, weather forecasting, and nowcasting of extreme rainfall and flooding events.

Another study, employing number of GNSS processing technique, considered one of the valleys in Switzerland ([91]Wilgan and Geiger, 2019). This study presents high-resolution models of tropospheric total refractivity and ZTDs for the challenging alpine area of Matter Valley in Switzerland. It is important to provide reliable measurements in the high mountains for monitoring avalanches, deformations, rock glacier activity, or landslides. Here, the authors presented the models based on the numerical weather prediction model COSMO-1 with a high spatial resolution of 1.1 km per 1.1 km, GNSS data from permanent geodetic stations, and GPS L1-only data from low-cost permanent stations. The tropospheric parameters were interpolated to the arbitrary locations by the least-squares collocation method using the software package COMEDIE (Collocation of Meteorological Data for Interpretation and Estimation of Tropospheric Pathdelays). The authors validated generated models against reference radiosonde measurements for total refractivity and GNSS data for ZTD. The accuracy of both GNSS- and NWP-based models was much higher than in previously reported studies e.g., by [90]Wilgan et al. (2017). This study used a denser GNSS network and NWP model of higher resolution. Thus, the authors concluded that high-resolution input data enhanced the overall accuracy of the tropospheric models.

3.6 GNSS troposphere in numerical weather systems and nowcasting applications efforts

Several studies will take a step further from analyzing severe weather signatures in GNSS signals. These studies demonstrate the application of GNSS observations directly in the weather model assimilation system. Researchers are currently looking into assimilating ZTDs, PWVs, and tomography refractivities.

[78]Rohm et al. (2019) presented the results of assimilating GNSS data into the Weather Research and Forecasting (WRF) NWP model using the WRF data assimilation (WRFDA) package. Two variational approaches, 3DVAR and 4DVAR, were used, and the assimilation procedure was modified to correct bias and observation errors. The assimilated GNSS data included ZTD, PWV, radiosonde (RS), and surface synoptic observations (SYNOP) using a 4DVAR assimilation scheme. Three experiments were conducted to analyze the impact of GNSS data assimilation on weather forecasting, including severe weather events in June 2013. The study revealed that GNSS data assimilation using the GPSPW operator significantly improved the moisture fields and rain forecasts in the WRF model. The strongest impact was observed after a 9-hour lead time. The assimilation of ZTD significantly reduced the mean error of relative humidity forecasts in a vertical profile by over 20%, starting from 2.5 km upward. Assimilation of PWV alone did not significantly improve, but the combination of PW, SYNOP, and radiosonde improved humidity distribution in the vertical profile by up to 12%. In all three analyzed severe weather cases, PWV improved the rain forecast, while ZTD reduced the humidity field bias. Binary rain analysis showed that GNSS parameters significantly impacted

the rain forecast in the class above 1 mm/h. Overall, the results suggest that assimilating GNSS data into the WRF model can significantly improve the accuracy of weather forecasting, particularly in moisture fields and rain forecasts.

Another study, led by researchers from the Australian Bureau of Meteorology ([47]Le Marshall et al., 2019), presented the application of the ZTD data provided by GNSS missions in NWP to enhance moisture specification of the atmosphere at up to nearly 40 km resolution across south-eastern Australia. These observations have an accuracy (often equivalent to 2-mm RMS error in total water vapor), which enables them to be of potential benefit for the NWP model and to be of value in the Australian region, which is in the data sparse southern hemisphere. Here the authors used ZTD, produced in real-time/near real-time by RMIT University and Geoscience Australia. It resulted in an enhanced database for the specification of moisture fields in the ACCESS C3 NWP system. The improved database resulted in improvements to 12- and 18-h rainfall forecasts which were measured using the Fractions Skill Score.

Other studies are looking into the innovative use of GNSS tomography refractivity profiles as an input to the NWP data assimilation system. [85]Trzcina and Rohm (2019) established an NRT GNSS troposphere tomographic solution for the area of Poland, using TOMO2 software developed at UPWr. The solution is based on the ZTD estimates for 167 GNSS stations from the EUREF Permanent Network, ASG-EUPOS, and Leica SmartNet networks. 3-dimensional reconstruction of the wet refractivity field in the troposphere up to 12 km altitude is provided every 1 hour, using tomographic principles. The NRT experiment and assimilation into the numerical weather prediction (NWP) model were performed to verify whether tomographic products can attain the required accuracy for utilization within operational NWP procedures. The assimilation of the TOMO2 output into a WRF model was performed using the WRF Data Assimilation (WRFDA) module and a GPSREF observation operator dedicated to radio occultation (RO) total refractivity data. Two selected analysis periods covered summer storms and autumn rainfalls. The resulting weather forecasts were validated with GNSS-derived IWV data, synoptic observations, radiosonde profiles, and ERA-Interim reanalysis. The analysis revealed the capability of the TOMO2 model outputs to improve 6-18 hours predictions of relative humidity (0.5%) and temperature (0.25°C), especially for precipitation events.

[25]Hanna et al., (2019) performed the first test on the assimilation of the GNSS tomography products to the Weather Research and Forecasting Data Assimilation System (WRF DA). The tomographic domain covered the area of central Europe. The wet refractivity fields were estimated using two tomographic models (TUW and UPWr) during heavy-precipitation events (May 29 - June, 14, 2013). The authors tested three sets of GNSS slant wet delays (SWDs) derived from ZTDs and horizontal gradients provided for 88 GNSS sites by Geodetic Observatory Pecny (GOP). The analyzed datasets consisted of 'set0' without compensation for hydrostatic anisotropic effects, 'set1' with compensation for this effect, and 'set2' cleaned by wet delays outside the inner voxel model. To perform the three-dimensional assimilation of the GNSS tomography products into the nested (12 km and 36 km horizontal resolution) WRF model, the authors used the radio occultation (GPSREF) observation operator. This operator enabled the assimilation of the total refractivity profiles; therefore, besides the tomographic wet refractivity field, the missing hydrostatic part of refractivity was derived from the ALADIN-CZ model. Moreover, the authors compared GNSS tomography data assimilation results to the radiosonde (RS) observations. The validation showed that the assimilation improved the relative humidity forecasts (bias and standard deviation) and temperature (standard deviation) during heavy-precipitation events.

Prior studies on the assimilation of numerical weather prediction models have utilized observation operators not optimized for GNSS tomography data. [86]Trzcina et al. (2020) introduced TOMOREF, an observation operator designed to assimilate 3-D fields of wet

refractivity derived from GNSS tomography data into a WRF DA system. TOMOREF was tested using wet refractivity fields obtained during a heavy precipitation event and validated using radiosonde observations, synoptic data, ERA5 reanalysis, and rain radar data. The results showed that assimilating GNSS tomography data positively impacted the forecast of relative humidity, with a reduction in root-mean-square error of up to 0.5%. Furthermore, the assimilation of GNSS tomography data improved precipitation forecasts within 1 hour after assimilation, as evidenced by a reduction in mean bias values of up to 0.1 mm. The results also demonstrated that GNSS tomography data had a greater impact on the WRF model than ZTDs, underscoring the potential of GNSS tomography data for weather forecasting.
Finally, the nowcasting of severe weather events using a machine learning approach with GNSS ground-based and tomography retrievals was investigated by [48]Los et al. (2020). The author focused on applying GNSS observations in nowcasting severe weather events, particularly summer storms, which can result in significant economic and societal losses. While previous studies have explored vertical IWV in weather nowcasting, the combination of IWV and vertical profiles of wet refractivity derived from GNSS tomography has not yet been fully utilized for short-range forecasts of storms. The study presented a machine learning approach to predict storms in Poland within a 0-2 hour window using the combined information of IWV and tomography-based vertical profiles. The model was found to be accurate, with a success rate exceeding 87%. However, the precision of the prediction was limited to about 30%. The wet refractivity below 6 km and IWV on the west side of the storm were identified as significant parameters with the potential to predict the location of the storm. Furthermore, the analysis of IWV highlighted a correlation between changes in IWV and the occurrence of storms

4. Ionosphere studies with GNSS

GNSS-based ionosphere sounding has always played a prominent role in the studies undertaken by the Polish scientific community. In this regard, the investigations are conducted toward ionospheric disturbance monitoring, regional and global ionosphere modeling, and enhancing the algorithms for mitigating ionosphere-originated errors in precise GNSS positioning.
The investigations aimed at high-latitude ionosphere monitoring were conducted at UWM. To provide a more detailed view of plasma irregularities, the authors employed two parameters, namely ROTI and relative STEC ([80]Sieradzki and Paziewski, 2019). The latter is a new approach that extracts signatures of large-scale ionospheric structures by estimating background STEC level with a 4-order polynomial. The main benefit of relative STEC value is its epoch-wise character without spatiotemporal interpolation. More importantly, the indicator can be easily extracted for entire GNSS networks, providing a more comprehensive view of the ionosphere. The comparison of statistics offered by ROTI and relative STEC demonstrated that the new algorithm is especially effective for massive plasma structures. As a consequence of these promising results, the new algorithm was applied to the first climatological study of polar patches using ground-based GNSS observables ([81]Sieradzki and Paziewski, 2022). These investigations revealed the equinoctial peak of polar patch occurrence and a good agreement between GNSS and SWARM measurements. A sparse divergence between both techniques was related to a different patch definition. The analysis also reported a transformation of the UT pattern depending on the ionospheric gradient between sub-auroral and polar areas. During the winter solstice, most patches occurred at post-noon UT hours, whereas in March, the maximum corresponded to morning hours. This variation was expected according to the theory, but it was confirmed for the first time.

Accepted

The climatology of ionospheric irregularities over Greenland was, in turn, investigated in the ESA-founded project "Forecasting Space Weather Impacts on Navigation Systems in the Arctic" (FORSWAR). The consortium of UWM, Universitat Politecnica de Catalunya (UPC), University in Oslo (UiO), and German Aerospace Center (DLR) studied modeling and reconstruction of ionospheric irregularities expressed in terms of ROTI by the method of Empirical Orthogonal Functions (EOFs) ([33]Jin et al., 2022). The applied method using ROTI as an input presented the long-term climatology (over two solar cycles) of TEC irregularities from a polar cap station. The climatology revealed variability with different time scales, i.e., solar cycle, seasonal, and diurnal variations. The FORSWAR project also provided a method based on the optical flow algorithm for forecasting ROTI (OFROTI) ([54]Monte-Moreno et al., 2021). It is a nonparametric method for predicting maps of rapid polar ROTI fluctuations. This prediction method involves modeling the ROTI spatial distribution as a time-evolving flow. The method works well in high/medium geomagnetic activity conditions, assuming that the regions of high ROTI values are concentrated with continuity.

The problem of precise positioning under such disturbed ionospheric conditions at high latitudes was investigated in [67]Paziewski et al. (2022). Specifically, the study addressed a research problem regarding the impact of ionospheric irregularities on precise GNSS positioning in Greenland. The authors assessed the performance of positioning methods that had not been comprehensively investigated but are desired by a wide range of users, namely single-frequency (SF) PPP and wide-area RTK. The datasets were acquired under three ionospheric storms: the St. Patrick's Day storm of March 17, 2015, the storm on June 22, 2015, and August 25-26, 2018, to provide a challenging scenario for experimentation. As expected, the results demonstrated noticeable implications of the ionospheric disturbances for the IAR performance and the coordinate accuracy in RTK positioning. More importantly, the authors revealed that the SF PPP model based on the GRAPHIC phase-code ionospheric free linear combination was generally resistant to ionospheric disturbances.

The UWM research group also contributed to developing the global ionosphere models. A new global ionosphere model was proposed based on processing undifferenced dual-frequency GPS+GLONASS carrier phase data from 260 permanent stations and several interpolation techniques. The employed approach is based on a three-step procedure and allows estimating the slant ionospheric delays. These values are derived using the geometry-free linear combination and carrier phase bias modeling. Then, VTEC values are converted into STEC at the ionospheric pierce points (IPP) locations. For this purpose, a Modified Single Layer Model (MSLM) mapping function was used. The application of different stochastic parametric modeling methods to interpolating TEC data in producing this global ionosphere model has been comprehensively examined. The theoretical background related to the parametrization of least-squares collocation (LSC) was studied in parallel with the other techniques from the kriging family, i.e., ordinary kriging (OKR) and universal kriging (UKR) ([32]Jarmolowski et al., 2021b). The studies on the local ionosphere model in southeastern Asia proved similar accuracy derived from different parametric modeling techniques ([29]Jarmolowski, 2019; [30]Jarmolowski et al., 2019). Special attention was paid to the parametrization and detrending problems related to kriging and LSC. More precisely, it was found that local detrending with higher-order polynomial surfaces applied in UKR adversely affects the kriging modeling results. Additionally, it was concluded that outliers occurrence also decreases kriging accuracy, especially in the case of local, higher-order detrending in UKR (Fig. 8).

Accepted Article

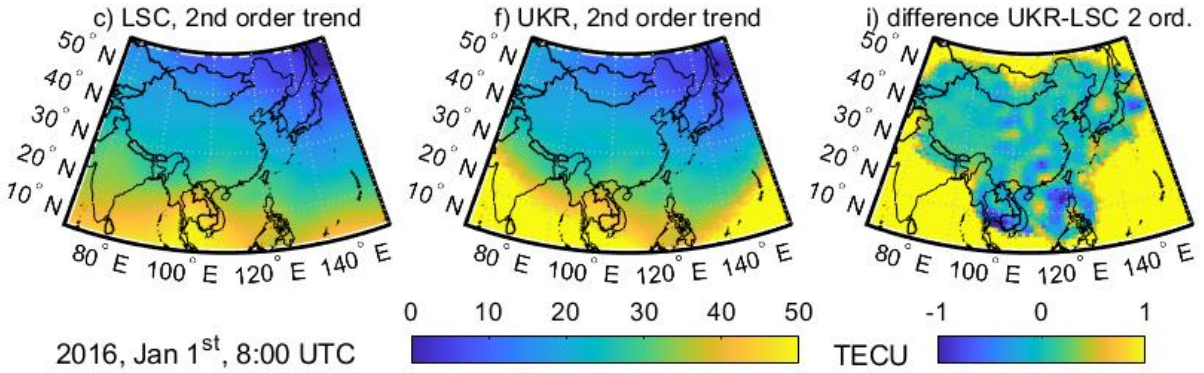

Fig. 8. Example epoch (January 1, 2016, 8:00 AM) of VTEC interpolated by LSC and UKR methods and differences between LSC and kriging for data with outliers

Kriging modeling was recently implemented in the new GIM by UWM. The global grid based on point VTEC data at IPPs was created by combining two kriging techniques in two modeling steps: ordinary kriging (OKR) and simple kriging (SKR) equivalent to LSC ([32]Jarmolowski et al., 2021b). The combination of OKR and SKR was justified mainly by the inhomogeneous geostatistical distribution of TEC point data due to equatorial ionization anomaly (EIA). It required the removal of the long-wavelength VTEC part to ensure work with a relatively homogeneous residual signal in the second step of precise modeling by SKR. The removal of the trend by OKR was an alternative to spherical harmonic detrending, which was more stable in the presence of significant data gaps over the ocean. The second step of precise residual modeling by SKR technique is based on VTEC residuals, which have a substantial advantage with respect to non-detrended VTEC due to an approximate geostatistical homogeneity of residual TEC signal after the elimination of EIA, and due to the narrow band of the processed signal. As a result, the final UWM GIMs are of 2.5 by 5.0 degrees spatial and 1-hour temporal resolution. The accuracy of the new ionosphere model by UWM under various geomagnetic conditions was verified by comparing it to the best available GIMs (Fig. 9). The models were analyzed for self-consistency during the most severe geomagnetic storm of 2018. RMS for UWM GIMs reached the lowest values among all tested models for the stormy day. In general, UWM maps offer a clear improvement over benchmark models provided by IGS and CODE ([89]Wielgosz et al., 2021).

Accepted Article

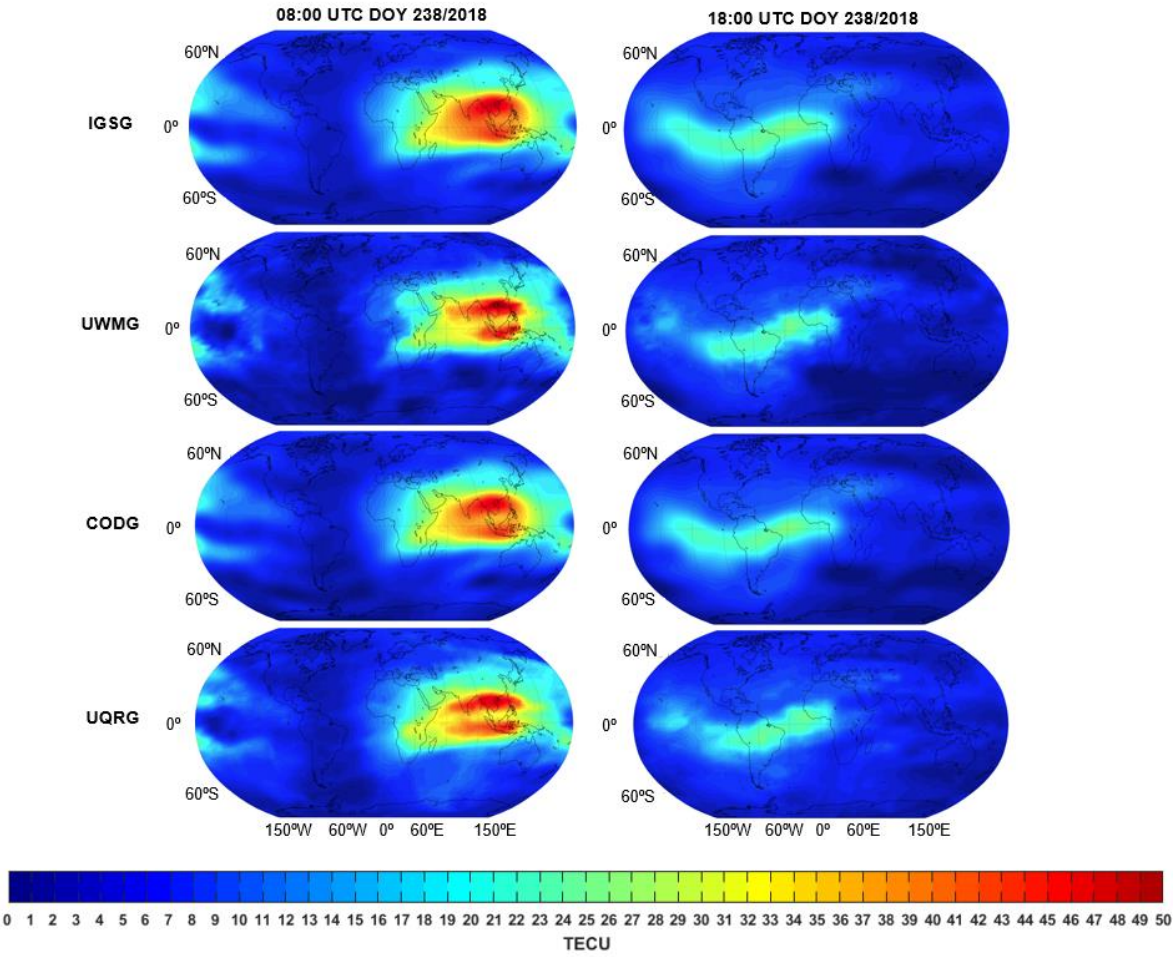

Fig. 9. Example TEC maps derived from IGSG, UWMG, CODG, and UQRG models on a stormy day (DOY 238) at 08.00 UTC (left) and 18.00 UTC (right)

5. Selected GNSS applications

GNSS positioning proved its high applicability and reliability in providing coordinate estimates. Studies stimulating progress in this area have mainly considered enhancing correction, functional and stochastic models, methods for integer ambiguity resolution and validation, and integration of multi-constellation GNSS signals. Consequently, GNSS positioning has been applied to numerous branches of industry and fields of human activity where high accuracy and reliability of the solution are required. These include surveying, mapping, transport, civil engineering, but also other applications such as geography, hydrology, and even tourism ([83]Szombara et al., 2020; [13]Chwedczuk et al., 2022). Moreover, GNSS positioning with smartphones is gaining popularity as it becomes more and more accurate ([38]Koziol and Maciuk, 2020).

In this section, we acknowledge selected studies reporting the achievements of Polish researchers related to the abovementioned selected GNSS applications. We recognize advances in low-cost and Android GNSS, GNSS seismogeodesy, geodynamics, structural health monitoring (SHM), antenna calibration, and satellite clock stability.

5.1 Positioning and applications with smartphones and low-cost GNSS receivers

Accepted

Recent advances in GNSS hardware inspired the scientific community to put a spotlight on the mass-market GNSS receivers and smartphones equipped with GNSS chipsets and the development of novel processing methods as a potential complement to the high-grade GNSS receivers in geoscience studies. By taking advantage of the ubiquity of such receivers, we may move towards a new era with multiple sensors acquiring multi-constellation and multi-frequency GNSS observations.

GNSS measurements of smart devices have been accessible through Application Programming Interface 24 on Android 7 since 2016, provoking studies in the field. Despite the unprecedented advances in GNSS chipsets embedded in smart devices, we still may list many constraints that hinder their use in the most demanding applications. The issues such as susceptibility to multipath, the inhomogeneous gain pattern, unmodelled lack of phase centers, and linear polarization affect smartphone GNSS antennas. What is more, high noise of observations, unaligned chipset initial phase biases, and other biases destroying the integer and time-constant properties of carrier-phase ambiguities must be addressed ([61]Paziewski, 2020; [27]Iakovidis et al., 2022).

These smartphone GNSS data limitations have spurred an effort by the scientific community to handle them. Initially, attention has been drawn to the quality of GNSS observations derived from smartphones. In [59]Paziewski et al. (2019a), the authors showed the poor quality of the smartphone GNSS phase data. Specifically, the analyses revealed that smartphone GNSS phase measurements are affected by discontinuities, a gradual accumulation of errors, and the duty cycling effect. These phenomena prevent correct IAR and consequently impede the application of smartphone phase measurement to high-precision positioning techniques such as RTK or PPP. Moreover, even if the most recent smartphones acquire observations on multiple frequencies, selected ones are still subject to unwanted effects that must be handled [65](Paziewski et al., 2021). Careful addressing of such constraints may catalyze an expansion of satellite navigation to novel science and market areas.

Considering such restrictions, an effort has been put into developing stochastic and functional models customized to smartphone observations. These algorithms aimed to address such limitations of smartphone observations as the low suppression to multipath, high observational noise, the carrier phase discontinuity driven by duty-cycle, and the existence of unwanted biases that destroy integer properties of phase ambiguities. In [59]Paziewski et al. (2019a), the authors suggested the application of wide-range DGNSS positioning to address the constraints of smartphone phase GNSS data. The following studies enhanced weighting schemes by introducing a novel one based on carrier-to-noise density ratio, thus suited for smartphone GNSS data ([75]Robustelli et al., 2021). More importantly, the feasibility of collaborative smartphone-to-smartphone GNSS RTK positioning with IAR has been shown for the first time ([65]Paziewski et al., 2021). In parallel, studies have been conducted on applying low-cost GNSS receivers to geodetic applications. First, a focus has been put on evaluating SDR low-cost receivers' observation quality and positioning performance ([76]Robustelli et al., 2022).

Next, the investigations explored the potential of low-cost receivers and antennas for surveying applications. In [88]Wielgocka et al. (2021), the authors employed the u-blox ZED-F9P receiver and the low-cost ANN-MB-00-00 antenna for assessing PPP, RTK, and relative static positioning performance. The results revealed that the ambiguity fixing rate might reach up to 80% in the static mode, thus providing a few centimeters of horizontal accuracy. A comparable level of accuracy is offered in RTK and Network RTK or PPP mode after at least 2.5 h of data collection. However, a noticeable deterioration was reported when a low-cost receiver was used as a base station for RTK positioning.

Finally, the current performance of single-frequency PPP with low-cost receivers has been evaluated in [66]Paziewski (2022). The author showed the most prominent constraint of such

Accepted Article

receivers and antennas, which is multipath, and demonstrated the benefit of applying a phase-code ionosphere-free linear combination to low-cost receiver GNSS data processing. Moreover, a great advantage of geodetic antennas over low-cost ones was revealed.
The quality of tropospheric estimates obtained from low-cost equipment was investigated to discuss their suitability for climate and weather applications (Stepniak and Paziewski, 2022). The experiment was based on GNSS data collected during two campaigns in diverse atmospheric conditions. Three collocated stations equipped with u-blox ZED F9P receivers and one station with a high-grade Trimble Alloy receiver were employed for data acquisition. Receivers were connected to two different types of GNSS antennas: a surveying-grade Leica AR10 and a patch ANN-MB antenna. Zenith tropospheric delays and horizontal gradients restored from GNSS data of mass-market receivers were validated against those of the high-grade receivers and the fifth-generation reanalysis for the global climate and weather - ERA5. The results showed that tropospheric parameters derived from low-cost receiver data could achieve high precision and reliability, only slightly lower than that of high-grade receivers. The accuracy of low-cost receiver tropospheric estimates can be better when a surveying-grade antenna is employed than the low-cost receiver + a patch antenna. A strong correspondence between GNSS-derived tropospheric parameters and these of the reanalysis was also revealed. Such an outcome proved that low-cost equipment might contribute to atmospheric studies by taking advantage of their low cost and thus ease of GNSS permanent network densification, increasing the spatial resolution of the soundings.

5.2 GNSS for geohazard and structural health monitoring

High-sampling rate of observations offered by geodetic GNSS receivers opened the door for this measurement technique to seismic, geohazard, and structural health monitoring studies. Such an application of navigation satellite systems is labeled as GPS seismology. The following research considered the determination of subsidence and seismic deformations caused by earthquakes, volcanoes, tsunamis, GPS-based systems for early warnings, and SHM systems. These investigations involved precise positioning techniques or dedicated processing algorithms directly retrieving displacements suited to the GNSS observations of high-grade receivers ([58]Paziewski et al., 2018).
Also, the Polish scientific community has recently contributed to developing and assessing the novel GNSS processing algorithms retrieving dynamic displacements. First, in [60]Paziewski et al. (2019b), the authors presented and validated an enhanced PPP-based approach for characterizing structural vibrations. Taking advantage of artificially triggered high-rate and low-scale vibrations, the authors proved that retrieving the amplitude of such sin-wave displacements at a millimeter-level accuracy is possible. Moreover, with the presented method, it is feasible to process observations even at a 100 Hz rate, which allows for meeting the specific demands of structural displacement monitoring.
Furthermore, in [64]Paziewski et al. (2020), the authors introduced an automatic system for Galileo + GPS high-rate data processing, which addresses the specific requirements of local seismic events monitoring. The system retrieves the displacement response to seismic events induced by mining exploitation based on medium-baseline multi-station positioning algorithms. The results proved that it is possible to offer millimeter-level accuracy of such derived displacements.
The following studies in the field investigated three strong natural earthquakes with HR-GNSS. In [41]Kudlacik (2019) the authors demonstrated the necessity of filtering the HR-GNSS displacement time series to resolve the reliable GNSS-waveforms comparable with seismic waveforms and the suitable filtering methodology that does not require additional reference

Accepted Article

HR-GNSS data. The presented procedure of denoising the HR-GNSS time series was then adopted into a small and shallow anthropogenic tremor of magnitude 3.7 in south-western Poland in Legnica-Glogow Copper District. This unique study revealed that with the HR-GNSS (limited to GPS), after a proper denoising procedure, small-amplitude vibrations induced by mining activity are reliably recognized compared to seismic sensors. The peak value of ground displacement was 2-14 mm, and the correlation coefficients between GPS and seismological displacement time series reached 0.92 ([42]Kudlacik et al., 2021). These results were also confirmed by [28]Ilieva et al. (2020). Figure 10 depicts the seismometer (SM) results overlayed by the GNSS displacements and the Pearson correlation coefficients showing the best agreement of SM and GNSS time series during the most significant displacements.

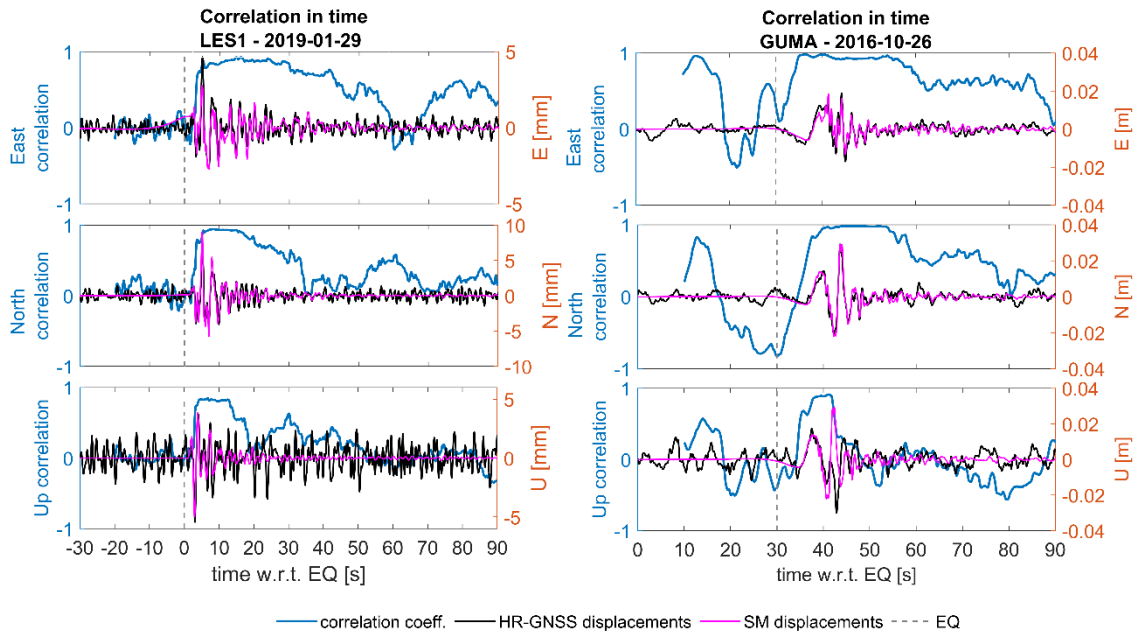

Fig. 10. Pearson's correlation coefficient change in time for mining-induced-tremor (left) and natural earthquake (right). The correlation between SM and GNSS displacements is the highest for the greatest peaks

Next, the studies explored the idea of applying multi-source satellite observations to the atmosphere and geohazard monitoring. UWM in Olsztyn was the Prime Contractor of the COSTO project (Contribution Of Swarm data to the prompt detection of Tsunamis and Other natural hazards), which also involved the National Observatory of Athens (NOA), Technical University of Munich (TUM/DGFI-TUM) and Technical University of Catalonia (UPC/UPC-IonSAT). The project objective was to characterize and understand coupling processes and interactions between the ionosphere/magnetosphere, the lower atmosphere, and the Earth's surface and sea level vertical displacements. For this purpose, the observations from the Swarm mission, GNSS, and seismic records were combined with information on earthquakes and tsunamis. Specifically, a relationship between seismic ionospheric disturbances and the earthquakes and tsunamis observed from low-Earth-orbit (LEO) satellites was investigated. This research was based on two Swarm data types: in-situ electron density (ED) measured by Langmuir Probes (LP) and total electron content (TEC) from precise orbit determination (POD) GNSS receivers ([31]Jarmolowski et al., 2021a). The mathematical tools applied in this kind of research were Fast Fourier Transform (FFT)-based high-pass and band-pass filters, and short-term Fourier transform (STFT) analysis of seismic ionospheric disturbances (SID) in

Accep

along-track satellite data. Swarm data processed using STFT was applied in detecting and preliminary classifying SIDs related to earthquakes and tsunamis. In contrast, ground GNSS data and seismic records were engaged in their validation. The analyses of Swarm data provided interesting observations of ionospheric disturbances not only directly related to the most significant earthquake events and tsunamis but also occurred during entire periods of enhanced seismic activity and at larger distances from the earthquake epicenter. The largest earthquake and tsunami examined using Swarm mission data was the Chilean Mw=8.3 earthquake. This event occurred on September 16th, 2015, on the coast of central Chile, near Illapel (Fig. 11). The seismic activity before and after the mainshock-induced SIDs were detected with Swarm and ground GNSS stations ([31]Jarmolowski et al., 2021a). Different ionospheric anomalies were recorded along Swarm satellite orbits located over earthquake/tsunami events at the time of these events or close to them in time and space when a related seismic activity took place. Filtered disturbing signals from Swarm and ground GNSS, observed in the same place and time, were analyzed together. STFT spectrograms were made for the selected Swarm along-track data samples and determined their spectral patterns. Keograms and scatter plotting for ground GNSS carrier phase geometry-free combination data (L_{GF}) from dense ground networks were used for the validation by the analysis of SID's spatiotemporal correlation (Fig. 11). STFT spectral approach to along-track Swarm data studied in the frame COSTO allowed distinguishing the signals of different origins.

The COSTO studies opened a way to analyze the system of seismically induced ionosphere anomalies for a wider range, also including internal validation of the observed anomalous signals. The research outcomes can constitute a basis of a prototype solution for investigating solid Earth-atmosphere-ionosphere coupling.

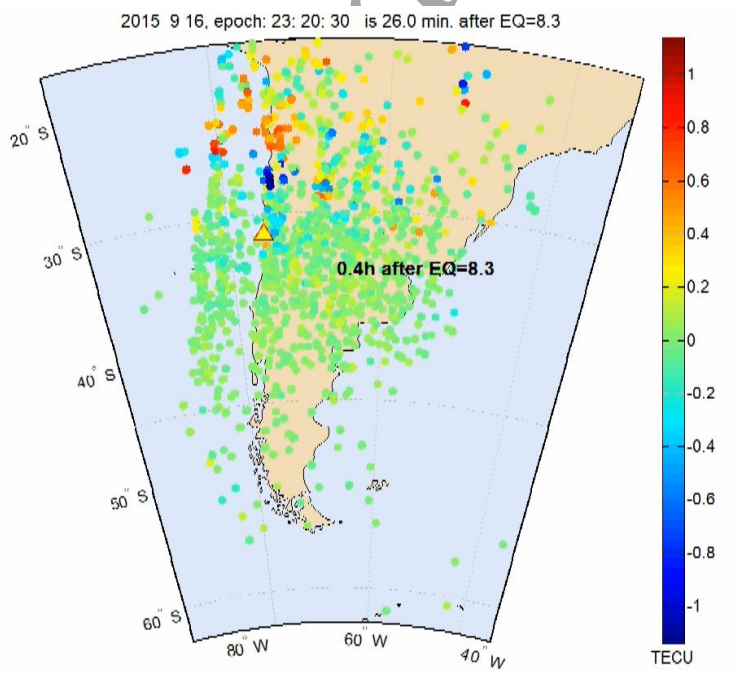

Fig. 11. Scatter map of detrended L_{GF} phase combination from ground GNSS stations of Chilean and Argentinian networks 0.4 h after 8.3 earthquake. The red/blue points in the vicinity of the earthquake denote SIDs, which move to the northeast

Extensive studies on applying LEO satellites such as Swarm, GRACE, COSMIC, and DORIS were continued at UWM. Interesting findings referred to the analyses of Swarm electron

Accepted Article

density (ED) and topside total electron content (TEC) data. The studies focused on the period of increased seismic activity in Papua New Guinea (PNG) and Solomon Islands in December 2016, including two major earthquakes with Mw=7.8 and 7.9 ([92]Yang et al., 2022). The analyses of Swarm data in the PNG region were based on high-pass filtered ED and POD GNSS TEC time series along the satellite tracks. The STFT and windowing using Tukey window were applied to provide spectrograms of ED and topside TEC over seismically active tectonic plate boundaries, over which the Swarm passes were recorded. Figure 12 presents an example spectrogram of a selected interesting Swarm passes over the PNG region recorded around 40 min after the second major earthquake with Mw=7.9 in PNG. The ED residual signal revealed significant power spectral density (PSD) values at different separated spectral periods, which is suspected to be characteristic for the ionosphere responses to sudden seismic activity detectable by LEO satellites. The observations of residual Swarm ED signal suggested that maximum PSD variations of Swarm ED are correlated with seismic activity starting from 5.0 magnitude in the region of two analyzed mainshocks. It can be observed that the most prominent peaks of ED PSD maxima at different periods occur with critical seismic activity, like the first earthquake after relaxation, a larger earthquake amongst some number of smaller earthquakes, or the largest earthquakes in the region. The lowest PSD of ED typically coincides with relaxation time. Swarm ED disturbances have specific spectral patterns in different moments of continuous tectonic activity. Therefore, these studies suggested that continuous tracking of seismic activity from the satellite orbit is fundamental in LEO-based seismology and can provide inputs to the research on earthquake forecasting. The validation of spectral analysis has been made to compare disturbed in-situ ED signal and topside TEC signal disturbed by the same seismic events. It should be pointed out that these two kinds of signals refer to geometrically different spatial locations. Therefore an approximate similarity could be only expected, rather than absolute coherency of the signals. Nevertheless, the similarity between ED and POD TEC was very high. The coincidence of PSD from LPs and GNSS TEC confirmed the ionospheric origin of the disturbances and excluded instrumental uncertainties.

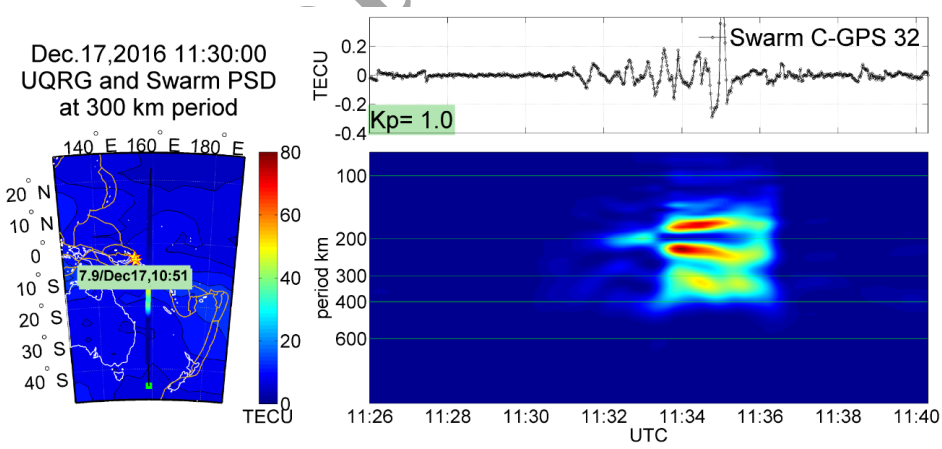

Fig. 12. STFT spectrogram of residual TEC from Swarm C POD GNSS receiver (phase measurements to PRN32) on December 17, 2016, around 40 min after major earthquake with Mw=7.9

5.3 GNSS antenna calibrations and the stability of satellite clocks

Introducing new carrier frequencies to the mature and developing GNSS systems requires updating the receiver antenna calibration models. Even now, most high-grade GNSS receivers acquire multi-constellation and multi-frequency signals. Therefore, all the geodetic antennas

Accepted Article

must be calibrated for the new signals shortly. In [40]Krzan et al. (2020), the authors analyzed the differences between phase center corrections (PCC) models of GNSS antennas obtained from field calibration and calibration performed in an anechoic chamber. They also examined the effect of using different PCC models on the EUREF Permanent GNSS Network (EPN) station position time series. The results showed that the calibration method has a noticeable effect on the PCC models. PCC differences determined for ionospheric-free linear combinations can reach up to 20 mm for some antenna signal reception areas, which directly propagates to the coordinate domain. Tests have shown that the differences in height components resulting from different PCC models can exceed 10 mm in some processing variants.

Other symptoms of GNSS modernization are the changes in equipment at reference stations. Hardware changes often cause jumps seen in the time series of station positions. The resulting shifts are assumed to be driven primarily by changes in carrier phase multipath effects after antenna replacement. However, the observed position shifts may also indicate an imperfect in antenna PCC models. In [16]Dawidowicz et al. (2023), the authors analyzed coordinate changes caused by antenna replacement at selected stations of the EPN network. The authors studied the correlation between the occurrence of jumps and the type of PCC model (type mean (IGS), individual robot-derived (ROBOT), individual chamber-derived (CHAMBER)), as well as multipath changes after antenna replacement. The results proved that antenna change is a critical moment in station coordinate stability. In most cases, it causes visible shifts in the time series of position components (Fig. 13). The discontinuities resulting from antenna changes were noted in the position time series in 75% of GPS+Galileo solutions. In contrast, multipath changes resulting from antenna replacement were responsible for 21%-42% of the jumps in the position components depending on the type of solution.

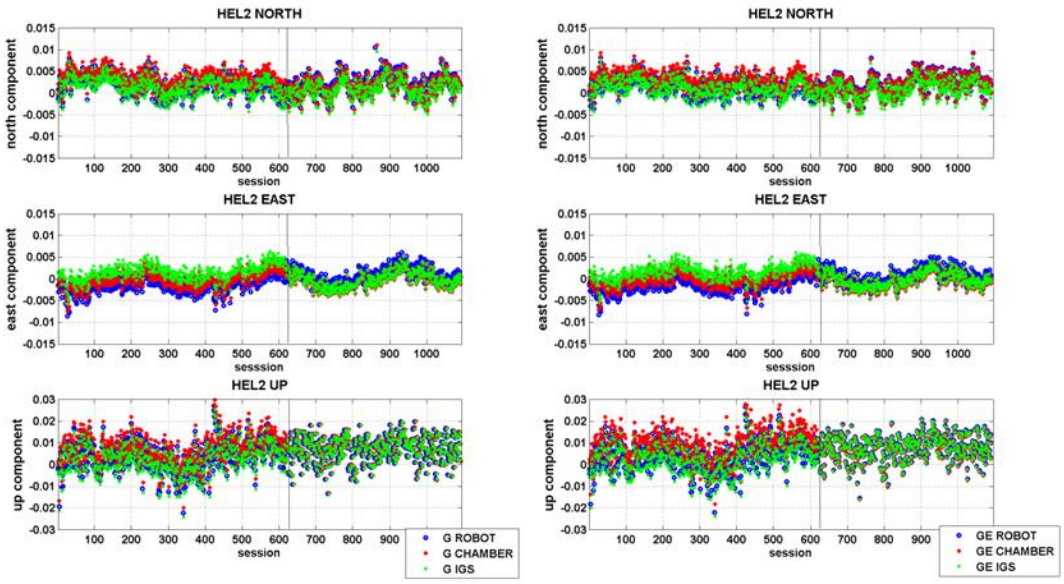

Fig. 13. Time series of NEU position components differences for HEL2 station using different PCC models in case of G-only (G) and GPS+Galileo (GE) observations processing (vertical line indicates the moment of antenna replacement on the station)

In 2019, the consortium of the UWM in Olsztyn and Astri Poland started an ESA-founded project to develop and implement a calibration procedure for multi-frequency and multi-GNSS. The concept of absolute field calibration inspired the methodology used in the project; however,

some innovations were introduced (Fig. 14). The first test results proved the correctness of the implemented calibration procedures ([15]Dawidowicz et al., 2021). The calibration results for the L1 GPS frequency showed good agreement with the values included in the IGS-type mean models. For signals from satellites on high elevations (20°-90°), the differences did not exceed 1.5 mm. For low elevation angles (0°-20°), the agreement of the results was slightly worse, with differences exceeding the 3 mm level in some cases.

Fig. 14. The test GNSS receiver antenna calibration facility at UWM Olsztyn

Also, MUT in Warsaw reported worth acknowledging findings on the effect of the antenna phase center modeling ([4]Araszkiewicz et al., 2019). The analysis compared IGS-type models and individual calibrations collected by EUREF Permanent GNSS Network (EPN) Central Bureau. The research was conducted using the example of the most popular antenna in the EPN installed in 2015 - Leica's model AR25 with LEIT radome (IGS code: LEIAR25.R3 LEIT). The analyses focused on the estimated heights, as previous investigations showed that this component is most affected by antenna modeling. The analysis of GPS observations of a full year from selected EPN stations revealed that the coordinate solutions are close regardless of the chosen phase center model. The study also demonstrated a relationship between the distribution of differences in the compared phase center correction and the differences in the estimated heights. At the same time, it has been proved that IGS-type mean models provide the same quality of coordinate time series as individual ones. In the following years, the MUT also analyzed how the estimated coordinates were affected by the interchangeable use of phase center corrections intended for the L2 frequency to the E5a frequency ([5]Araszkiewicz and Kiliszek, 2020). Tests were conducted to model the phase position of the antennas in different ways so that the magnitude of the introduced error could be determined. The results demonstrated that using L2 corrections for the E5a frequency introduces a systematic error close to 8 mm. Such simplification applies to nearly half of the EPN stations acquiring Galileo observation at that time.

Furthermore, [9]Borowski et al. (2022) noticed significant inconsistencies in the antenna PCC model between the IGS model and actual antenna characteristics. They used two co-located stations, i.e., KRAW equipped with ASH70195C_M SNOW antenna, which originated from the '90s, and KRA1, having individual calibration provided in 2019. Various experiments were performed using several calculation strategies, software, and PCC models. The benchmark difference of heights between antennas ARP's points was defined by precise spirit leveling. Surprisingly, the PPP methods performed by network solution or calculated in Bernese Software obtained worse results than those in popular engineering software, such as Trimble

Accepted Article

Business Centre, GNSS Solutions, or Geonet 2006 (Fig. 15). Authors emphasized that the stations included in CORS networks need individual antenna calibration, and the antennas from the '90s should be replaced by new ones supporting all constellations.

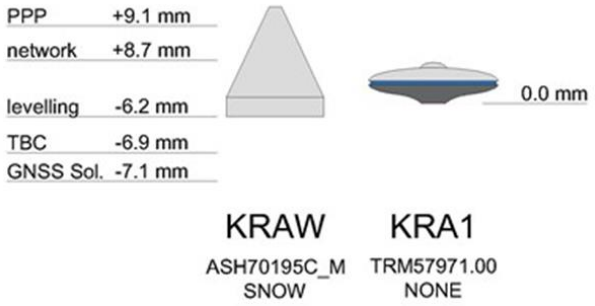

Fig. 15. The height difference between the antenna reference points (ARP) defined by different methods (PPP - PPP calculated in Bernese, network - EPN weekly solutions, TBC - Trimble Business Centre 3.5, GNSS Sol. - GNSS Solution 3.80.8)

Also, the GNSS satellite onboard clocks were of interest to Polish researchers. [52]Maciuk et al. (2021) analyzed the stability of GPS and Galileo onboard oscillators. At the same time [49]Maciuk (2019a), and [51]Maciuk and Lewinska (2019) carried out GPS clock stability analyses based on the original 1Hz clock correction product calculated with the Bernese GNSS Software. It was demonstrated that the stability of the hydrogen maser clock is by one order of magnitude and by half order of magnitude better than for the internal and cesium clocks, respectively. In the following studies, Galileo and BeiDou clocks were also taken into consideration. [50]Maciuk (2019b) noticed some events of unexpected and unexplained jumps in Galileo's clock corrections as well as he analyzed anomalous trends and frequency behavior in the clock characteristics. [3]Ai et al. (2021) focused on determining the noise characteristic of the different types of clocks (rubidium, cesium, hydrogen masers), the type of GNSS system, and the duration of satellites in orbit.

6. Summary and conclusions

This review paper acknowledged the most important research activities concerning GNSS positioning and applications conducted at Polish research institutions in the period of 2019-2022. In particular, we discussed the advances in PPP and relative positioning, troposphere, and ionosphere sounding, smartphone and low-cost GNSS data processing, and other specific studies such as those on satellite antenna calibration and clock stability. Still, we recognize numerous emerging and inevitable issues related to, e.g., multi-constellation signals fusion and biases, which need to be carefully handled. Nonetheless, in light of these recent advances in theories and algorithms, continuous progress in GNSS performance is thought to be maintained in the future, and GNSS applications are expected to continue to proliferate.

We offer special words of thanks to the researchers who contributed to this review with their articles. We anticipate their studies will spark further innovations in geodesy, geomatics, and related applications. We also express our gratitude to the Committee on Geodesy of the Polish Academy of Science, which initiated this review article reporting the recent contribution of the Polish research community to GNSS science.

Accepted Article

Author contributions

Conceptualization: J.P., T.H., W.R., P.W.; writing original draft preparation: J.P., T.H., W.R., P.W.; writing – review and editing: J.P., T.H., W.R., P.W.

Data availability statement

No datasets were used in this research.

Acknowledgements

The review paper was elaborated in the framework of the Committee on Geodesy of the Polish Academy of Sciences. Valuable help was provided by: Andrzej Araszkiewicz, Zofia Baldysz, Lukasz Borowski, Slawomir Cellmer, Karol Dawidowicz, Natalia Hanna, Pawel Hordyniec, Wojciech Jarmolowski, Jan Kaplon, Damian Kiliszek, Anna Klos, Iwona Kudlacik, Anna Krypiak-Gregorczyk, Grzegorz Krzan, Elzbieta Lasota, Krzysztof Nowel, Kamil Maciuk, Grzegorz Marut, Dominik Prochniewicz, Rafal Sieradzki, Damian Tondas, Estera Trzcina, Karina Wilgan, and Radoslaw Zajdel.

References

[1]Adavi, Z., Rohm, W., and Weber, R. (2020). Analyzing Different Parameterization Methods in GNSS Tomography Using the COST Benchmark Dataset. *IEEE J. Sel. Top. Appl. Earth Obs. Remote Sens.*, 13, 6155-6163. DOI: 10.1109/JSTARS.2020.3027909.

[2]Adavi, Z., Weber, R., and Rohm, W. (2022). Pre-analysis of GNSS tomography solution using the concept of spread of model resolution matrix. *J. Geod.*, 96, 27. DOI: 10.1007/s00190-022-01620-1.

[3]Ai, Q., Maciuk, K., Lewinska, P. et al. (2021). Characteristics of Onefold Clocks of GPS, Galileo, BeiDou and GLONASS Systems. *Sensors*, 21, 2396. DOI: 10.3390/s21072396.

[4]Araszkiewicz, A., Kiliszek, D., and Podkowa, A. (2019). Height Variation Depending on the Source of Antenna Phase Centre Corrections: LEIAR25.R3 Case Study. *Sensors*, 19, 4010. DOI: 10.3390/s19184010.

[5]Araszkiewicz, A., and Kiliszek, D. (2020). Impact of Using GPS L2 Receiver Antenna Corrections for the Galileo E5a Frequency on Position Estimates. *Sensors*, 20, 5536. DOI: 10.3390/s20195536.

[6]Araszkiewicz, A., Kiliszek, D., Mierzwiak, M. et al. (2021). GPS-Based Multi-Temporal Variation in Precipitable Water over the Territory of Poland. *Remote Sens.*, 13, 2960. DOI: 10.3390/rs13152960.

[7]Baldysz, Z., and Nykiel, G. (2019). Improved Empirical Coefficients for Estimating Water Vapor Weighted Mean Temperature over Europe for GNSS Applications. *Remote Sens.*, 11, 1995. DOI: 10.3390/rs11171995.

[8]Baldysz, Z., Nykiel, G., Latos, B. et al. (2021). Interannual Variability of the GNSS Precipitable Water Vapor in the Global Tropics. *Atmosphere*, 12, 1698. DOI: 10.3390/atmos12121698.

[9]Borowski, L., Kudrys, J., Kubicki, B. et al. (2022). Phase Centre Corrections of GNSS Antennas and Their Consistency with ATX Catalogues. *Remote Sens.*, 14, 3226. DOI: 10.3390/rs14133226.

Accepted Article

[10]Brenot, H., Rohm, W., Kačmařík, M. et al. (2019). Cross-Comparison and Methodological Improvement in GPS Tomography. *Remote Sens.*, 12, 30. DOI: 10.3390/rs12010030.
[11]Cellmer, S., Nowel, K., and Fischer, A. (2022a). A search step optimization in an ambiguity function-based GNSS precise positioning. *Surv. Rev.*, 54, 117-124. DOI: 10.1080/00396265.2021.1885947.
[12]Cellmer, S., Nowel, K., and Fischer, A. (2022b). Reduction as an improvement of a precise satellite positioning based on an ambiguity function. *J. Appl. Geod.*, 16, 385-392. DOI: 10.1515/jag-2022-0005.
[13]Chwedczuk, K., Cienkosz, D., Apollo, M. et al. (2022). Challenges related to the determination of altitudes of mountain peaks presented on cartographic sources. *Geodetski vestnik*, 66, 49-59. DOI: 10.15292/geodetski-vestnik.2022.01.49-59.
[14]Dawidowicz, K. (2019). Sub-hourly precise point positioning accuracy analysis - case study for selected ASG-EUPOS stations. *Surv. Rev.*, 52, 341-351. DOI: 10.1080/00396265.2019.1579988
[15]Dawidowicz, K., Rapinski, J., Smieja, M. et al. (2021). Preliminary Results of an Astri/UWM EGNSS Receiver Antenna Calibration Facility. *Sensors*, 21, 4639. DOI: 10.3390/s21144639.
[16]Dawidowicz, K., Krzan, G., and Wielgosz, P., (2023). Offsets in the EPN station position time series resulting from antenna/radome changes: PCC type-dependent model analyses. *GPS Solut.*, 27, 9. DOI: 10.1007/s10291-022-01339-8.
[17]Ejigu, Y.G., Teferle, F.N., Klos, A. et al. (2021). Monitoring and prediction of hurricane tracks using GPS tropospheric products. *GPS Solut.*, 25, 76. DOI: 10.1007/s10291-021-01104-3.
[18]Fischer, A., Cellmer, S., and Nowel, K. (2022). Regularizing ill-posed problem of single-epoch precise GNSS positioning using an iterative procedure. *J. Appl. Geod.*, 16, 247-264. DOI: 10.1515/jag-2021-0031.
[19]Hadas, T., Kazmierski, K., and Sosnica, K. (2019). Performance of Galileo-only dual-frequency absolute positioning using the fully serviceable Galileo constellation. *GPS Solut.*, 23. DOI: 10.1007/s10291-019-0900-9.
[20]Hadas, T., Hobiger, T., and Hordyniec, P. (2020). Considering different recent advancements in GNSS on real-time zenith troposphere estimates. *GPS Solut.*, 24. DOI: 10.1007/s10291-020-01014-w.
[21]Hadas, T., and Hobiger, T. (2021). Benefits of Using Galileo for Real-Time GNSS Meteorology. *IEEE Geosci. Remote Sens. Lett.*, 18, 1756-1760. DOI: 10.1109/LGRS.2020.3007138.
[22]Hadas, T., Bender, M., Marut, G. et al. (2021). Real-Time GNSS Meteorology in Europe - Hurricane Lorenzo Case Study. In: 2021 IEEE International Geoscience and Remote Sensing Symposium IGARSS. Presented at the IGARSS 2021 - 2021 IEEE International Geoscience and Remote Sensing Symposium, IEEE, Brussels, Belgium, pp. 8321-8323. DOI: 10.1109/IGARSS47720.2021.9554690.
[23]Haji-Aghajany, S., Amerian, Y., Verhagen, S. et al. (2020). An Optimal Troposphere Tomography Technique Using the WRF Model Outputs and Topography of the Area. *Remote Sens.*, 12, 1442. DOI: 10.3390/rs12091442.
[24]Haji-Aghajany, S., Amerian, Y., Verhagen, S. et al. (2021). The effect of function-based and voxel-based tropospheric tomography techniques on the GNSS positioning accuracy. *J. Geod.*, 95, 78. DOI: 10.1007/s00190-021-01528-2.
[25]Hanna, N., Trzcina, E., Möller, G. et al. (2019). Assimilation of GNSS tomography products into the Weather Research and Forecasting model using radio occultation data assimilation operator. *Atmos. Meas. Tech.*, 12, 4829-4848. DOI: 10.5194/amt-12-4829-2019.

Accepted Article

[26]Hordyniec, P., Huang, C.-Y., Liu, C.-Y. et al. (2019). GNSS radio occultation profiles in the neutral atmosphere from inversion of excess phase data. *Terr. Atmos. Ocean. Sci.*, 30, DOI: 10.3319/TAO.2018.10.12.01.
[27]Iakovidis, D.K., Ooi, M., Kuang, Y.C. et al. (2022). Roadmap on signal processing for next generation measurement systems. *Meas. Sci. Technol.* ,33, 012002. DOI: 10.1088/1361-6501/ac2dbd.
[28]Ilieva, M., Rudzinski, L., Pawluszek-Filipiak, K. et al. (2020). Combined Study of a Significant Mine Collapse Based on Seismological and Geodetic Data - 29 January 2019, Rudna Mine, Poland. *Remote Sens.*, 12, 1570. DOI: 10.3390/rs12101570.
[29]Jarmolowski, W. (2019). On the relations between signal spectral range and noise variance in least-squares collocation and simple kriging: example of gravity reduced by EGM2008 signal. *BGTA*. DOI: 10.4430/bgta0265.
[30]Jarmolowski, W., Ren, X., Wielgosz, P. et al. (2019). On the advantage of stochastic methods in the modeling of ionospheric total electron content: Southeast Asia case study. *Meas. Sci. Technol*., 30, 044008. DOI: 10.1088/1361-6501/ab0268.
[31]Jarmolowski, W., Belehaki, A., Hernández Pajares, M. et al. (2021a). Combining Swarm Langmuir probe observations, LEO-POD-based and ground-based GNSS receivers and ionosondes for prompt detection of ionospheric earthquake and tsunami signatures: case study of 2015 Chile-Illapel event. J. *Space Weather Space Clim*., 11, 58. DOI: 10.1051/swsc/2021042.
[32]Jarmolowski, W., Wielgosz, P., Ren, X. et al. (2021b). On the drawback of local detrending in universal kriging in conditions of heterogeneously spaced regional TEC data, low-order trends and outlier occurrences. *J. Geod.*, 95, 2. DOI: 10.1007/s00190-020-01447-8.
[33]Jin, Y., Clausen, L.B.N., Miloch, W.J. et al. (2022). Climatology and Modeling of Ionospheric Irregularities over Greenland Based on Empirical Orthogonal Function Method. *J. Space Weather Space Clim.* DOI: 10.1051/swsc/2022022.
[34]Kazmierski, K., Hadas, T., and Sosnica, K. (2018). Weighting of Multi-GNSS Observations in Real-Time Precise Point Positioning. *Remote Sens*., 10, 84. DOI: 10.3390/rs10010084.
[35]Kazmierski, K., Zajdel, R., and Sosnica, K. (2020). Evolution of orbit and clock quality for real-time multi-GNSS solutions. *GPS Solut.*, 24. DOI: 10.1007/s10291-020-01026-6.
[36]Kiliszek, D., and Kroszczynski, K. (2020). Performance of the precise point positioning method along with the development of GPS, GLONASS and Galileo systems. *Measurement*, 164, 108009. DOI: 10.1016/j.measurement.2020.108009.
[37]Kiliszek, D., Kroszczynski, K., and Araszkiewicz, A. (2022). Analysis of Different Weighting Functions of Observations for GPS and Galileo Precise Point Positioning Performance. *Remote Sens.*, 14, 2223. DOI: 10.3390/rs14092223.
[38]Koziol, K., and Maciuk, K. (2020). New heights of the highest peaks of Polish mountain ranges. *Remote Sens.*, 12, 1446. DOI: 10.3390/rs12091446.
[39]Krasuski, K., and Wierzbicki, D. (2021). New Methodology for Computing the Aircraft's Position Based on the PPP Method in GPS and GLONASS Systems. *Energies*, 14, 2525. DOI: 10.3390/en14092525.
[40]Krzan, G., Dawidowicz, K., and Wielgosz, P. (2020). Antenna phase center correction differences from robot and chamber calibrations: the case study LEIAR25. *GPS Solut*., 24, 44. DOI: 10.1007/s10291-020-0957-5.
[41]Kudlacik, I. (2019). Seismic phenomena in tke light high-rate GPS precise point positioning results. *Acta Geodyn. et Geomater.*, 99-112. DOI: 10.13168/AGG.2019.0008.
[42]Kudlacik, I., Kaplon, J., Lizurek, G. et al. (2021). High-rate GPS positioning for tracing anthropogenic seismic activity: The 29 January 2019 mining tremor in Legnica- Glogow

Accepted Article

Copper District, Poland. *Measurement*, 168, 108396. DOI: 10.1016/j.measurement.2020.108396.
[43]Lasota, E., Rohm, W., Guerova, G. et al. (2020a). A Comparison Between Ray-Traced GFS/WRF/ERA and GNSS Slant Path Delays in Tropical Cyclone Meranti. *IEEE Trans. Geosci. Remote Sens.*, 58, 421-435. DOI: 10.1109/TGRS.2019.2936785.
[44]Lasota, E., Steiner, A.K., Kirchengast, G. et al. (2020b). Tropical cyclones vertical structure from GNSS radio occultation: an archive covering the period 2001-2018. *Earth Syst. Sci. Data*, 12, 2679-2693. DOI: 10.5194/essd-12-2679-2020.
[45]Lasota, E. (2021). Comparison of different machine learning approaches for tropospheric profiling based on COSMIC-2 data. *Earth Planets Space*, 73, 221. DOI: 10.1186/s40623-021-01548-4.
[46]Lasota, E., Slavchev, M., Guerova, G. et al. (2022). Combined Space- and Ground-Based GNSS Monitoring of Two Severe Hailstorm Cases in Bulgaria. *J. Atmos. Ocean. Technol.*, 39, 649-665. DOI: 10.1175/JTECH-D-21-0100.1.
[47]Le Marshall, J., Norman, R., Howard, D. et al. (2019). Using GNSS Data for Real-time Moisture Analysis and Forecasting over the Australian Region I. The System. *JSHESS*, 69, 1-21. DOI: 10.22499/3.6901.009.
[48]Los, M., Smolak, K., Guerova, G. et al. (2020). GNSS-Based Machine Learning Storm Nowcasting. *Remote Sens.*, 12, 2536. DOI: 10.3390/rs12162536.
[49]Maciuk, K. (2019a). Satellite clock stability analysis depending on the reference clock type. *Arab. J. Geosci.*, 12. DOI: 10.1007/s12517-018-4069-2.
[50]Maciuk, K. (2019b). Monitoring of Galileo on-board oscillators variations, disturbances &amp$\mathsemicolon$ noises. *Measurement*, 147, 106843. DOI: 10.1016/j.measurement.2019.07.071.
[51]Maciuk, K., and Lewinska, P. (2019). High-Rate Monitoring of Satellite Clocks Using Two Methods of Averaging Time. *Remote Sens.*, 11, 2754. DOI: 10.3390/rs11232754.
[52]Maciuk, K., Kudrys, J., Skorupa, B. et al. (2021). Testing the product quality of Galileo and GPS on-board oscillators. *Measurement*, 167, 108261. DOI: 10.1016/j.measurement.2020.108261.
[53]Marut, G., Hadas, T., Kaplon, J. et al. (2022). Monitoring the Water Vapor Content at High Spatio-Temporal Resolution Using a Network of Low-Cost Multi-GNSS Receivers. *IEEE Trans. Geosci. Remote Sens.*, 60, 1-14. DOI: 10.1109/TGRS.2022.3226631.
[54]Monte-Moreno, E., Hernandez-Pajares, M., Yang, H. et al. (2021). Method for Forecasting Ionospheric Electron Content Fluctuations Based on the Optical Flow Algorithm. *IEEE Trans. Geosci. Remote Sens.*, 60, 1-1. DOI: 10.1109/TGRS.2021.3126888.
[55]Mota, G.V., Song, S., and Stepniak, K. (2019). Assessment of Integrated Water Vapor Estimates from the iGMAS and the Brazilian Network GNSS Ground-Based Receivers in Rio de Janeiro. *Remote Sens.*, 11, 2652. DOI: 10.3390/rs11222652.
[56]Nowel, K., Cellmer, S., and Fischer, A. (2021). Validation of GNSS baseline observation models using information criteria. *Surv. Rev.*, 53, 402-414. DOI: 10.1080/00396265.2020.1790168.
[57]Nykiel, G., Figurski, M., and Baldysz, Z. (2019). Analysis of GNSS sensed precipitable water vapour and tropospheric gradients during the derecho event in Poland of 11th August 2017. *J. Atmos. Sol. Terr. Phys.*, 193, 105082. DOI: 10.1016/j.jastp.2019.105082.
[58]Paziewski, J., Sieradzki, R., and Baryla, R. (2018). Multi-GNSS high-rate RTK, PPP and novel direct phase observation processing method: application to precise dynamic displacement detection. *Meas. Sci. Technol.*, 29, 035002. DOI: 10.1088/1361-6501/aa9ec2.

Accepted Article

[59]Paziewski, J., Sieradzki, R., and Baryla, R. (2019a). Signal characterization and assessment of code GNSS positioning with low-power consumption smartphones. *GPS Solut.*, 23, 98. DOI: 10.1007/s10291-019-0892-5.
[60]Paziewski, J., Sieradzki, R., Baryla, R. (2019b). Detection of Structural Vibration with High-Rate Precise Point Positioning: Case Study Results Based on 100 Hz Multi-GNSS Observables and Shake-Table Simulation. *Sensors*, 19, 4832. DOI: 10.3390/s19224832.
[61]Paziewski, J. (2020). Recent advances and perspectives for positioning and applications with smartphone GNSS observations. *Meas. Sci. Technol*., 31, 091001. DOI: 10.1088/1361-6501/ab8a7d.
[62]Paziewski, J., and Sieradzki, R. (2020a). Enhanced wide-area multi-GNSS RTK and rapid static positioning in the presence of ionospheric disturbances. *Earth Planets Space*, 72, 110. DOI: 10.1186/s40623-020-01238-7.
[63]Paziewski, J., and Sieradzki, R. (2020b). On the performance of selected ionospheric modelling schemes in Precise Point Positioning. In: 2020 International Conference on Localization and GNSS (ICL-GNSS). Presented at the 2020 International Conference on Localization and GNSS (ICL-GNSS), IEEE, Tampere, Finland, pp. 1-5. DOI: 10.1109/ICL-GNSS49876.2020.9115506.
[64]Paziewski, J., Kurpinski, G., Wielgosz, P. et al. (2020). Towards Galileo + GPS seismology: Validation of high-rate GNSS-based system for seismic events characterisation. *Measurement*, 166, 108236. DOI: 10.1016/j.measurement.2020.108236.
[65]Paziewski, J., Fortunato, M., Mazzoni, A. et al. (2021). An analysis of multi-GNSS observations tracked by recent Android smartphones and smartphone-only relative positioning results. *Measurement*, 175, 109162. DOI: 10.1016/j.measurement.2021.109162.
[66]Paziewski, J. (2022). Multi-constellation single-frequency ionospheric-free precise point positioning with low-cost receivers. *GPS Solut.*, 26, 23. DOI: 10.1007/s10291-021-01209-9.
[67]Paziewski, J., Høeg, P., Sieradzki, R. et al. (2022). The implications of ionospheric disturbances for precise GNSS positioning in Greenland. *J. Space Weather Space Clim.*, 12, 33. DOI: 10.1051/swsc/2022029.
[68]Pelc-Mieczkowska, R. (2020). Preliminary Analysis of the Applicability of the GPS PPP Method in Geodynamic Studies. *Geomat. Environ. Eng.*, 14, 57-68. DOI: 10.7494/geom.2020.14.4.57.
[69]Pelc-Mieczkowska, R., and Tomaszewski, D. (2020). Space State Representation Product Evaluation in Satellite Position and Receiver Position Domain. *Sensors*, 20, 3791. DOI: 10.3390/s20133791.
[70]Poniatowski, M., and Nykiel, G. (2020). Degradation of Kinematic PPP of GNSS Stations in Central Europe Caused by Medium-Scale Traveling Ionospheric Disturbances During the St. Patrick's Day 2015 Geomagnetic Storm. *Remote Sens.*, 12, 3582. DOI: 10.3390/rs12213582.
[71]Prochniewicz, D., Szpunar, R., Kozuchowska, J. et al. (2020). Performance of Network-Based GNSS Positioning Services in Poland: A Case Study. *J. Surv. Eng.*, 146, 05020006. DOI: 10.1061/(ASCE)SU.1943-5428.0000316.
[72]Prochniewicz, D., and Grzymala, M. (2021). Analysis of the Impact of Multipath on Galileo System Measurements. *Remote Sens.*, 13, 2295. DOI: 10.3390/rs13122295.
[73]Prochniewicz, D., Wezka, K., and Kozuchowska, J. (2021). Empirical Stochastic Model of Multi-GNSS Measurements. *Sensors*, 21, 4566. DOI: 10.3390/s21134566.
[74]Prochniewicz, D., Kudrys, J., and Maciuk, K. (2022). Noises in Double-Differenced GNSS Observations. *Energies*, 15, 1668. DOI: 10.3390/en15051668.
[75]Robustelli, U., Paziewski, J., and Pugliano, G. (2021). Observation Quality Assessment and Performance of GNSS Standalone Positioning with Code Pseudoranges of Dual-Frequency Android Smartphones. *Sensors*, 21. DOI: 10.3390/s21062125.

Accepted Article

[76]Robustelli, U., Cutugno, M., Paziewski, J. et al. (2022). GNSS-SDR pseudorange quality and single point positioning performance assessment. *Appl Geomat.* DOI: 10.1007/s12518-022-00457-9.
[77]Rohm, W., and Bosy, J. (2009). Local tomography troposphere model over mountains area. *Atmos. Res.*, 93, 777-783. DOI: 10.1016/j.atmosres.2009.03.013.
[78]Rohm, W., Guzikowski, J., Wilgan, K. et al. (2019). 4DVAR assimilation of GNSS zenith path delays and precipitable water into a numerical weather prediction model WRF. *Atmos. Meas. Tech*., 12, 345-361. DOI: 10.5194/amt-12-345-2019.
[79]Sá, A., Rohm, W., Fernandes, R.M. et al. (2021). Approach to leveraging real-time GNSS tomography usage. *J. Geod.*, 95, 8. DOI: 10.1007/s00190-020-01464-7.
[80]Sieradzki, R., and Paziewski, J. (2019). GNSS-based analysis of high latitude ionospheric response on a sequence of geomagnetic storms performed with ROTI and a new relative STEC indicator. *J. Space Weather Space Clim.*, 9, A5. DOI: 10.1051/swsc/2019001.
[81]Sieradzki, R., and Paziewski, J. (2022). Towards a reliable ionospheric polar patch climatology with ground-based GNSS. *IEEE Trans. Geosci. Remote Sens.*, 60, 1-14. DOI: 10.1109/TGRS.2022.3149635.
[82]Stepniak, K., Bock, O., Bosser, P. et al. (2022). Outliers and uncertainties in GNSS ZTD estimates from double-difference processing and precise point positioning. *GPS Solut*., 26, 74. DOI: 10.1007/s10291-022-01261-z.
[83]Szombara, S., Lewinska, P., Zadlo, A. et al. (2020). Analyses of the Prądnik riverbed shape based on archival and contemporary data sets—old maps, LiDAR, DTMs, orthophotomaps and cross-sectional profile measurements. *Remote* Sens., 12, 2208. DOI: 10.3390/rs12142208.
[84]Tondas, D., Kaplon, J., and Rohm, W. (2020). Ultra-fast near real-time estimation of troposphere parameters and coordinates from GPS data. *Measurement*, 162, 107849. DOI: 10.1016/j.measurement.2020.107849.
[85]Trzcina, E., and Rohm, W. (2019). Estimation of 3D wet refractivity by tomography, combining GNSS and NWP data: First results from assimilation of wet refractivity into NWP. *Q.J.R. Meteorol. Soc.*, 145, 1034-1051. DOI: 10.1002/qj.3475.
[86]Trzcina, E., Hanna, N., Kryza, M. et al. (2020). TOMOREF Operator for Assimilation of GNSS Tomography Wet Refractivity Fields in WRF DA System. *J. Geophys. Res. Atmos*., 125. DOI: 10.1029/2020JD032451.
[87]Van Malderen, R., Pottiaux, E., Klos, A. et al. (2020). Homogenizing GPS Integrated Water Vapor Time Series: Benchmarking Break Detection Methods on Synthetic Data Sets. *Earth Space Sci.*, 7. DOI: 10.1029/2020EA001121.
[88]Wielgocka, N., Hadas, T., Kaczmarek, A. et al. (2021). Feasibility of Using Low-Cost Dual-Frequency GNSS Receivers for Land Surveying. *Sensors*, 21, 1956. DOI: 10.3390/s21061956.
[89]Wielgosz, P., Milanowska, B., Krypiak-Gregorczyk, A. et al. (2021). Validation of GNSS-derived global ionosphere maps for different solar activity levels: case studies for years 2014 and 2018. *GPS Solut*., 25, 103. DOI: 10.1007/s10291-021-01142-x.
[90]Wilgan, K., Hurter, F., Geiger, A. et al. (2017). Tropospheric refractivity and zenith path delays from least-squares collocation of meteorological and GNSS data. *J. Geod.*, 91, 117-134. DOI: 10.1007/s00190-016-0942-5.
[91]Wilgan, K., and Geiger, A. (2019). High-resolution models of tropospheric delays and refractivity based on GNSS and numerical weather prediction data for alpine regions in Switzerland. *J. Geod*., 93, 819-835. DOI: 10.1007/s00190-018-1203-6.
[92]Yang, H., Hernandez-Pajares, M., Jarmolowski, W. et al. (2022). Systematic Detection of Anomalous Ionospheric Perturbations Above LEOs From GNSS POD Data Including Possible

Accepted Article

Tsunami Signatures. IEEE Trans. Geosci. *Remote Sens.* 60, 1-23. DOI: 10.1109/TGRS.2022.3182885.
[93]Yuan, P., Hunegnaw, A., Alshawaf et al. (2021). Feasibility of ERA5 integrated water vapor trends for climate change analysis in continental Europe: An evaluation with GPS (1994-2019) by considering statistical significance. *Remote Sens. Environ.*, 260, 112416. DOI: 10.1016/j.rse.2021.112416.
[94]Zajdel, R., Kazmierski, K., and Sosnica, K. (2022). Orbital Artifacts in Multi-GNSS Precise Point Positioning Time Series. *J. Geophys. Res. Solid Earth*, 127. DOI: 10.1029/2021jb022994.

Accepted Article

Global Geodetic Observing System in Poland 2019-2022

Krzystof Sosnica*, Radoslaw Zajdel, Jaroslaw Bosy

Wroclaw University of Environmental and Life Science, Wroclaw, Poland,
*Corresponding author: Krzysztof Sosnica, e-mail: krzysztof.sosnica@upwr.edu.pl

Abstract: This paper summarizes the contribution of Polish scientific units to the development of the Global Geodetic Observing System (GGOS) in recent years. We discuss the issues related to the integration of space geodetic techniques and co-location in space onboard Global Navigation Satellites Systems (GNSS) and Low Earth Orbiters (LEO), as well as perspectives introduced by the new European Space Agency's (ESA) mission GENESIS. We summarize recent developments in terms of the European Galileo system and its contribution to satellite geodesy and general relativity, as well as ESA's recent initiative – Moonlight to establish a satellite navigation and communication system for the Moon. Recent progress in troposphere delay modeling in Satellite Laser Ranging (SLR) allowed for better handling of systematic errors in SLR, such as range biases and tropospheric biases. We discuss enhanced tropospheric delay models for SLR based on numerical weather models with empirical corrections, which improve the consistency between space geodetic parameters derived using different techniques, such as SLR, GNSS, and Very Long Baseline Interferometry (VLBI). Finally, we review recent progress in the development of Polish GGOS scientific infrastructure in the framework of the European Plate Observing System project EPOS-PL+.

Keywords: GNSS, GGOS, SLR, space ties, GENESIS

Accepted Article

1. Introduction

The Global Geodetic Observing System (GGOS) introduced a challenge to space geodesy requiring the accuracy of the realization of the terrestrial reference frame of 1 mm and 0.1 mm per year for its stability ([38]Plug and Pearlman, 2009). These requirements are dictated by the need of moving the boundaries of knowledge about subtle phenomena occurring in the Earth system, such as sea level rise, as well as changes in the cryosphere, land hydrology, and lithosphere. The current accuracy of the terrestrial reference frame realization exceeds about four times the GGOS requirements ([1]Altamimi et al., 2022). Therefore, many efforts have been undertaken to accomplish the GGOS criteria by improving the global infrastructure in terms of the distribution of the stations, performance and accuracy, mitigation of systematic errors included in observations, modeling of geophysical and geodynamic background models, proposing new satellite missions and observation types to improve the space segment and orbit determination, as well as enhancing the connection of various space geodetic techniques by space ties, tropospheric ties, and global ties.

This article has been accepted for publication in the journal Advances in Geodesy and Geoinformation, issue 72/1, 2023. It has not yet undergone the process of copyediting, typesetting, pagination and proofreading. This may lead to differences between this version and the final published version. The article may be cited as DOI: 10.24425/agg.2022.141925.

2. Co-location in space onboard GNSS satellites

Currently, local ties are used for the realization of the international terrestrial reference frames, e.g., ITRF2020 ([1]Altamimi et al., 2022). Local ties are measured at the GGOS stations equipped with more than one space geodetic technique: VLBI, GNSS, SLR, and DORIS ([24]Kallio et al., 2022). The measurements require a very high accuracy because all potential errors in local tie measurements may directly leak into the ITRF realization as an inconsistency between space geodetic techniques and affect the accuracy of the ITRF realization. Local ties are typically measured once over several years at GGOS stations because of the high costs and efforts required for the measurement process.

Instead of conducting laborious local tie measurements, the space ties onboard satellites can be used for the ITRF realization (see Fig. 1). A space tie link is possible whenever more than one space geodetic technique is targeted toward a common object. [9]Bury et al. (2021a) showed that the space ties onboard Galileo and GLONASS can be used for the connection between SLR and GNSS techniques because all Galileo and GLONASS satellites are equipped with laser retroreflectors for SLR. The independent space tie is available whenever an SLR station tracks GNSS satellites and the GNSS receiver at the station provides observations to the same satellites. The quality of space ties on-board GNSS satellites in terms of the standard deviation of differences between GNSS and SLR solutions is about 40-50 mm in 1-day solutions for individual stations. However, the long-term mean of space ties agrees to 3-4 millimeters with local tie measurements ([9]Bury et al., 2021a). The co-location in space requires proper handling of SLR range biases because biases and detector-specific signature effects constitute the major factors that limit the accuracy of SLR data processing. For flat laser retroreflectors installed onboard GNSS, only the correction between the satellite center-of-mass and the retroreflector centroid is considered when processing SLR data. The single-shot laser pulse can be reflected by any corner cube of the retroreflector array. Detectors installed at SLR stations may operate in single-photon, few-photon, or multi-photon regimes which results in different mapping of the GNSS retroreflector array depending on the incidence angle of the incoming laser pulse. Different SLR detectors' regimes result in systematic effects observed at SLR stations, which are called the signature effect ([54]Strugarek et al., 2021b).

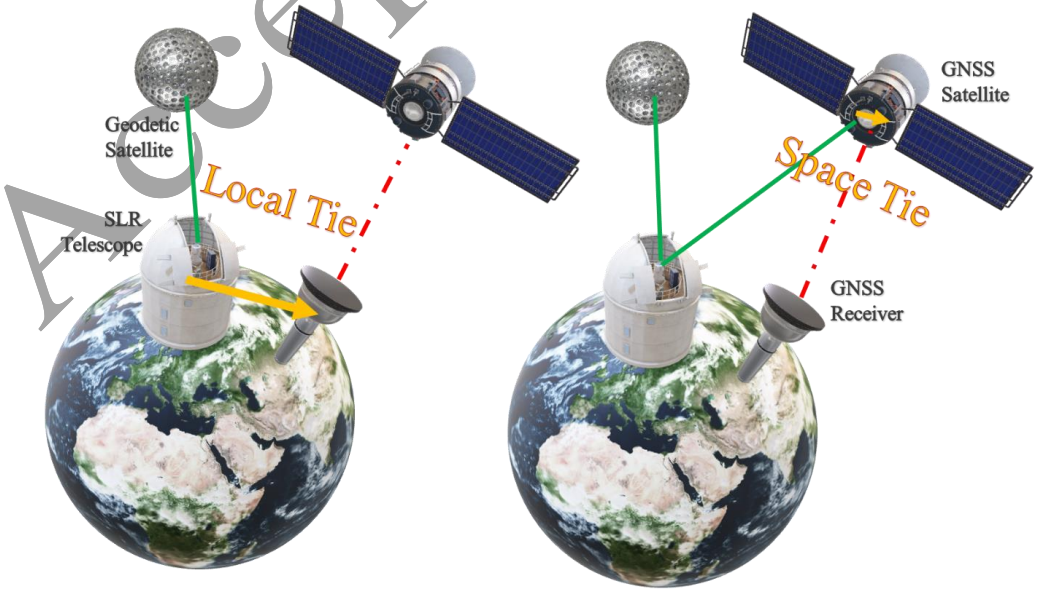

Fig. 1. SLR-GNSS co-location in space onboard GNSS satellites, after [9]Bury et al. (2021a)

Accepted Article

3. Co-location in space onboard LEO satellites

Due to the recent progress in GNSS data modeling, the accuracy of GNSS-based LEO orbits has essentially improved ([3]Arnold et al., 2019). The largest improvement of LEO orbits emerges from 1) using satellite macromodels to account for the solar radiation pressure, albedo, and atmospheric drag, 2) resolving phase ambiguities, 3) enhanced LEO antenna calibrations, 4) and proper satellite attitude modeling ([52]Strugarek 2019b; [34]Montenbruck et al., 2022). Many LEO satellites requiring the highest quality of determined orbits are equipped with laser retroreflectors for SLR, GNSS receivers, and DORIS receivers. Therefore, LEO can be used as the platform for co-location in space. [51]Strugarek et al. (2019a) used the SLR observations to GNSS-based Sentinel 3A and 3B orbits to derive global geodetic parameters. Such an approach allows for the deriving of global geodetic parameters and SLR station coordinates with comparable quality to that derived from LAGEOS observations. [51]Strugarek et al. (2019a) tested different network constraints and different lengths of the solutions. However, 3-day and 5-day solutions turned out to be insufficient to derive global parameters due to missing observations from at least four continents, thus, 7-day solutions are optimum for SLR. [51]Strugarek et al. (2019a) also proposed an SLR-based precise point positioning (PPP) solution, in which no network constraints are required because only station coordinates are estimated, whereas satellite orbits and Earth rotation parameters are derived from GNSS. Such a solution allows for deriving SLR station coordinates individually for each site. The concept of the SLR-PPP technique was further employed using the SWARM-A/B/C constellation ([54]Strugarek et al., 2021b).

[45]Sosnica et al. (2019) used integrated SLR observation to Galileo, GLONASS, BeiDou, GPS, and QZSS for deriving global geodetic parameters. [53]Strugarek et al. (2021a) extended the possibilities of deriving SLR station coordinates and geodetic parameters by integrating SLR observations to active satellites at different heights: LEO and Galileo, as well as passive geodetic satellites: LARES and LAGEOS (see Fig. 2). Such a solution, allowed for deriving SLR station coordinates of superior quality when compared to LAGEOS-based products provided that proper weighting is employed. Using equal weights for all SLR targets may result in solution deterioration ([53]Strugarek et al. 2021a).

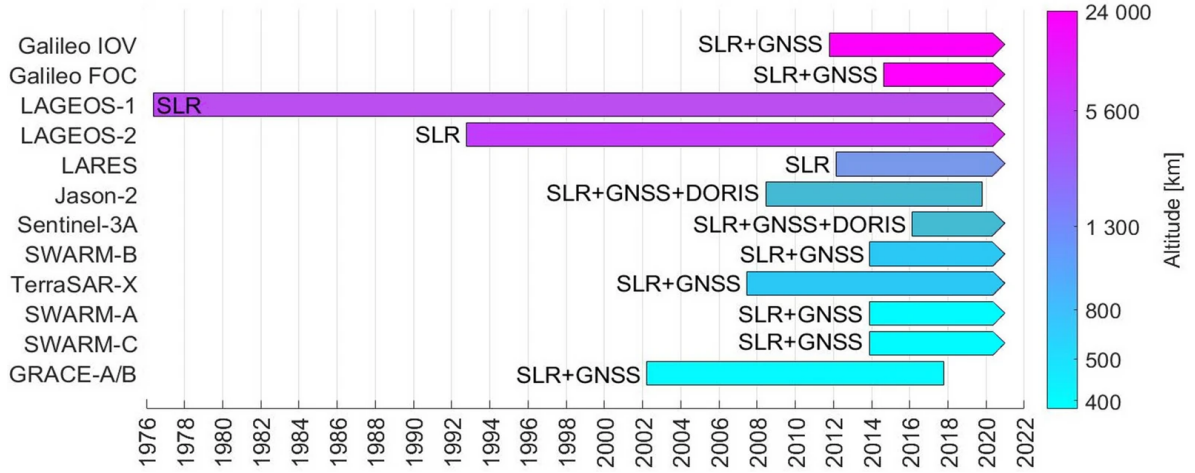

Fig. 2. Satellite missions allowing for the co-location in space as described in the paper by [53]Strugarek et al. (2021a)

One of the errors affecting the SLR observations is the blue-sky effect caused by the atmospheric pressure loading because the dominating SLR observations are collected during

Accepted Article

cloudless weather conditions when the Earth's crust is deformed by high atmospheric pressure. [7]Bury et al. (2019c) assessed the impact of the blue-sky effect based on SLR observations to GNSS satellites. The missing loading corrections can be reconstructed a posteriori by translating the SLR network. However, a considerable part of the loading effect affects not only the network origin but also all estimated parameters, such as orbits, pole coordinates, and length of day; thus, loading corrections should be applied a priori at the observation level to ensure the highest solution accuracy ([7]Bury et al., 2019c).

The Synthetic Aperture Radar (SAR) satellites together with active transponders have been tested in terms of the height system unification and sea level research for the countries near the Baltic Sea ([17]Gruber et al., 2020). The SAR transponders were co-located with GNSS receivers and the tide gauges, resulting in the agreement at the several-centimeter level between different techniques ([12]Czikhardt et al., 2021; [18]Gruber et al., 2022). Hence, the SAR technique introduces a novel opportunity for co-location in space geodesy, however, the SAR applicability for the reference frame realization requires further studies.

4. Co-location in space onboard GENESIS

So far, VLBI was the only technique missing for the successful co-location onboard artificial Earth satellites. Some tests of tracking CubeSat LEO using VLBI have been conducted ([21]Hellerschmied et al., 2018), but the results remained unsatisfactory for geodetic purposes. In 2022, ESA decided to fund a mission dedicated to space geodesy (see Fig. 3). The GENESIS platform will carry onboard all the geodetic instruments referenced to one another through carefully calibrated space ties. The co-location of the techniques in space will solve the inconsistencies and biases between the different geodetic techniques, and pave new opportunities for reference frame realization to bring us closer to the fulfillment of the GGOS goals ([13]Delva et al., 2023).

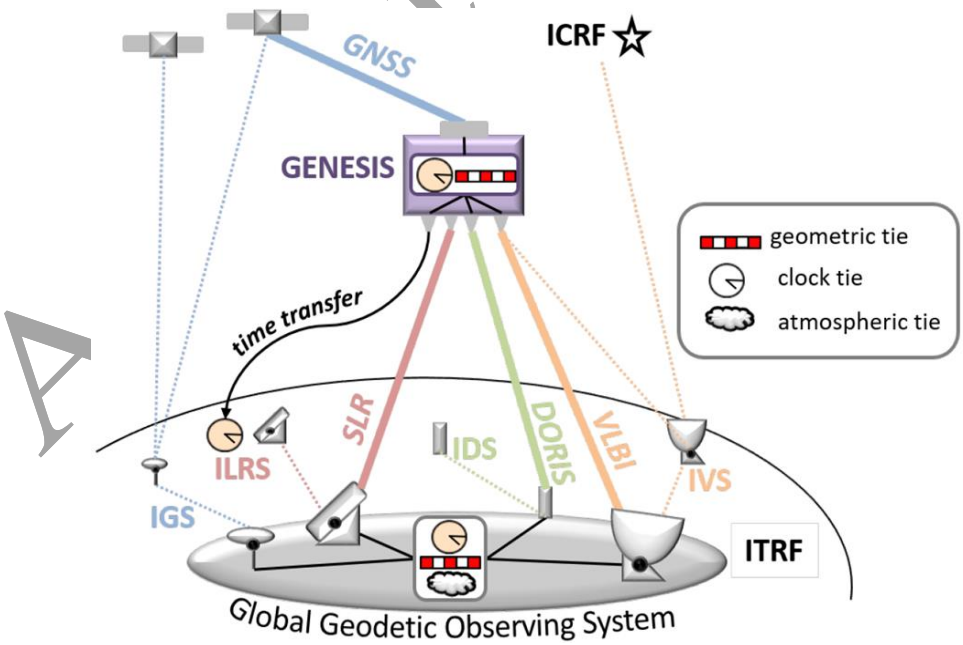

Fig. 3. Concept of the GENESIS mission for the SLR, GNSS, DORIS, and VLBI co-location in space, after [13]Delva et al. (2023)

Accepted Article

5. GNSS orbit modeling

Precise GNSS orbits are a prerequisite for obtaining all derivative products – geodetic parameters based on GNSS. A huge progress in the precise orbit determination of Galileo was possible due to the publication of satellite metadata. The Galileo metadata included indispensable information for orbit determination, e.g., satellite components' size and surface properties – reflection, absorption and dispersion coefficients, modified yaw-steering law, laser retroreflector offsets, as well as antenna offsets and variations based on calibrated data.

[5]Bury et al. (2019a) developed a box-wing model for Galileo In-Orbit Validation (IOV) and Full Operational Capability (FOC) satellites based on published satellite metadata. To fully exploit the potential of the box-wing model, the number of empirical orbit parameters had to be reduced excluding the twice-per-revolution and quadruple terms proposed by [2]Arnold et al. (2015) for the new Empirical CODE orbit model (ECOM). The box-wing model improves the Galileo orbits, especially for the eclipsing periods – the standard deviation of SLR residuals decreases from 37 to 25 mm between the solution based on the extended empirical ECOM with twice-per-rev parameters and the solution based on the box-wing model and a reduced number of ECOM parameters to the five main terms.

[8]Bury et al. (2020) assessed the impact of the non-gravitational force modeling on Galileo satellites, including the direct solar radiation pressure, albedo, Earth infrared radiation, and navigation antenna thrust. The authors concluded that the published Galileo metadata are capable of absorbing about 97% of the total non-gravitational perturbing forces, whereas the remaining part must be absorbed by additionally estimated empirical orbit parameters.

Further improvement of the orbit determination can be obtained by integrating SLR and GNSS data. [10]Bury et al. (2021b) showed that the orbits in the periods when the Sun is almost perpendicular to the orbital plane, resulting in orbit modeling issues due to large correlations between orbit parameters, are improved when combining SLR with GNSS for precise orbit determination (see Fig. 4). However, the SLR and GNSS observations require proper weighting because assuming that the SLR observations and phase GNSS data are of the same quality introduces spurious effects in determined orbits. Therefore, down-weighting of the SLR by a factor of four for Galileo ([10]Bury et al., 2021b) and satellite-dependent weighting for GLONASS with even further reduced weights ([11]Bury et al., 2022) is indispensable for obtaining high-quality combined orbits.

SLR observations to GNSS satellites can also be used for deriving their orbits, however, the cross-track component is poorly observed by SLR, whereas the orbits of cm-level quality require SLR observations collected from different continents for each satellite arc, which occurs only during intensive SLR tracking campaigns ([6]Bury et al., 2019b). Therefore, the combination of SLR and GNSS data is preferable for GNSS precise orbit determination.

Accepted Article

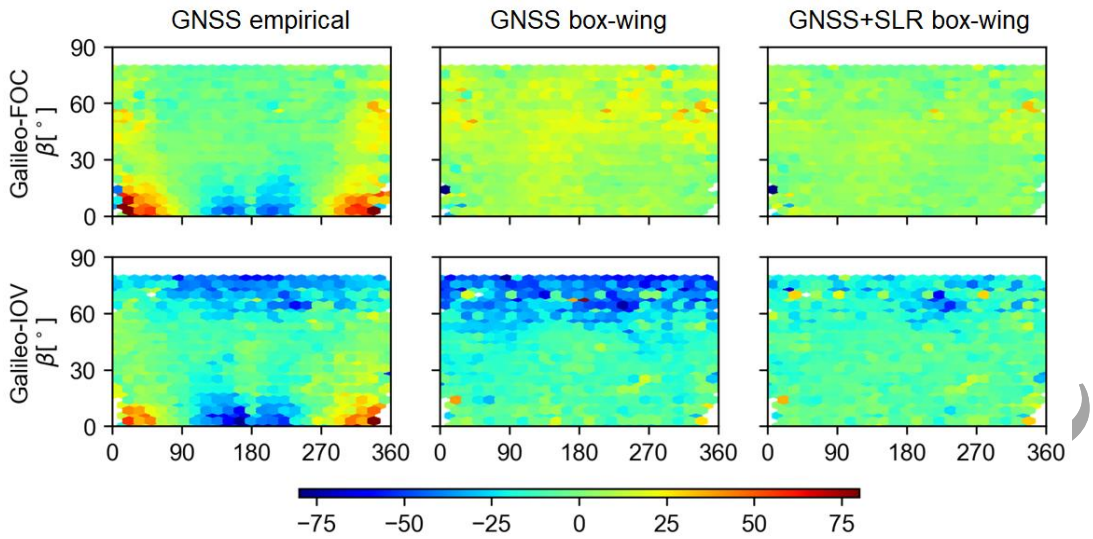

Fig. 4. Progress in Galileo orbit modeling and reducing systematic patterns – SLR residuals to Galileo orbits for the GNSS-based empirical orbit solution (left), GNSS-based box-wing orbit model solution with estimating five ECOM parameters (middle), and the combination of GNSS and SLR data with the box-wing model and estimating five ECOM parameters (right). All values are in millimeters. After [10]Bury et al. (2021b)

For the Galileo satellites of the second generation, the inter-satellite links are considered which would increase the independence of the system with respect to the ground-based control segment. [30]Kur et al. (2021), and [29]Kur and Kalarus (2021) studied different configurations of inter-satellite links and their impact on the accuracy of satellite orbits, clocks, and geodetic parameters. The authors employed the variance component estimation for relative weighting of simulated inter-satellite links and GNSS measurements to further benefit from new observation types for precise orbit determination ([31]Kur and Liwosz, 2022).

The current ITRF realizations struggle with the increasing number of contributing stations and longer time series, and thus, the increasing number of discontinuities in the station coordinate time series caused by equipment changes, earthquakes, electromagnetic interference, and other reasons. [35]Najder (2020) studied the possibility of using automatic algorithm of detecting discontinuities and velocity changes in GNSS data and compared those to the events considered in the ITRF realization. [4]Baselga and Najder (2022) employed similar automatic tools for detecting EUREF permanent GNSS network stations' discontinuities due to earthquake events. Although the automatic tools for the analysis of the station coordinates still require manual adaptation of the threshold levels for significant events, these automated tools are very useful for processing large-scale GNSS networks.

6. Realization of the reference frame scale based on GNSS

The ITRF is the basis for almost all applications in geosciences by providing the reference for observations, and the monitoring of geophysical phenomena occurring in the Earth system. In the ITRF history, the scale was realized in several ways: from SLR or VLBI observations only, as a combination of selected periods from SLR, VLBI and GPS solutions, or by an alignment to the previous ITRF solution. Throughout the ITRF history, the scale differences between consecutive ITRF solutions reach up to 1 ppb. Most commonly, these could be explained by modeling errors and inter-technique inconsistencies. For ITRF2014, the individual solutions

Accepted Article

from SLR and VLBI had a corresponding offset of 0.4 and − 0.4 ppb, respectively. Meanwhile, thanks to the improved procedure of the SLR range bias handling, the ITRF2020 results show a substantial scale consistency improvement, as the level of agreement between SLR and VLBI intrinsic scales is now at the level of 0.15 ± 0.05 ppb ([1]Altamimi et al., 2022).
Antenna calibrations provided in Galileo metadata allow for the realization of the global scale. In the framework of the ITRF2020 realization, Galileo has been processed for the first time together with GPS and GLONASS data. However, due to the inconsistencies in the scale realization between GNSS, SLR and VLBI, the official ITRF2020 realization does not employ the Galileo-based scale ([1]Altamimi et al., 2022) and the scale is based only on VLBI and SLR. Interestingly, the DTRF2020, that is the DGFI-TUM realization of the terrestrial reference frame, incorporates the Galileo-based scale together with the VLBI-based scale ([41]Seitz et al., 2022).
The two following GNSS contributors allow for the independent GNSS-based contribution to the ITRF scale realization. Both GPS-III and BDS-3 manufacturers released information about the satellite antenna calibrations. [66]Zajdel et al. (2022b) tested different combinations of frequencies for the BeiDou-3 system, for which the antenna calibrations have been provided, in terms of their applications to the global scale realization. [66]Zajdel et al. (2022b) found that the GNSS-based scale realization can be frequency-dependent and is strongly vulnerable to orbit modeling. Therefore, the issue of the GNSS scale realization requires further investigation.

7. Deriving global geodetic parameters based on multi-GNSS data

Galileo provides superior global geodetic parameters due to the recent developments in orbit modeling, advanced technology employed, available metadata, and the characteristics of the satellite orbits. Due to the deep resonance 1:2 between the Earth rotation and satellite revolution for GPS, some diurnal and semidiurnal parameters cannot be reliably derived, whereas the GPS-based length-of-day data typically result in an offset which translates into a secular drift of UT1-UTC values. Galileo satellites are not affected by a deep orbit resonance with the Earth rotation ([64]Zajdel et al., 2021b), therefore, the diurnal and semidiurnal signals can be derived with superior quality when compared to GPS. [62]Zajdel et al. (2020) tested the Earth rotation parameters derived from GPS, GLONASS, and Galileo data and found that the accumulated length-of-day values based on Galileo have a secular rate up to fourteen times smaller than GPS-based values. The GLONASS-based pole coordinates are strongly affected by the orbit modeling issues and thus are not as reliable as the GPS and Galileo results (see Fig. 5).
[63]Zajdel et al. (2021a) studied the impact of solar radiation pressure modeling on GNSS-based geocenter coordinates. The authors found that six orbital planes of the GPS system stabilize the geocenter motion recovery. The largest orbit modeling issues for GNSS systems including three orbital planes take place when the Sun illuminates one orbital plane almost perpendicularly (i.e., the Sun elevation angle above the orbital plane is maximum) and the Sun elevation angle above two other orbital planes is similar. Such a configuration results in substantial correlations between empirical orbit parameters and the Z component of the geocenter motion. [63]Zajdel et al. (2021a) found that this phenomenon is strengthened for the new ECOM model with additional twice-per-revolution terms when compared to the classical ECOM model. Therefore, estimating the minimum number of empirical orbit parameters is preferable.
GLONASS-based geocenter motion is unreliable due to three orbital planes and orbit modeling issues. However, despite that the Galileo system nominally consists of three orbital planes, the E14 and E18 Galileo FOC satellites, accidentally launched into eccentric orbits, form the fourth

Accepted Article

orbital plane stabilizing the Galileo solutions. Therefore, the geocenter motion provided by the Galileo system is only slightly worse when compared to that provided by GPS, whereas the GPS+Galileo combination provides superior results ([63]Zajdel et al., 2021a).

[61]Zajdel et al. (2019b) tested the reliability of the GNSS-based geocenter estimates and compared the GNSS station coordinates between the solution with and without imposing the no-net-translation constraint on the GNSS network. The errors of station heights increase by a factor of three when the no-net-translation constraint is not imposed on the GNSS network, despite not estimating the geocenter coordinates as an additional parameter. Therefore, the GNSS network solution based on double differences has a limited sensitivity to the network origin and the GNSS-based geocenter motion includes not only the geophysical signals but also the limitations of the global GNSS solutions to sense the Earth's center-of-mass. [61]Zajdel et al. (2019b) recommend that the not-net-translation constraint should always be imposed on the global GNSS solution despite the lack of direct solution singularity. A different situation occurs in the SLR solutions based on LAGEOS observations ([61]Zajdel et al., 2019b). When imposing the no-net-translation constraint, the estimated geocenter parameter includes the geocenter motion; whereas when not imposing no-net-translation, estimated SLR station coordinates fully absorb the geocenter motion, and the formal errors of station heights are not increased. Therefore, the no-net-translation constraint is not obligatory in the SLR global solutions; and thus, one can choose whether the SLR-based results should be provided in the center-of-mass frame (without no-net-translation) or the center-of-network frame (with no-net-translation constraint). Such a prospect is not possible in GNSS solutions, which always require the no-net-translation constraint.

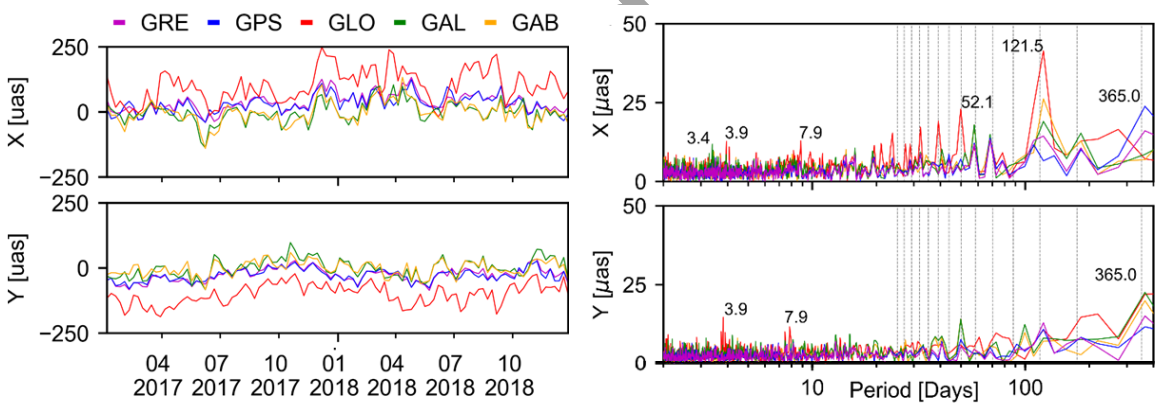

Fig. 5. Pole coordinates derived from GPS, GLONASS (GLO), Galileo based on empirical orbit model (GAL), Galileo based on box-wing model (GAB), and GPS+GLONASS+Galileo (GRE) combination as a difference with respect to IERS-14-C04 series (left) with a corresponding spectrum analysis (right), after [61]Zajdel et al. (2021b)

Accepted Article

8. Orbital signals in global geodetic parameters

The time series of geodetic parameters typically contain spurious signals that are related to: (1) orbital resonances between the satellite revolution period and Earth rotation, (2) aliasing between the sub-daily background models and resulting parameter sampling, (3) draconitic errors due to the orbit modeling issues. These errors have been found in GNSS-based Earth rotation parameters ([62]Zajdel et al., 2020), sub-daily polar motion ([64]Zajdel et al., 2021b), geocenter coordinates ([63]Zajdel et al., 2021a), sub-daily station coordinates derived from PPP

([65]Zajdel et al., 2022a), and tropospheric parameters ([20]Hadas and Hobiger, 2021; [65]Zajdel et al., 2022a). Moreover, the troposphere parameters and station coordinates based on different GNSS may result in an inter-system bias ([56]Wilgan et al. 2022, [57]2023).
[62]Zajdel et al. (2020, [65]2022a) found that the orbital resonances can be mitigated by the multi-satellite combinations (see Fig. 6). In the multi-satellite solutions, satellites with different revolution periods are employed, resulting in the de-correlation between global geodetic parameter estimation intervals and satellite ground track repeatabilities. The aliasing issues must be mitigated by improving the background models of high-frequency phenomena, e.g., better sub-daily Earth rotation models based on geophysical ocean tide models with libration corrections or empirical models based on space geodetic data ([64]Zajdel et al., 2021b). The draconitic errors can be reduced by improved orbit modeling, e.g., by using satellite macromodels for mitigating the impact of solar radiation pressure with the minimum number of estimated empirical orbit parameters ([62]Zajdel et al., 2020, [63]2021a). However, GLONASS has been found to provide station coordinates of inferior quality, therefore, its contribution had to be down-weighted to avoid the degradation of multi-GNSS PPP solutions ([65]Zajdel et al., 2022a).

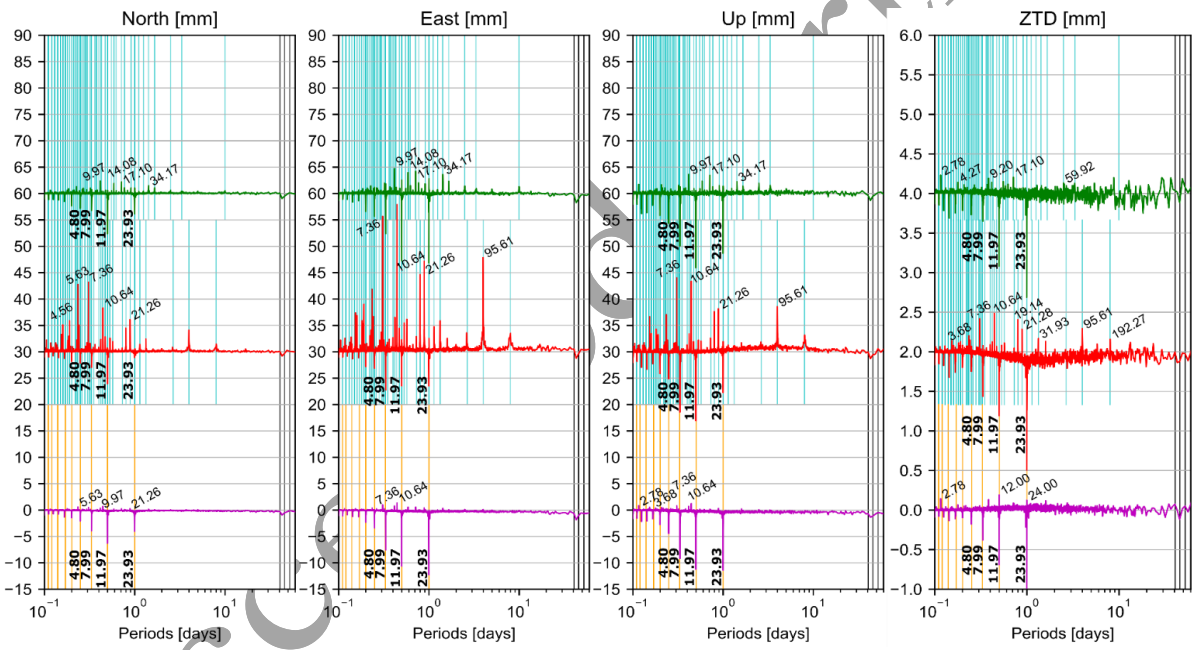

Fig. 6. Stacked differential periodograms of station coordinates for the North, East, and Up components and zenith total delay correction (ZTD). Top: the difference between Galileo and GPS, middle: the difference between GLONASS and GPS, bottom: the difference between multi-GNSS and GPS. Positive values denote that the signals have larger amplitudes in system-specific solutions than in GPS, and negative values denote a reduction of the signals that occurred in GPS-only solutions. Blue lines denote orbital signals for Galileo and GLONASS, whereas orange lines denote the harmonics of the sidereal day (orbital signals for GPS). Labels are in hours. After: [65]Zajdel et al. (2022a)

9. New perspectives for Galileo and BeiDou

Galileo and BeiDou are the new GNSS systems, for which the metadata have been released allowing for advanced orbit modeling and scale realization. However, some parameters provided for BeiDou are still incomplete, e.g., satellite surface properties, whereas some

Accepted article

antenna offset parameters seem to be invalid for some BeiDou-3 satellites ([66]Zajdel et al., 2022b).

The International GNSS Service (IGS) provided an initial orbit product by combining GPS, GLONASS, Galileo, BeiDou, and QZSS orbits provided by different IGS analysis centers, including those contributing to the multi-GNSS experiment (MGEX). The initial orbit combination service was evaluated by [46]Sosnica et al. (2020) showing that substantial efforts must be undertaken by MGEX centers to reach the same quality of orbits for new systems as currently obtained for the best-performing systems.

Despite that all BeiDou-3 satellites are equipped with laser retroreflector arrays, only three of them are being tracked by SLR stations. The SLR tracking of BeiDou-3 requires orbit predictions of high reliability and quality ([36]Najder and Sosnica, 2021). The International Laser Ranging Service plans to track 20 out of 30 BeiDou-3 satellites in the future instead of GLONASS satellites, whose tracking stopped after the Russian invasion on Ukraine in 2022.

[26]Kazmierski et al. (2020) evaluated the real-time orbits and clocks provided by the CNES IGS analysis center ([25]Katsigianni et al., 2019). The authors found that despite modeling issues included in the Galileo orbits, some errors in the orbit radial direction are absorbed and compensated by clock corrections. This is only possible in the GNSS systems that are equipped with superior clocks, such as Galileo with pairs of hydrogen masers compensated by rubidium clocks ([26]Kazmierski et al., 2020). The time transfer based on Galileo is of similar quality to GPS results or even better despite that the Galileo system still did not reach its full operational capability ([33]Mikos et al., 2023). Galileo satellites are homogeneous as opposed to GPS satellites employing different technologies and frequencies for different blocks. Moreover, the broadcast messages of Galileo satellites are being updated more frequently than in the case of GPS, GLONASS, and BeiDou. Therefore, the PPP based on Galileo broadcast data with no further corrections allows for the positioning with decimeter-level accuracy ([19]Hadas et al., 2019) – more than a factor of three better than those based on GPS.

High-quality orbits allow for the validation of effects emerging from general relativity, such as the Schwarzschild, Lense-Thirring, and De Sitter (geodetic precession) effects. [47]Sosnica et al. (2021) derived formulas of theoretical changes in Keplerian parameters and satellite revolution periods due to three main effects emerging from general relativity. The authors calculated the magnitude of periodical and secular orbit perturbations for GNSS, LAGEOS, LARES, and geostationary orbits. The periodical variations of the semi-major axis due to the Schwarzschild effect and the secular rates of the ascending node due to Lense-Thirring and De Sitter turned out to be measurable using GNSS orbits as they reach the centimeter level within 3-day arcs. Accumulating the long-term GNSS solutions may even further improve the confirmation of general relativistic effects.

[48]Sosnica et al. (2022) used GPS, GLONASS, and Galileo orbits to detect the impact of the Schwarzschild effect on the semi-major axis and eccentricity of GNSS orbits. The Galileo satellites in eccentric orbits provided a very good agreement with theoretically derived values. The change of the satellite semi-major axis equaled +28.3 and -7.8 mm when eccentric Galileo satellites are in their perigees and apogees, respectively. When considering the full constellation of GPS, GLONASS, and Galileo, the mean observed semi-major offset is -17.41 mm, which gives a relative error versus the expected value from the theory of 0.36% ([48]Sosnica et al. 2022). Therefore, GNSS satellites with enhanced orbit modeling considerably contribute to fundamental physics.

Accepted Article

10. Progress in SLR data modeling

Some of the global geodetic parameters can be derived entirely reliably only from the SLR technique, e.g., Earth's oblateness term ([59]Yu et al., 2021b), geocenter coordinates ([61]Zajdel et al., 2019b; [27]Kosek et al., 2020; [58]Yu et al., 2021a) or the standard gravitational product GM (Perlman et al., 2019). Moreover, the combination of GNSS-based LEO kinematic orbits and SLR data can be used for deriving the low-degree gravity field parameters and fill up the gap between GRACE and GRACE Follow-On missions ([32]Meyer et al. 2019; [67]Zhong et al., 2021). Despite significant progress in SLR data processing, the SLR-based parameters are still affected by systematic errors.

One of the major systematic error sources in SLR data is the modeling of the troposphere delay. SLR stations rely on the meteorological data collected at the SLR stations to derive the corrections for the slant tropospheric delays. For the delay in the zenith direction, the barometer with water vapor data are employed, whereas, for the mapping function, the temperature records collected at the station are used. Due to the point meteorological measurements, the full symmetry of the atmosphere is assumed for the SLR tropospheric delay modeling.

[15]Drozdzewski et al. (2019) proposed employing numerical weather models to account for the asymmetry of the atmosphere above the SLR stations. The horizontal gradients and mapping functions based on numerical models improved the SLR solutions, however, the zenith delays turned out to be more accurate when based on direct meteorological data collected at SLR stations than numerical weather models. Using the hybrid approach with barometer data and horizontal gradients and mapping functions from numerical models, the SLR-based pole coordinates improved by about 20 μas ([15]Drozdzewski et al., 2019) and became more consistent with the results obtained from other space geodetic techniques, especially GNSS.

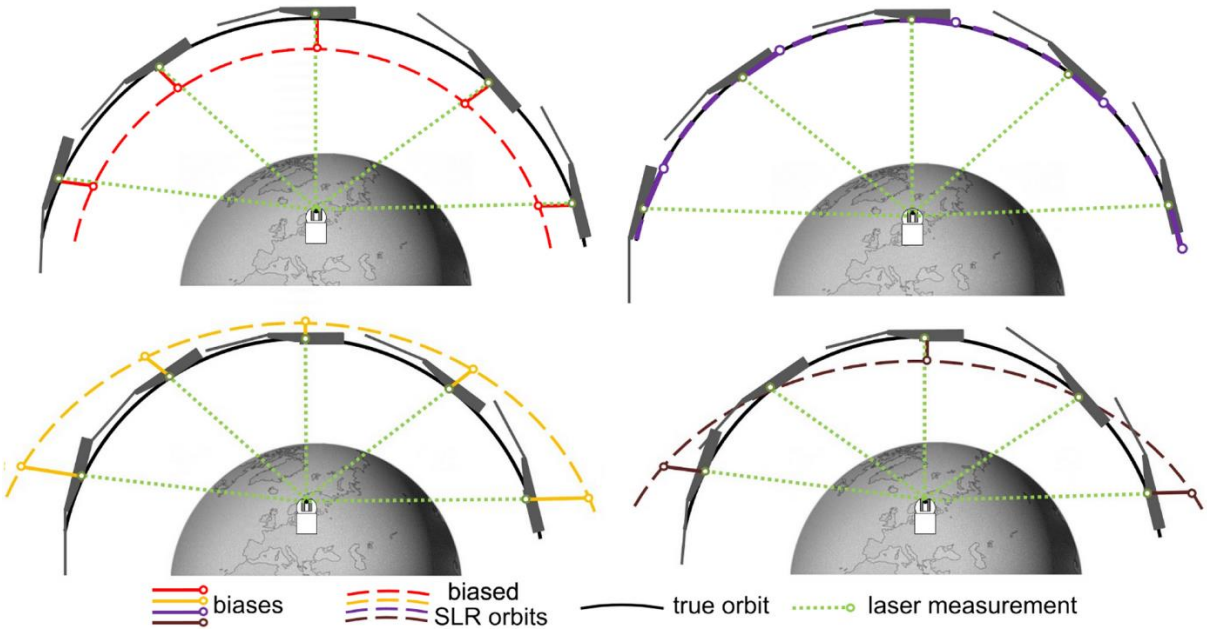

Fig. 7. Geometry of systematic errors in SLR. Range bias (top-left, red), time bias (top-right, purple), tropospheric bias (bottom-left, yellow), and sum of errors (bottom-right, brown), after [37]Otsubo et al. (2019) and [55]Strugarek et al. (2022)

Despite the calibrations, some SLR stations seemed to be affected by barometer biases resulting in tropospheric biases ([16]Drozdzewski and Sosnica, 2021). Therefore, the estimation of

Article

tropospheric biases has been proposed for SLR. The estimation of tropospheric biases improves the repeatability of SLR station coordinates, changes the geocenter mean offset at the millimeter level ([16]Drozdzewski and Sosnica, 2021), and substantially reduce the SLR residuals to LEO satellites – from the level of 10 to 6 mm for high-performing SLR stations ([55]Strugarek et al., 2022). Due to the elevation-dependency of tropospheric biases, they are much better suited to account for systematic errors in SLR data than range biases, which are independent of the elevation angle (see Fig. 7). Therefore, estimating tropospheric biases is beneficial for SLR solutions, whereas estimating range biases may result of biased SLR-based parameters, especially the height component of station coordinates and the global scale ([16]Drozdzewski and Sosnica, 2021).

11. ESA's new initiatives

Besides the GENESIS initiative, ESA will support a new mission in the framework of the Moonlight program. For future lunar missions, the satellite navigation and communication system is indispensable. Navigation and positioning on the Moon using a satellite system require a high-accuracy lunar reference frame realization, connection to the terrestrial reference frame, lunar-specific time system definitions, and time transfer between the UTC time on the Earth and lunar satellites and receivers. The high-quality lunar reference frames can be provided by the laser retrorefectors on the Moon installed by Apollo and Luna missions, as well as future Arthemis missions ([22]Iess et al., 2022). The high-quality orbits of lunar orbiters can be provided by range, range-rate, and Doppler observations by a dedicated ESA network as well as by GNSS receivers that are planned to be placed on the lunar orbiters ([42]Sesta et al., 2023). ESA funded the project ATLAS (Fundamental techniques, models and algorithms for a Lunar Radio Navigation system) to define the requirements and technologies needed to establish the navigation system ([22]Iess et al., 2022). The role of the Polish partner in the ATLAS project is to define the structure of the broadcast navigation message with orbit representation, to evaluate the impact of orbit perturbations for eccentric lunar orbiters, simulate the orbits with extended gravitation and non-gravitational orbit perturbations, to analyze the visibility of the satellites, to assess possible inconsistencies in the origin, rotation, and translation of the lunar reference frame realizations with their impact on positioning, and to analyze the possibility of receiving faint GNSS signals at lunar distances ([14]Di Benedetto et al., 2022; [49]Sosnica et al., 2023).

12. New GGOS infrastructure in Poland

Two GGOS observatories in Poland have been recently supported by new infrastructure in the framework of the European Plate Observing System – EPOS-PL+. The Astrogedynamical Observatory in Borowiec belonging to the Space Research Center of the Polish Academy of Sciences bought the tidal gravimeter gPhone-X that shall support the routine SLR and GNSS observations and provide corrections to high-accuracy clocks, such as cesium fountain. The local tidal parameters can be derived from SLR data ([23]Jagoda et al., 2020) and then compared with those directly obtained from gPhone-X gravimeter. The Borowiec SLR Observatory continues tracking geodetic targets ([39]Schillak et al., 2021, [40]2022) and contributes to new initiatives dedicated to space debris tracking ([43]Smaglo et al., 2021). The new, independent laser system is planned to be installed in the near future ([50]Suchodolski, 2022), whereas the legacy SLR system will be supported by a new detector – compensated single photon avalanche diode (CSPAD) and kilohertz laser ([43]Smaglo et al., 2021), which

Accepted Article

allows for the spin determination of geodetic satellites and time transfer based on laser observations ([28]Kucharski et al., 2019).
The GGOS infrastructure at the Institute of Geodesy and Geoinformatics UPWr has been recently supported by the gravimeter CG-6, which is also used as a tidal gravimeter parallel to gPhone-X when not employed for field measurements. Besides the existing GNSS stations, such as WROC and WROE, a number of GNSS receivers based on low-cost and geodetic-grade antennas and chipsets have been tested. The WROC IGS station has been operating for 26 years and since 2017 has been supported by a microwave radiometer ([44]Sosnica and Bosy, 2019). Soon, the link via a black optical fiber between Wroclaw and Borowiec is planned which will allow for the connection of the WROC and WROE stations to a hydrogen maser or a cesium fountain. The optical link will allow for the time transfer using a direct connection as well as multi-GNSS observations ([33]Mikos et al., 2023). Finally, the robot acquired in the EPOS-PL+ will provide antenna calibrations for low-cost antennas increasing their accuracies and reliabilities for high-accuracy geodetic applications.

13. Conclusions and Outlook

We provided a review of the recent contribution of Polish scientific units to GGOS in terms of the development of models and processing procedures, as well as new geodetic infrastructure. Considerable progress in GNSS data processing was possible due to metadata release for Galileo and BeiDou-3 systems allowing for improved satellite orbit models, and thus, also global geodetic parameters. Thanks to multiple satellites distributed on different orbital planes and characterized by different orbital revolution periods, one can derive station coordinates, tropospheric parameters, pole coordinates, and length-of-day excess values with unprecedented quality. Antenna calibrations provided for Galileo allow for the scale realization of reference frames and were employed in DTRF2020 along with the VLBI for the scale realization. Two techniques of space geodesy co-located onboard Galileo, GLONASS, and BeiDou – SLR and GNSS – allow for co-location in space. However, only four BeiDou-3 satellites are tracked by SLR stations, and since 2022 the stations ceased to track GLONASS. Therefore, a successful co-location is currently possible only via Galileo satellites. Co-location in space of GNSS and SLR can be conducted onboard LEO missions, such as GRACE, GOCE, and SWARM, whereas Sentinel-6A, Sentinel-3A/B, and Jason-3 offer the co-location of three techniques, as they track the signals from DORIS beacons in addition. The future ESA's GENESIS mission will provide X-band and S-band signals for VLBI tracking, allowing for the co-location in space of all four space geodetic techniques for the first time.
Better orbit models reduced the draconitic errors embedded in GNSS-based global geodetic parameters, such as station coordinates and Earth rotation parameters. Estimating tropospheric biases in SLR solutions improved the station height estimates and the SLR residuals to GNSS-based LEO orbits, whereas the horizontal gradients based on numerical weather models improved the SLR-based polar motion estimates and enhanced the consistency between SLR and other space geodetic techniques.
Future progress in quality improvement of the global geodetic parameters is expected from the full exploitation of high-quality clocks onboard GNSS satellites and on the ground via stochastic modeling, proper integration of all GNSS systems with understanding the sources of inter-system biases, reducing systematic errors, such as SLR signature effects and tropospheric biases, better modeling of geodynamic phenomena, such as tides and non-tidal loading effects. More consistent antenna calibrations and more complete information about satellite surface properties will entail better orbit models and translate into a superior quality of geodetic

Accepted Article

parameters and confirmation of general relativity effects with smaller uncertainties. Finally, new observation types, such as inter-satellite links or direct connections to lunar orbiters will pave novel opportunities not only for Earth sciences but also for better understanding processes in the entire Earth-Moon system.

Author contributions

Conceptualization: K.S., J.B.; literature review: K.S, R.Z.; writing - original draft preparation: K.S., R.S.; writing - review and editing: J.B.; funding acquisition: K.S., J.B.

Data availability statement

No datasets were used in this research.

Acknowledgements

We would like to thank all authors of papers referenced in this review article. This work was supported by the EPOS-PL+ project no. POIR.04.02.00-00-C005/19.

References

[1]Altamimi, Z., Rebischung, P., Collilieux, X. et al. (2022). ITRF2020: main results and key performance indicators. In EGU General Assembly Conference, 4-8 May 2020, Vienna, Austria. DOI: 10.5194/egusphere-egu22-3958.
[2]Arnold, D., Meindl, M., Beutler, G. et al. (2015). CODE's new solar radiation pressure model for GNSS orbit determination. *J. Geod.*, 89(8), 775-791. DOI: 10.1007/s00190-015-0814-4.
[3]Arnold, D., Montenbruck, O., Hackel, S. et al. (2019). Satellite laser ranging to low Earth orbiters: orbit and network validation. *J. Geod.*, 93(11), 2315-2334. DOI: 10.1007/s00190-018-1140-4.
[4]Baselga, S., and Najder, J. (2022). Automated detection of discontinuities in EUREF permanent GNSS network stations due to earthquake events. *Surv. Rev.*, 54(386), 420-428. DOI: 10.1080/00396265.2021.1964230.
[5]Bury, G., Zajdel, R., and Sosnica, K. (2019a). Accounting for perturbing forces acting on Galileo using a box-wing model. *GPS Solut.*, 23 (74), 1-12. DOI: 10.1007/s10291-019-0860-0.
[6]Bury, G., Sosnica, K., and Zajdel, R. (2019b). Multi-GNSS orbit determination using satellite laser ranging. *J. Geod.*, 93 (12), 2447-2463. DOI: 10.1007/s00190-018-1143-1.
[7]Bury, G., Sosnica, K., and Zajdel, R. (2019c). Impact of the Atmospheric Non-tidal Pressure Loading on Global Geodetic Parameters Based on Satellite Laser Ranging to GNSS. *IEEE Trans. Geosci. Remote Sens.*, 57(6), 3574-3590. DOI: 10.1109/TGRS.2018.2885845.
[8]Bury, G., Sosnica, K., Zajdel, R. et al. (2020). Toward the 1-cm Galileo orbits: challenges in modeling of perturbing forces. *J. Geod.*, 94 (16), 1-19. DOI: 10.1007/s00190-020-01342-2.
[9]Bury, G., Sosnica, K., Zajdel, R. et al. (2021a). Geodetic datum realization using SLR-GNSS co-location onboard Galileo and GLONASS. *J. Geophys. Res. Solid Earth*, 126(10), 1-23. DOI: 10.1029/2021JB022211.

Accepted Article

[10]Bury, G., Sosnica, K., Zajdel, R. et al. (2021b). Determination of precise Galileo orbits using combined GNSS and SLR observations. *GPS Solut.*, 25(11), 1-13. DOI: 10.1007/s10291-020-01045-3.
[11]Bury, G., Sosnica, K., Zajdel, R. et al.. (2022). GLONASS precise orbit determination with identification of malfunctioning spacecraft. *GPS Solut.*, 26(36), 1-13. DOI: 10.1007/s10291-021-01221-z.
[12]Czikhardt, R., van der Marel, H., Papco, J. et al. (2021). On the Efficacy of Compact Radar Transponders for InSAR Geodesy: Results of Multiyear Field Tests. *IEEE Trans. Geosci. Remote Sens.*, 60, 1-13. DOI: 10.1109/TGRS.2021.3119917.
[13]Delva, P., Altamimi, Z., Blazquez, A. et al. (2023). GENESIS: Co-location of geodetic techniques in space. *Earth Planets Space*, 1752. DOI: 10.1186/s40623-022-01752-w.
[14]Di Benedetto, M., Boscagli, G., De Marchi, F. et al. (2022). An architecture for a lunar navigation system: orbit determination and time synchronization. In: Proceedings of the ESA's 8th International Colloquium on Scientific and Fundamental Aspects of GNSS, 14-16 September 2022, Sofia, Bulgaria.
[15]Drozdzewski, M., Sosnica, K., Zus, F. et al. (2019). Troposphere delay modeling with horizontal gradients for satellite laser ranging. *J. Geod.*, 93(10), 1853-1866. DOI: 10.1007/s00190-019-01287-1.
[16]Drozdzewski, M., and Sosnica, K. (2021). Tropospheric and range biases in Satellite Laser Ranging. *J. Geod.*, 95(100), 1-18. DOI: 10.1007/s00190-021-01554-0.
[17]Gruber, T., Ågren, J., Angermann, D. et al. (2020). Geodetic SAR for Height System Unification and Sea Level Research-Observation Concept and Preliminary Results in the Baltic Sea. *Remote Sens.*, 12, 3747. DOI: 10.3390/rs12223747.
[18]Gruber, T., Ågren, J., Angermann, D. et al. (2022). Geodetic SAR for Height System Unification and Sea Level Research-Results in the Baltic Sea Test Network. *Remote Sens.*, 14, 3250. DOI: 10.3390/rs14143250.
[19]Hadas, T., Kazmierski, K., and Sosnica, K. (2019). Performance of Galileo-only dual-frequency absolute positioning using the fully serviceable Galileo constellation. *GPS Solut.*, 23(108), 1-12. DOI: 10.1007/s10291-019-0900-9.
[20]Hadas, T., and Hobiger, T. (2021). Benefits of Using Galileo for Real-Time GNSS Meteorology. *IEEE Geosci. Remote Sens. Lett.*, 18(10), 1756-1760. DOI: 10.1109/LGRS.2020.3007138.
[21]Hellerschmied, A., McCallum, L., McCallum, J. et al. (2018). Observing APOD with the AuScope VLBI array. *Sensors*, 18(5), 1587. DOI: 10.3390/s18051587.
[22]Iess, L., Sosnica, K., Racioppa, P. et al. (2022). 'ATLAS-Fundamental techniques, models and algorithms for a lunar radio navigation system': a proposal for a lunar navigation system infrastructure. In 44th COSPAR Scientific Assembly, 16-24 July 2022, Athens, Greece.
[23]Jagoda, M., Rutkowska, M., Lejba, P. et al. (2020). Satellite Laser Ranging for Retrieval of the Local Values of the Love h2 and Shida l2 Numbers for the Australian ILRS Stations. *Sensors*, 20, 6851. DOI: 10.3390/s20236851.
[24]Kallio, U., Rouhiainen, P., Raja-Halli, A. et al. (2022). Validation of GNSS-based reference point monitoring of the VGOS VLBI telescope at Metsähovi. In 5th Joint International Symposium on Deformation Monitoring (JISDM), 20-22 June 2022, Valencia, Spain. DOI: 10.4995/JISDM2022.2022.16057.
[25]Katsigianni, G., Loyer, S., Perosanz, F. et al. (2019). Improving Galileo orbit determination using zero-difference ambiguity fixing in a Multi-GNSS processing. *Adv. Space Res.*, 63 (9), 2952-2963. DOI: 10.1016/j.asr.2018.08.035.

Accepted Article

[26]Kazmierski, K., Zajdel, R., and Sosnica, K. (2020). Evolution of orbit and clock quality for real-time multi-GNSS solutions. *GPS Solut.*, 24 (111), 1-12. DOI: 10.1007/s10291-020-01026-6.
[27]Kosek, W., Popinski, W., Wnek, A. et al. (2020). Analysis of Systematic Errors in Geocenter Coordinates Determined From GNSS, SLR, DORIS, and GRACE. *Pure Appl. Geophys.*, 177, 867-888. DOI: 10.1007/s00024-019-02355-5.
[28]Kucharski, D., Kirchner, G., Otsubo, T. et al. (2019). Hypertemporal photometric measurement of spaceborne mirrors specular reflectivity for Laser Time Transfer link model. *Adv. Space Res.*, 64(4), 957-963. DOI: 10.1016/j.asr.2019.05.030.
[29]Kur, T., and Kalarus, M. (2021). Simulation of Inter-Satellite Link schemes for use in precise orbit determination and clock estimation. *Adv. Space Res.*, 68(12), 4734-4752. DOI: 10.1016/j.asr.2021.05.011
[30]Kur, T., Liwosz, T., and Kalarus, M. (2021). The application of inter-satellite links connectivity schemes in various satellite navigation systems for orbit and clock corrections determination: simulation study. *Acta Geodaet. Geophys.*, 56(1), 1-28. DOI: 10.1007/s40328-020-00322-4.
[31]Kur, T., and Liwosz, T. (2022). Simulation of the Use of Variance Component Estimation in Relative Weighting of Inter-Satellite Links and GNSS Measurements. *Remote Sens.*, 14(24), 6387. DOI: 10.3390/rs14246387.
[32]Meyer, U., Sosnica, K., Arnold, D. et al. (2019). SLR, GRACE and Swarm Gravity Field Determination and Combination. *Remote Sens.*, 11 (8), 956. DOI: 10.3390/rs11080956.
[33]Mikos, M., Kazmierski, K., and Sosnica K. (2023). Characteristics of the IGS receiver clock performance from multi-GNSS PPP solutions. *GPS Solut.*, 27, 55. DOI: 10.1007/s10291-023-01394-9.
[34]Montenbruck, O., Kunzi, F., and Hauschild, A. (2022). Performance assessment of GNSS-based real-time navigation for the Sentinel-6 spacecraft. *GPS Solut.*., 26(1), 1-11. DOI: 10.1007/s10291-021-01198-9
[35]Najder, J. (2020). Automatic detection of discontinuities in the station position time series of the reprocessed global GNSS network using Bernese GNSS Software. *Acta Geodyn. Geomater.*, 17(4), 439-451. DOI: 10.13168/AGG.2020.0032.
[36]Najder, J., and Sosnica, K. (2021). Quality of Orbit Predictions for Satellites Tracked by SLR Stations. *Remote Sens.*, 13(7), 1377. DOI: 10.3390/rs13071377.
[37]Otsubo, T., Müller, H., Pavlis, E.C. et al. (2019). Rapid response quality control service for the laser ranging tracking network. *J. Geod.*, 93(11), 2335-2344. DOI: 10.1007/s00190-018-1197-0.
[38]Plag, H., and Pearlman, M. (2009). *Global Geodetic Observing System*. Springer-Verlag: Berlin Heidelberg. DOI: 10.1007/978-3-642-02687-4.
[39]Schillak, S., Lejba, P., and Michalek, P. (2021). Analysis of the Quality of SLR Station Coordinates Determined from Laser Ranging to the LARES Satellite. *Sensors*, 21(3), 737. DOI: 10.3390/s21030737.
[40]Schillak, S., Lejba, P., Michalek, P. et al. (2022). Analysis of the Results of the Borowiec SLR Station (7811) for the Period 1993–2019 as an Example of the Quality Assessment of Satellite Laser Ranging Stations. *Sensors*, 22(2), 616. DOI: 10.3390/s22020616.
[41]Seitz, M., Bloßfeld, M., Glomsda, M. et al. (2022). DTRF2020: the ITRS 2020 realization of DGFI-TUM. In IAG International Symposium on Reference Frames for Applications in Geosciences, 17-19 October, 2022, Thessaloniki, Greece.
[42]Sesta, A., Di Benedetto, M., Durante, D. et al. (2023). Orbit Determination and Time Transfer for a Lunar Radio Navigation System. EGU General Assembly Conference, 23-28 April 2023, Vienna, Austria. DOI: 10.5194/egusphere-egu23-15933.

Accepted Article

[43]Smaglo, A., Lejba, P., Schillak, S. et al. (2021). Measurements to space debris in 2016-2020 by laser sensor at Borowiec Poland. *Artif. Satell. J. Planet. Geod.*, 56. DOI: 10.2478/arsa-2001-0009.
[44]Sosnica, K., and Bosy, J. (2019). Global Geodetic Observing System 2015–2018. *Geod. Cartogr.*, 68(1). DOI: 10.24425/gac.2019.126090.
[45]Sosnica, K., Bury, G., Zajdel, R. et al. (2019). Estimating global geodetic parameters using SLR observations to Galileo, GLONASS, BeiDou, GPS, and QZSS. *Earth Planets Space*, 71(20), 1-11. DOI: 10.1186/s40623-019-1000-3.
[46]Sosnica, K., Zajdel, R., Bury, G. et al. (2020). Quality assessment of experimental IGS multi-GNSS combined orbits. *GPS Solut*., 24 (54), 1-14. DOI: 10.1007/s10291-020-0965-5.
[47]Sosnica, K., Bury, G., Zajdel, R. et al. (2021). General relativistic effects acting on the orbits of Galileo satellites. *Celest. Mech. Dyn. Astron.*, 133(14), 1-31. DOI: 10.1007/s10569-021-10014-y.
[48]Sosnica K., Bury G., Zajdel R. et al. (2022). GPS, GLONASS, and Galileo orbit geometry variations caused by general relativity focusing on Galileo in eccentric orbits. *GPS Solut.*, 26(5), 1-12. DOI: 10.1007/s10291-021-01192-1.
[49]Sosnica, K., Zajdel, R., Bury, G. et al. (2023). Precise orbits for the lunar navigation system: challenges in the modeling of perturbing forces and broadcast orbit representation. In EGU General Assembly Conference, 23-28 April 2023, Vienna, Austria. DOI: 10.5194/egusphere-egu23-5575.
[50]Suchodolski, T. (2022). Active Control Loop of the BOROWIEC SLR Space Debris Tracking System. *Sensor*s, 22(6), 2231. DOI: 10.3390/s22062231.
[51]Strugarek, D., Sosnica, K., Arnold, D. et al. (2019a). Determination of Global Geodetic Parameters Using Satellite Laser Ranging Measurements to Sentinel-3 Satellites. *Remote Sens*., 11 (19), 2282. DOI: 10.3390/rs11192282.
[52]Strugarek, D., Sosnica, K., and Jäggi, A. (2019b). Characteristics of GOCE orbits based on Satellite Laser Ranging. *Adv. Space* Res., 63(1), 417-431. DOI: 10.1016/j.asr.2018.08.033.
[53]Strugarek, D., Sosnica, K., Arnold, D. et al. (2021a). Determination of SLR station coordinates based on LEO, LARES, LAGEOS, and Galileo satellites. *Earth Planets Space*, 73(87), 1-21. DOI: 10.1186/s40623-021-01397-1.
[54]Strugarek, D., Sosnica, K., Zajdel, R. et al. (2021b). Detector-specific issues in Satellite Laser Ranging to Swarm-A/B/C satellites. *Measurement*, 182(109786), 1-12. DOI: 10.1016/j.measurement.2021.109786.
[55]Strugarek, D., Sosnica, K., Arnold, D. et al. (2022). Satellite laser ranging to GNSS-based Swarm orbits with handling of systematic errors. *GPS Solut.*, 26 (104), 1-14. DOI: 10.1007/s10291-022-01289-1.
[56]Wilgan, K., Dick, G., Zus, F. et al. (2022). Towards operational multi-GNSS tropospheric products at GFZ Potsdam. *Atmos. Meas. Tech*., 15(1), 21-39. DOI: 10.5194/amt-15-21-2022.
[57]Wilgan, K., Dick, G., Zus, F. et al. (2023). Tropospheric parameters from multi-GNSS and numerical weather models: case study of severe precipitation and flooding in Germany in July 2021. *GPS Solut*., 27, 49. DOI: 10.1007/s10291-022-01379-0.
[58]Yu, H., Sosnica, K., and Shen, Y. (2021a). Separation of Geophysical Signals in the LAGEOS Geocenter Motion based on Singular Spectrum Analysis. *Geophys. J. Int.*, ggab063, 1-25. DOI: 10.1093/gji/ggab063.
[59]Yu, H., Chen, Q., Sun, Y. et al. (2021b). Geophysical Signal Detection in the Earth's Oblateness Variation and Its Climate-Driven Source Analysis. *Remote Sens*., 13(10), 1-18. DOI: 10.3390/rs13102004.

Accepted Article

[60]Zajdel, R., Sosnica, K., Dach, R. et al. (2019a) Network effects and handling of the geocenter motion in multi-GNSS processing. *J. Geophys. Res. Solid Earth*, 124(6), 5970-5989. DOI: 10.1029/2019JB017443.
[61]Zajdel, R., Sosnica, K., Drozdzewski, M. et al. (2019b). Impact of network constraining on the terrestrial reference frame realization based on SLR observations to LAGEOS. *J. Geod*., 93(11), 2293-2313. DOI: 10.1007/s00190-019-01307-0.
[62]Zajdel, R., Sosnica, K., Bury, G. et al. (2020). System-specific systematic errors in earth rotation parameters derived from GPS, GLONASS, and Galileo. *GPS Solut*., 24(74), 1-15. DOI: 10.1007/s10291-020-00989-w.
[63]Zajdel, R., Sosnica, K., and Bury, G. (2021a). Geocenter coordinates derived from multi-GNSS: a look into the role of solar radiation pressure modeling. *GPS* Solut., 25(1), 1-15. DOI: 10.1007/s10291-020-01037-3.
[64]Zajdel, R., Sosnica, K., Bury, G. et al. (2021b). Sub-daily polar motion from GPS, GLONASS, and Galileo. *J. Geod*., 95 (3), 1-27. DOI: 10.1007/s00190-020-01453-w.
[65]Zajdel R., Kazmierski K., and Sosnica K. (2022a). Orbital artifacts in multi-GNSS Precise Point Positioning time series. *J. Geophys. Res. Solid Earth*, 127(2), e2021JB022994. DOI: 10.1029/2021JB022994.
[66]Zajdel R., Steigenberger P., and Montenbruck O. (2022b). On the potential contribution of BeiDou-3 to the realization of the terrestrial reference frame scale. *GPS Solut*., 26(109), 1-18. DOI: 10.1007/s10291-022-01298-0.
[67]Zhong, L., Sosnica, K., Weigelt, M. et al. (2021). Time-Variable Gravity Field from the Combination of HLSST and SLR. *Remote Sens*., 13(17), 3491. DOI: 10.3390/rs13173491.

Accepted Article

Research on general theory and methodology in geodesy in Poland in 2019-2022

Anna Klos[1]*, Marcin Ligas[2], Marek Trojanowicz[3]

[1]Military University of Technology, Warsaw, Poland,
[2]AGH University of Science and Technology, Krakow, Poland,
[3]Wroclaw University of Environmental and Life Science, Wroclaw, Poland,
*Corresponding author: Anna Klos, e-mail: anna.klos@wat.edu.pl

Abstract: We present a summary of research carried out in 2019-2022 in Poland in the area of general theory and methodology in geodesy. The study contains a description of original contributions by authors affiliated with Polish scientific institutions. It forms part of the national report presented at the 28th General Assembly of the International Union of Geodesy and Geophysics (IUGG) taking place on 11-20 July 2023 in Berlin, Germany. The Polish authors developed their research in the following thematic areas: robust estimation and its applications, prediction problems, cartographic projections, datum transformation problems and geometric geodesy algorithms, optimization and design of geodetic networks, geodetic time series analysis, relativistic effects in GNSS (Global Navigation Satellite System) and precise orbit determination of GNSS satellites. Much has been done on the subject of estimating the reliability of existing algorithms, but also improving them or studying relativistic effects. These studies are a continuation of work carried out over the years, but also they point to new developments in both surveying and geodesy. We hope that the general theory and methodology will continue to be so enthusiastically developed by Polish authors because although it is not an official pillar of geodesy, it is widely applicable to all three pillars of geodesy.

Keywords: robust estimation, relativistic effects, prediction problems, datum transformation, geodetic time series

Accepted Article

1. Introduction

This contribution is part of the Polish National Report on geodesy to the International Association of Geodesy (IAG) presented at the General Assembly of the International Union of Geodesy and Geophysics (IUGG) on the topic of general theory and methodology in geodesy. The research described below was carried out by authors affiliated with Polish scientific institutions in the period 2019-2022. The report is, so to speak, a continuation of the previous report published by [4]Borkowski et al. (2019), which described the original achievements of Polish researchers in the period 2015-2018. Most of the studies published by Polish researchers were carried out within international collaboration and published in JCR-indexed journals. They included analyses conducted on robust estimation and its applications, prediction problems, cartographic projections, datum transformation problems, geometric geodesy algorithms, optimization and design of geodetic networks, geodetic time series analysis, relativistic effects in the Global Navigation Satellite System (GNSS) and precise orbit determination of GNSS satellites. The research reported focused on discussing the Msplit

This article has been accepted for publication in the journal Advances in Geodesy and Geoinformation, issue 72/1, 2023. It has not yet undergone the process of copyediting, typesetting, pagination and proofreading. This may lead to differences between this version and the final published version. The article may be cited as DOI: 10.24425/agg.2023.144592.

estimation and developing its modifications to achieve better stability of the method. Within the topic of prediction problems, the authors concentrated on improving the least squares collocation method and its comparison with kriging for different types of geodetic datasets. Much has also been done to improve cartographic projections and improve transformation between different geodetic coordinates. The attempts have been made to analyse geodetic networks, to assess their reliability and optimise them. An effort has also been made to estimate the defect of the existing networks. An issue that is also frequently addressed by Polish authors concerns geodetic time series analysis. In this field, the authors estimated the effectiveness of existing methods, but also improved existing approaches resulting in the increase of the applicability of time series. Finally, the attempts were made to explain relativistic effects using GNSS observations.

2. Robust estimation and its applications

Since its introduction by [54]Wisniewski (2009, [55]2010) M_{split} estimation has been experiencing constant development. Recent advancements by [13]Duchnowski and Wisniewski (2019, [14]2020) consider robustness of $M_{split(q)}$ estimation method from both theoretical and empirical perspectives. M_{split} estimation is a method that can be derived as a development (or generalization) of *M*-estimation theory, under an assumption that a functional model for observations may be broken up into q competitive ones. To study the issue of robustness of $M_{split(q)}$ estimation local and global breakdown points are introduced, denoted as (LBdP), and (GBdP), respectively. In general, a breakdown point informs how many blunders a method may handle until it fails to provide acceptable results. Since $M_{split(q)}$ estimation concerns q competitive models, LBdP measures robustness of adjacent pair of parameters θ_i, $\theta_{(i+1)}$ whilst GBdP measures the overall robustness of estimates coming from all competitive models. The authors state that the maximum value of LBdP is 50% but, what is striking, exceeding this value, $M_{split(q)}$ estimation does not break down. This is explained by swapping places by adjacent estimates and the point is called a reversal point. On the other hand, from general perspective $M_{split(q)}$ is not robust to outliers since GBdP is zero, but if the number of competitive functional models will be extended to q+1 then outlying observations will be included therein. This operation cleans the remaining functional models and this may be perceived as robustness of M_{split} estimation method. Empirical analysis shows equivalence between empirical LBdP and corresponding theoretical derivations. However, GBdP strongly relies on prescribed number of competitive models q. If the value matches reality M_{split} method is a good alternative to conventional *M*-estimation what has been proven empirically with the use of Huber's method. Conversely, when q is mismatched then the method may fail. Also, [57]Wisniewski and Zienkiewicz (2021a) examined robustness of (squared) M_{split} estimation confirming high efficiency of the method in identifying gross errors and assigning them to competitive model with respect to a model that includes clean observations. The authors point out also very important feature of M_{split} estimation which is the independence of subjectively selected parameters controlling robustness (e.g., tuning constants). This particular feature should attract attention and contribute to further development of the family of M_{split} estimation methods.
Generalization of M_{split} estimation in the framework of errors-in-variables (EIV) model was introduced by [59]Wisniewski (2022) under the name of Total M_{split} estimation. The EIV model allows for inclusion random errors in both observations and a design matrix what makes it more realistic. The procedure itself is similar to that one of conventional M_{split} estimation with the replacement of classical versions of competitive models with EIV ones. Such a replacement makes the optimization problem much more complex than it is in the conventional case. A

Accepted Article

Lagrange objective function, that takes into account EIV competitive models as side conditions, is used to derive the solution algorithm that is based on the Gauss-Newton method applied to linearized EIV models. TM_{split} estimation absorbs M_{split} estimation in a sense that if a design matrix **A** is not contaminated by random errors, then TM_{split} and M_{split} estimators coincide.
On the other hand, [60]Wyszkowska and Duchnowski (2019) proposed a modification of M_{split} estimation where the least-squares based objective function is replaced with L1 norm optimization problem. This new variant is called the absolute M_{split} estimation (AMS). The authors found this variant less sensitive to outliers or inadequate assignment of an observation to one of the competitive functional models than the conventional squared M_{split} estimation (SMS). Also, the solution seems to be more stable with respect to an adopted initial guess that begins the iterative procedure.
Interesting and up-to-date application of M_{split} estimation was presented by [61]Wyszkowska and Duchnowski (2022). The authors apply the method to processing of Terrestrial Laser Scanning (TLS) data. In fact, they modify the method to satisfy the needs of robustness against outliers since the basic variant of M_{split} estimation was not meant to be such a method in conventional understanding of *M*-estimation. This improvement relies on modification of original influence functions (also objective and weighting functions) of SMS and AMS estimations into Huber's and Tukey's like influence function and are named SMSH, SMST and AMSH, AMSR, respectively. Practical aspect of this contribution concentrates on processing heterogenous TLS data (including outliers) with newly developed methods and confronting results obtained with their classical counterparts. The study shows that SMS and AMS may fail whilst SMST and AMSR provide satisfactory results. Huber's like variants seem to be more sensitive to outliers. The examples reveal that the newly introduced robustified version of M_{split} estimation outperforms considered *M*-estimators which fail when a data set includes a relatively high number of blunders. In addition, M_{split} estimation may yield correct results even if the percentage of outliers exceeds 50%.
[62]Zienkiewicz (2022) proposed a new version of the squared M_{split} estimation which allows the estimation of competitive parameters in a split functional model in constrained datums. The emphasis is put on robustness and efficiency of the method in geodetic network deformation analysis. The presented approach can be successfully used in the process of identifying reference datum.
In [58]Wisniewski and Zienkiewicz (2021b) the theory of $M_{split(q)}$ estimation has been supplemented with the valuable missing element that is a derivation of covariance matrices for $M_{split(q)}$ estimators. This extends the possible use of the method since accuracy analysis is, in fact, a fundamental step in every adjustment procedure. Construction of appropriate covariance matrices is based on an empirical influence function and estimators of variance coefficients (scale factors). The paper presents two versions of covariance matrices for M_{split} estimators originating from a single general formula but derived with different assumptions and applying different variance coefficients. Despite the fact that they differ in assumptions they provide comparable values of standard deviations of M_{split} estimates.

3. Prediction problem

The Least Squares Collocation (LSC) method, introduced by Torben Krarup and Helmut Moritz, has been of interest to the surveying community since its development in the 1960s, and this interest has been sustained to the present. [29]Ligas (2022) compared LSC with geostatistical method of kriging. The methods are compared under the same conditions, however, it is known that they were created to satisfy different needs thus they are equipped

Accepted Article

with specialized tools needed in particular field of application. The author demonstrates equivalence between the methods under the assumption of a second-order structure of a random function. It is shown that simple kriging (constant and known mean value) is equivalent to the least-squares prediction (interpolation) formula whilst filtered version of simple kriging is a counterpart of least-squares collocation with random errors. Universal kriging (unknown and spatially varying mean value – trend) as a filter and its special case ordinary kriging (unknown and constant mean) are equivalent to least-squares collocation with parameters. The paper clarifies also the issue of exact and filtered prediction. These two variants provide the same values on newly predicted (out-of-sample) points and filtered kriging, in this case, has a smaller prediction variance since the total signal is less variable than observed data. On the other hand, they provide different prediction results on observed data-points (in-sample). In this case, the exact model honors the data giving the same value of prediction as observed at a given point with zero prediction variance. In contrast, the filtered model provides the predicted value different from observed one (non-exact prediction) with non-zero prediction variance. Both versions provide exactly the same outcomes (in corresponding configurations of points) when there is no noise present in the data (or it is neglected).

The problem of uncorrelated noise variance in least-squares spatial prediction was studied numerically, with the application of local gravity data and EGM2008 model by [17]Jarmolowski (2019). The meaning of noise variance level is explained in this paper, and the sources of the noise are carefully examined. The studies applied LSC and revealed its relationships with the spectral signal properties. The terrestrial Bouguer anomalies, have a large variance at higher signal frequencies, i.e. their power spectral density (PSD) decreases slowly when the spatial resolution increases. The same quantity was calculated from the EGM2008 model using various degrees of spherical harmonic expansion. The different degrees of harmonics were used to remove some spectral part of the signal from the data, which revealed the relation of the noise variance with medium and high-frequency signal parts. The observed statistical quantities proved that the noise level is related with signal spectral range and data spatial resolution. The paper provided a relevant proof that the noise is not solely dependent on the measurement error and explained geometrical meaning of the regularization requirement.

The use of techniques from the kriging family to the interpolation of ionospheric total electron content (TEC) data was the subject of research by a team from the University of Warmia and Mazury (UWM). The work is focused on the local TEC models but also on new global ionosphere map (GIM) developed at UWM. The detrending and parametrization of LSC, which is equivalent to Simple Kriging (SKR), Ordinary Kriging (OKR) and Universal Kriging (UKR) were studied with respect to ionospheric TEC determined at GNSS stations ([18]Jarmolowski et al., 2021). The studies proved similar accuracy derived from different parametric modelling techniques, but a special attention should be put on the parametrization and detrending issues. It was found that local detrending with higher order polynomial surfaces applied to UKR deform kriging modeling results. This deformation is especially high in case of outliers occurrence together with a higher-order detrending in UKR.

[56]Wisniewski and Kaminski (2020) introduced a method for estimating and predicting vertical deformations based on a total least squares collocation method (TLSC). It is a generalization of least squares collocation in which conventional solution was replaced with that of total least squares. Vertical deformation field is treated therein as a random field, i.e., a collection of random variables indexed by a set of planar coordinates. It is assumed that the model underlying observed deformations consists of deterministic and stochastic parts. Generality of LSC in this particular application manifests itself through the opportunity of prediction of displacements on points not being a part of a control network (named extended control points therein) in a single coherent numerical procedure. This extends monitoring of

Accepted Article

deformations to points that are not observed directly due to different reasons like covering, no access etc. TLSC solution is iterative and the convergence is usually reached after 8–10 iterations but this is dependent on the magnitude of noise present or assumed in data, on the covariance function model and its parameters adopted for computations. In addition, TLSC approach allows not only for the determination of the deterministic and random displacements on control points and extended control points, but also for the estimation of the value of random disturbance at these points.

4. Cartographic projections, datum transformation problems and geometric geodesy algorithms

The problem of triaxiality of reference ellipsoids approximating shapes of celestial bodies, including the Earth and Moon, has attracted attention of geodesists and cartographers for the last decades ([5]Burša and Šima, 1980). This led to the development of algorithms concerning conversion between Cartesian and planetographic coordinates ([15]Feltens, 2009), geodesic lines ([41]Panou, 2013), fitting triaxial ellipsoids ([42]Panou et al., 2020), and cartographic projections ([40]Nyrtsov et al., 2013; [43]Pedzich, 2017) to mention only a few contributions. The work by [44]Pedzich (2019) inscribes in this stream. It presents a construction of a low distortion conformal projection of a triaxial ellipsoid that is based on Chebyshev's theorem on minimization of distortions in the class of conformal projections. The procedure of constructing such a projection consists of several steps which in brief may be listed out as: determination of conformal coordinates on a triaxial ellipsoid, finding formulas for a scale of linear distortion and convergence of meridians, determination of projection functions that link rectangular coordinates to conformal coordinates and determining the coefficients of the polynomials used to approximate the conformal projection that meets Chebyshev's criterion. This elaborate procedure may be examined step-by-step therein. It is worth mentioning that development of cartographic projections for triaxial ellipsoids is driven by outer space exploration since many of the celestial objects as a first approximation may be considered as bodies of such shapes (e.g., Mimas, Enceladus moons of Saturn, or Amalthea a moon of Jupiter, asteroids) therefore it is an up-to-date research field within cartography.

Conversion between Cartesian x, y, z and geodetic φ, λ, h coordinates belongs to classical problems of computational geodesy. Although it has already many solutions, new ones are constantly emerging. [19]Kadaj (2020) has modified Getchell's method ([16]Getchell, 1972) by applying new initial guess to the original iterative procedure of Getchell's reducing at the same time the number of necessary iterations. The author includes also Newton's iteration for the solution of the Getchell's nonlinear equation. Both modifications are equipped with a theoretical convergence analysis. The methods keep stability in the entire range of latitudes (-90^{o}, 90^{o}) and a practical range of geodetic heights. The exception is the geocenter region where a great majority of conversion algorithms lose their stability or ability to converge. The implementations of the algorithms in DELPHI programming language are provided in the appendix of the paper what is particularly valuable.

In addition to the problem of coordinate conversion, a problem that is constantly attracting the attention of the academic community is the issue of coordinate transformations. [30]Ligas and Prochniewicz (2021) gave a closed-form solution to the point-wise weighted rigid-body transformation (only rotations and translations involved, weights assigned to points not to separate coordinates) for asymmetric and symmetric cases. Asymmetric case assumes that either a source system or a target system is subject to random errors. On the other hand, symmetric case enables the inclusion of random errors in both systems simultaneously. A

Accepted Article

collection of developed estimation algorithms use Procrustean framework to find solutions for transformation parameters in all considered adjustment scenarios. The solutions are based on the use of polar decomposition and singular value decomposition of matrices resulting from the optimality criteria. Provided solutions are attractive since they require neither linearisation nor iteration. In addition, formulas are universal in the sense that they fit to 2D and 3D transformation problems without modifications. Theoretical considerations are supplemented with step-by-step algorithms and numerical examples. [28]Ligas (2020) extends the solution given for a rigid-body transformation to the general similarity transformation (Helmert's transformation) also applying point-wise weighting scheme and solving the problem with Procrustean approach. For asymmetric cases, i.e., either a source system (Q) or a target system (P) is subject to random errors, the solutions may be presented in closed-form. The most general case, where both coordinate systems are considered erroneous simultaneously, does not have such a solution. It can be solved iteratively but avoiding linearization process, with an initial guess for parameters obtained from, e.g., a closed-form asymmetric case. Nevertheless, the general case have some special instances which may be presented in closed-form. Those special instances include: equal weight matrices for both coordinate systems $\mathbf{W}_Q = \mathbf{W}_P = \mathbf{W}$ (for arbitrary $\mathbf{W}$), $\mathbf{W}_Q = \mathbf{W}_P = k\mathbf{I}$ (a scalar multiple of an identity matrix), and $\mathbf{W}_Q = \frac{1}{k_Q}\mathbf{W}$, $\mathbf{W}_P = \frac{1}{k_P}\mathbf{W}$ (different scalar multiples of the same weight matrix). The approach presented in this work absorbs the solutions presented by [9]Chang (2015, [10]2016). In case of the scale factor $s = 1$, the solutions reduce to the ones of a rigid-body transformation given by [30]Ligas and Prochniewicz (2021). They are based on polar decomposition of a certain matrix resulting from optimality criterion (minimization of a Frobenius norm under the side conditions for a rotation matrix) and fit to both 2D and 3D transformation problems without modification.

The work by [20]Kadaj (2021a) relates PL-ETRF89 and PL-ETRF2000 frames through transformational approach using two variants, i.e., theoretical and empirical ones. The first one is solely based on 7-parameter transformation model (Helmert transformation) fit to 330 points of the POLREF network. The second variant is based on the same 330 POLREF points with additional points of the adjusted first class triangulation network (app. 6500 points) that were used to generate an interpolation grid. Gridded differences between coordinates of two systems are the input data for a bilinear interpolation. Comparison of two approaches shows that the similarity transformation alone is not able to fully model the relation between the two reference frames. On the other hand, the empirical approach recommended for practical use reduces to some degree local deformations of the PL-ETRF89 (older) while converting coordinates of points to the PL-ETRF2000 (newer).

Another problem of geometric geodesy – geodesic line on a rotation ellipsoid – that has a rich history dating back to 18th century and strong Polish accent due to works by Thaddeus Vincenty (Tadeusz Szpila) ([53]Vincenty, 1975) was again undertaken by [37]Nowak and Nowak Da Costa (2022). They presented new and effective solutions for geodesic related problems. The authors use a cylindrical coordinate system and a newly introduced geometric construction, i.e., an equatorial geodesic triangle, to derive a novel set of formulas for the longitude, distance along the geodesic and the area of a geodesic polygon. The novelty of the contribution is multifaceted. It introduces an already mentioned equatorial geodesic triangle as a supportive tool for determining the area of a geodesic polygon. It uses Napier's rules to determine the difference between forward and reverse azimuths of a geodesic arc. It also applies a new parameterization of the geodetic inverse problem. The solution is equally well suited for oblate and prolate ellipsoids. The phenomenon of bifurcation having impact on the solution of the inverse geodetic problem is studied. In fact, the paper constitutes a significant contribution to studies on the behavior of a geodesic line on rotational ellipsoids.

Accepted Article

5. Optimization and Design of Geodetic Networks

Analyses of control networks

Monitoring of deformation of the engineering structures is an important function of surveying and geodesy. Periodically measured geodetic control networks usually represents the area or object of investigation and the results of their analyses indicate the condition of the tested object. Fundamental role in those analyses plays the identification of stable potential reference points (PRPs). In this issue the robust S-transformation approach has already been used by [11]Chen (1983) and [8]Caspary and Borutta (1987). This approach is still being developed and modified along with the development of geodetic network analysis methods. In this terms, a new approach for the identification of stable potential reference points was proposed by [38]Nowel (2019). The idea of the approach is inspired by the theory of squared $M_{split(q)}$ estimation and lies in the assumption that between the control networks adjusted in two considered epochs can simultaneously exist many congruences (matchings) which differ by the transformation parameters; in the conventional robust S-transformation existence of one congruence is assumed. That is, one model is assumed to realize a congruence in a subgroup of stable PRPs, and other models may realize different congruences in unstable PRPs. [38]Nowel (2019) proposed statistical hypothesis tests to determine the number of congruence models in a given case and whether the best model is correct. The presented approach was evaluated on the basis of four experiments described in detail.

The deformation congruence models were also investigated in the study of [39]Nowel (2020). The author discussed two widely used approaches to the specification of deformation congruence models: the global congruence test (GCT) procedure and new concept involving combinatorial possibilities (two methods) pointing out their weaknesses. The GCT procedure is based on consecutive point-by-point specification and may suffer from so-called displacement smearing. The combinatorial methods generate another weakness, namely the problem of comparison of different-dimensional models. To address this weaknesses, [39]Nowel (2020) discussed a new combinatorial procedure, denoted as CIDIA (combinatorial iterative detection–identification–adaptation (DIA) testing procedure). This new procedure relied on the appropriate use of combinatorics capabilities and generalized likelihood ratio tests performed in DIA steps, and overcame both of the aforementioned weaknesses. To demonstrate the proposed CIDIA procedure against existing methods, the author presented four experiments.

In the problem of analyses of geodetic control networks also an important role plays the network sensitivity analyses and the Minimal Detectable Displacement (MDD) as its measure. This problem was introduced to the scientific discussion by [1]Baarda (1968) and [45]Pelzer (1972), and became an element of network analysis ([34]Niemeier 1982; [35]Niemeier et al., 1982). This issue was later the subject of many scientific discussions. A new perspective on the problem was proposed by [48]Proszynski and Lapinski (2021). The authors considered the possibility of using MDD as a source of supporting information in a priori analyses of control networks accuracy and in significance tests of displacements. [48]Proszynski and Lapinski (2021) formulated a theoretical basis that would enable to investigate the problem and examine the possibility of modifying these procedures so as to use the supporting information contained in the MDD. The investigations were focused on a probabilistic aspect of combining detectability and confidence as well as significance and detectability by the superimposition of the corresponding ellipsoids and their joint analysis. Based on the analysis of MDD support, the authors proposed two options of modifying the confidence and significance thresholds related to single point displacements for practical use. As they emphasize, the task has not yet

Accepted Article

been the subject of research presented in the literature in the field of geodetic control networks so, the presented approach can be considered as a new proposal extending the application area of the MDD.

Reliability of geodetic networks analyses

An important element of the analysis of geodetic networks is the reliability of the network and problems related to the measures of this reliability. In that respect [46]Proszynski and Kwasniak (2019) investigated the effect of observation correlations on the basic characteristics of reliability matrix as oblique projection operator. The authors developed the theoretical basis for the use of reliability matrices in designing the positioning systems. They formulate (connected with the effect of observation correlations) properties of an oblique projection operator and provide a more detailed knowledge on variability of the response-based reliability measures with respect to the increase in observation correlations. They also compare the behavior of the response-based reliability measures and of the so-called testing-based measures (i.e. generalized reliability numbers and MDBs) with the increase in observation correlations.

The issue of reliability of geodetic networks was also raised by [47]Proszynski and Lapinski (2019). The authors studied reliability of non-distorting connection (NDC) of engineering survey network. They developed and analysed reliability measures for both, joint and two step adjustment models of NDC networks. The theory was illustrated by numerical examples based on two test networks. The authors showed that the reliability description based on indices obtained from the joint model should be supplemented with the indices from the two-step model. They also identified a relationship between the strength of a new network in terms of internal reliability and mutual controllability of the coordinates of connection points. The provided indices of external reliability include information related to individual connection points and the transformation parameters, so they are more meaningful for the design of non-distorting network connection.

Optimization of geodetic networks

Another current problem concerning the analysis of geodetic networks in engineering surveying is their optimization. An interesting approach presented by [32]Mrowczynska and Sztubecki (2021) consists of the optimization of the measurement and control network structure based on minimizing the objective function defined in the form of information entropy and evolutionary algorithms. The authors accepted the minimum value of the parameter vector entropy as the objective function, whereas evolutionary algorithms were used as an optimization method. Theoretical considerations were supported by numerical analyses based on a test network in three versions: with linear only, angular only and mixed (linear and angular) observations. The proposed approach allows to establish a hierarchy of importance of the individual linear and angular observations as well as determination of the optimal observations number and their mutual distribution in geodetic networks before measurements. In connection to this it allows for shortening the measurement time without reducing the accuracy of the network, and for optimizing the geodetic network structure.

Configuration defect of geodetic networks

The classical problem of identifying and locating local configuration defects of geodetic networks was considered by [21]Kadaj (2021b). The problem of incorrectly defined network structure due to missing data or errors in point numbering prevents the adjustment of such a network. In networks with a small number of points, this problem can be easily detectable and solved by simple, non-automatic analyses of the network structure. In large networks, automatic procedures for identifying and locating this kind of defect must be applied. The author described

Accepted Article

the use of Tikhonov's regularization method for this purpose. The approach was implemented by the author into the GEONET system and its effectiveness has been confirmed on the example of the adjustment of a large network consisting of over 6,000 network points..

6. Geodetic time series analysis

Geodetic time series analysis has been quite popular in Poland in 2019-2022. First of all, it concerns time series analysis of GNSS station displacements. The researchers used various GNSS permanent station networks, and analyzed both the deterministic as well as the stochastic part of the displacements. [23]Klos et al. (2020) presented two alternative approaches to modelling the deterministic part of GNSS station displacement time series. The authors compared the conventional approach, which takes into account the trend, the annual component and the semi-annual component, to an approach in which the seasonal curves are replaced with a high-resolution hydrological model assimilating GRACE. The effectiveness of using both approaches was tested by determining the nature of the stochastic part of the time series. The authors proved that the new approach to determining the deterministic part allows reducing the correlation present in the residuals, i.e. whitening them. This is due to the fact that frequencies higher than half a year are modelled by the hydrological model. This proves that some stations are sensitive to short-term changes in the terrestrial hydrosphere. These results have quite large implications especially for the use of GNSS permanent stations as hydrological sensors. [36]Nistor et al. (2021) analysed solutions for a set of 200 EPN GNSS stations obtained in a second reprocessing campaign (Repro-2). The authors focused on determining the nature of the stochastic part of the series. They found that the displacement time series for most of the European stations have a flicker noise character and that the uncertainties of station velocity are significantly lower using the classical Maximum Likelihood Estimation (MLE; [26]Langbein and Svarc, 2019) method than using the MIDAS (Median Interannual Difference Adjusted for Skewness) method ([2]Blewitt et al., 2016). This is quite understandable, as the latter method is advertised by the authors as being robust to offsets and therefore does not require offsets to be removed before velocity determination. [49]Ray et al. (2019) analyzed the displacement time series of 13 permanent GNSS stations located in the Himalayan region of Nepal. They used the Lomb-Scargle method and the nonlinear Levenberg-Marquardt algorithm to determine the index of the power-law noise based on the spectra of time series. They found that the character of the time series depends on the frequency band, i.e. the series has the character of white noise from the highest frequencies up to the frequency of 21 days, and the character of power-law noise for the rest of the frequencies.

Attempts have also been made to study the effectiveness of the algorithms used for geodetic time series analysis, and even to improve them. [33]Najder (2020) analysed the effectiveness of the Finding Outliers and Discontinuities In Time Series (FODITS) program for detecting offsets in GNSS displacement time series. The program is implemented in the Bernese GNSS Software environment ([12]Dach et al., 2015). The author concluded that although automatic detection of spike epochs is much faster than manual detection, one should take into account the errors generated by the algorithm. [31]Maciuk et al. (2020) proposed a simplified presentation of results on the nature of the stochastic part of time series obtained by the Allan variance method. The authors applied the method for five-year-long time series of GPS satellite clock corrections and declared that the method allows qualitative and quantitative expression of the type of noise using the Allan variance without the need for integration steps.

[22]Klos et al. (2019) showed how important the correct analysis of time series is in terms of application, and how the integration of parameters determined for different techniques can

Accepted Article

support the interpretability of the results. The authors performed analyses for the eastern Pacific area, which is characterized by frequent earthquakes. The largest earthquake, called Tohoku-Oki, affected the area in 2010. It was clearly recorded by GNSS permanent stations located in the area and is visible in the time series of position changes as a function of postseismic deformation. The earthquake was also recorded in observations of sea-level changes at tide-gauges, which show a clear offset in the series at the earthquake epoch. This offset will cause the trends of sea-level to be biased. The authors proposed that the amplitude of the offset should be determined from the time series of GNSS station displacements, whose sensitivity to earthquakes has already been proven, and this value should be implemented to correct tide-gauge observations. The above approach makes the changes in sea-level estimated from tide-gauge observations have better agreement with altimetric observations than before. This is of great importance when including tide-gauges from the Pacific area in studies of sea-level changes.

A definite novelty is the analysis of determining the sensitivity of GNSS stations to environmental effects. [24]Klos et al. (2021) attempted to identify the sensitivity of a GNSS system to environmental crustal loading effects: non-tidal atmospheric, non-tidal oceanic and hydrospheric loading. The authors used time series of vertical displacement changes recorded for GNSS stations located in Asia. The study area was chosen because the atmospheric effect is highly significant there and reliably modelled in present-day environmental loading models. It was observed that the GNSS system is sensitive to changes in environmental loading at different time scales. The hydrospheric effect is well visible in the displacement time series for time scales from seasonal above, the oceanic effect is only visible for short periods, while the atmospheric effect is visible on all time scales, but with varying intensity.

In addition to time series analyses of GNSS station displacements, crustal displacements resulting from terrestrial hydrosphere loading were also analysed. [27]Lenczuk et al. (2020) analyzed river catchments across Europe. Displacements were estimated based on hydrological models and observations from GRACE (Gravity Recovery and Climate Experiment; [52]Tapley et al., 2004) gravity mission. They found that the hydrology-induced displacements of Earth's crust are pronounced for the eastern European area, with a clear trend indicating a long-term decrease in water resources and a pronounced amplitude of the annual signal indicating large variations in water resources through the year. They then used the Singular Spectrum Analysis (SSA) method to determine inter-annual signals. The differences between the displacements derived for GRACE and those predicted by two hydrological models were analysed. They found that the hydrological models underestimate the trend and inter-annual signals observed by GRACE for eastern Europe. The above analyses can support the interpretation of displacements recorded by other surveying techniques, or serve as a reference when testing their sensitivity to changes in the hydrosphere.

7. Relativistic effects in GNSS

The satellites of the Galileo navigation system are orbiting in general on circular orbits. Unfortunately, the first pair of the system accidentally has been launched into highly eccentric orbits. This misplacement of satellites was exploited by [50]Sosnica et al. (2021) to investigate the impact of general relativistic effects on the satellites orbits. The authors used the post-Newtonian parameterization of general relativity and first-order Gaussian perturbations to derive formulas describing theoretical perturbations of Keplerian parameters of Earth-orbiting satellites. The study focused on three general relativity effects: Schwarzschild effect, Lense-Thirring effect and geodetic precession – De Sitter effect. [50]Sosnica et al. (2021) found that

Accepted Article

the change of the semi-major axis Δa for circular orbits ($e = 0$) is independent of the orbital height and equals on average:

$$\Delta a = -4\frac{GM}{c^2} = -17.74 \text{ mm} \quad (1)$$

for all Earth orbiting satellites. *G* denotes the gravity constant, *M* is the mass of the Earth, *c* is the speed of the light. The mean changes of the semi-major axis is equal to the double value of the Schwarzschild radius for the Earth, i.e., the hypothetical size of the black hole of the mass equal to the Earth's mass. For eccentric orbits, the mean offset due to the Schwarzschild effect changes over time and equals to -7.8 and -28.3 mm in perigee and apogee, respectively for Galileo E14 and E18 ([50]Sosnica et al., 2021). De Sitter and Lense-Thirring cause small offsets of the semi-major axis for a satellite at Galileo orbit heights of about +0.46 and −0.07 mm, respectively.

The authors also found that the geodetic precession depends on the elevation of the Sun above the orbital plane. The rate of the ascending node depends on the maximum possible elevation of the Sun above the orbital plane, which was not considered before in the literature (the constant rate due to the geodetic precession was considered so far). A nodal rate of 55.6 and 6.8 μas/day is caused by De Sitter and Lense-Thirring, respectively, on Galileo satellite in eccentric orbits. Thus, the total effect changes the position of the Galileo orbit node by 8.46 mm after one day and more than 3 m when accumulating data from 1 year. Thus, the effect is measurable using the current techniques of space geodesy.

The effect of general relativity on satellite orbits geometry has also been the subject of research provided by [51]Sosnica et al. (2022). The authors used three years of GPS, GLONASS, and Galileo data to retrieve the general relativistic effects acting on the orbit geometry described as the semi-major axis and eccentricity. The mean observed offset of the semi-major axis is -17.41 mm, which gives a relative error versus the expected value of 0.36% when estimating the post-Newtonian parameters

8. Precise orbit determination of GNSS satellites

Satellite position errors are one of the most important factors affecting the accuracy of positioning with the use of the GNSS. Research to improve this accuracy focuses, among others, on evaluation of various factors crucial for the precise orbit determination like infrared radiation, albedo and direct solar radiation pressure. In that regard [6]Bury et al. (2020) studied the impact of the aforementioned forces on GNSS satellites. The authors focused on evaluation of the magnitude and the characteristic periods of accelerations caused by the forces. The studies were conducted in relation to Empirical Orbit Model (ECOM), which in the Sun-satellite-Earth reference frame, decompose the accelerations acting on the GNSS satellite in three directions: D-from the satellite toward the Sun, Y-along the solar panel rotation axis and B-perpendicular to D and Y axes, completing the right-handed orthogonal frame. The authors pointed and assessed the perturbations absorbed by the extended ECOM2 and the consequences of neglecting higher order of ECOM coefficients. They reported that the largest periodic perturbations absorbed by the ECOM2 in B and D directions are at 371 and $146\,mm$ respectively. However, Galileo in eccentric orbits - E14 and E18 - are subject to the different perturbing forces. As a result, the non-considered once-per-revolution accelerations in D and twice-per revolution acceleration in B cause the errors up to 154 and $37\,mm$, respectively. Therefore, using the proper a priori model for Galileo satellites is indispensable to achieve the highest quality of the geodetic products ([7]Bury et al., 2021). The authors developed also the

Accepted Article

equation describing the relation between the periodic error of the position (A_m) and the periodic acceleration acting on satellites in direction Q:

$$A_m = \sqrt{Q_{cn_{\mathrm{ref}}}^2 + Q_{sn_{\mathrm{ref}}}^2} \cdot \frac{1}{n_{\mathrm{ref}}^2} \cdot \left(\frac{T}{2\pi}\right)^2, \quad (2)$$

where $n_{\mathrm{ref}} = 1,2,3, \ldots$ denotes the perturbation of the once-, twice-, ternary-, quadruple-per-revolution, etc., T is the satellite revolution period and Q_c and Q_s denote the sine and cosine acceleration components.

On the other hand [25]Kur et al. (2021) investigated the possible consequences of introducing Inter-Satellite Links (ISL) in the orbit determination process. The of three constellation types of orbital planes (GPS-like with 24 satellites on six orbital planes, GPS-real with real satellite positions and Galileo-like with 24 satellites on three orbital planes) and seven different ISL connectivity schemes (intra-plane closed, intra-plane open), nearest (inter-plane, dual one-way), nearest (general, dual one-way), nearest (general, one-way), sequential (dual one-way) and sequential (one-way)) were investigated. Simulated ISL measurements were included in the orbit and clock estimation process. The authors demonstrated strong contribution of ISLs to minimize of the orbit errors, in general, and help to minimize satellite clock estimation errors.

9. Conclusions

Although general theory and methodology is not an official pillar of geodesy, the field is widely developed because it allows for the improvement of algorithms used in all three pillars of geodesy. The results of the researches presented in this study are an overview of the achievements of Polish scientists in this field in the period of 2019-2022. On the one hand, the studies are continuation of work carried out for years, the summary of which can be found in the studies, e.g. [3]Borkowski and Kosek (2015) and [4]Borkowski et al. (2019). On the other hand, they indicate new directions of development in both geodesy and surveying. The most important achievements include:

- new approach for the identification of stable potential reference points inspired by the theory of squared $M_{split(q)}$ estimation proposed by [38]Nowel (2019) and investigations of the deformation congruence models based on combinatorial methods ([39]Nowel, 2020);
- new proposal of application of the use of Minimal Detectable Displacement in the network sensitivity analyses derived by [48]Proszynski and Lapinski (2021);
- development of the theoretical basis for the use of reliability matrices in designing the positioning systems ([46]Proszynski and Kwasniak, 2019) and reliability analysis for non-distorting connection (NDC) of engineering survey network ([47]Proszynski and Lapinski, 2019);
- new approach of the optimization of the measurement and control network structure proposed by [32]Mrowczynska and Sztubecki (2021). The approach is based on minimizing of the objective function defined in the form of information entropy and evolutionary algorithms;
- analyzes regarding of the classical problem of identifying and locating local configuration defects of geodetic networks ([21]Kadaj, 2021b);
- investigations on the impact of general relativistic effects on the satellites orbits ([50]Sosnica et al., 2021; [51]2022);
- research to improve the accuracy of satellites orbits based on the study of perturbing forces on GNSS satellites ([6]Bury et al., 2020; [7]2021) as well as introducing Inter-Satellite Links in the orbit determination process ([25]Kur et al., 2021);

Accepted Article

- development of cartographic projections for triaxial ellipsoids and their applications for mapping of celestial bodies ([44]Pedzich, 2019);
- research on closed-form solutions for a similarity transformation and its variants (e.g., a rigid-body transformation) within the Procrustean framework ([28]Ligas, 2020; [30]Ligas and Prochniewicz, 2021);
- derivation of novel set of formulas for the longitude, distance along the geodesic and the area of a geodesic polygon ([37]Nowak and Nowak Da Costa, 2022);
- continuous development of M_{split} estimation in terms of robustness analysis, introduction of errors-in-variables (EIV) solution, further robustification against outliers, accuracy analysis, e.g., [13]Duchnowski and Wisniewski (2019, [14]2020), [57]Wisniewski and Zienkiewicz (2021a); [59]Wisniewski (2022), [61]Wyszkowska and Duchnowski (2022);
- demonstration of equivalence between the least squares collocation and geostatistical method of kriging for scalar random fields under the assumption of 2nd order stationarity ([29]Ligas, 2022);
- investigations on noise-related problems and detrending issues in least squares collocation and kriging, application of total least squares collocation to deformation analysis ([17]Jarmolowski, 2019; [18]Jarmolowski et al., 2021; [56]Wisniewski and Kaminski, 2020);
- improved understanding of geophysical processes through better modelling of geodetic time series ([22]Klos et al., 2019, [23]2020, [24]2021; [27]Lenczuk et al., 2020; [31]Maciuk et al., 2020; [33]Najder, 2020; [36]Nistor et al., 2021).

Author contributions

Conceptualization: AK, ML, MT; original draft preparation, editing and reviewing: AK, ML, MT.

Data availability statement

No datasets were used in this research.

Acknowledgements

We thank the editors of Advances in Geodesy and Geoinformation and the anonymous reviewers for their valuable comments.

References

[1]Baarda, W. (1968). *A testing procedure for use in geodetic network*. Publications on Geodesy, New Series, Netherlands Geodetic Commission, Delft.

[2]Blewitt, G., Kreemer, C., Hammond, W.C. et al. (2016). MIDAS robust trend estimator for accurate GPS station velocities without step detection. *J. Geophys. Res. Solid Earth*, 121(3), 2054-2068. DOI: 10.1002/2015JB012552.

[3]Borkowski, A., and Kosek, W. (2015). Theoretical geodesy. *Geod. Cartogr.*, 64(2), 261-279. DOI: 10.1515/geocart-2015-0015.

[4]Borkowski, A., Kosek, W., and Ligas, M. (2019). Geodesy: General theory and methodology 2015–2018. *Geod. Cartogr.*, 68(1), 145-162. DOI: 10.24425/gac.2019.126092.

Accepted Article

[5]Burša, M, and Šima, Z (1980). Tri-axiality of the Earth, the Moon and Mars. *Stud. Geoph. et Geod*., 24(3), 211-217.
[6]Bury, G., Sosnica, K., Zajdel, R. et al. (2020). Toward the 1-cm Galileo orbits: challenges in modeling of perturbing forces. *J. Geod.*, 94, 16. DOI: 10.1007/s00190-020-01342-2.
[7]Bury, G., Sosnica, K., Zajdel, R. et al. (2021). Geodetic datum realization using SLR-GNSS co-location onboard Galileo and GLONASS. *J. Geophys. Res. Solid Earth*, 126, 10. DOI: 10.1029/2021JB022211.
[8]Caspary, W.F. and Borutta, H. (1987). Robust estimation in deformation models. *Surv. Rev*., 29(223), 29-45.
[9]Chang, G. (2015). On least-squares solution to 3D similarity transformation problem under Gauss-Helmert model. *J. Geod.*, 89(6), 573-576. DOI: 10.1007/s00190-015-0799-z.
[10]Chang, G. (2016). Closed form least-squares solution to 3D symmetric Helmert transformation with rotational invariant covariance structure. *Acta Geod. Geophys.*, 51, 237-244. DOI: 10.1007/s40328-015-0123-7.
[11]Chen, Y.Q. (1983). *Analysis of deformation surveys – a generalized method*. Technical Report No. 94. University of New Brunswick: Fredericton.
[12]Dach, R., Lutz, S., Walser, P. et al. (2015). Bernese GNSS Software Version 5.2. DOI: 10.7892/boris.72297.
[13]Duchnowski, R., and Wisniewski, Z. (2019). Robustness of Msplit(q) estimation: a theoretical approach. *Stud. Geophys. Geod.*, 63(3), 390-417. DOI: 10.1007/s11200-018-0548-x.
[14]Duchnowski, R., and Wisniewski, Z. (2020). Robustness of squared Msplit(q) estimation: Empirical analyses. *Stud. Geophys. Geod.*, 64(2), 153-171. DOI: 10.1007/s11200-019-0356-y.
[15]Feltens, J. (2009). Vector method to compute the Cartesian (X, Y, Z) to geodetic (φ, λ, h) transformation on a triaxial ellipsoid. *J. Geod*., 83, 129-137. DOI: 10.1007/s00190-008-0246-5.
[16]Getchell, B.C. (1972). Geodetic latitude and altitude from geocentric coordinates. *Celestial Mechanics*, 5, 300-302.
[17]Jarmolowski, W. (2019). On the relations between signal spectral range and noise variance in least-squares collocation and simple kriging: example of gravity reduced by EGM2008 signal. *Bollettino di Geofisica Teorica et Applicata*, 60(3), 457-474. DOI: 10.4430/bgta0265.
[18]Jarmolowski, W., Wielgosz, P., Ren, X. et al. (2021). On the drawback of local detrending in universal kriging in conditions of heterogeneously spaced regional TEC data, low-order trends and outlier occurrences. *J. Geod.*, 95(1), 1-19. DOI: 10.1007/s00190-020-01447-8.
[19]Kadaj, R. (2020). Conformal and empirical transformation between the PL-ETRF89 and PL-ETRF2000 reference frames using the new adjustment of the former Polish I class triangulation network. *Geod. Cartogr.*, 70(2). DOI: 10.24425/gac.2021.136680.
[20]Kadaj, R. (2021a). Getchell's method for conversion of Cartesian-geocentric to geodetic coordinates – Its properties and Newtonian alternative. *J. Appl. Geod.*, 15(1), 47-60. DOI: 10.1515/jag-2020-0034.
[21]Kadaj, R. (2021b). The method of detection and localization of configuration defects in geodetic networks by means of Tikhonov regularization. *Reports on Geodesy and Geoinformatics*, 112(1), 19-25. DOI: 10.2478/rgg-2021-0004.
[22]Klos, A., Kusche, J., Fenoglio-Marc, L. et al. (2019). Introducing a vertical land motion model for improving estimates of sea level rates derived from tide gauge records affected by earthquakes. *GPS Solut.*, 23, 102. DOI: 10.1007/s10291-019-0896-1.
[23]Klos, A., Karegar, M.A., Kusche, J. et al. (2020). Quantifying Noise in Daily GPS Height Time Series: Harmonic Function Versus GRACE Assimilating Modeling Approaches. *IEEE Geosci. Remote Sens. Lett.*, 18, 4. DOI: 10.1109/LGRS.2020.2983045.

Accepted Article

[24]Klos, A., Dobslaw, H., Dill, R. et al. (2021). Identifying sensitivity of GPS to non-tidal loadings at various time resolutions: examining vertical displacements from continental Eurasia. *GPS Solut.*, 25, 89. DOI: 10.1007/s10291-021-01135-w.
[25]Kur, T., Liwosz, T., and Kalarus, M. (2021). The application of inter-satellite links connectivity schemes in various satellite navigation systems for orbit and clock corrections determination: simulation study. *Acta Geod. Geophys*., 56, 1-28. DOI: 10.1007/s40328-020-00322-4.
[26]Langbein, J., and Svarc, J.L. (2019). Evaluation of temporally correlated noise in Global Navigation Satellite System time series: Geodetic monument performance. J Geophys Res Solid Earth, 124, 925–942. DOI: 10.1029/2018JB016783.
[27]Lenczuk, A., Leszczuk, G., Klos, A. et al. (2020). Study on the inter-annual hydrology-induced deformations in Europe using GRACE and hydrological models. *J. Appl. Geod*., 14(4). DOI: 10.1515/jag-2020-0017.
[28]Ligas, M. (2020). Point-wise weighted solution for the similarity transformation parameters. *Appl. Geomat.*, 12, 371-377. DOI: 10.1007/s12518-020-00306-7.
[29]Ligas, M. (2022). Comparison of kriging and least-squares collocation – Revisited. *J. Appl. Geod.*, 16(3), 217-227. DOI: 10.1515/jag-2021-0032
[30]Ligas, M., and Prochniewicz, D. (2021). Procrustes based closed-form solution to the point-wise weighted rigid-body transformation in asymmetric and symmetric cases. *J. Spatial. Sci.*, 66:3, 445-457. DOI: 10.1080/14498596.2019.1684394.
[31]Maciuk, K., Kudrys, J., Bagherbandi, M. et al. (2020). A new method for quantitative and qualitative representation of the noises type in Allan (and related) variances. *Earth Planets Space*, 72, 186. DOI: 10.1186/s40623-020-01328-6.
[32]Mrowczynska, M., and Sztubecki, J. (2021). The network structure evolutionary optimization to geodetic monitoring in the aspect of information entropy. *Measurement*, 179, 1-15. DOI: 10.1016/j.measurement.2021.109369.
[33]Najder, J. (2020). Automatic detection of discontinuities in the station position time series of the reprocessed global GNSS network using Bernese GNSS Software. *Acta Geodyn. Geomater.*, 17, 4, 439-451. DOI: 10.13168/AGG.2020.0032.
[34]Niemeier, W. (1982). Principal component analysis and geodetic networks – some basic considerations. *Proc. Surv. Control Netw. Heft*, 7, 275-291.
[35]Niemeier, W., Teskey, W.F., and Lyall, R.G. (1982). Precision, reliability and sensitivity aspects of an open pit monitoring network. *Aust. J. Geod. Photogramm. Surv.*, 37, 1-27.
[36]Nistor, S., Suba, N.-S., Maciuk, K. et al. (2021). Analysis of Noise and Velocity in GNSS EPN-Repro 2 Time Series. *Remote Sens*., 13, 2783. DOI: 10.3390/rs13142783.
[37]Nowak, E., and Nowak Da Costa, J. (2022). Theory, strict formula derivation and algorithm development for the computation of a geodesic polygon area. *J. Geod.*, 96, 20. DOI: 10.1007/s00190-022-01606-z.
[38]Nowel, K. (2019). Squared Msplit(q) S-transformation of control network deformations. *J. Geod.*, 93(7), 1025-1044. DOI: 10.1007/s00190-018-1221-4.
[39]Nowel, K. (2020). Specification of deformation congruence models using combinatorial iterative DIA testing procedure. *J. Geod.*, 94(12), 118. DOI: 10.1007/s00190-020-01446-9.
[40]Nyrtsov, M.V., Fleis, M.E., Borisov, M.M. et al. (2013). Equal-area projections of the tri-axial ellipsoid: first time derivation and implementation of cylindrical and azimuthal projections for small solar system bodies. *Cartogr. J.*, 52 (2), 114-124. DOI: 10.1080/00087041.2015.1119471.
[41]Panou, G. (2013). The geodesic boundary value problem and its solution on a triaxial ellipsoid. *J. Geod. Sci*., 3(3), 240-249. DOI: 10.2478/jogs-2013-0028.

Accepted Article

[42]Panou, G., Korakitis, R., and Pantazis, G. (2020). Fitting a triaxial ellipsoid to a geoid model. *J. Geod. Sci.*, 10, 1, 69-82. DOI: 10.1515/jogs-2020-0105.
[43]Pedzich, P. (2017). Equidistant map projections of a tri-axial ellipsoid with the use of reduced coordinates. *Geod. Cartogr.*, 66, 271-290. DOI: 10.1515/geocart-2017-0021.
[44]Pedzich, P. (2019). A low distortion conformal projection of a tri-axial ellipsoid and its application for mapping of extra-terrestrial objects. *Planet Space Sci*., 178, 1-9. DOI: 10.1016/j.pss.2019.104697.
[45]Pelzer, H. (1972). *Nachweis von Staumauerdeformationen unter Anwendung statistischer Verfahren. Berichte Arbeitsgruppe B*. Deutscher Geodätentag: Braunschweig.
[46]Proszynski, W., and Kwasniak, M. (2019). The effect of observation correlations upon the basic characteristics of reliability matrix as oblique projection operator. *J. Geod*., 93, 1197-1206. DOI: 10.1007/s00190-019-01236-y.
[47]Proszynski, W., and Lapinski, S. (2019). Reliability analysis for non-distorting connection of engineering survey networks. *Surv. Rev*., 51, 366, 219-224. DOI: 10.1080/00396265.2018.1425605.
[48]Proszynski, W., and Lapinski, S. (2021). Investigating support by minimal detectable displacement in confidence region determination and significance test of displacements. *J. Geod.*, 95(10), 1-12. DOI: 10.1007/s00190-021-01550-4.
[49]Ray, J.D., Vijayan, M.S.M., Godah, W. et al. (2019). Investigation of background noise in the GNSS position time series using spectral analysis: A case study of Nepal Himalaya. *Geod. Cartogr*, 68(2), 375-388. DOI: 10.24425/gac.2019.128468.
[50]Sosnica, K., Bury, G., Zajdel, R. et al. (2021). General relativistic effects acting on the orbits of Galileo satellites. *Celest. Mech. Dyn. Astron.*, 133, 14. DOI:10.1007/s10569-021-10014-y.
[51]Sosnica, K., Bury, G., Zajdel, R. et al. (2022). GPS, GLONASS, and Galileo orbit geometry variations caused by general relativity focusing on Galileo in eccentric orbits. *GPS Solut*., 26, 5. DOI: 10.1007/s10291-021-01192-1.
[52]Tapley, B.D., Bettadpur, S.V., Watkins, M.M. et al. (2004). The gravity recovery and climate experiment: mission overview and early results. *Geophys. Res. Lett*., 31, 9. DOI: 10.1029/2004GL019920.
[53]Vincenty, T. (1975). Direct and inverse solutions on the ellipsoid with application of nested equations. *Surv. Rev.*, 23(176), 88-93. DOI: 10.1179/sre.1975.23.176.88.
[54]Wisniewski, Z. (2009). Estimation of parameters in a split functional model of geodetic observations (Msplit estimation). *J. Geod.*, 83, 105-120. DOI: 10.1007/s00190-008-0241-x.
[55]Wisniewski, Z. (2010). Msplit(q) estimation: estimation of parameters in a multi split functional model of geodetic observations. *J. Geod.*, 84, 355-372. DOI: 10.1007/s00190-010-0373-7.
[56]Wisniewski, Z., and Kaminski W. (2020). Estimation and prediction of vertical deformations of random surfaces, applying the total least squares collocation method. *Sensors*, 20(14), 1-24, DOI: 10.3390/s20143913.
[57]Wisniewski, Z., and Zienkiewicz, H. (2021a). Empirical analyses of robustness of the square Msplit estimation. *J. Appl. Geod.*, 15 (2), 87-104. DOI: 10.1515/jag-2020-0009.
[58]Wisniewski, Z., and Zienkiewicz, M.H. (2021b). Estimators of covariance matrices in Msplit(q) estimation. *Surv. Rev.*, 53(378), 263-279. DOI: 10.1080/00396265.2020.1733817.
[59]Wisniewski, Z. (2022). Total Msplit estimation. *J. Geod.*, 96 (10), 1-23. DOI: 10.1007/s00190-022-01668-z.
[60]Wyszkowska, P., and Duchnowski, R. (2019). Msplit estimation based on L1 norm condition. *J. Surv. Eng.*, 145, 3. DOI: 10.1061/(ASCE)SU.1943-5428.0000286.

Accepted Article

[61]Wyszkowska, P., and Duchnowski, R. (2022). Processing TLS heterogeneous data by applying robust Msplit estimation. *Measurement*, 197, 111298. DOI: 10.1016/j.measurement.2022.111298.
[62]Zienkiewicz, M. (2022). Identification of Unstable Reference Points and Estimation of Displacements Using Squared Msplit Estimation. *Measurement*, 195, 111029. DOI: 10.1016/j.measurement.2022.111029.

Accepted Article